CONCISE STEREOSELECTIVE SYNTHESIS OF ASPIDOALBIDINE ALKALOIDS & SPLICEOSTATIN DERIVATIVES

by

Joshua R. Born

A Dissertation

Submitted to the Faculty of Purdue University

In Partial Fulfillment of the Requirements for the degree of

Doctor of Philosophy

Department of Chemistry

West Lafayette, Indiana

May 2020

THE PURDUE UNIVERSITY GRADUATE SCHOOL
STATEMENT OF COMMITTEE APPROVAL

Dr. Arun K. Ghosh, Chair

Departments of Chemistry and Medicinal Chemistry

Dr. Mark Lipton

Department of Chemistry

Dr. Chris Uyeda

Department of Chemistry

Dr. Abram Axelrod

Department of Medicinal Chemistry and Molecular Pharmacology

Approved by:

Dr. Christine Hrycyna

This dissertation is dedicated to my family and friends for their love, support, and complete bewilderedness as to why I'm still at Purdue after eight years.

ACKNOWLEDGEMENTS

I would like to thank my father Tim and mother Brenda, brother Jason and wife Alex, sister Jennifer and husband Jerad, and all my nieces and nephews for their guidance, love, and understanding during my graduate studies.

I would like to thank Professor Arun K. Ghosh for his acceptance of me into his research laboratory during the Fall of 2016. His drive, direction, and unwavering confidence in me inspired me become the scientist I am today. His "always learning" mindset has helped me feel both greatly humbled and awed at the vast expanse of chemistry I have yet to learn, a challenge that I wouldn't be up for if it weren't for my supportive group members. I would specifically like to thank my mentors Dr. Emilio Cardenas and Dr. Luke Kassekert, as well as current members Abdulkhaliq Alawaed, Abhijith Anil, Amartyo Basu, Caesar Gomez, Daniel Lee, Hannah Simpson, Miranda Belcher, Monika Yadav, Jennifer Mishevich, John Gulliver, Will Robinson, Dr. Che-Sheng Hsu, Dr. Dana Shahabi, Dr. Jinfei Yang, Dr. Joseph Bungard, Dr. Raghavaiah Jakka, Dr. Satish Kovela, Dr. Shivaji Markad, Dr. Srinivasa Rao Allu, Dr. Zilei Xia, and Suzanne Snoeberger; and former members Dr. Alessandro Grillo, Dr. Anindya Sarkar, Dr. Anne Veitschegger, Dr. Anthony Tomaine, Dr. Chandu Reddy, Dr. Heather Osswald, Dr. Jacqueline Williams, Dr. Margherita Brindisi, Dr. Nicola Relitti, Dr. Prasanth Nyalapatla, MSc. Samantha Ebner, Dr. Samuel Rodriguez, and Dr. Vasudeva Dodda.

Finally, I would like to thank my committee members Professor Mark Lipton, Professor Christopher Uyeda, and Professor Abram Axelrod for their academic tutelage, professional guidance, and collaborative research groups that they themselves maintain.

TABLE OF CONTENTS

LIST OF TABLES

LIST OF FIGURES

LIST OF SCHEMES

LIST OF ABBREVIATIONS

acac	Acetylacetone
Addn	Addition
AcOH	Acetic acid
AIBN	Azobisisobutyronitrile
B.A.	Brønsted Acid
BMS	Borane-dimethyl sulfide
BRSM	Based on recovered starting material
BuLi	Butyl lithium
Bu	Butyl
BuOH	Butanol
CBS	Corey–Bakshi–Shibata
CDI	Carbonyldiimidazole
DBU	1,8-Diazabicyclo(5.4.0)undec-7-ene
DCB	Dichlorobenzene
DCE	Dichloroethane
DCM	Dichloromethane/Methylene Chloride
DFT	Density functional theory
Diox	1,4-Dioxane
DIPEA	Diisopropylethylamine/Hünig's base
DMAP	4-Dimethylaminopyridine
DMF	*N*,*N*-Dimethylformamide
DMS	Dimethylsulfide
DMSO	Dimethylsulfoxide
DNA	Deoxyribonucleic Acid
DMP	Dess-Martin Periodinane
DMPU	N,N'-Dimethylpropyleneurea
dr	Diastereomeric excess
EDCI	1-Ethyl-3-(3-dimethylaminopropyl)carbodiimide
ee	*Enantiomeric excess*

Elim	Elimination
Et_2O	Diethyl Ether
EtOAc	Ethyl acetate
EtOH	Ethanol
GI_{50}	Half maximal inhibitory of cell proliferation
G-II	Grubbs Catalyst 2nd Generation
HFIP	1,1,1,3,3,3-Hexafluoro-propan-2-ol
HMPA	Hexamethylphosphoramide
HPLC	High performance liquid chromatography
HRMS	High resolution mass spectrometry
Hz	Hertz
IC_{50}	Half maximal inhibitory concentration
Imid	Imidazole
IPA	*iso*-propanol
KHMDS	Potassium hexamethyldisilazide/potassium bis(trimethylsilyl)amide
L.A.	Lewis Acid
LAH	Lithium aluminum hydride
LDA	Lithium *N*,*N*-diisopropyl amide
LLS	Longest linear sequence
LRMS	Low resolution mass spectrometry
m	*meta*
MeCN	Acetonitrile
MeOH	Methanol
mRNA	Messenger ribonucleic acid
MTBE	methyl tert-butyl ether
n	*normal*
NaHMDS	Sodium hexamethyldisilazide/sodium bis(trimethylsilyl)amide
nM	nanomolar
NMP	*N*-Methyl-2-pyrrolidone
NMR	Nuclear
o	*ortho*

OMe	Methoxide
p	*para*
pH	Potential of hydrogen
pKa	Acid dissociation constant, logarithmic scale
PhMe	Toluene
PhH	Benzene
PHOX	2-[2-(diphenylphosphino)phenyl]-2-oxazoline
PMB	*para*-methoxybenzyl
ppm	parts per million
PTSA•H_2O	*para*-toluene sulfonic acid monohydrate
Pyr	pyridine
Ra-Ni	Raney-Nickel
RCM	Ring closing metathesis
RNA	Ribonucleic acid
rr	regioisomeric ratio
RSM	Recovered starting material
SAR	Structure activity relationship
sNRP	Small nuclear ribonucleoproteins
ss	Splicing site
t	*tert*
TBAF	Tetrabutylammonium Fluoride
TBAI	Tetrabutylammonium Iodide
TBDPS	*tert*-butyldiphenylsilane
TBS	*tert*-butyldimethylsilane
TC	Thiophene carboxylate
TEA	Triethylamine
TEMPO	(2,2,6,6-Tetramethylpiperidin-1-yl)oxyl
TES	Triethylsilane
Tf	Trifluoromethanesulfonate
TFA	Trifluoroacetic acid
TFAA	Trifluroacetic anhydride

THF	Tetrahydrofuran
THP	Tetrahydropyran
TLC	Thin-layer chromatography
TMEDA	N,N,N’,N’-Tetramethylethylene-1,2-diamine
TMS	Trimethyl silane
Tol	Toluene
Trisyl	2,4,6-Triisopropylbenzenesulfonyl
Ts	Tosylate
α	alpha
β	beta
γ	gamma

ABSTRACT

Enantioselective syntheses of hexacyclic aspidoalbidine alkaloids (+)-fendleridine and (+)-acetylaspidoalbidine are described. These syntheses feature an asymmetric decarboxylative allylation and photocyclization of a highly substituted enaminone. Also, the synthesis highlights the formation of a C19-hemiaminal ether via a reduction/condensation/intramolecular cyclization cascade with the C21-alcohol. The present synthesis provides convenient access to the aspidoalbidine hexacyclic alkaloid family in an efficient manner.

A copper-catalyzed cross-coupling is described. Use of Cu(I) salts in the presence of allyl bromides and organostannyl furans were found to undergo catalytic turnover under ambient conditions and afford the coupled products in good to great yields. Model substrate screening led to conditions used in the concise formal synthesis of FR901464 analogues. Optimization of the described coupling step led to suppression of undesired isomers and byproducts affording the desired diene coupled product in high yield, stereo-, and regioselectivity on a multigram scale. Novel protection of the resulting diene moiety as an unconventional protecting group, and a facile four-step single column chromatographic stereoselective sequence are also reported.

CHAPTER 1. ENANTIOSELECTIVE TOTAL SYNTHESES OF (+)-FENDLERIDINE AND (+)-ACETYLASPIDOALBIDINE

The structures of (+)-Fendleridine (aspidoalbidine, **1**) and (+)-Acetylaspidoalbidine (**2**) are that of highly functionalized hexacyclic indolines with 4 contiguous chiral centers and feature a hemiaminal ether on the C19 carbon (Figure 1.1). This chapter provides background information on the isolation, synthesis, and characterization of these molecules. Previous synthetic efforts by Boger[1] and Movassaghi[2] are described within. Initial failed attempts made by us at the syntheses of these molecules, addressal, and the resulting solutions are described. Characterization of a desired key intermediate via chemical derivatization and 2D NMR characterization, facile construction of the pentacyclic core via a cascade reaction, along with support and full characterization of the minor rotamer found to be present in (+)-**2** are also described.

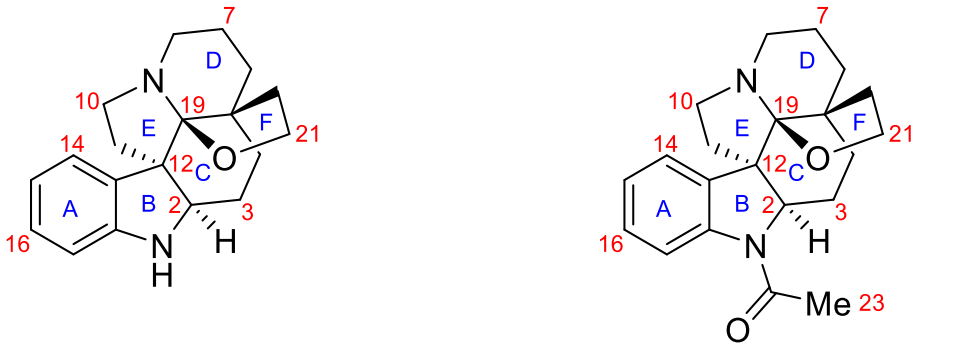

Figure 1.1 Structures of (+)-Fendleridine and its N-Acyl Derivative (+)-Acetylaspidoalbidine

1.1 Introduction

Aspidosperma alkaloids constitute a large family of monoterpene natural products with over 250 members.[3–9] The pentacyclic core comes from that of the core molecule (+)-Aspidospermidine (**3**, Figure 1.2). The likely biosynthetically ethyl-oxidized analogue (+)-Limaspermidine (**4**) has also been found to be a natural product, and through means of further oxidation of the C19 carbon a hemiaminal ether connection would form (+)-Fendleridine **2**. This molecule represents the hexacyclic core of a subset known as *Aspidoalbidine* alkaloids. Several Aspidosperma and Aspidoalbidine alkaloids have been shown to have attributed bioactivity;[3,9–11] of note (+)-Haplocidine **5** has been shown to be a potent caspase 8 inhibitor, with an IC_{50} value of 0.4 μM. Due to caspase 8's over expression in the pathogenesis of multiple sclerosis, Parkinson's, and Alzheimer's disease, inhibition of these apoptosis-inducing proteases provides a novel therapeutic target.[12] The bioactivity of these closely related molecules and the prevalence of natural product use in medicinal chemistry[13] motivated us to construct a concise route to this family of molecules through the synthesis of (+)-Fendleridine (**1**) and (+)-Acetylaspidoalbidine (**2**).

1.2 Isolation of (+)-Fendleridine and (+)-Acetylaspidoalbidine

(+)-Fendleridine (**1**) was isolated from the dried seeds of the Venezuelan tree *Aspidosperma fendleri* in 1964 by Medina and coworkers along with other Aspidoalbidine natural products,[14] only constituting 0.04% of the isolated compound mixture. Later in 1979 it was also isolated from the Venezuelan tree species *Aspidosperma rhombeosignatum* by the same group. Although the name for Fendleridine comes from the tree from which it was isolated, it's also referred to as "Aspidoalbidine" in the isolation literature, hence where the name *Acetyl*aspidoalbidine for the corresponding *N*-acetyl derivative comes from. Acetylaspidoalbidine (**2**), was isolated from the Peruvian plant *Vallesia dichotoma* in 1963 by Djerassi and coworkers, and again from the Bolivian tree *Aspidosperma pyrifolium* in 1996 by Mitaine and coworkers, in which it was mislabeled as "dehydroxyhaplocidine".[15] In this discovery, it was noted to make up ~0.1% of the alkaloid mixture of the other isolated *Aspidosperma* and *Aspidoalbidine* alkaloids. It's worth noting that several of these plants have been attributed to the prementioned medicinal and biological activities likely due to the presence of said alkaloids.[16–18]

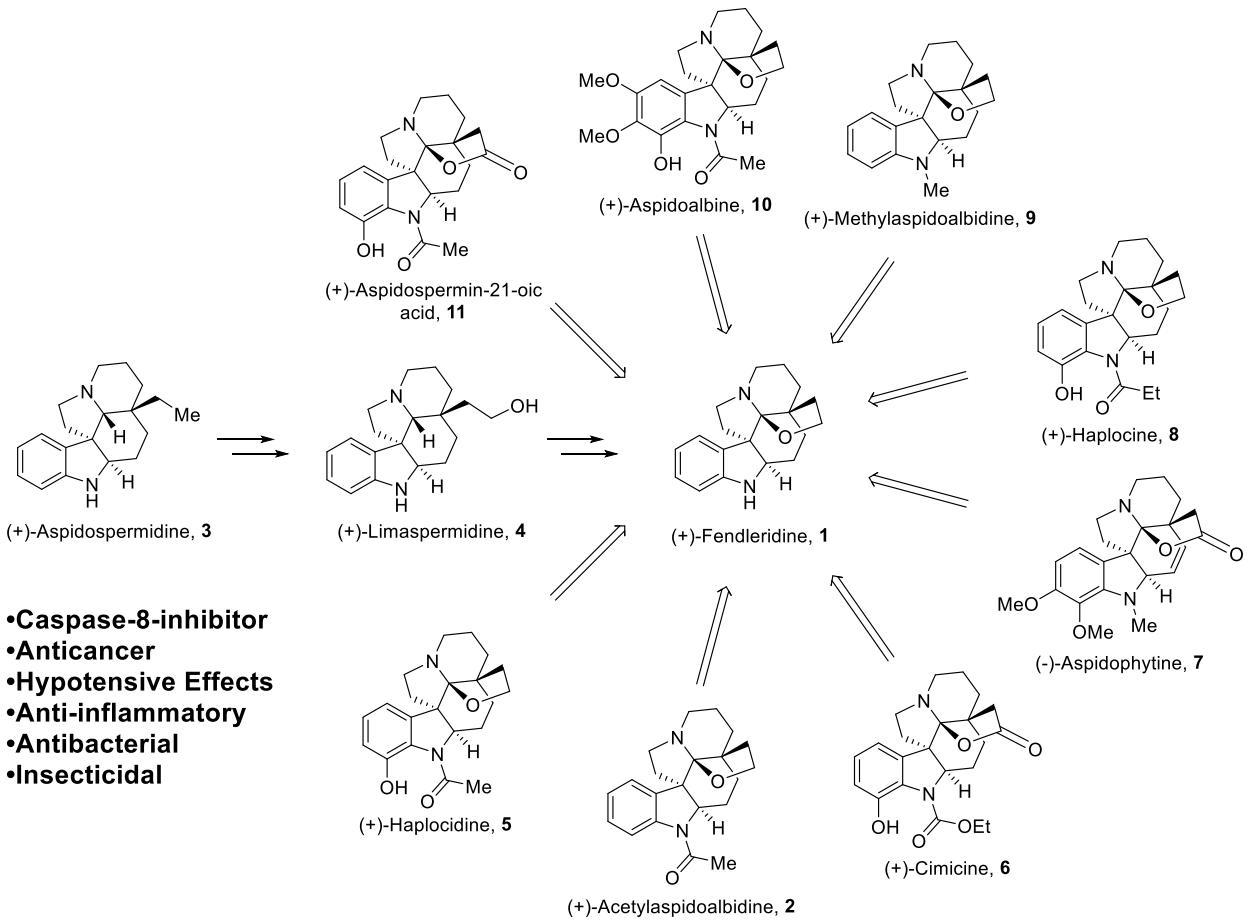

Figure 1.2 Fendleridine and Select Natural Products of the Aspidoalbidine Family

1.3 Boger's Total Synthesis

1.3.1 Retrosynthesis

Boger and coworkers published the first enantioselective total syntheses of (+)-Fendleridine and (+)-Acetylaspidoalbidine in 2010, assigning the absolute configuration for the first time.[1] Their synthesis of enantiopure **1** came from reductive manipulations of racemic xanthate **12**, in which the desired enantiomer was separated out by chiral HPLC and assigned via X-ray crystallography before being carried on (Scheme 1.1). (±)-**12** came from silyl ether (±)-**13**, which is the product of his tandem [4+2]/[3+2] cycloaddition used in his past work[19] (Figure 1.3) The starting material **14** for the cycloaddition was coupled from **15** and **16**, which each in turn would come from starting materials **18** and **20** after a number of chemical transformations.

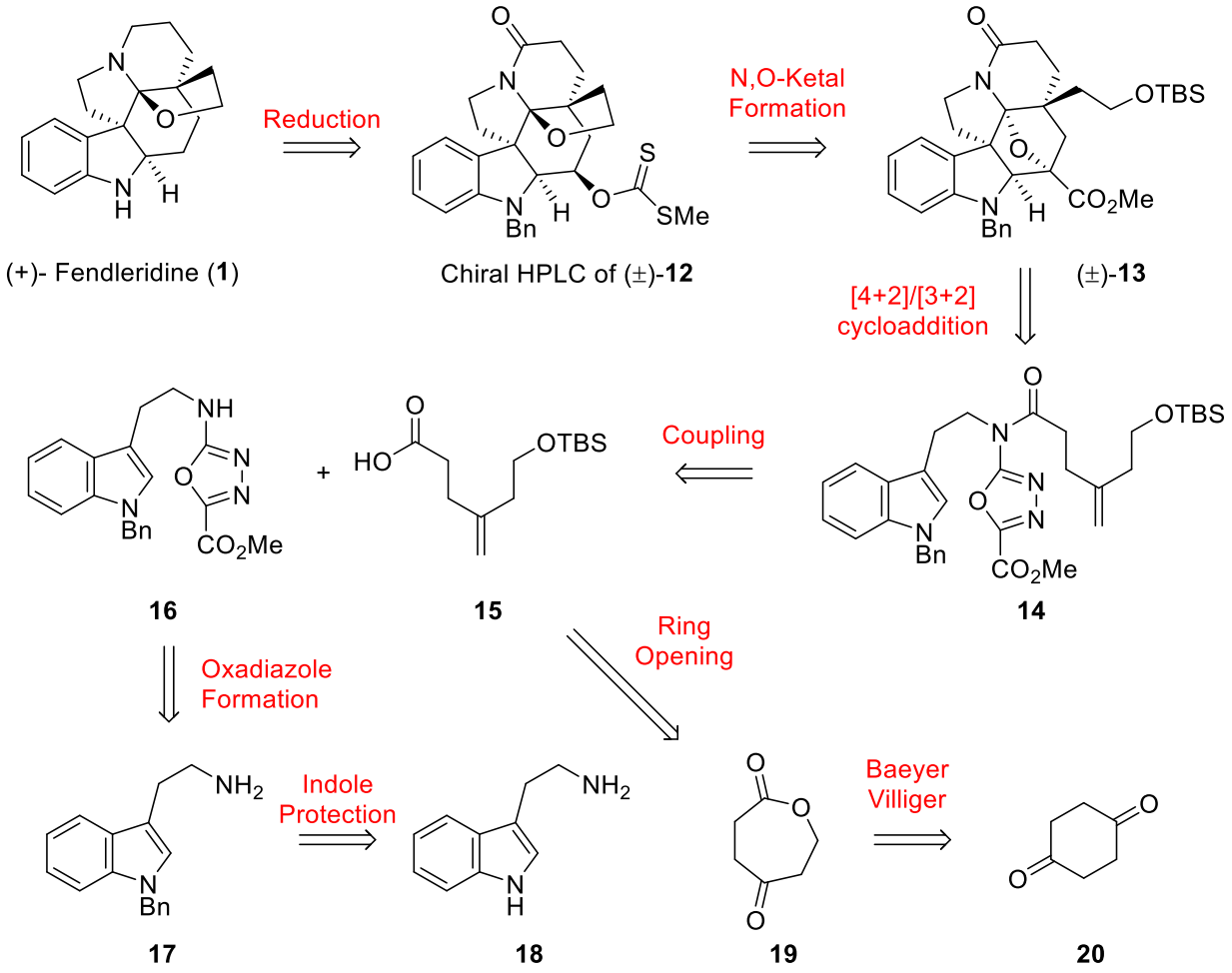

Scheme 1.1 Boger and Coworkers Retrosynthetic Analysis of (+)-Fendleridine

1.3.2 [4+2}/[3+2] Cycloaddition

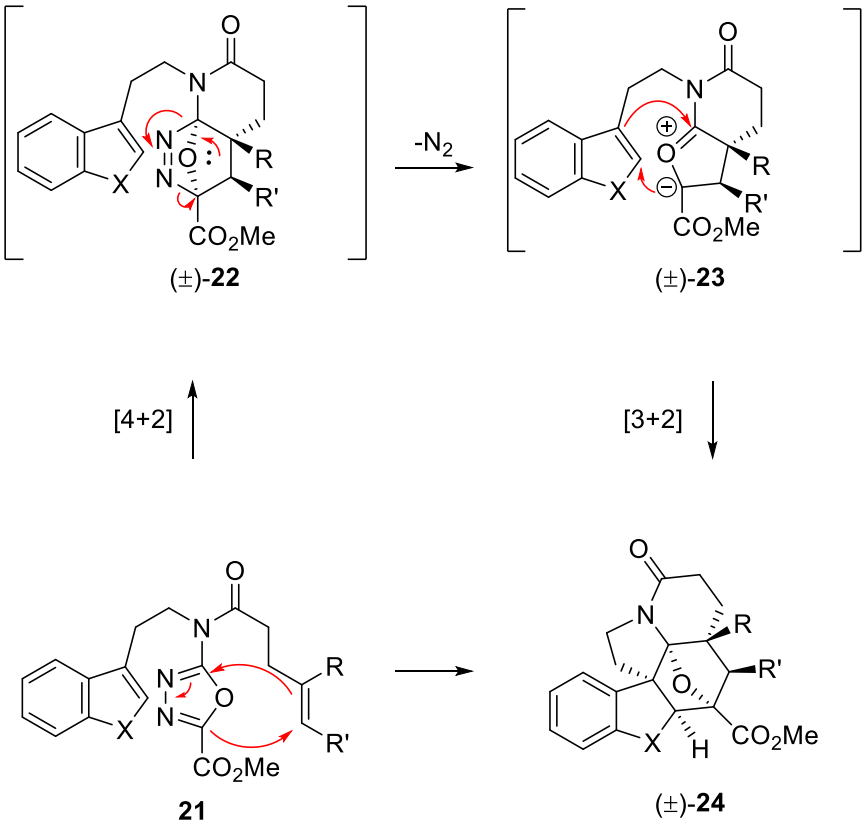

Figure 1.3 Boger's Tandem [4+2]/[3+2] Cycloaddition

The mechanism behind Boger's tandem cycloaddition is that, once heated up, the oxadiazole moiety in **21** undergoes a [4+2] with the intramolecular olefin, creating racemic (±)-**22**. Extrusion of nitrogen gas forms the 1,3 dipole (±)-**23** *in situ*, which then undergoes a [3+2] with the unsaturation in the heterocycle, leading to the product (±)-**24**.

1.3.3 Synthesis

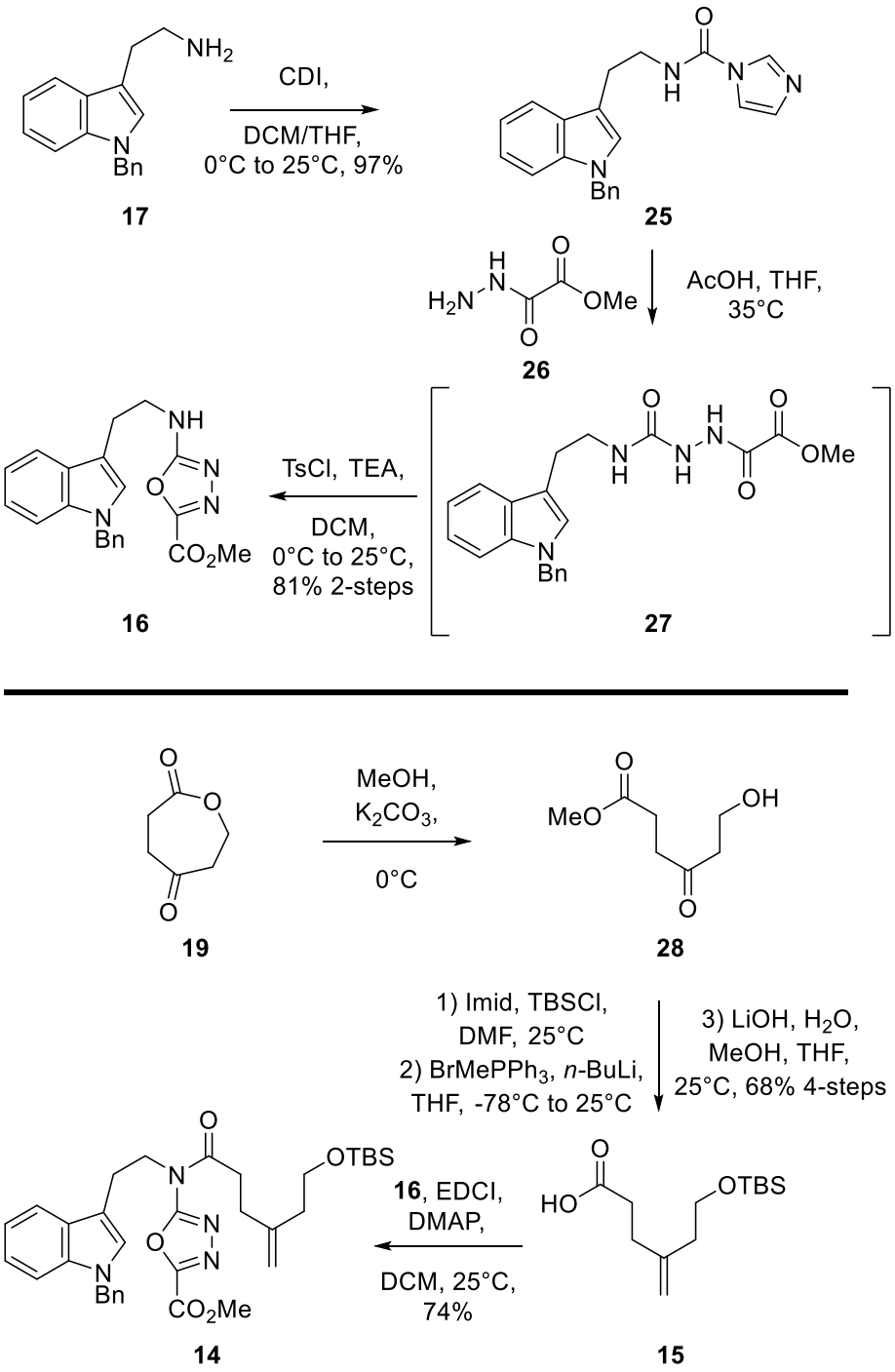

Scheme 1.2 Synthesis of Coupled Cycloaddition Precursor **14**

Their synthesis began from **17** and **19** (Scheme 1.2), which were prepared from tryptamine and 1,4-cyclohexanedione in 3[20] and 1[21] steps respectively. Coupling tryptamine **17** with CDI

afforded urea **25** in 97%, which was then reacted with hydrazide **26** (formed in one step[22]) to form crude **27**. Dehydration with TsCl and TEA then afforded the requisite **16** in 81% over 2-steps. Meanwhile, oxepane **19** could be subjected to methanolysis to yield **28**, then silyl protection, Wittig olefination, and saponification yielded carboxylic acid **15** in 68% yield over 4 steps. Coupling of carboxylic acid **15** and oxadiazole compound **16** with EDCI afforded the compound **14** in 74%.

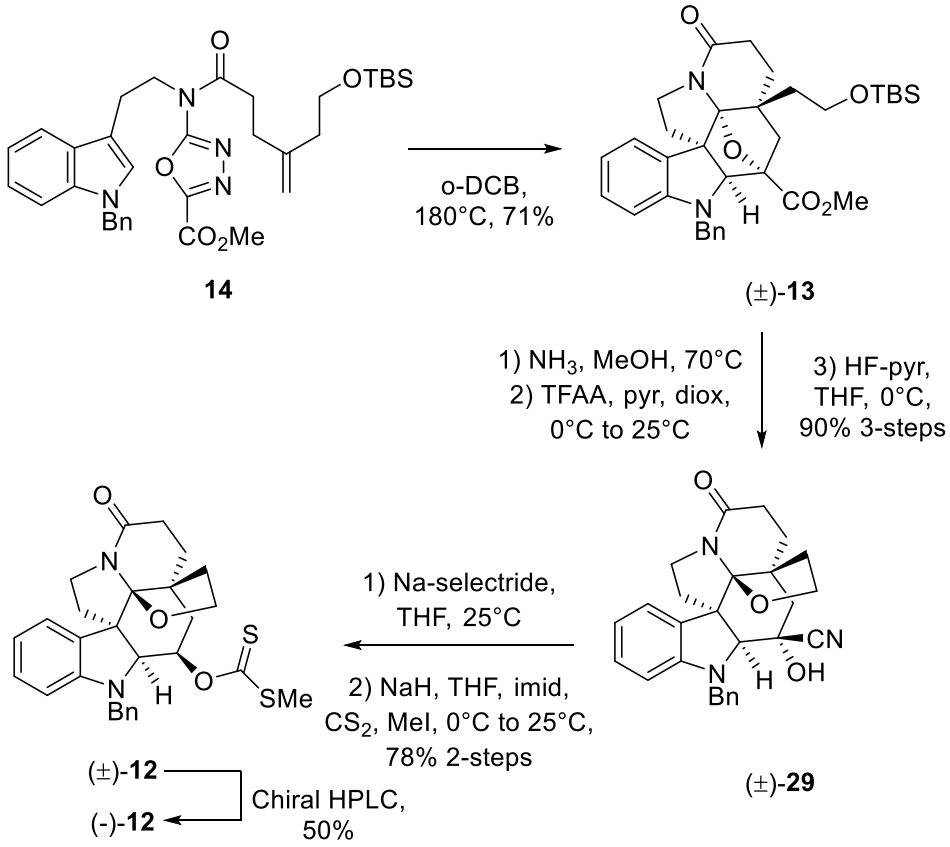

Scheme 1.3 Synthesis of Xanthate **12**

Heating **14** in o-DCB afforded a racemic mixture of their desired compound (±)-**13** in 71% (Scheme 1.3). Aminolysis followed by dehydration of the resulting amide and then silyl deprotection to collapse the resultant alkoxide afforded the nitrile, alcohol, and hemiaminal moieties present in (±)-**29** in 90% over 3 steps. Diastereoselective reduction of the *in-situ* formed ketone followed by xanthate formation afforded (±)-**12**, which was then separated at this late stage via chiral HPLC to afford (-)-**12** in 39% over 2-steps and one resolution.

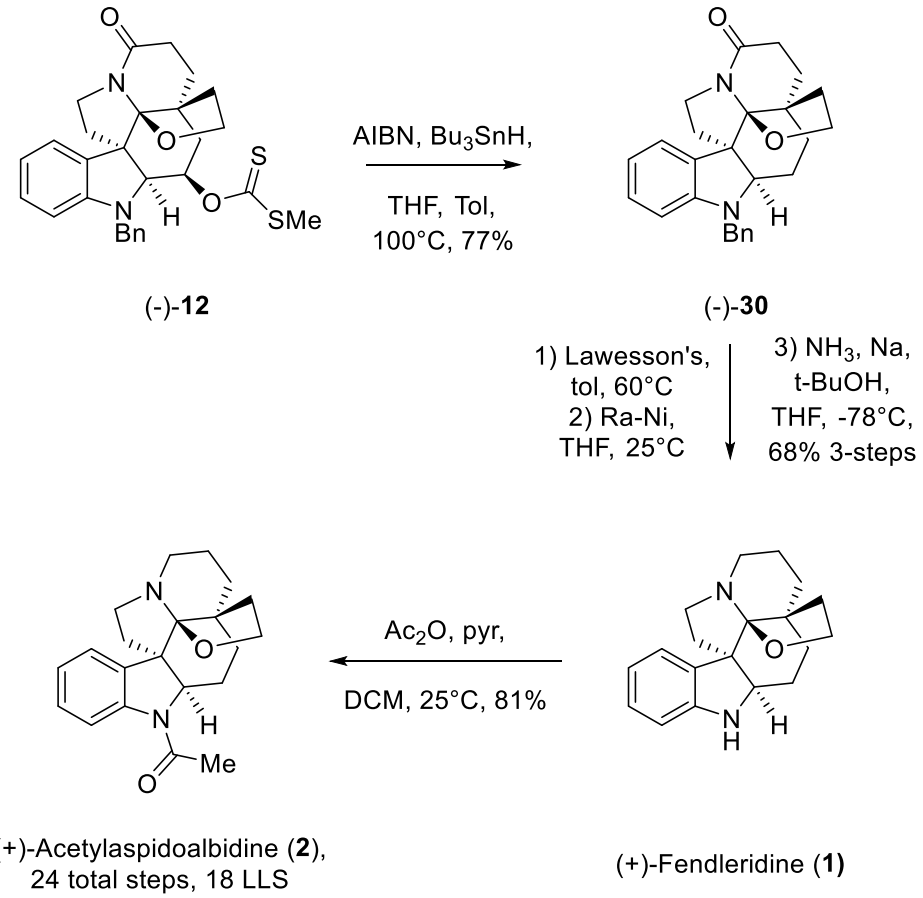

Scheme 1.4 Boger's Completion of (+)-Fendleridine (**1**) and (+)-Acetylaspidoalbidine (**2**)

(-)-**12** was then taken forward, and Barton-McCombie conditions afforded amide (-)-**30** in 77% yield (Scheme 1.4). Formation of the thioamide, subsequent reduction to the amine, and Birch conditions afforded (+)-Fendleridine (**1**) in 68% over three steps. Typical acetylation conditions then afforded (+)-Acetylaspidoalbidine (**2**) in 81% yield thus completing their syntheses of the two molecules. Overall, Boger's synthesis included 24 total steps from commercially available tryptamine **18** and 1,4-cyclohexanedione **20**, 18 steps longest linear sequence (LLS) and utilized late-stage chiral separation.

1.4 Movassaghi's Total Synthesis

1.4.1 Retrosynthesis

Movassaghi and coworkers followed up with their syntheses of (+)-Fendleridine (**1**) and (+)-Acetylaspidoalbidine (**2**) in 2016.[2] Retrosynthetically, the hemiaminal in **1** came from the alcohol (-)-**31**, which was made racemically and enzymatically resolved at a late stage (Scheme 1.5). (±)-**31** came from a ring-closing metathesis of allyl amide **32**, which in turn came from the ester **33** after Friedel-Crafts type alkylations. This divinyl moiety was the product of the alkylation of indole **35** and diene **34**, which came from *o*-iodoaniline **36** and trans-crotonyl chloride **37** respectively after a number of chemical transformations.

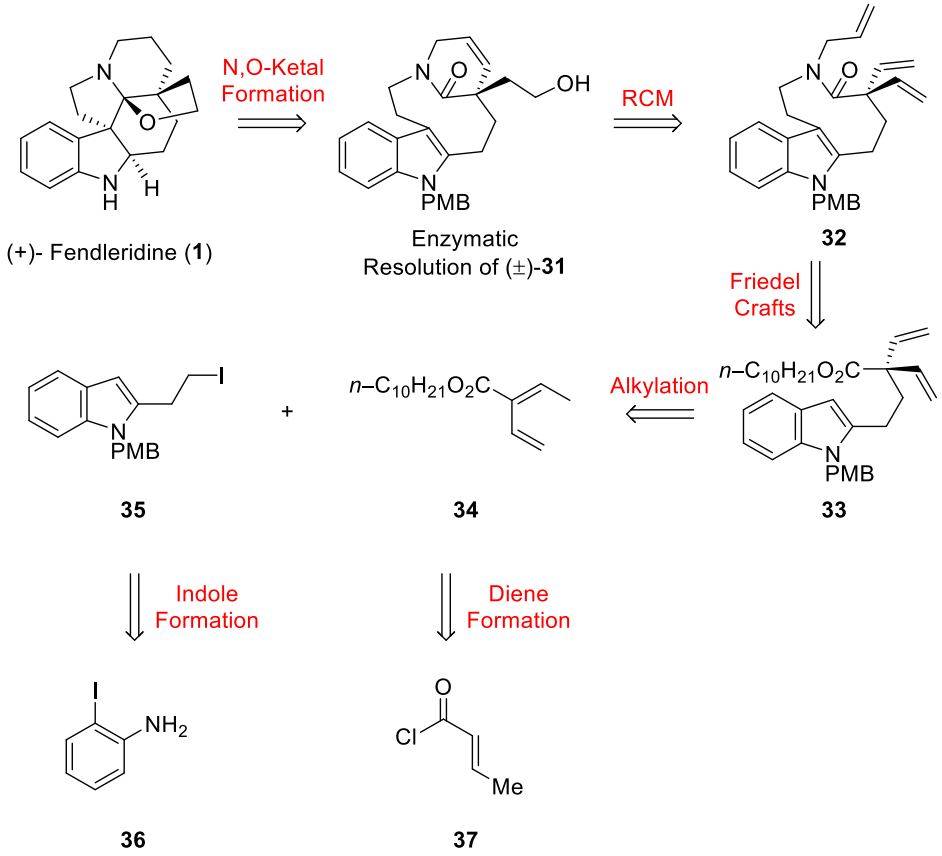

Scheme 1.5 Movassaghi and Coworkers Retrosynthetic Analysis of (+)-Fendleridine

1.4.2 Synthesis

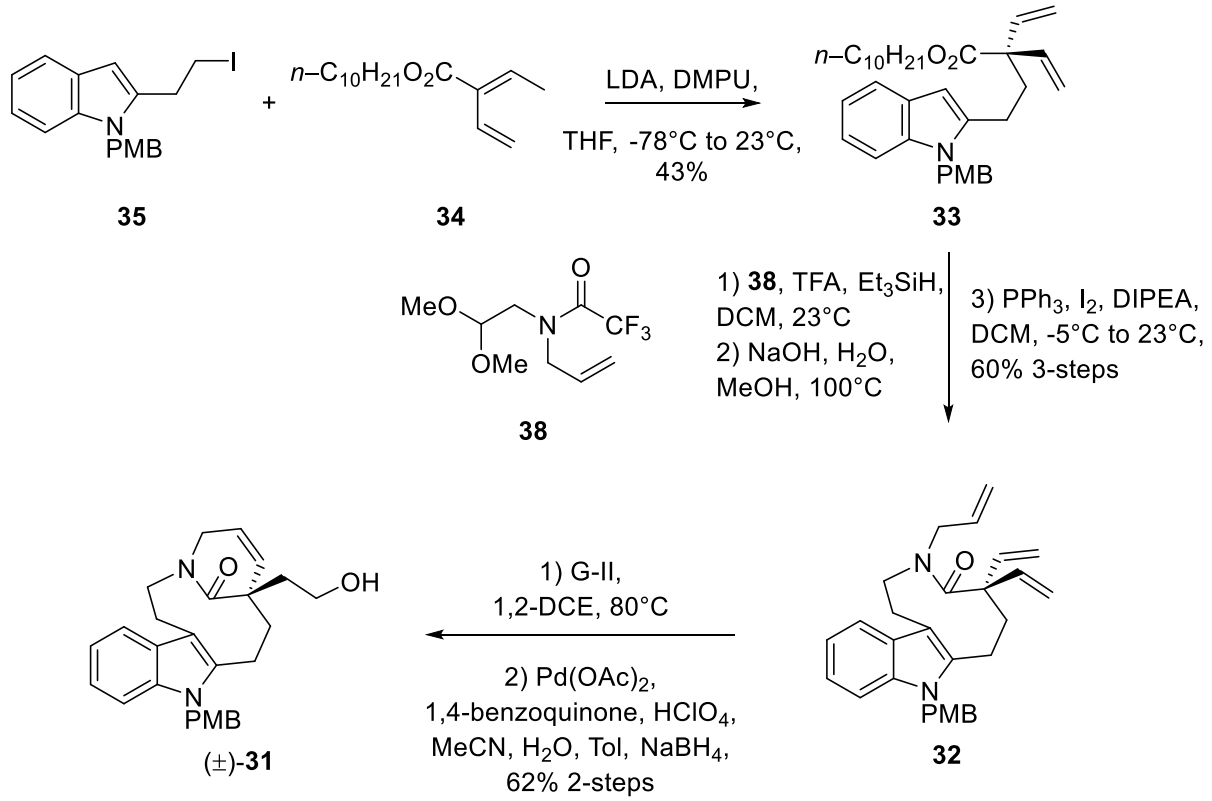

Scheme 1.6 Synthesis of Racemic Alcohol **31**

Their synthesis began with indole **35** and diene **34**, which were made from *o*-iodoaniline **36** and trans-crotonyl chloride **37** in 4^{23} and 3^{2} steps respectively (Scheme 1.6). Coupling of the two using LDA and DMPU afforded the divinyl compound **33** in 43% yield. A Friedel-Crafts type alkylation could be made through the indole C2-C3 unsaturation to attach dimethyl acetal **38** (made in 2-steps[23]) and subsequent hydrolysis and ring closure formed **32** in 60% over 3-steps. Grubbs metathesis and a subsequent Wacker-Tsuji oxidation resulted in the racemic alcohol (±)-**31** in 62% over two steps.

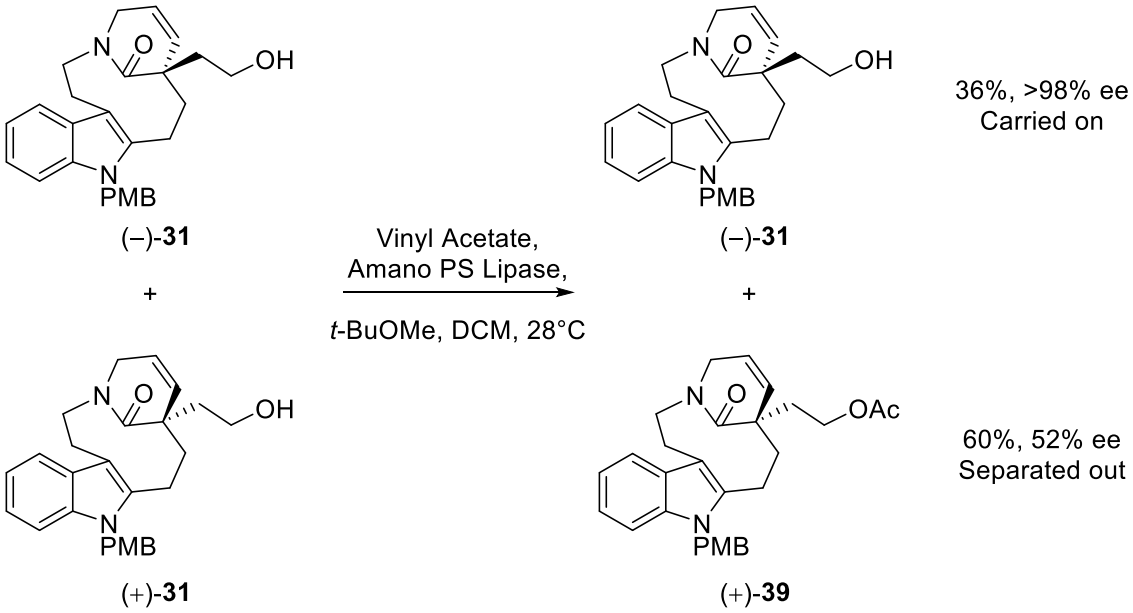

Scheme 1.7 Enzymatic Resolution of Racemic Alcohol **31**

Their enzymatic resolution began with a screening of different enzymes and conditions, and they concluded Amano PS Lipase afforded the best *ee* in regards to (-)-**31** (Scheme 1.7).[2] To this end, they were able to get >98% *ee* of the desired enantiomer, however in order to increase the *ee* the yield took a hit, resulting in undesirable yield (36% yield of the desired enantiomer).

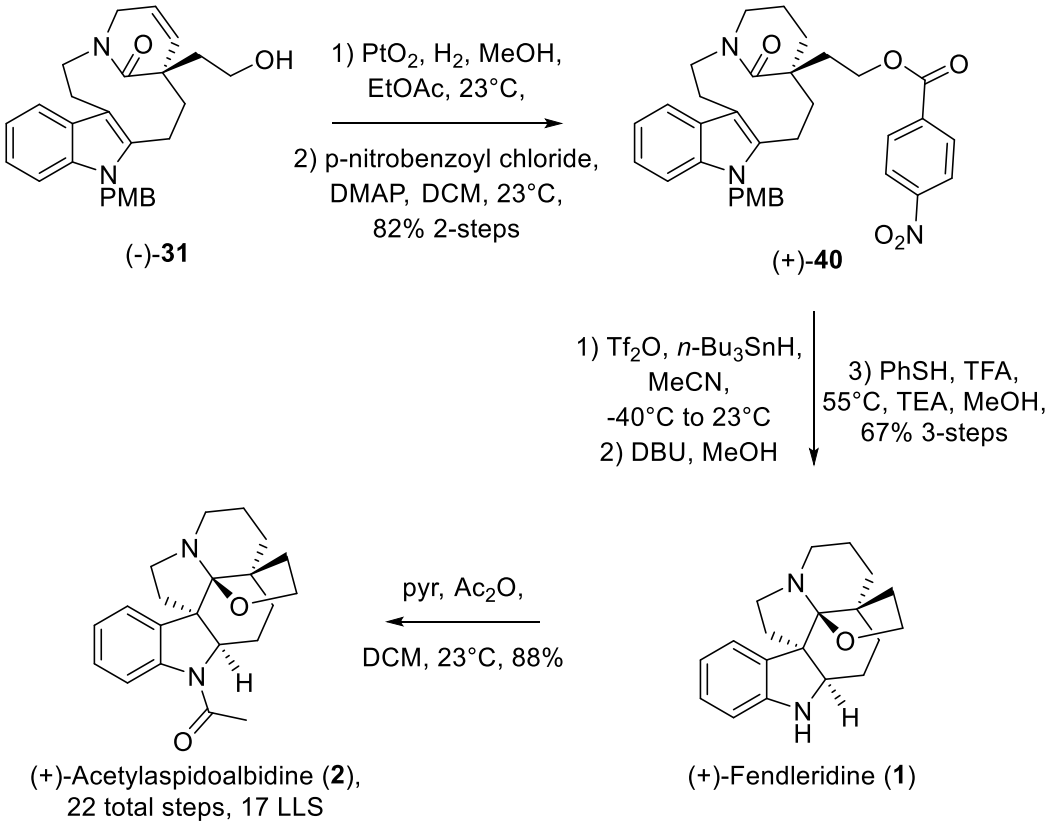

Scheme 1.8 Movassaghi's Completion of (+)-Fendleridine & (+)-Acetylaspidoalbidine

Carrying forward (-)-**31**, reduction of the cis-olefin followed by p-nitrobenzoylation afforded (+)-**40** in 82% over 2-steps (Scheme 1.8). Reduction with tributyltin hydride and triflic anhydride followed by DBU addition then resulted in the alcohol cyclizing to form the hemiaminal ether, and deprotection of the PMB ether with thiophenol and triflic acid followed by TEA addition resulted in (+)-Fendleridine (**1**) in 67% over 3-steps. Typical acetylation conditions then afforded (+)-Acetylaspidoalbidine (**2**) in 88% yield thus completing their synthesis of the two molecules. Overall, Movassaghi's synthesis included 22 total steps from *o*-iodoaniline **36** and trans-crotonyl chloride **37**, 17 steps longest linear sequence (LLS), and utilized late-stage enzymatic resolution.

1.5 Results and Discussion

1.5.1 Retrosynthetic Analysis of (+)-Fendleridine and (+)-Acetylaspidoalbidine

Based upon the prior work by Boger and Movassaghi (Chapters 1.3 & 1.4), we envisioned a more concise synthetic route towards the construction of the (+)-Fendleridine core, circumventing the use of both late-stage chiral HPLC and enzymatic resolution. Our retrosynthetic analysis is outlined in Scheme 1.9. The formation of our hemiaminal ether moiety would come from trapping the iminium ion in **41** by the resultant alcohol of the deprotected silyl ether. The iminium ion would come from a cascade reaction in which reduction of a nitrile group would result in amine **42** and concomitantly cyclize twice to form the pentacyclic framework. The *syn* relationship of the C2 and C12 substituents would come from the alkylation of the indoline **43**. The trans substituted indoline **43** would come from the 6π-conrotatory photocyclization of enaminone **44**, whose C5 stereochemically defined chiral center would be constructed via Stoltz Decarboxylative Allylation chemistry. Thus, our synthesis would begin from commercially available enaminone **45**.

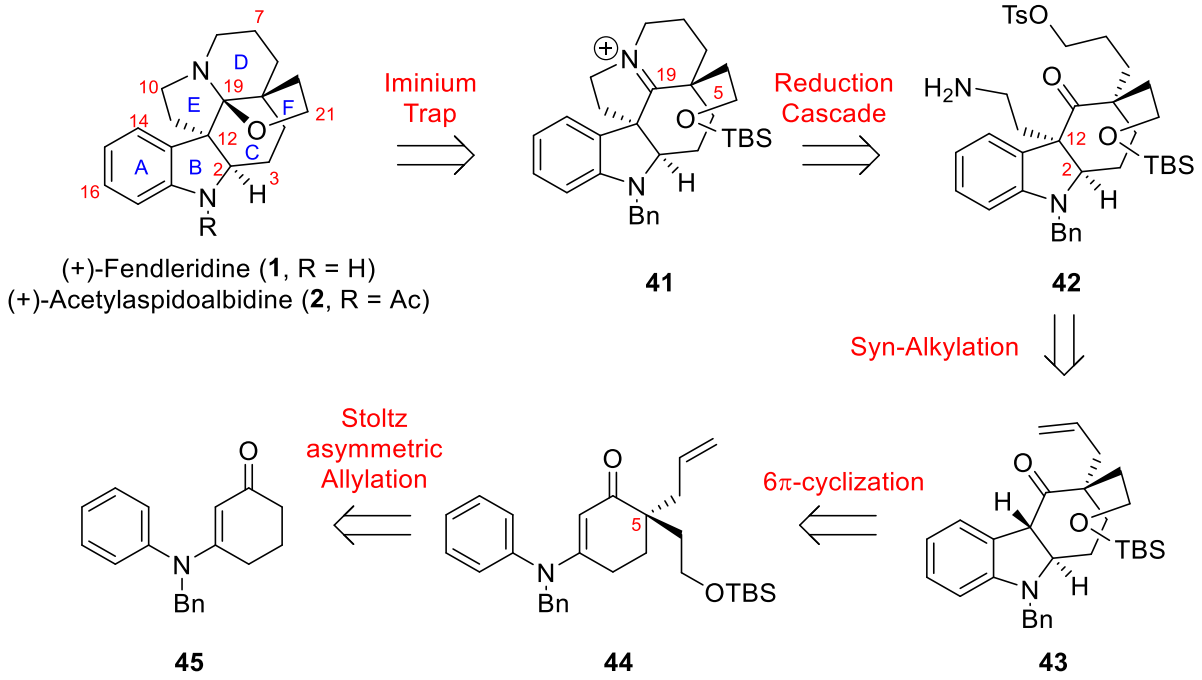

Scheme 1.9 Born & Ghosh Retrosynthesis of (+)-Fendleridine and (+)-Acetylaspidoalbidine.

1.5.2 Initial Attempts at Desymmetrization of the Quaternary Center

Our initial attempt at the synthesis of (+)-**1** and (+)-**2** are shown in Scheme 1.10. Our synthesis started with commercially available **45**, which if needed could also be made on a decagram scale in one step from very cheap starting materials (less than $1/gram)[24], but is also commercially available in kilogram quantities. Photocyclization of the material followed by alkylation produced the *syn*-alkylated material (±)-**46**. Allylation at this point however consistently resulted in diallylated product (±)-**47**, and multiple attempts to desymmetrize the material proved difficult. Thus, another route depicted in Scheme 1.11 was undertaken.

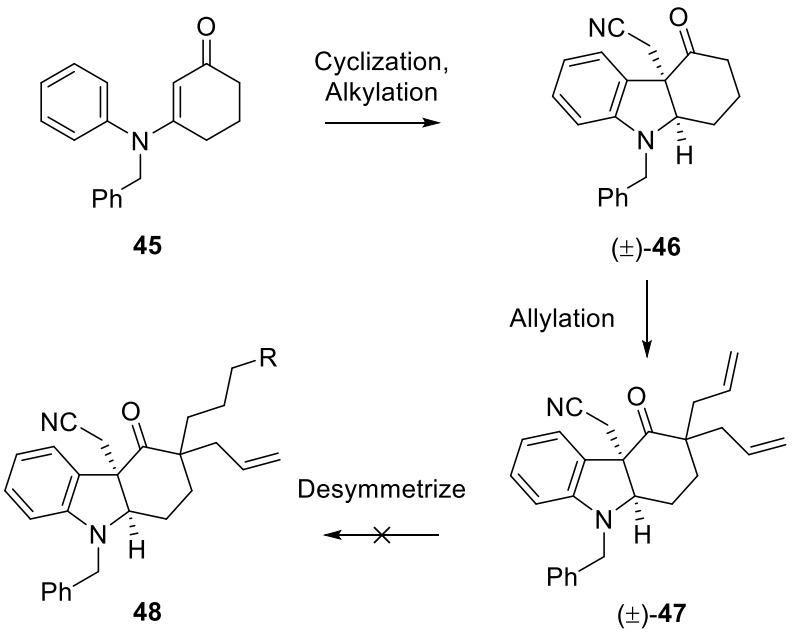

Scheme 1.10 Attempted Functionalization of Indoline (±)-**47**

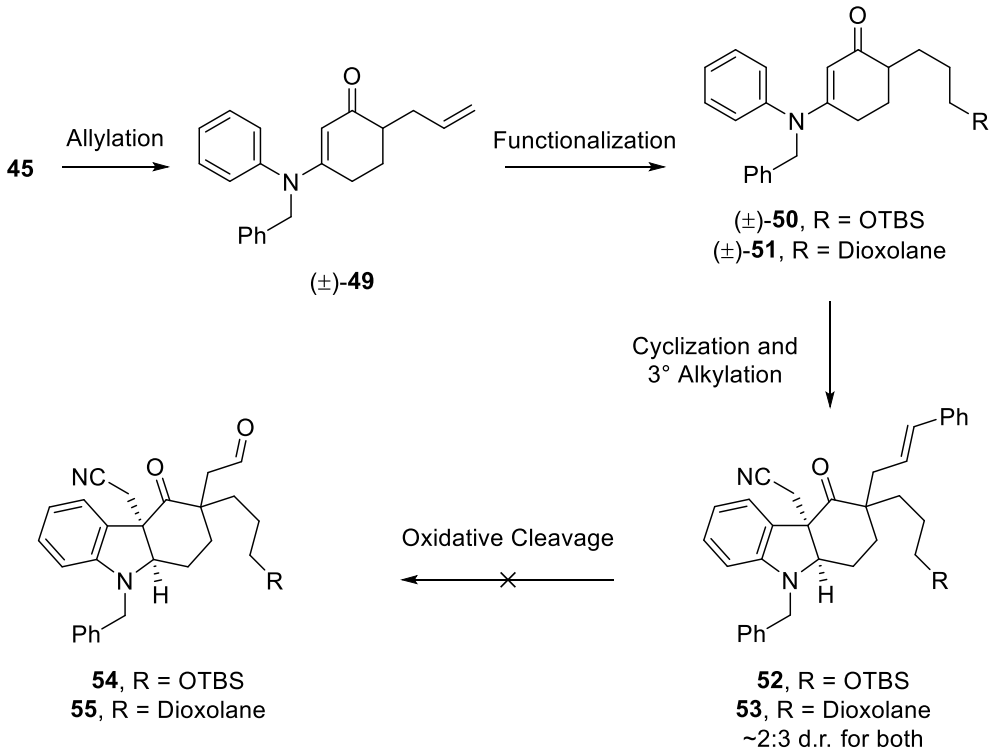

Scheme 1.11 Attempted Oxidative Cleavage of **52** & **53**

In this attempt, allylation of starting material **45** was undertaken, achieving the monoallylated material (±)-**49**. Functionalization of this material via hydroboration-oxidation followed by either protection of the alcohol as a silyl ether or oxidation and protection as a dioxolane group gave **50** and **51** respectively. Photocyclization and *syn*-alkylation followed by alkylation with cinnamyl bromide successfully formed the quaternary center in products **52** and **53**, albeit in poor d.r. (~2:3). Attempts to perform ozonolysis or dihydroxylation followed by oxidative cleavage to yield **54** or **55** proved unfruitful. It was at this point that we were inspired by the efforts of Stoltz in his enantioselective Tsuji allylation modification.[25]

1.5.3 Construction of Quaternary Center for Stoltz Allylation

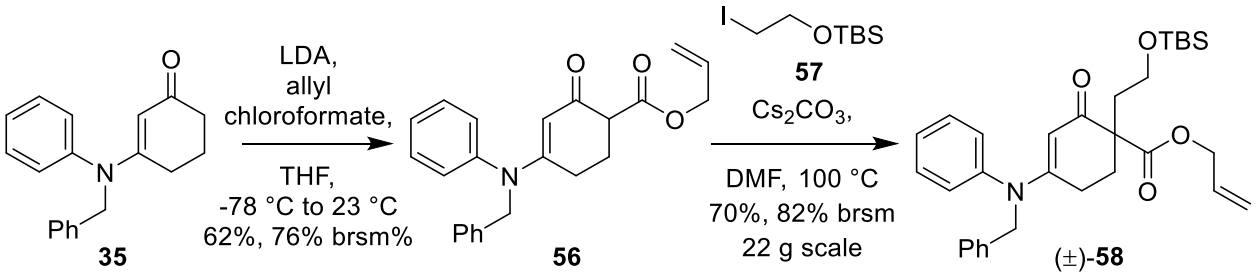

Scheme 1.12 Alkylation of Tertiary Center in **56**

Enaminone **35** was alkylated with allyl chloroformate using LDA at low temperature in THF to afford the dicarbonyl species **56** in 62%, 76% BRSM**,** avoiding the production of any dialkylated material (Scheme 1.12). Due to the alpha proton's much lower pKa, Cs_2CO_3 was able to perform the deprotonation of the difficult tertiary center by heating the reaction to 100°C in DMF, and upon addition of iodo silyl ether **57**, (±)-**58** was produced in 70% yield, 82% BRSM on a 22 gram scale. This species is now set up to undergo the Stoltz decarboxylative allylation.

1.5.4 Stoltz Decarboxylative Allylation

1.5.4.1 Proposed Mechanism

The Stoltz Decarboxylative Enantioselective Allylation was first described in by Stoltz and coworkers in 2004[25], as an expansion upon the seminal work done by Tsuji[26] and Trost[27]. Mechanistic support for this transformation was supported in 2012 by Goddard and Stoltz[28]. Upon heating, loss of CO_2 in alloxycarbonyl substrate (±)-**58** will result in an η^3-allyl palladium complex with chelation of the chiral ligand (**59**, Figure 1.4). Approach of the enolate **60** drives the allyl group to an η^1 complex, and thus the square planar Pd^{II} intermediate **61** exists. Insertion of the allyl moiety to the preferenced face of the enolate during reductive elimination is the reasoning behind the resulting stereoselectivity, resulting in our desired compound (-)-**44**.

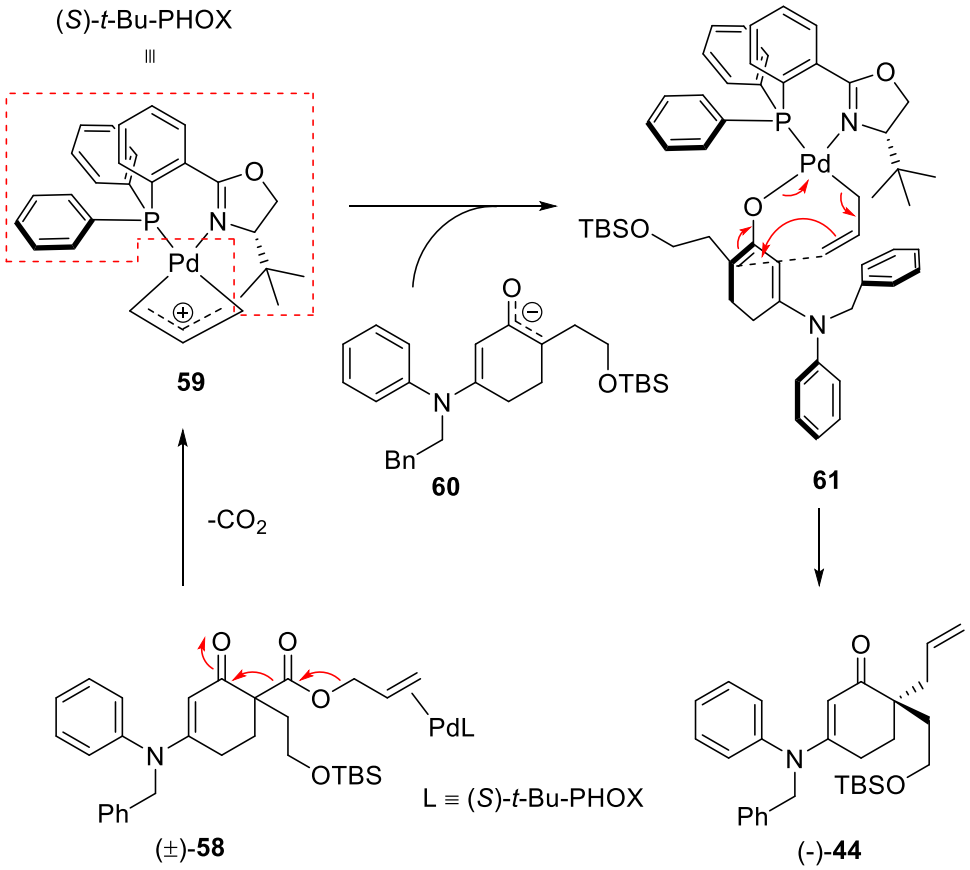

Figure 1.4 Proposed Mechanism of Our Stoltz Decarboxylative Enantioselective Allylation

1.5.4.2 Reaction Optimization and Determination of *ee*

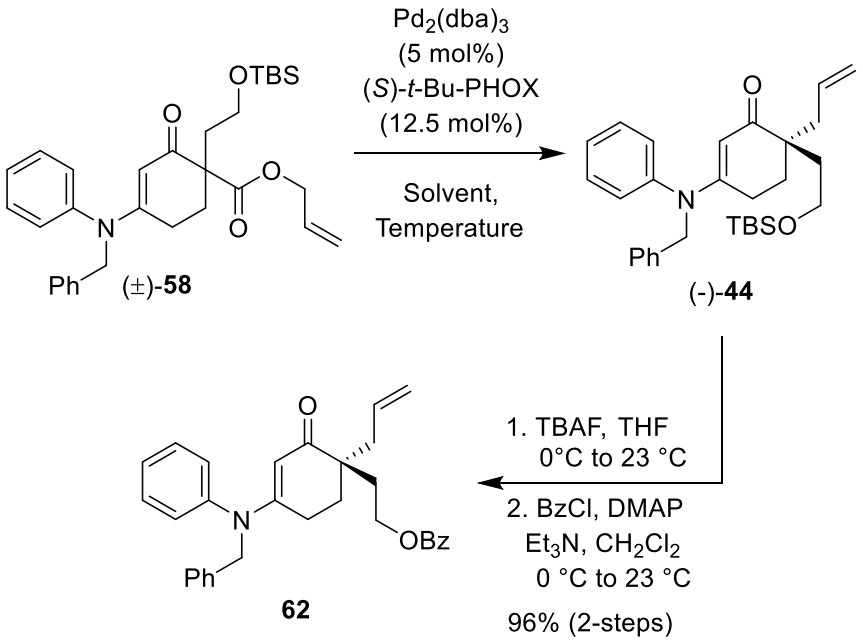

Scheme 1.13 Stoltz Decarboxylative Allylation Conditions and Transformation to **62** for Determination of %*ee*

Based on this hypothesis, (±)-**58** was subjected to Stoltz decarboxylation conditions, using 5 mol % tris(dibenzylidene acetone)dipalladium (0) as the catalyst and 12.5 mol % (*S*)-*t*-Bu-PHOX as the chiral ligand (Scheme 1.13). A small screening of the solvent influence on the reaction is shown in Table 1.1. If the solvent wasn't freshly degassed by bubbling argon through it for several hours beforehand, it led to trace amount of product formed, recovering majority of starting material along with the commonly seen dealkylated byproduct (first entry).[29] MTBE also proved to be insufficient in the transformation. THF, benzene, and toluene all provided near quantitative yields of (-)-**44** on a small scale. However, toluene was determined to give the best %*ee* in respect to **62**, and in the best yield on a multigram scale (last entry). **62** was made by deprotecting the silyl ether and protecting it as a benzoate, which was needed as it resolved more easily via chiral HPLC in order to determine the enantiomeric excess accurately. The yield of these two reactions were 96% over 2-steps. This 91:9 e.r. is reflective of the scarce examples of enaminone asymmetric allylations as reported by Stoltz and coworkers.[30] Traces of these chiral HPLCS are shown in Figure 1.5 through Figure 1.7.

Table 1.1 Screening of Solvent Effect in the Enantioselective Allylation

Solvent	Temp	Duration	Percent Yield of (-)-44	%ee of 62
Toluene[a]	70°C	12 h	Trace	N/A
MTBE	40°C	12 h	Trace	N/A
THF	70°C	30 min	97%	77%
Benzene	70°C	30 min	98%	81%
Toluene[b]	70°C	30 min	88%	82%

[a] Solvent not degassed. [b] Reaction carried out on multigram scale.

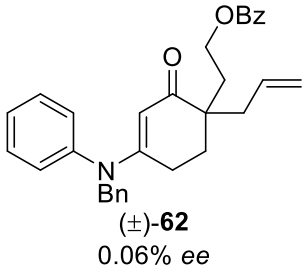

(±)-**62**
0.06% *ee*

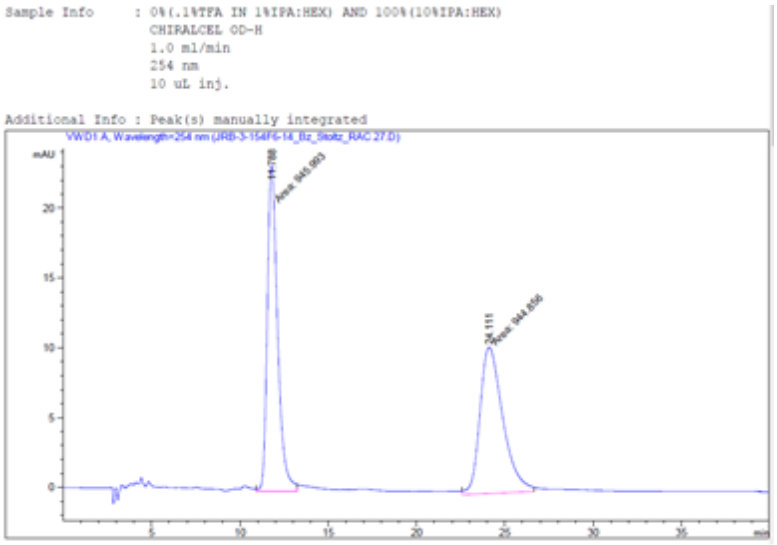

Signal 1: VWD1 A, Wavelength=254 nm

Peak #	RetTime [min]	Type	Width [min]	Area [mAU*s]	Height [mAU]	Area %
1	11.788	MM	0.6761	945.99347	23.31872	50.0301
2	24.111	MM	1.5055	944.85553	10.46018	49.9699

Figure 1.5 HPLC Trace of **62** Synthesized Racemically

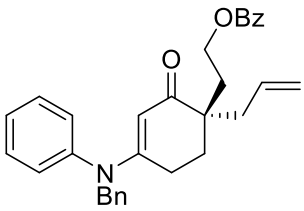

62 from Stoltz Allylation
in THF
76.5% *ee*

```
Sample Info     : 0.1%TFA in 10%IPA:Hex
                  CHIRALCEL OD-H
                  1.0  mL/min
                  254 nm
                  5 uL inj.

Additional Info : Peak(s) manually integrated
```

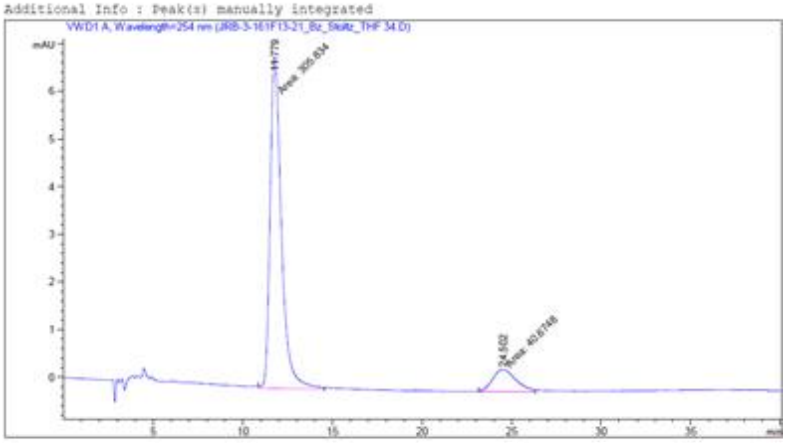

Signal 1: VWD1 A, Wavelength=254 nm

Peak #	RetTime [min]	Type	Width [min]	Area [mAU*s]	Height [mAU]	Area %
1	11.779	MM	0.7316	305.83365	6.96752	88.2615
2	24.502	MM	1.4758	40.67484	4.59342e-1	11.7385

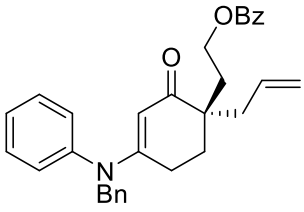

62 from Stoltz Allylation
in Benzene
80.5% *ee*

```
Sample Info     : 0.1%TFA in 10%IPA:Hex
                  CHIRALCEL OD-H
                  1.0  mL/min
                  254 nm
                  5 uL inj.

Additional Info : Peak(s) manually integrated
```

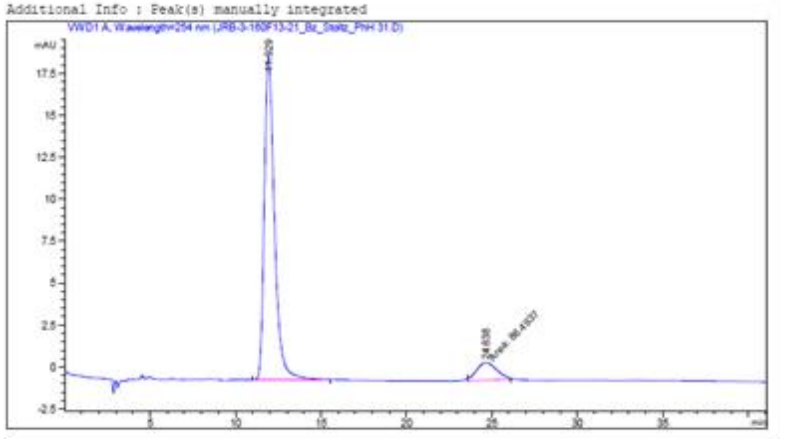

Signal 1: VWD1 A, Wavelength=254 nm

Peak #	RetTime [min]	Type	Width [min]	Area [mAU*s]	Height [mAU]	Area %
1	11.929	BB	0.6287	800.73853	19.27262	90.2513
2	24.638	MM	1.3742	86.49369	1.04900	9.7487

Figure 1.6 HPLC Traces of **62** from THF and Benzene Stoltz Allylations

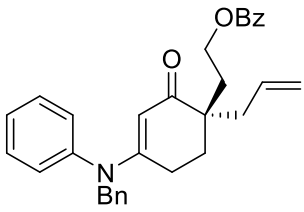

62 from Stoltz Allylation
in Toluene
81.7% *ee*

```
Sample Info      : 0%(.1%TFA IN 1%IPA:HEX) AND 100%(10%IPA:HEX)
                   CHIRALCEL OD-H
                   1.0 ml/min
                   254 nm
                   10 uL inj.

Additional Info : Peak(s) manually integrated
```

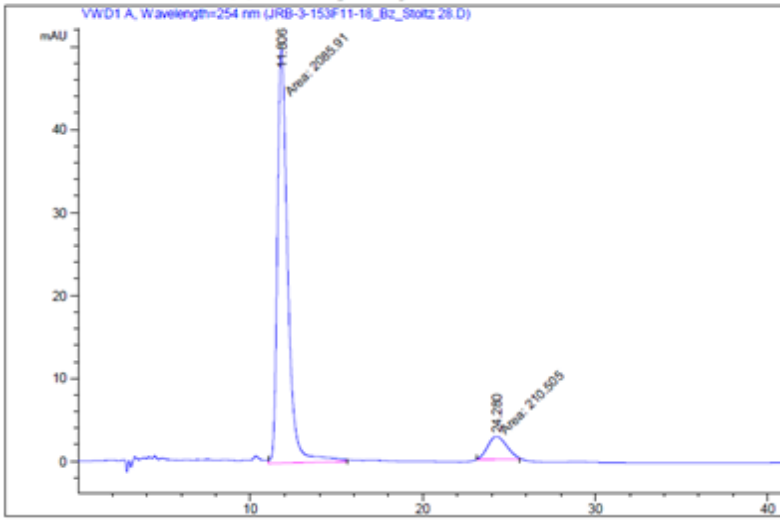

Signal 1: VWD1 A, Wavelength=254 nm

Peak #	RetTime [min]	Type	Width [min]	Area [mAU*s]	Height [mAU]	Area %
1	11.806	MM	0.6976	2085.91260	49.83364	90.8333
2	24.280	MM	1.2746	210.50478	2.75247	9.1667

Figure 1.7 HPLC Trace of **62** from Toluene Stoltz Allylation

1.5.5 6π—Conrotatory Photocyclization Mechanism

The 6π-photocyclization of *N*-phenyl enaminones to form indolines was pioneered by Gramain and coworkers in the 1980's and 90's.[31–33] Due to the presence of six pi electrons, Woodward-Hofmann[34] rules dictate a conrotatory mechanism, thus when **63** is introduced to 366 nm light the result is 1,3-dipole (±)-**64** (Figure 1.8). This intermediate would then rapidly undergo a hydride transfer to yield enantiomers (*S*,*R*)-**65** and (*R*,*S*)-**65**. While this basic mechanism was proposed, support as to whether the hydride transfer occurs via two consecutive [1,2]-transfers or a concerted suprafacial [1,4]-transfer was debated. It wasn't until very recently before our publication in 2019 that this was investigated by Bach and coworkers[35]. Via deuteration of the aniline ring, it's proposed that if the reaction were to go via two [1,2]-hydride migrations, the major product would be (±)-**69**. If it were to undergo the concerted [1,4]-migration, the major product would be (±)-**70**. When they performed the experiment with compound Boc-protected **71**, it was seen that (±)-**73** was the major product of the reaction, thus supporting the concerted suprafacial [1,4]-hydride migration.

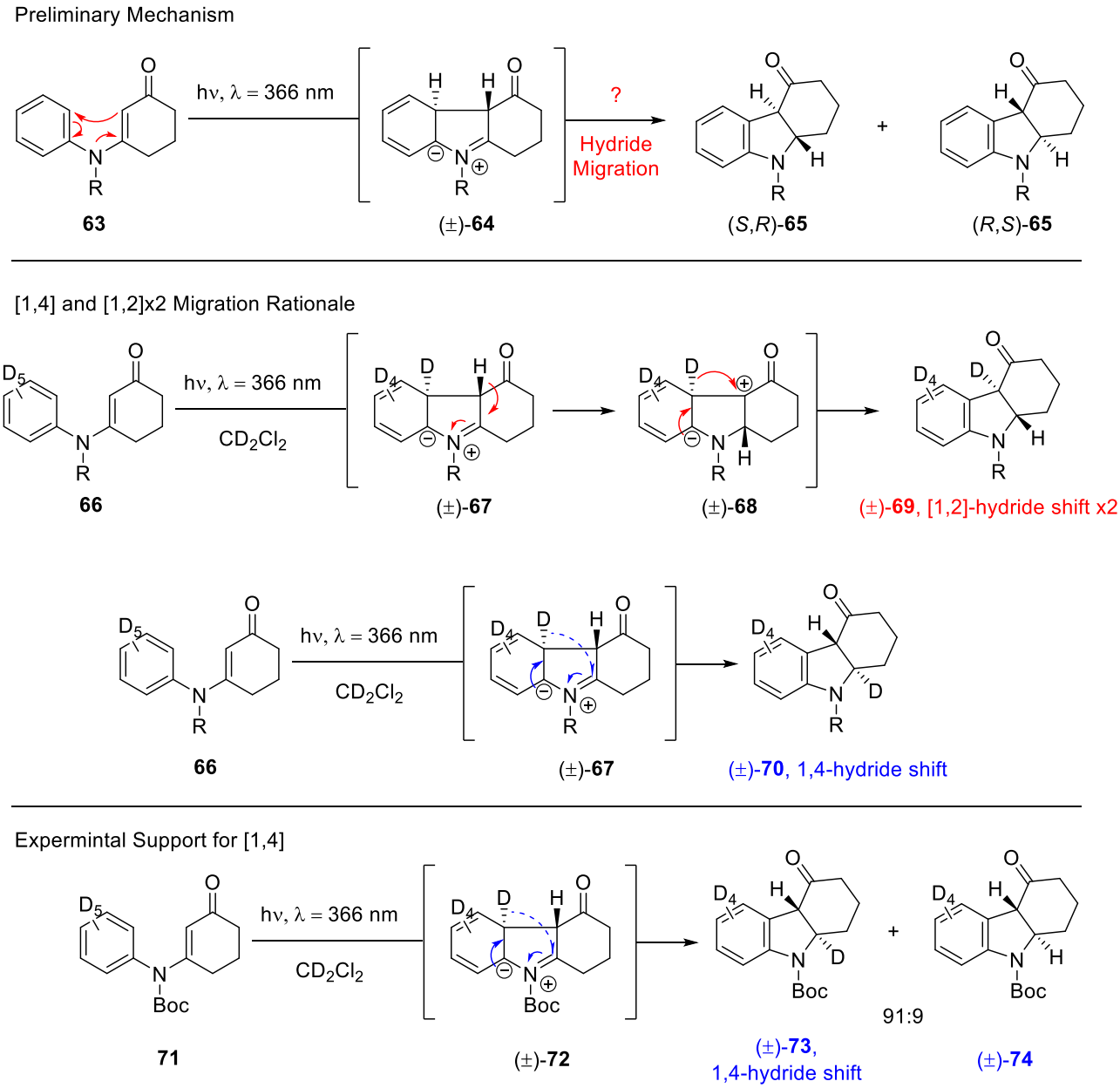

Figure 1.8 Mechanistic Support for the Photocyclization of *N*-Phenyl Enaminones

1.5.6 Synthesis of Alcohol Diastereomers

Thus, we undertook the photocyclization of our enantioenriched product (-)-**44**. Initial attempts to photocyclize the material utilizing a mercury lamp (450 W) in benzene as the solvent provided *trans*-diastereomeric indolines **75** and **76** along with corresponding indole byproduct **77** as an inseparable mixture (Scheme 1.14). Attempts to inhibit the formation of indole byproduct **77** via means of antioxidant additives, solvent variation, and concentration either didn't improve the ratio or resulted in no reaction. Instead, it was found that carefully degassing the apparatus by repeatedly evacuating and flushing the system with argon along with stopping the reaction before complete consumption of starting material yielded indolines **75** and **76** as the major products along with only trace indole **77**. The origin of **77** comes from indolines **75** and **76**'s proclivities to oxidize to the indole byproduct**.**[31,35] Thus to eliminate further formation of this byproduct, we submitted the diastereomers as a crude mixture for subsequent alkylation immediately. The crude mixture of **75** and **76** was subjected to KHMDS and bromoacetonitrile to yield *cis*-diastereomers **78** and **79** in 63% yield over two steps as an inseparable mixture.[31] These crude products were carried forward and subjected to hydroboration oxidation conditions using *in-situ* formed dicyclohexylborane to afford the alcohols **80** and **81** as a 1:1 mixture of diastereomers in 98% overall yield. The alcohols as suspected were seperable via column chromatography thus circumventing the use of late stage chiral HPLC and enzymatic resolution in our synthesis.

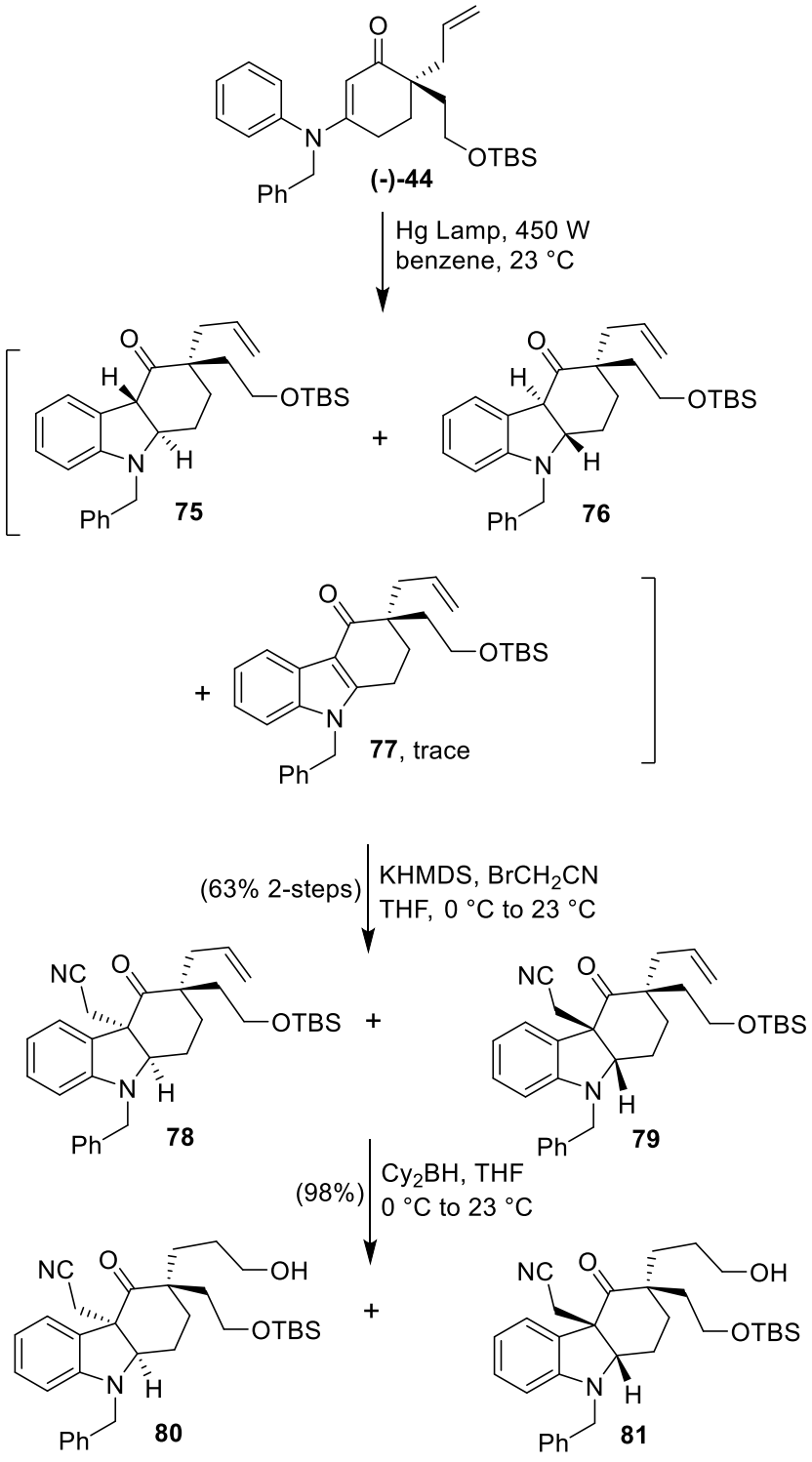

Scheme 1.14 Synthesis of Seperable Alcohol Diastereomers **80** and **81**

1.5.7 Synthesis of Ketals for 2D NMR Studies

The alcohols **80** and **81** were characterized via ^{1}H and ^{13}C NMR, however their absolute identities initially remained a mystery pertaining to their C2 and C12 configuration. Initial 2D NMR showed one plausible interaction supporting the identity of **81**, however more support was needed as the theorized interaction through space didn't appear plausible, and the expected interactions didn't occur (Scheme 1.15). We hypothesized that constructing a more rigid bicyclic system to constrain protons in space would promote the observations of the desired NOESY interactions. To this end, we carried forth both reactions separately and tosylated the free alcohols, leading to compounds **82** and **83** in 79% and 85% respectively. TBAF deprotection then resulted in the free alcohol cyclizing onto the carbonyl, and the resultant alkoxide cyclizing onto the tosylated carbon, creating the rigid pentacyclic ketals **84** and **85** in near quantitative yields. With this rigidity set, we theorized that we would now observe the suspected interactions with the alpha nitrile protons to the front or back rings. To our surprise we did not, and instead observed more interactions with the sp^2 hybridized phenyl carbon. We theorize that due to the folding of the molecules from the *cis* relationships of the C2 and C12 substituents, the ring is then brought in close proximity with either the front THF ring (ketal **85**, derived from alcohol **81**) or the back THP ring (ketal **84**, derived from **80**). Thus, our initial observation for the suspected absolute identity of **81** was supported, and we assigned alcohol **80** as the desired diastereomer.

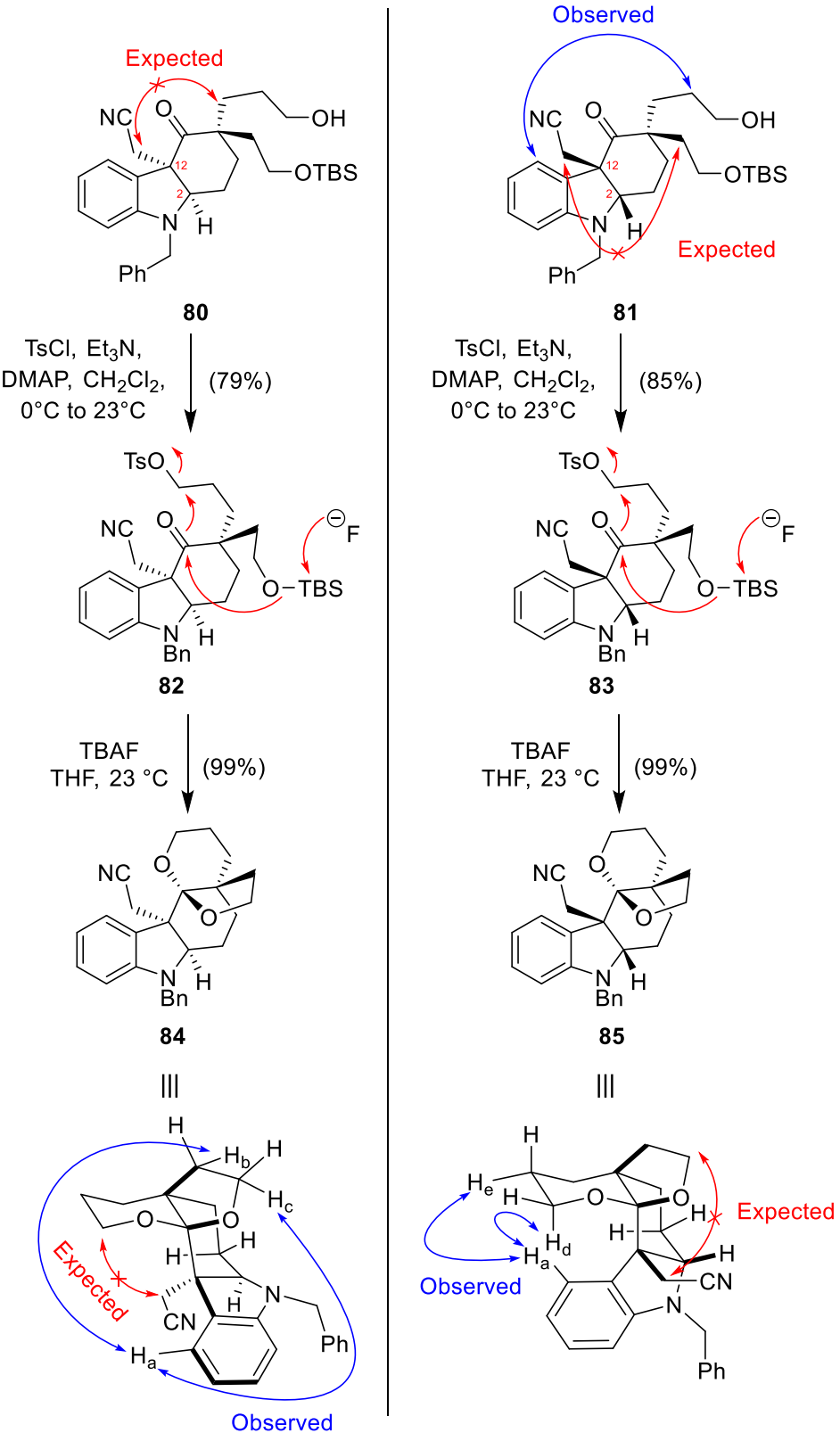

Scheme 1.15 Synthesis of Ketals for Absolute Characterization of Alcohols **80** and **81**

1.5.8 Synthesis of Imine for Characterization Support

Based on our new stereochemical assignments, we theorized that if we were to carry forward the undesired tosylate **83** over the next planned cascade step, the iminium ion wouldn't form due to the intermediate imine nitrogen of **86** not being in proximity to the tosylate carbon (Scheme 1.16). However, with our desired tosylate **82** it would. This was supported by subjecting undesired tosylate **83** to Raney Nickel under an H_2 pressurized atmosphere, resulting in imine **86** in 91% yield.

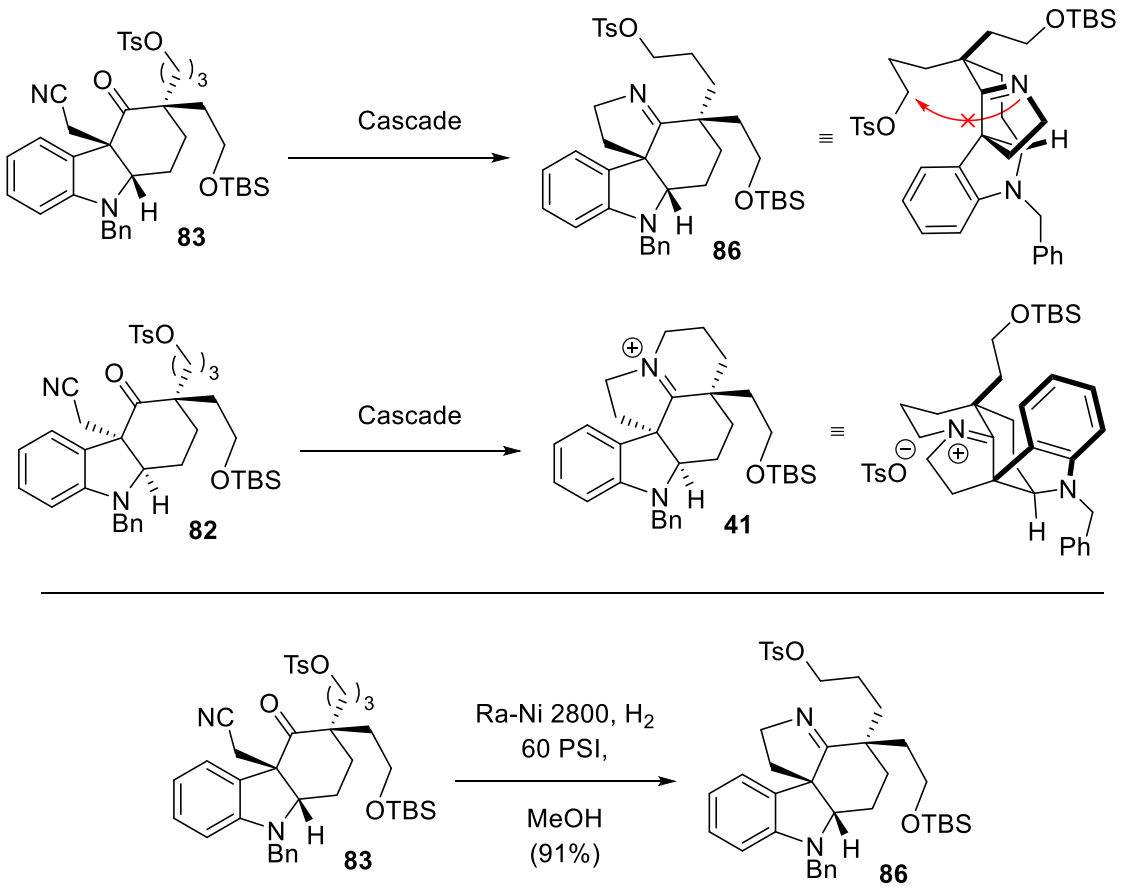

Scheme 1.16 Corroboration of Stereochemical Assignments via Chemical Transformation

1.5.9 Attempts at Full Cascade Reaction to Achieve (+)-Fendleridine

With the desired tosylate **82** in hand, we theorized that in one step we would be able to achieve (+)-Fendleridine (**1**). We proposed that use of a catalyst under a pressurized H_2 atmosphere would reduce the nitrile, concomitantly cyclize onto the ketone, and further cyclize to form the iminium ion **41** (Scheme 1.17). From here, it's been shown that some silyl groups are prone to deprotection under hydrogenation conditions,[36,37] and thus the resultant alcohol would cyclize onto the iminium ion carbon to form the hemiaminal ether **87**. Finally, the reduction of the *N*-benzyl group could theoretically be accomplished in the same pot to achieve (+)-**1**.

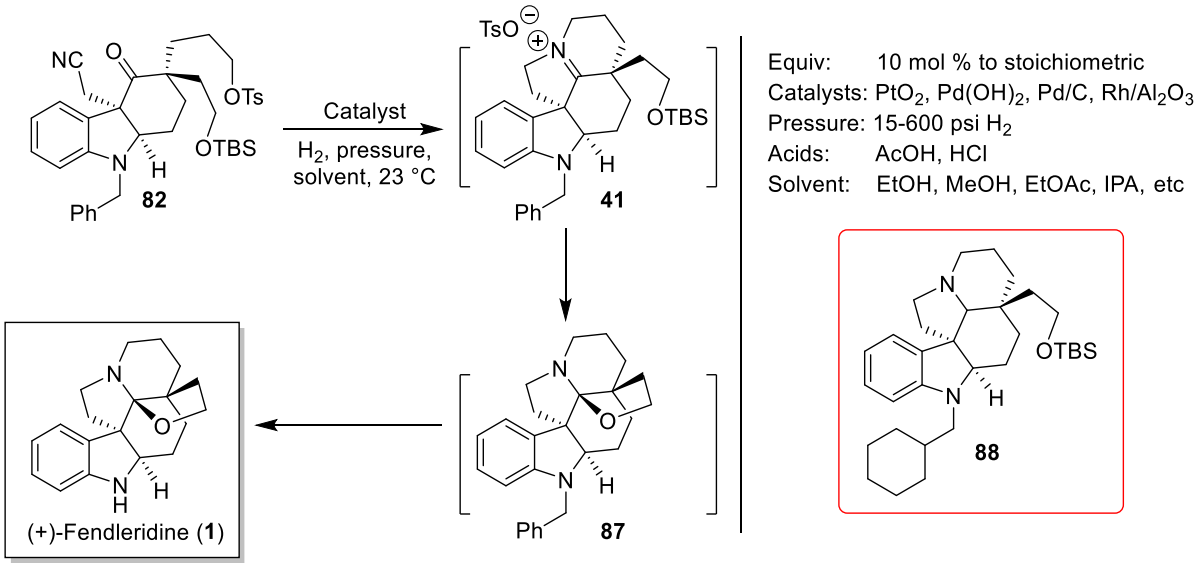

Scheme 1.17 Attempted Full Cascade from Tosylate **82** to (+)-**1** and Interesting Byproduct **88**.

Many attempts were made at this transformation. The use of palladium on carbon, Pearlman's and Adam's catalyst, and rhodium on alumina were all varied in 10 mol % to stoichiometric amounts of loading. Addition of acids to activate the catalysts *in situ* was also tried, along with pressure screening from 1 atmosphere to 600 psi. Finally, solvent variation (EtOAc, MeOH, IPA, etc) was tried to promote said hydrogenations. Unfortunately, it was observed that the desired transformations didn't occur, with either the starting material **82** unreacting or fully degrading in some instances. Interestingly, the use of Adam's catalyst at increased pressures appeared to reduce the phenyl ring of the *N*-benzyl moiety down to a cyclohexyl before removal of the silyl ether or full *N*-benzyl deprotection (Structure **88**).

1.5.10 Synthesis of (+)-Fendleridine and (+)-Acetylaspidoalbidine

With the above results observed, we elected to finish our synthesis of **1** in a stepwise fashion (Scheme 1.18). Submission of the desired tosylate **82** to catalytic reduction provided the crude iminium ion **41** as theorized. Subjecting this material to TBAF deprotection resulted in the hemiaminal ether **87** in 62% over two steps. It's worth noting that purification of this step was initially difficult, as the hemiaminal ether appeared to degrade on the slightly acidic silica. Use of alumina columns on this material and the subsequent natural products however afforded the desired substrates cleanly. Finally, the debenzylation of **87** was attempted. It became apparent that the material quickly degraded using traditional palladium catalysts and methods like those described in Chapter 1.5.9. Therefore a 1-electron Birch reduction process was used and afforded (+)-**1** in 70% yield. The difficulty in this final debenzylation step provides insight as to why our initial full cascade reaction attempts were unfruitful.

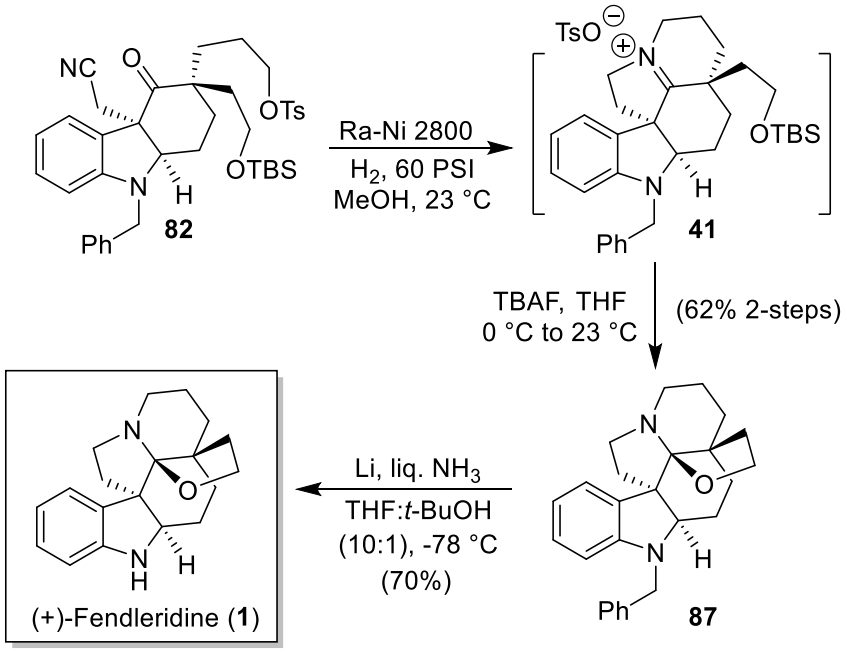

Scheme 1.18 Synthesis of (+)-Fendleridine (**1)**

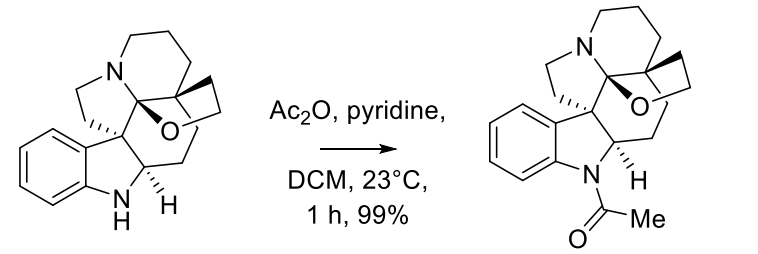

(+)-Fendleridine (**1**) (+)-Acetylaspidoalbidine (**2**)

Scheme 1.19 Synthesis of (+)-Acetylaspidoalbidine (**2**)

Acetylation using standard conditions were carried out to yield (+)-Acetylaspidoalbidine (**2**) in near quantitative yield (Scheme 1.19). A minor rotamer was observed as has been suggested in the literature,[1,2] however, no variable temperature experiments had been done before to support this claim. Thus, we heated our sample up to 55°C and ^{1}H NMR was taken, observing coalesced peaks within the sample (Figure 1.9). Cooling the sample back to ambient temperature also supported that no degradation/side reaction occurred, supporting the presence of this rotamer.

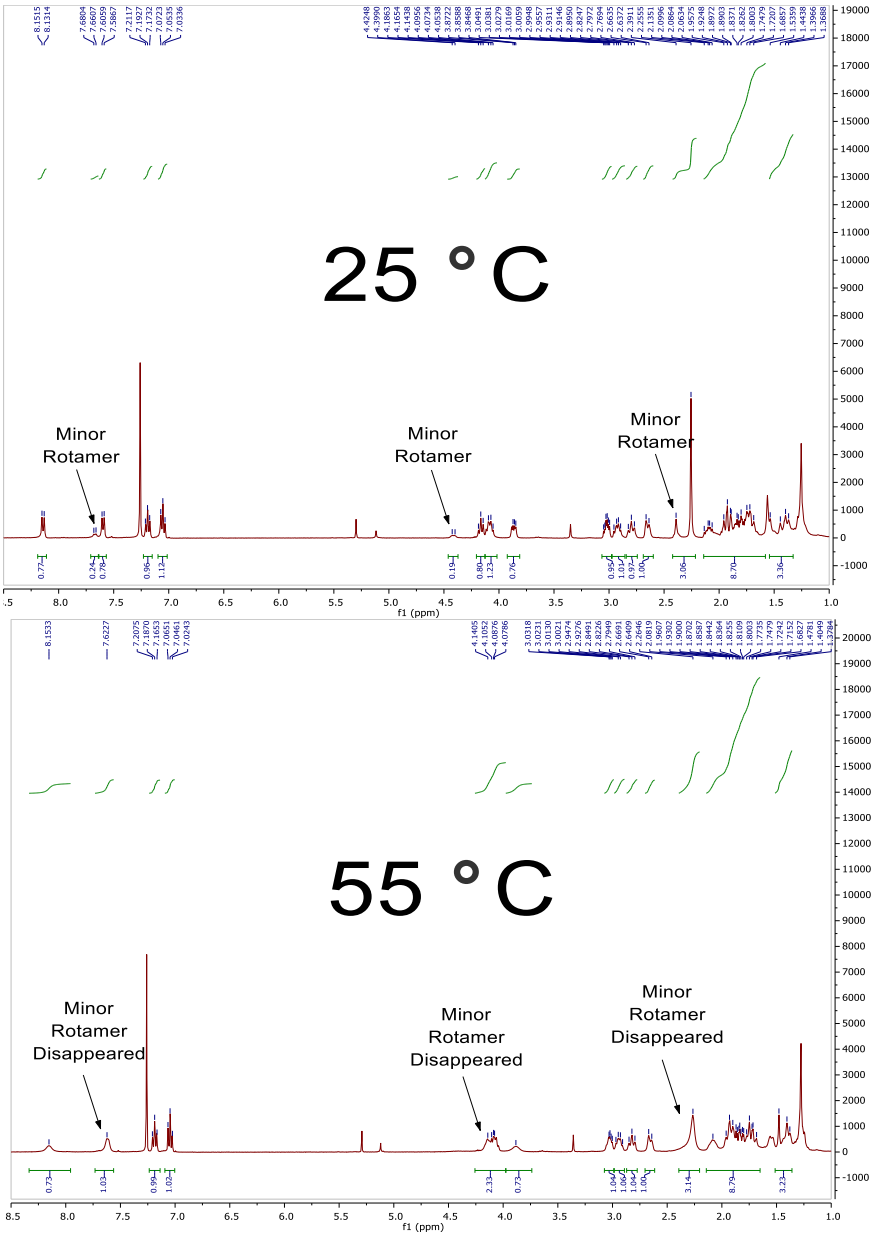

Figure 1.9 Variable Temperature Experiments in the Support of (+)-**2** and Minor Rotamer

1.5.11 Comparison with Prior Literature

With the synthesis completed, we underwent comparative NMR and rotational data. In Table 1.2, our ^{1}H data matched up closely with that of the priorly reported. However, the indoline proton appears to have been misassigned within Boger's supporting information, and ours agrees more with Movassaghi's synthesis[1,2].

Table 1.2 (+)-(**1**) ^{1}H NMR Comparison with Prior Literature ($CDCl_3$)

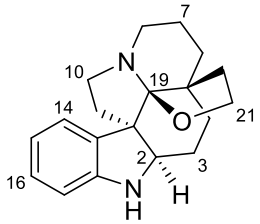

Assignment	Boger 600 MHz	Movassaghi 400 MHz, 25°C	This Work 800 MHz, 25°C
N1	5.90 (bs, 1H)	3.50 (bs, 1H)	3.52 (bs, 1H)
C2	3.40 (dd, *J* = 9.1, 4.8 Hz, 1H)	3.40 (dd, *J* = 8.9, 5.1 Hz, 1H)	3.40 (dd, *J* = 9.5, 4.8 Hz, 1H)
C3	1.92–1.66 (m, 2H)	2.00–1.55 (m, 2H)	1.91-1.60 (m, 2H)
C4	1.92–1.66 (m, 1H) 1.35 (d, *J* = 13.1 Hz, 1H)	2.00–1.55 (m, 1H) 1.36 (d, *J* = 12.6 Hz, 1H)	1.91-1.60 (m, 1H) 1.35 (d, *J* = 13.0 Hz, 1H)
C5	-	-	-
C6	1.92–1.66 (m, 1H) 1.45 (dt, *J* = 13.6, 4.4 Hz, 1H)	2.00–1.55 (m, 1H) 1.46 (dt, *J* = 13.6, 4.6 Hz, 1H)	1.91-1.60 (m, 1H) 1.45 (dt, *J* = 13.8, 4.8 Hz, 1H)
C7	1.92–1.66 (m, 1H) 1.52 (dd, *J* = 7.7, 4.6 Hz, 1H)	2.00–1.55 (m, 1H) 1.52 (dt, *J* = 11.8, 3.3 Hz, 1H)	1.91-1.60 (m, 1H)1.51 (dt, *J* = 12.1, 3.2 Hz, 1H)
C8	2.79 (td, *J* = 11.5, 2.6 Hz, 1H) 2.65 (d, *J* = 11.4 Hz, 1H)	2.79 (t, *J* = 10.8 Hz, 1H) 2.65 (d, *J* = 10.3 Hz, 1H)	2.79 (t, *J* = 11.4 Hz, 1H) 2.65 (d, *J* = 11.1 Hz, 1H),
C10	3.01 (td, *J* = 8.7, 4.3 Hz, 1H) 2.92 (dt, *J* = 14.6, 7.3 Hz, 1H)	3.01 (ddd, *J* = 9.4, 8.1, 4.3 Hz, 1H) 2.93 (ddd, *J* = 10.1, 8.2, 6.2 Hz, 1H)	3.00 (td, *J* = 8.7, 4.1 Hz, 1H) 2.92 (dt, *J* = 15.6, 8.2 Hz, 1H)
C11	2.25 (ddd, *J* = 15.0, 9.1, 6.3 Hz, 1H) 1.92–1.66 (m, 1H)	2.25 (ddd, *J* = 13.3, 8.7, 5.9 Hz, 1H) 2.00–1.55 (m, 1H)	2.24 (ddd, *J* = 13.4 8.7, 5.9 Hz, 1H) 1.91-1.60 (m, 1H)
C12	-	-	-
C13	-	-	-
C14	7.46 (d, *J* = 7.8 Hz, 1H)	7.45 (d, *J* = 7.5 Hz, 1H)	7.45 (d, *J* = 7.5 Hz, 1H)
C15	6.73 (t, *J* = 7.2 Hz, 1H)	6.73 (app-t, *J* = 7.6 Hz, 1H)	6.73 (t, *J* = 7.5 Hz, 1H)
C16	7.01 (t, *J* = 7.8 Hz, 1H)	7.01 (app-t, *J* = 7.5 Hz, 1H)	7.01 (t, *J* = 7.6 Hz, 1H)
C17	6.61 (d, *J* = 7.8 Hz, 1H)	6.60 (d, *J* = 7.9 Hz, 1H)	6.60 (d, *J* = 7.7 Hz, 1H)
C18	-	-	-
C19	-	-	-
C20	1.92–1.66 (m, 1H) 1.25 (d, *J* = 5.4 Hz, 1H)	2.00–1.55 (m, 1H) 1.25 (ddd, *J* = 12.0, 5.4, 1.8 Hz, 1H)	1.91-1.60 (m, 1H) 1.24 (dd, *J* = 11.9, 5.5 Hz, 1H)
C21	4.01–3.98 (m, 2H)	4.05–3.91 (m, 2H)	4.03 – 3.95 (m, 2H)

Table 1.3 (+)-(**1**) ^{13}C NMR Comparison with Prior Literature ($CDCl_3$)

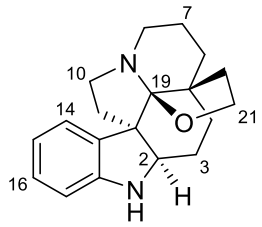

Assignment	Boger 150 MHz	Movassaghi 100 MHz, 25°C	This Work 200 MHz, 25°C	Δδ = δ (this work)–δ (Boger Report)	Δδ = δ (this work)–δ (Movassaghi Report)
C2	66.3	66.6	66.6	0.3	0.0
C3	27.0	27.3	27.3	0.3	0.0
C4	33.9	34.1	34.1	0.2	0.0
C5	39.1	39.2	39.2	0.1	0.0
C6	26.8	27.0	27.0	0.2	0.0
C7	21.3	21.5	21.5	0.2	0.0
C8	43.9	44.1	44.1	0.2	0.0
C10	49.1	49.3	49.3	0.2	0.0
C11	35.6	37.0	37.0	1.4	0.0
C12	58.8	59.0	58.9	0.1	0.1
C13	134.4	134.5	134.4	0.0	0.1
C14	125.9	126.1	126.1	0.2	0.0
C15	119.3	119.5	119.4	0.1	0.1
C16	127.1	127.3	127.3	0.2	0.0
C17	109.9	110.0	110.0	0.1	0.0
C18	150.0	150.3	150.3	0.3	0.0
C19	101.9	102.1	102.1	0.2	0.0
C20	35.7	35.8	35.8	0.1	0.0
C21	64.8	64.9	64.9	0.1	0.0

Table 1.4 (+)-(**2**) ^{1}H NMR Comparison of Isolation and Boger ($CDCl_3$)

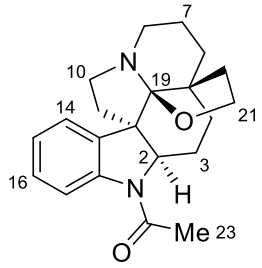

Assignment	Zeches-Hanrot's Isolation 300 MHz	Boger 600 MHz
C2	3.85 (dd, *J* = 10.6, 5.8 Hz, 1H)	3.86 (dd, *J* = 10.9, 5.1 Hz, 1H)
C3	2.1–1.6	2.1–1.6
C4	2.1–1.6, 1.45 (dt, *J* = 13.7, 3.5 Hz, 1H)	1.99–1.66 (m, 1H), 1.43 (dt, *J* = 13.9, 3.3 Hz, 1H)
C5	-	-
C6	2.1–1.6 (m, 1H), 1.35 (br-d, *J* = 8.0 Hz, 1H)	1.99-1.66 (m, 1H), 1.38 (br d, *J* = 11.4 Hz, 1H)
C7	1.55 (m, 1H)	1.55 (dd, *J* = 12.1 Hz, 1H)
C8	2.8 (td, *J* = 8.5, 4.3 Hz, 1H), 2.6 (m, 1H)	2.79 (t, *J* = 9.6 Hz, 1H), 2.65 (d, *J* = 10.8 Hz, 1H)
C10	3.0 (td, *J* = 8.5, 4.3 Hz, 1H), 2.9 (m, 1H)	3.02 (td, *J* = 8.7, 4.2 Hz, 1H), 2.92 (dd, *J* = 15.4, 9.1 Hz, 1H)
C11	2.1–1.6 (m, 1H)	2.13–2.06 (m, 1H)
C12	-	-
C13	-	-
C14	8.1 (dd, *J* = 7.7, 1.3 Hz, 1H)	8.14 (d, *J* = 8.0 Hz, 1H)
C15	7.1 (td, *J* = 7.7 Hz, 1H)	7.05 (t, *J* = 7.5 Hz, 1H)
C16	7.2 (td, *J* = 7.7, 1.3 Hz, 1H)	7.19 (t, *J* = 7.7 Hz, 1H)
C17	7.6 (dd, *J* = 7.7, 1.3 Hz, 1H)	7.59 (d, *J* = 7.6 Hz, 1H)
C18	-	-
C19	-	-
C20	2.1–1.6 (m, 2H)	1.99–1.66 (m, 2H)
C21	4.15 (t, *J* = 10.8 Hz, 1H), 4.05 (ddd, *J* = 10.8, 8.2, 6.0 Hz, 1H)	4.16 (t, *J* = 8.5 Hz, 1H), 4.08 (dd, *J* = 8.5 Hz, 1H)
C22	-	-
C23	2.3 (s, 3H)	2.25 (s, 3H)

Table 1.5 (+)-(**2**) ^{1}H NMR Comparison of Movassaghi and Born ($CDCl_3$)

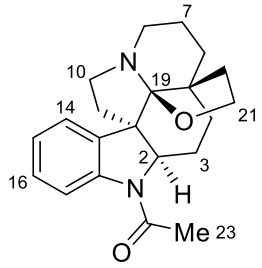

Assignment	Movassaghi 400 MHz, 25°C	This Work 800 MHz, 25°C
C2	3.86 (dd, *J* = 10.9, 5.1 Hz, 1H)	3.86 (dd, *J* = 11.0, 5.2 Hz, 1H)
C3	1.99–1.64 (m, 2H)	1.96-1.70 (m, 2H)
C4	1.99–1.64 (m, 1H), 1.46–1.30 (m, 1H)	1.96-1.70 (m, 1H) 1.43 (dt, *J* = 14.0, 3.9 Hz, 1H)
C5	-	-
C6	1.99–1.64 (m, 1H) 1.46–1.30 (m, 1H)	1.96-1.70 (m, 1H) 1.38 (d, *J* = 12.9 Hz, 1H)
C7	1.99–1.64 (m, 1H) 1.62–1.46 (m, 1H)	1.96-1.70 (m, 1H) 1.55 (dt, *J* = 12.7, 3.6 Hz, 1H)
C8	2.80 (t, *J* = 9.8 Hz, 1H) 2.65 (d, *J* = 10.9 Hz, 1H)	2.80 (td, *J* = 11.5, 2.8 Hz, 1H) 2.65 (d, *J* = 10.7 Hz, 1H),
C10	3.02 (td, *J* = 8.8, 4.2 Hz, 1H) 2.98–2.86 (m, 1H)	3.02 (td, *J* = 8.8, 4.1 Hz, 1H) 2.93 (dd, *J* = 15.7, 9.0 Hz, 1H)
C11	2.10 (ddd, *J* = 14.4, 9.1, 5.9 Hz, 1H) 1.99–1.64 (m, 1H)	2.10 (ddd, *J* = 14.6, 9.1, 6.1 Hz, 1H) 1.96-1.70 (m, 1H)
C12	-	-
C13	-	-
C14	7.60 (d, *J* = 7.7 Hz, 1H)	7.60 (d, *J* = 7.7 Hz, 1H)
C15	7.05 (app-td, *J* = 7.4, 1.1 Hz, 1H)	7.05 (t, *J* = 7.5 Hz, 1H)
C16	7.19 (app-t, *J* = 7.8 Hz, 1H)	7.19 (t, *J* = 7.7 Hz, 1H)
C17	8.14 (d, *J* = 8.0 Hz, 1H)	8.14 (d, *J* = 8.0 Hz, 1H)
C18	-	-
C19	-	-
C20	1.99–1.64 (m, 1H) 1.30–1.18 (m, 1H)	1.96-1.70 (m, 1H) 1.27 (m, 1H).
C21	4.17 (t, *J* = 8.6 Hz, 1H) 4.09 (dt, *J* = 11.1, 7.6 Hz, 1H)	4.16 (t, *J* = 8.6 Hz, 1H) 4.09 (dt, *J* = 10.5, 7.5 Hz, 1H)
C22	-	-
C23	2.26 (s, 3H)	2.26 (s, 3H)

Table 1.6 (+)-(**2**) ^{13}C NMR Comparison of Boger & Born ($CDCl_3$)

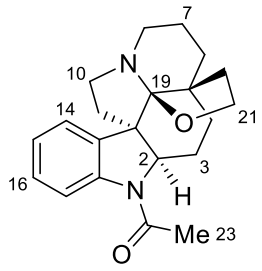

Assignment	Boger 150 MHz	This Work 200 MHz, 25°C	Δδ = δ (this work)– δ (Boger Report)
C2	68.8	69.0	0.2
C3	25.3	25.5	0.2
C4	33.0	33.2	0.2
C5	39.6	39.8	0.2
C6	26.4	26.6	0.2
C7	21.0	21.2	0.2
C8	43.9	44.1	0.2
C10	48.9	49.1	0.2
C11	37.1	37.3	0.2
C12	58.2	58.4	0.2
C13	137.8	137.9	0.1
C14	124.8	124.9	0.1
C15	124.7	124.8	0.1
C16	127.3	127.5	0.2
C17	117.8	117.9	0.1
C18	141.1	141.2	0.1
C19	102.0	102.2	0.2
C20	34.6	34.9	0.3
C21	65.0	65.1	0.1
C22	168.1	168.2	0.1
C23	23.4	23.5	0.1

Table 1.7 (+)-(**2**) ^{13}C NMR Comparison of Movassaghi & Born ($CDCl_3$)

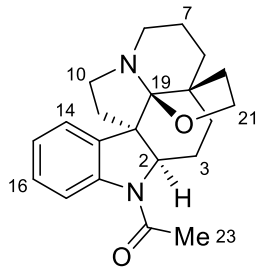

Assignment	Movassaghi 125MHz, 25°C	This Work 200 MHz, 25°C	Δδ = δ (this work)–δ (Movassaghi Report)	Movassaghi Minor Rotamer, 125MHz, 25°C	This Work Minor Rotamer, 200 MHz, 25°C	Δδ = δ (this work)–δ (Movassaghi Report)
C2	68.9	69.0	0.1	67.0	67.1	0.1
C3	25.5	25.5	0.0	24.3	24.4	0.1
C4	33.2	33.2	0.0	33.4	33.5	0.1
C5	39.8	39.8	0.0	39.6	39.6	0.0
C6	26.5	26.6	0.1	26.7	26.8	0.1
C7	21.2	21.2	0.0	-	21.2	N/A
C8	44.0	44.1	0.1	44.0	43.9	0.1
C10	49.0	49.1	0.1	48.9	48.9	0.0
C11	37.2	37.3	0.1	36.9	37.0	0.1
C12	58.3	58.4	0.1	57.2	57.2	0.0
C13	137.9	137.9	0.0	-	140.1	N/A
C14	124.9	124.9	0.0	126.1	126.1	0.0
C15	124.8	124.8	0.0	124.3	124.3	0.0
C16	127.5	127.5	0.0	127.1	127.1	0.0
C17	117.9	117.9	0.0	115.1	115.1	0.0
C18	141.2	141.2	0.0	-	140.6	N/A
C19	102.1	102.2	0.1	102.5	102.5	0.0
C20	34.8	34.9	0.1	35.1	35.2	0.1
C21	65.1	65.1	0.0	65.0	65.0	0.0
C22	168.2	168.2	0.0	168.0	168.0	0.0
C23	23.5	23.5	0.0	23.7	23.8	0.1

In Table 1.3 through Table 1.7, it's shown again that our data matches closely with the reported values. Of note, we are the first to fully characterize the minor rotamer found in (+)-**2**. Pertaining to carbons C7, C13, & C18, previously reported data didn't assign corresponding signals. It is our belief the C7 minor rotamer signal overlays the major rotamer signal (δ 21.2). As for C13 and C17 we've assigned our own minor rotamer signals, likely not appearing in the previously reported data due to lower S/N. With regards to the optical rotation found in our synthesis $[\alpha]_D^{20}$: + 30.2 (c, 0.15, $CHCl_3$), it matches quite closely to that of the past two synthetic samples by Boger and coworkers[1] $[\alpha]_D^{24}$: +38 (c = 0.2, $CHCl_3$), and Whïte and Movassaghi[2] $[\alpha]_D^{24}$: +39 (c = 0.18, $CHCl_3$). However, two known optical rotations are known to exist for naturally isolated (+)-Acetylaspidoalbidine. $[\alpha]_D$: +1° (c 0.2, $CHCl_3$) was found by Mitaine and coworkers,[15] as well as $[\alpha]_D^{15}$: + 46° ($CHCl_3$) by Djerassi and coworkers.[38]

1.6 Conclusion

In summary, we have accomplished a concise stereoselective total synthesis of (+)-Fendleridine and (+)-Acetylaspidoalbidine. Our overall synthetic scheme is summarized in Scheme 1.20. These syntheses were completed in 10 and 11-steps from commercially available starting material, significantly cutting down the enantioselective synthetic routes proposed previously[1,2]. Highlights of this synthesis include a multi-gram scale Stoltz decarboxylative enantioselective allylation, 6-π conrotatory photocyclization of the enantioenriched hexahydrocarbazolone ring system, and a Ra-Ni catalyzed cascade reaction to form the pentacyclic iminium structure followed by collapse of a resultant alcohol to construct the hexacyclic hemiaminal ether with 4 contiguous stereocenters. Synthesis of two diastereomeric alcohols allowed for simple flash chromatographic separation of the isomers and circumvented the need for late stage chiral HPLC[1] and enzymatic resolution.[2] Detailed 2D NMR and chemical transformations were used to support the absolute identity of a key desired intermediate. VT NMR was also used to identify the presence of a minor rotamer in (+)-**2** and was fully characterized via ^{13}C NMR for the first time. This synthesis provides convenient access to the Aspidoalbidine family thus creating an efficient route towards the synthesis of these potentially therapeutic alkaloids.

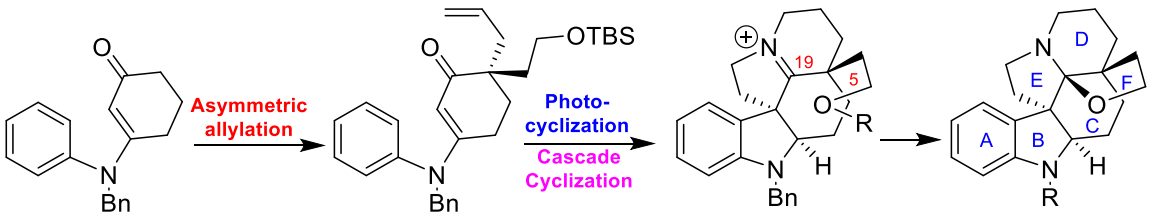

Scheme 1.20 Summarized Scheme for the Total Syntheses of (+)-**1** and (+)-**2**

1.7 Experimental Conditions

1.7.1 General Experimental Methods

All reactions were performed in oven-dried round-bottom flasks followed by flame-drying in the case of moisture-sensitive reactions. The flasks were fitted with rubber septa and kept under a positive pressure of argon. Cannula were used in the transfer of moisture-sensitive liquids. Heated reactions were allowed to run using an oil bath on a hot plate equipped with a temperature probe. Hydrogenations were carried out using a Parr shaking apparatus inside a thick-walled nonreactant borosilicate glass vessel. Photochemical transformations were done using a Hanovia 450 W Hg lamp. TLC analysis was conducted using glass-backed thin-layer silica gel chromatography plates (60 Å, 250 μm thickness, F-254 indicator) or with glass-backed thin-layer alumina N chromatography plates (250 μm thickness, UV 254). Flash chromatography was done using a 230–400 mesh, a 60 Å pore diameter silica gel, or a with 80–200 mesh alumina. Organic solutions were concentrated at 30–35 °C on rotary evaporators capable of achieving a minimum pressure of ∼30 Torr and further concentrated on a Hi-vacuum pump capable of achieving a minimum pressure of ∼4 Torr. ^{1}H NMR spectra were recorded on 400, 500, and 800 MHz spectrometers. ^{13}C NMR spectra were recorded at 100, 125, and 200 MHz on the respective NMRs. Chemical shifts are reported in parts per million and referenced to the deuterated residual solvent peak (CDCl3, 7.26 ppm for ^{1}H and 77.16 ppm for ^{13}C). NMR data are reported as δ value (chemical shift), J-value (Hz), and integration, where s = singlet, bs = broad singlet, d = doublet, t = triplet, q = quartet, p = quintet, m = multiplet, dd = doublet doublets, and so on. Optical rotations were recorded on a digital polarimeter. Low-resolution mass spectra (LRMS) spectra were recorded using a quadrupole LCMS under positive electrospray ionization (ESI+). High-resolution mass spectrometry (HRMS) spectra were recorded at the Purdue University Department of Chemistry Mass Spectrometry Center. These experiments were performed under ESI+ and positive atmospheric pressure chemical ionization (APCI+) conditions using an Orbitrap XL Instrument.

1.7.2 Experimental Procedures

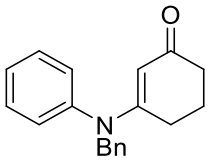

45

Enaminone **45**.[24,33] To a 500 mL one-neck round bottom flask equipped with a stir bar and 1,3-dicyclohexadiene (15 g, 133.8 mmol, 1.0 equiv), *N*-benzylaniline (26.97 g, 147.2 mmol, 1.1 equiv), and *p*-toluenesulfonic acid monohydrate (4.07 g, 21.4 mmol, 0.16 equiv) were added sequentially. A Dean-Stark apparatus with a reflux condenser was then attached and the entire vessel evacuated and flushed with Argon several times. Toluene (267 mL) was added and the reaction heated at 160 °C for 40 h. After this period, the reaction was cooled, diluted with EtOAc, washed with 1 M NaOH, brine, dried over Na_2SO_4, and concentrated. The crude mixture was purified via column chromatography over silica gel using 100% EtOAc as the eluent. Enaminone **45** was obtained as brown oil (34.57 g, 93%) TLC: Silica Gel (100% EtOAc), Rf = 0.31. ^{1}H NMR (400 MHz, $CDCl_3$) δ 7.36 – 7.15 (m, 8H), 7.11 (d, *J* = 7.1 Hz, 2H), 5.36 (s, 1H), 4.80 (s, 2H), 2.28 (dd, *J* = 14.2, 6.4 Hz, 4H), 1.88 (p, *J* = 6.4 Hz, 2H); ^{13}C{^{1}H} NMR (101 MHz, $CDCl_3$) δ 197.6, 164.9, 144.4, 136.3, 129.6, 128.6, 127.7, 127.5, 127.4, 126.8, 101.6, 56.6, 36.1, 28.6, 22.5; LRMS-ESI (+) *m/z* 278.1 $[M + H]^+$.

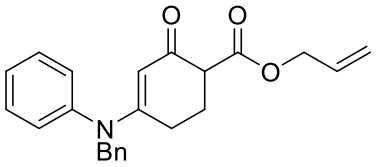

(±)-**56**

Ally Carbonate (±)-**56**. To a flame-dried 1L one-neck round bottom flask under Argon, diisopropylamine (34.1 mL, 243 mmol, 2.5 equiv) in freshly distilled THF (144 mL) was added. To this solution at 0 °C, *n*-BuLi (1.6 M in hexanes, 152 mL, 243 mmol, 2.5 equiv) was added and the reaction was stirred for 50 min. In a separate flame-dried 1 L flask enaminone **45** (27 g, 97.2 mmol, 1 equiv) was dissolved in THF (125 mL) and the solution was cannulated to the yellow solution of above LDA at –78 °C. The resulting mixture was stirred at –78°C for 1 h then allyl chloroformate (13.4 mL, 126.4 mmol, 1.3 equiv) was added dropwise. The resulting reaction was

allowed to warm slowly to 23 °C for 12 h. The reaction was quenched with saturated NH_4Cl (250 mL), extracted with EtOAc (3x), washed with brine, dried over Na_2SO_4, and concentrated. The crude mixture was purified via column chromatography over silica gel to provide allyl carbonate (±)-**56** as a viscous dark red oil (21.8 g, 62% yield), and unreacted starting material (4.9 g) was recovered (76% yield, brsm). TLC: Silica Gel (50% EtOAc:Hexanes), Rf = 0.34. ^{1}H NMR (400 MHz, $CDCl_3$) δ 7.37 – 7.20 (m, 6H), 7.17 (d, *J* = 7.0 Hz, 2H), 7.11 (d, *J* = 7.0 Hz, 2H), 5.90 (ddt, *J* = 17.2, 10.5, 5.6 Hz, 1H), 5.39 (s, 1H), 5.31 (dq, *J* = 17.2, 1.5 Hz, 1H), 5.19 (dq, *J* = 10.4, 1.2 Hz, 1H), 4.82 (s, 2H), 4.69 – 4.58 (m, 2H), 3.32 (dd, *J* = 8.7, 5.0 Hz, 1H), 2.57 – 2.46 (m, 1H), 2.36 – 2.23 (m, 2H), 2.17 – 2.06 (m, 1H); ^{13}C{^{1}H} NMR (101 MHz, $CDCl_3$) δ 191.0, 170.7, 164.6, 144.0, 136.0, 132.0, 129.7, 128.7, 127.8, 127.7, 127.5, 126.9, 118.1, 100.5, 65.5, 56.7, 51.5, 26.6, 25.2; HRMS-ESI (+) *m/z* calcd for $C_{23}H_{23}NO_3$ $[M + H]^+$: 362.1751, found 362.1755.

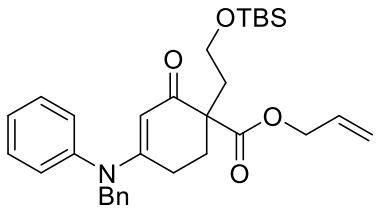

(±)-**58**

Silyl ether (±)-**58.** To a flame-dried 1L round bottom flask under Argon equipped with a stir bar and reflux condenser, racemic **56 (**21.8 g, 60.2 mmol, 1 equiv) in DMF (500 mL) was added. To this solution, *tert*-butyl(2-iodoethoxy)dimethylsilane **57** (33.4 mL, 150.4 mmol, 2.5 equiv) followed by Cs_2CO_3 (39.2 g, 120.4 mmol, 2.0 equiv) was added. The resulting reaction was heated in an oil bath to 100 °C for 32 h. After this period, the reaction was quenched with H_2O and brine (100 mL each). The resulting mixture was extracted with CH_2Cl_2, washed with 5% aqueous LiCl solution. The crude mixture was concentrated and purified via column chromatography over silica gel using 25 - 55% EtOAc/Hexanes as the eluent to yield silyl ether (±)-**58**, (21.9 g, 70.1% yield) as an orange amorphous solid. Unreacted starting material was recovered (3.2 g, 82 % yield, brsm). TLC: Silica Gel (25% EtOAc:Hexanes), Rf = 0.2. ^{1}H NMR (400 MHz, $CDCl_3$) δ 7.38 – 7.27 (m, 5H), 7.25 (d, *J* = 7.0 Hz, 1H), 7.18 (d, *J* = 6.7 Hz, 2H), 7.10 (d, *J* = 6.8 Hz, 2H), 5.89 (ddt, *J* = 17.2, 10.7, 5.5 Hz, 1H), 5.36 (s, 1H), 5.29 (dq, *J* = 16.8, 1.4 Hz, 1H), 5.19 (dq, *J* = 10.5, 1.4 Hz, 1H), 4.81 (s, 2H), 4.61 (dtdd, *J* = 14.9, 13.4, 5.0, 1.5 Hz, 2H), 3.72 (t, *J* = 6.6 Hz, 2H), 2.60 – 2.26 (m, 4H), 1.98 (dq, *J* = 14.0, 7.4, 6.6 Hz, 2H), 0.85 (s, 9H), 0.02 (d, *J* = 2.7 Hz, 6H); ^{13}C{^{1}H}

NMR (101 MHz, $CDCl_3$) δ 193.5, 172.2, 163.9, 144.2, 136.3, 132.2, 129.8, 128.8, 127.9, 127.8, 127.6, 127.0, 118.0, 100.3, 65.5, 60.2, 56.7, 54.4, 36.5, 29.6, 26.0, 25.9, 18.3, -5.3; HRMS-ESI (+) *m/z* calcd for $C_{31}H_{42}NO_4Si$ $[M + H]^+$: 520.2878, found 520.2874.

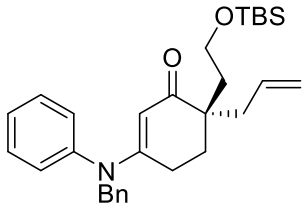

(-)-**44**

Allyl (-)-**44**. To a flame-dried round bottom flask under Argon equipped with a stir bar and reflux condenser, (*S*)-*t*Bu-Phox (429.6 mg, 1.11 mmol, 12.5 mol%) and $Pd_2(dba)_3$ (406 mg, 0.44 mmol, 5 mol %) were added. Deoxygenated toluene (61 mL) was added and the resulting mixture was stirred at 23 °C for 30 min. A solution of silyl ether (±)-**58** (4.61 g, 8.87 mmol, 1 equiv) in toluene (61 mL) was then slowly cannulated to the orange solution containing the catalyst at 23 °C. The resulting reaction mixture was heated to 70 °C for 35 min. After this period, the orange reaction mixture was cooled and then filtered over Celite®. The filter cake was washed with CH_2Cl_2. The solvent was concentrated and the residue was purified via column chromatography over silica gel using 15 – 20% EtOAc:Hexanes as the eluent to provide allylated product (-)-**44** (3.69 g, 88% yield) as viscous brown oil. TLC: Silica Gel (15% EtOAc:Hexanes), Rf = 0.16. $[\alpha]_D^{20}$ -2.9 (*c* 0.068, $CHCl_3$); ^1H NMR (500 MHz, $CDCl_3$) δ 7.37 – 7.27 (m, 5H), 7.24 (ml, 1H), 7.19 (d, *J* = 7.2 Hz, 2H), 7.12 (d, *J* = 7.1 Hz, 2H), 5.82 – 5.70 (m, 1H), 5.29 (s, 1H), 5.04 (s, 1H), 5.02 (d, *J* = 4.3 Hz, 1H), 4.82 (s, 2H), 3.72 (ddd, *J* = 10.1, 8.5, 6.2 Hz, 1H), 3.63 (ddd, *J* = 10.3, 8.7, 5.7 Hz, 1H), 2.42 (m, 2H), 2.30 (dt, *J* = 17.5, 5.7 Hz, 1H), 2.21 (dd, *J* = 13.9, 8.0 Hz, 1H), 1.87 – 1.78 (m, 3H), 1.75 – 1.69 (m, 1H), 0.87 (s, 9H), 0.03 (s, 6H); $^{13}C\{^1H\}$ NMR (126 MHz, $CDCl_3$) δ 200.5, 163.2, 144.5, 136.7, 135.2, 129.8, 128.8, 128.0, 127.59, 127.55, 127.1, 117.6, 100.9, 59.9, 56.7, 44.5, 40.3, 37.9, 31.0, 26.1, 25.5, 18.4, -5.1, -5.2; HRMS-ESI (+) *m/z* calcd for $C_{30}H_{42}NO_2Si$ $[M + H]^+$: 476.2979, found 476.2969.

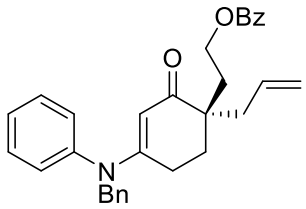

62

Benzoate **62**. To a flame-dried round bottom flask under argon equipped with a stir bar allyl derivative (-)-**44** (21 mg, 0.04 mmol, 1.0 equiv) in freshly distilled THF (0.5 mL, 0.1 M) was added. To this solution, TBAF (1.0 M in THF, 46 µL, 0.05 mmol, 1.05 equiv) was added dropwise at 0 °C and the resulting mixture was stirred at 0 °C to 23 °C for 12 h. Reaction was then quenched with H_2O and brine (~0.5 mL each), extracted with EtOAc (3x), washed brine, dried Na_2SO_4, and concentrated. The crude mixture was purified via silica gel column chromatography, using 65% EtOAc:Hexanes as the eluent to provide the corresponding alcohol as an amorphous solid (16 mg, 100% yield). TLC: Silica (65% EtOAc:Hexanes), Rf = 0.50 (UV and PMA). ^{1}H NMR (400 MHz, $CDCl_3$) δ 7.40 – 7.19 (m, 6H), 7.19 (m, 2H), 7.13 (m, 2H), 5.72 (m, 1H), 5.34 (s, 1H), 5.09 (m, 1H), 5.06 (m, 1H), 4.84 (s, 2H), 3.86 (bs, 1H), 3.81 (ddd, *J* = 12.1, 8.2, 4.4 Hz, 1H), 3.64 (dt, *J* = 10.7, 4.9 Hz, 1H), 2.46 – 2.29 (m, 4H), 1.84 – 1.67 (m, 4H). ^{13}C{^{1}H} NMR (101 MHz, $CDCl_3$) δ 202.6, 164.4, 144.2, 136.3, 134.2, 129.9, 128.9, 127.9 (2C), 127.7, 127.1, 118.4, 100.5, 58.9, 56.9, 45.0, 38.9, 37.9, 32.0, 25.4. LRMS-ESI (+) *m/z* 362.1[M + H]$^+$.

To a flame-dried round bottom flask under Argon, equipped with a stir bar, above alcohol (15 mg, 41 µmol, 1.0 equiv) in CH_2Cl_2 (0.5 mL) was added. To this solution at 0 °C, DMAP (1.0 mg, 8 µmol, 0.2 equiv), triethylamine (8.4 mg, 12 µL, 0.08 mmol, 2.0 equiv), and benzoyl chloride (7 mg, 6 µL, 0.05 mmol, 1.2 equiv) were added. The resulting reaction mixture was stirred at 0 °C to 23 °C for 2.5 h. Reaction was then quenched with H_2O and brine (~0.5 mL each), extracted with CH_2Cl_2 (3x), washed brine, dried Na_2SO_4, and concentrated. The crude mixture was purified via column chromatography over silica gel to provide benzoate **62** (18.5 mg, 96% yield) as an oil. TLC: Silica (30% EtOAc:Hexanes), Rf = 0.32 (UV and PMA) ^{1}H NMR (400 MHz, $CDCl_3$) δ 8.01 (d, *J* = 7.1 Hz, 2H), 7.54 (t, *J* = 7.4 Hz, 1H), 7.41 (t, *J* = 7.7 Hz, 2H), 7.35 (t, *J* = 7.5 Hz, 2H), 7.31 – 7.22 (m, 4H), 7.18 (d, *J* = 6.8 Hz, 2H), 7.12 (d, *J* = 7.6 Hz, 2H), 5.85 – 5.75 (m, 1H), 5.34 (s, 1H), 5.09 (s, 1H), 5.06 (d, *J* = 4.4 Hz, 1H), 4.81 (s, 2H), 4.44 – 4.34 (m, 2H), 2.48 – 2.28 (m, 4H), 2.23 – 2.16 (m, 1H), 1.93 – 1.85 (m, 3H). ^{13}C{^{1}H} NMR (101 MHz, $CDCl_3$) δ 199.78, 166.71,

163.20, 144.34, 136.49, 134.45, 132.92, 130.51, 129.82, 129.69, 128.86, 128.44, 127.97, 127.70, 127.60, 127.02, 118.25, 100.73, 62.13, 56.71, 44.42, 40.41, 33.79, 30.44, 25.32. LRMS-ESI (+) *m/z* 466.2 $[M + H]^+$.

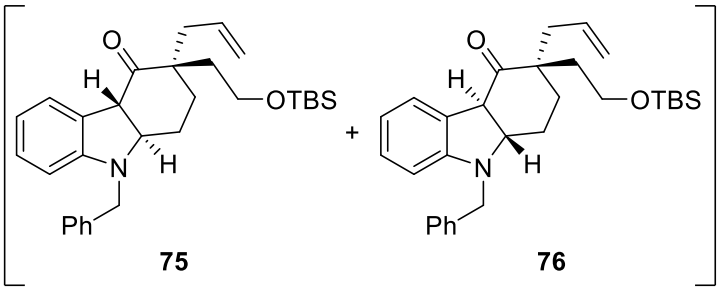

75 **76**

Indolines **75** and **76**. To a flame-dried round bottom flask under Argon fitted with a reflux condenser and stir bar, allylated (-)-**44** (1.55 g, 3.26 mmol, 1.0 equiv**)** was added. Deoxygenated Benzene (163 mL) was added and the resulting mixture was flushed under Argon multiple times. Photocyclization reaction then was carried out with a 450 W Hg lamp for 1.5 h. After this period, the reaction was concentrated under reduced pressure in the dark. The resulting crude product was immediately subjected to next step.

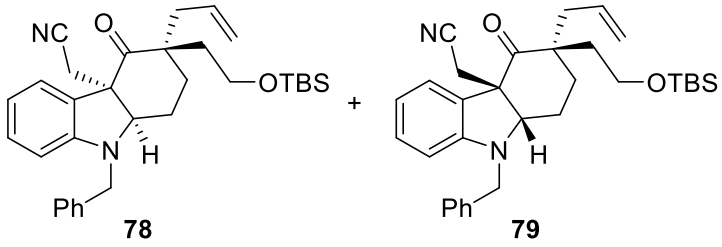

78 **79**

Nitriles **78** and **79**. To the above mixture, freshly-distilled THF (21.7 mL), and KHMDS (0.7 M in toluene, 5.12 mL, 3.58 mmol, 1.1 equiv) were added sequentially at 23 °C (solution went from orange gold to dark brown). The reaction cooled to 0 °C and after 10 min, $BrCH_2CN$ (238 µL, 3.42 mmol, 1.05 equiv) was added dropwise. The resulting mixture was stirred for 40 min at 0 °C. After this period, the reaction was quenched with saturated NH_4Cl (15 mL). Reaction extracted with EtOAc (3x), the combined extracts were washed brine, dried with Na_2SO_4, and concentrated. The crude mixture was purified via column chromatography over silica gel using 5% EtOAc:Hexanes as the eluent to provide nitriles **78** and **79** as an inseparable mixture as an oil (1.05 g, 63% over two steps). TLC: Silica Gel (15% EtOAc:Hexanes), Rf = 0.44. ^1H NMR (500 MHz, $CDCl_3$) δ 7.40 – 7.28 (m, 5H), 7.13 (t, *J* = 7.0 Hz, 1H), 6.93 (d, *J* = 7.6 Hz, 1H), 6.66 (t, *J* =

8.7 Hz, 1H), 6.49 (d, *J* = 7.9 Hz, 1H), 5.76 (m, 0.5H), 5.54 (m, 0.5H), 5.08 (m, 1H), 5.00 (d, *J* = 10.1 Hz, 0.5H), 4.87 (d, *J* = 17.0 Hz, 0.5H), 4.53 (d, *J* = 12.4 Hz, 1H), 4.32 (d, *J* = 12.4 Hz, 1H), 3.95 (m, 1H), 3.68 (t, *J* = 7.1 Hz, 1H), 3.50 – 3.45 (m, 0.5H), 3.42 – 3.38 (m, 0.5H) 3.07 (d, *J* = 10.4 Hz, 1H), 2.59 – 2.52 (m, 1.5H), 2.28 (dd, *J* = 11.1, 6.38, Hz, 0.5H), 2.09 – 2.05 (m, 0.5H), 2.02 – 1.96 (m, 1H), 1.91 – 1.45 (m, 5.5H), 0.89 (s, 5H), 0.83 (s, 4H), 0.06 (d, *J* = 4.1 Hz, 3H), -0.04 (d, *J* = 9.4 Hz, 3H). $^{13}C\{^{1}H\}$ NMR (126 MHz, $CDCl_3$) δ 210.9, 210.5, 150.1, 149.9, 137.7, 137.7, 133.9, 132.6, 130.5, 130.4, 128.9, 127.7, 127.5, 127.03, 126.97, 124.0, 123.8, 118.9, 118.8, 118.5, 118.3, 117.69, 117.67, 107.7, 68.99, 68.97, 59.6, 59.0, 58.2, 57.9, 49.7, 49.6, 49.5, 43.2, 41.0, 40.3, 39.3, 31.7, 27.2, 26.7, 26.6, 26.1, 26.0, 25.4, 22.8, 22.3, 22.2, 18.4, 18.3, 14.2, -5.2, -5.3; HRMS-ESI (+) *m/z* calcd for $C_{32}H_{43}N_2O_2Si$ $[M + H]^+$: 515.3088, found 515.3095.

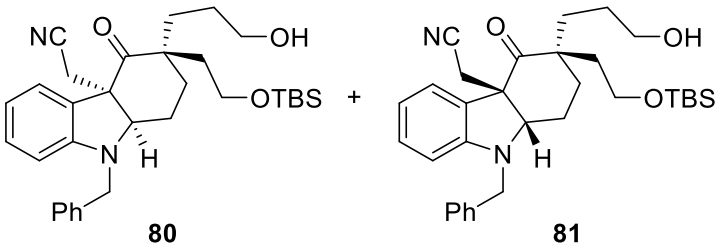

80 **81**

Alcohols **80** and **81**. To a flame-dried round bottom flask under Argon equipped with a stir bar cyclohexene (1.4 mL, 13.9 mmol, 6.5 equiv) was added to freshly distilled THF (6 mL) was added at 0°C. To this solution at 0 °C, borane dimethyl sulfide complex (neat, 607 µL, 6.4 mmol, 3.0 equiv) added dropwise. A thick white slurry started to form after 1 min. Additional amounts of THF (1 mL) was added and the reaction was continued to stir at 0 °C for 1 h. After this period, a solution of **78** and **79** (1.10 g, 2.1 mmol, 1.0 equiv), in THF (5 mL) was cannulated in at 0 °C and the resulting reaction was warmed slowly to 23 °C for 2.5 h. The reaction was quenched with slow addition of $NaBO_3$•$4H_20$ (3.3 g, 21.3 mmol, 10 equiv) and H_2O (7 mL, 0.3M), and the resulting reaction mixture was continued to stir for 12 h. The reaction was diluted in brine, extracted with EtOAc (3x), dried with Na_2SO_4, and concentrated. The crude mixture was purified via column chromatography over silica gel using 40% EtOAc:Hexanes as the eluent to provide alcohol diastereomers **80** and **81** (1.12 g, 98% combined yield) which were separated. TLC: Silica Gel (40% EtOAc:Hexanes), Rf = 0.52 and 0.38 (lower spot desired diastereomer).

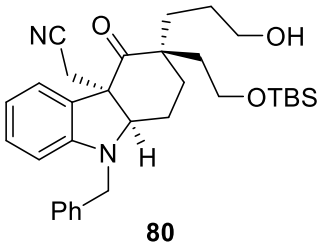

80

Alcohol **80**. $[\alpha]_D^{20}$ -144 (*c* 0.08, $CHCl_3$); ^1H NMR (500 MHz, $CDCl_3$) δ 7.39 – 7.28 (m, 5H), 7.12 (td, *J* = 7.7, 1.3 Hz, 1H), 6.91 (dd, *J* = 7.5, 1.2 Hz, 1H), 6.66 (td, *J* = 7.5, 0.9 Hz, 1H), 6.48 (d, *J* = 7.9 Hz, 1H), 4.52 (d, *J* = 15.4 Hz, 1H), 4.30 (d, *J* = 15.4 Hz, 1H), 3.93 (m, 1H), 3.62 (m, 2H), 3.47 (m, 1H), 3.39 (m, 1H), 3.08 (d, *J* = 16.3 Hz, 1H), 2.52 (d, *J* = 16.3 Hz, 1H), 1.87 – 1.76 (m, 4H), 1.69 – 1.59 (m, 3H), 1.55 (m, 1H), 1.51 – 1.40 (m, 2H), 0.81 (s, 9H), -0.06 (d, *J* = 9.4 Hz, 6H); $^{13}C\{^1H\}$ NMR (126 MHz, $CDCl_3$) δ 211.4, 149.8, 137.7, 130.4, 129.0, 127.8, 127.5, 127.3, 123.8, 118.6, 117.9, 107.9, 69.0, 63.3, 59.0, 58.1, 49.6, 49.4, 40.3, 32.5, 27.6, 27.3, 26.6, 26.0, 22.1, 18.3, -5.3; HRMS-ESI (+) *m/z* calcd for $C_{32}H_{44}N_2O_3SiNa$ $[M + Na]^+$: 555.3013, found 555.3009.

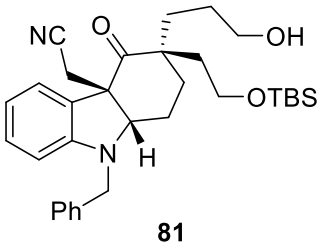

81

Alcohol **81**. ^1H NMR (500 MHz, $CDCl_3$) δ 7.39 – 7.28 (m, 5H), 7.12 (td, *J* = 7.7, 1.3 Hz, 1H), 6.90 (dd, *J* = 7.5, 1.2 Hz, 1H), 6.64 (td, *J* = 7.5, 1.0 Hz, 1H), 6.49 (d, *J* = 7.8 Hz, 1H), 4.53 (d, *J* = 15.5 Hz, 1H), 4.31 (d, *J* = 15.5 Hz, 1H), 3.95 (dd, *J* = 7.1, 4.3 Hz, 1H), 3.65 (m, 2H), 3.35 (m, 2H), 3.04 (d, *J* = 16.4 Hz, 1H), 2.56 (d, *J* = 16.4 Hz, 1H), 2.04 (m, 1H), 1.88 – 1.65 (m, 5H), 1.44 – 1.35 (m, 1H), 1.34 – 1.29 (m, 2H), 1.25 (m, 1H), 0.88 (s, 9H), 0.05 (d, *J* = 3.9 Hz, 6H); $^{13}C\{^1H\}$ NMR (126 MHz, $CDCl_3$) δ 210.6, 150.0, 137.6, 130.6, 129.0, 127.8, 127.6, 127.1, 123.6, 118.1, 117.8, 107.9, 69.1, 62.9, 59.6, 58.0, 49.6, 49.4, 38.7, 35.0, 28.4, 26.9, 26.7, 26.1, 22.5, 18.4, -5.2; LRMS-ESI (+) *m/z* 533.3 $[M + H]^+$.

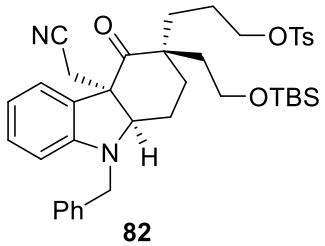

82

Tosylate **82**. To a flame-dried round bottom under Argon flask equipped with a stir bar, TsCl (50.1 mg, 0.26 mmol, 2.0 equiv) and DMAP (1.6 mg, 0.01 mmol, 10 mol %) in 0.3 mL CH_2Cl_2 were added at 0°C. To this solution, alcohol **80** (70 mg, 0.13 mmol, 1.0 equiv) in CH_2Cl_2 (0.3 mL), followed by triethylamine addition (20.1 µL, 0.14 mmol, 1.1 equiv) was added. Additional amounts of TsCl and trimethylamine (0.5 and 0.4 equiv, respectively) were further added. The resulting reaction was warmed to 23 °C, quenched with saturated $NaHCO_3$, (5 mL) extracted with CH_2Cl_2 (3x), washed with brine, dried Na_2SO_4, and concentrated. The crude mixture was purified via column chromatography over silica gel using 10 - 15% EtOAc:Hexanes as the eluent to provide tosylate **82** as an oil (71.4 mg, 79% yield). TLC: Silica Gel (20% EtOAc:Hexanes), Rf = 0.31. $[\alpha]_D^{20}$ -101.20 (*c* 0.171, $CHCl_3$); ^{1}H NMR (500 MHz, $CDCl_3$) δ 7.78 (d, *J* = 8.3 Hz, 2H), 7.39 – 7.28 (m, 7H), 7.12 (td, *J* = 7.7, 1.3 Hz, 1H), 6.87 (dd, *J* = 7.5, 1.2 Hz, 1H), 6.65 (td, *J* = 7.5, 1.0 Hz, 1H), 6.47 (d, *J* = 7.9 Hz, 1H), 4.51 (d, *J* = 15.4 Hz, 1H), 4.28 (d, *J* = 15.4 Hz, 1H), 4.00 (m, 2H), 3.89 (dd, *J* = 7.4, 4.5 Hz, 1H), 3.46 – 3.40 (m, 1H), 3.38 – 3.31 (m, 2H), 3.03 (d, *J* = 16.3 Hz, 1H), 2.48 (d, *J* = 16.3 Hz, 1H), 2.44 (s, 3H), 1.84 – 1.77 (m, 2H), 1.77 – 1.65 (m, 3H), 1.58 – 1.47 (m, 4H), 1.40 (ddd, *J* = 14.0, 8.3, 5.7 Hz, 1H), 0.80 (s, 9H), -0.07 (d, *J* = 9.0 Hz, 6H); ^{13}C{^{1}H} NMR (126 MHz, $CDCl_3$) δ 210.9, 149.6, 144.9, 137.6, 133.1, 130.5, 130.0, 129.0, 128.1, 127.8, 127.5, 127.2, 123.7, 118.6, 117.8, 107.9, 71.0, 68.9, 58.8, 58.1, 49.5, 49.3, 40.0, 32.3, 27.3, 26.4, 26.0, 24.0, 22.0, 21.8, 18.3, -5.3; HRMS-ESI (+) *m/z* calcd for $C_{39}H_{51}N_2O_5SSi$ $[M + H]^+$: 687.3283, found 687.3276.

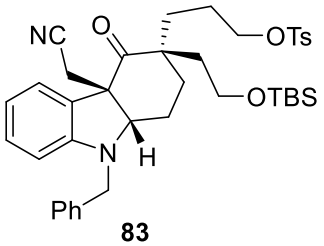

83

Tosylate **83**. Same experimental as in the transformation of **80** to **82**. The crude mixture was isolated via column chromatography over silica gel using 15-20% EtOAc:Hexanes as the eluent to provide tosylate **83** as yellow oil (463.2 mg, 85% yield). TLC: Silica (20% EtOAc:Hexanes), Rf = 0.29. ^{1}H NMR (400 MHz, $CDCl_3$) δ 7.68 (d, *J* = 8.3 Hz, 2H), 7.40 – 7.28 (m, 7H), 7.11 (td, *J* = 7.7, 1.3 Hz, 1H), 6.80 (dd, *J* = 7.6, 1.3 Hz, 1H), 6.58 (td, *J* = 7.4, 0.9 Hz, 1H), 6.49 (d, *J* = 7.9 Hz, 1H), 4.52 (d, *J* = 15.5 Hz, 1H), 4.30 (d, *J* = 15.5 Hz, 1H), 3.97 – 3.87 (m, 1H), 3.76 (m, 1H), 3.67 (m, 1H), 3.59 (td, *J* = 6.8, 1.5 Hz, 2H), 3.00 (d, *J* = 16.3 Hz, 1H), 2.53 (d, *J* = 16.4 Hz, 1H), 2.45 (s, 3H), 1.95 (m, 1H), 1.84 – 1.65 (m, 4H), 1.61 (m, 1H), 1.54 – 1.44 (m, 1H), 1.44 – 1.32 (m, 1H), 1.27 (td, *J* = 12.7, 4.5 Hz, 2H), 1.09 (td, *J* = 13.1, 3.4 Hz, 1H), 0.86 (s, 9H), 0.02 (d, *J* = 2.6 Hz, 6H); ^{13}C{^{1}H} NMR (101 MHz, $CDCl_3$) δ 210.4, 150.1, 144.8, 137.6, 133.1, 130.7, 129.9, 129.0, 128.0, 127.8, 127.6, 126.8, 123.4, 118.3, 117.7, 107.9, 70.4, 69.0, 59.5, 58.0, 49.7, 49.1, 38.4, 34.7, 28.3, 26.7, 26.1, 23.4, 22.5, 21.8, 18.4, -5.2; LRMS-ESI (+) *m/z* 687.3 $[M + H]^+$.

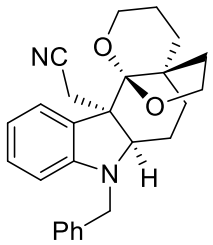

84

Ketal (+)-**84**. To a flame-dried round bottom flask under Argon equipped with a stir bar, tosylate **82** (27 mg, 39 μmol, 1.0 equiv) was dissolved in freshly distilled THF (0.4 mL, 0.1 M). To this solution at 23 °C, TBAF (1.0 M in THF, 47 μL, 47μmol, 1.2 equiv) was added dropwise and the reaction mixture was stirred for 12 h. Reaction was then quenched with H_2O and brine (~0.5 mL each), extracted with EtOAc (3x), washed brine, dried Na_2SO_4, and concentrated. The crude mixture was purified via column chromatography over silica gel using 15% EtOAc:Hexanes as the eluent to provide ketal **84** (15.7 mg, 99% yield) as a white amorphous solid. TLC: Silica

(20% EtOAc:Hexanes), Rf = 0.34. $[\alpha]_D^{20}$ +45.13 (*c* 0..203, $CHCl_3$); ^1H NMR (400 MHz, Chloroform-d) δ 7.34 – 7.24 (m, 6H), 7.07 (td, J = 7.7, 1.3 Hz, 1H), 6.62 (td, *J* = 7.4, 1.0 Hz, 1H), 6.34 (d, *J* = 8.3 Hz, 1H), 4.45 (d, *J* = 16.0 Hz, 1H), 4.35 (d, *J* = 16.0 Hz, 1H), 4.09 (ddd, *J* = 10.8, 8.4, 6.2 Hz, 1H), 3.91 (td, *J* = 8.6, 1.1 Hz, 1H), 3.77 (m, 2H), 3.68 (m, 1H), 2.95 (d, *J* = 16.6 Hz, 1H), 2.80 (d, *J* = 16.6 Hz, 1H), 2.02 (tt, J = 13.6, 3.5 Hz, 1H), 1.81 – 1.58 (m, 6H), 1.54 – 1.36 (m, 3H); $^{13}C\{^1H\}$ NMR (101 MHz, Chloroform-*d*) δ 152.1, 138.9, 129.9, 129.5, 128.7, 127.4, 127.2, 125.9, 119.3, 117.2, 108.8, 105.9, 68.3, 67.3, 61.3, 54.9, 50.9, 41.4, 38.6, 36.5, 31.3, 28.0, 24.9, 21.3; HRMS-APCI (+) *m/z* calcd for $C_{26}H_{29}N_2O_2$ $[M + H]^+$: 401.2223, found 401.2220.

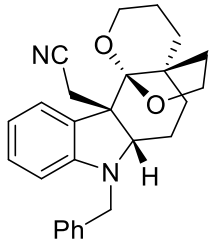

85

Ketal (-)-**85**. To a flame-dried round bottom flask under Argon equipped with a stir bar, compound **83** (30 mg, 44 µmol, 1.0 equiv) in freshly distilled THF (0.44 mL, 0.1 M) was added. To this solution at 23 °C, TBAF (1.0 M in THF, 52 µL, 52 µmol, 1.2 equiv) was added and the resulting reaction was stirred for 12 h. Reaction was then quenched with H_2O (0.5 mL), extracted with EtOAc (3x), washed brine, dried Na_2SO_4, and concentrated. The crude mixture was purified via column chromatography over silica gel using 20% EtOAc:Hexanes as the eluent to provide ketal **85** (17.5 mg, quantitative yield) as amorphous white solid. TLC: Silica (20% EtOAc:Hexanes), Rf = 0.30. $[\alpha]_D^{20}$ -68.82 (*c* 0.364, $CHCl_3$); ^1H NMR (500 MHz, $CDCl_3$) δ 7.53 (dd, *J* = 7.5, 1.3 Hz, 1H), 7.37 – 7.30 (m, 4H), 7.26 (m, 1H), 7.05 (td, *J* = 7.7, 1.4 Hz, 1H), 6.58 (td, *J* = 7.5, 1.0 Hz, 1H), 6.30 (dd, *J* = 7.9, 0.9 Hz, 1H), 4.47 (d, *J* = 15.9 Hz, 1H), 4.39 (d, *J* = 15.9 Hz, 1H), 4.17 (ddd, *J* = 10.6, 8.7, 4.9 Hz, 1H), 3.98 (ddd, *J* = 12.0, 9.8, 1.9 Hz, 1H), 3.93 (ddd, *J* = 9.6, 8.6, 7.5 Hz, 1H), 3.75 (ddd, *J* = 12.3, 10.4, 6.9 Hz, 1H), 3.66 (d, *J* = 3.7 Hz, 1H), 2.98 (d, *J* = 16.6 Hz, 1H), 2.93 (d, *J* = 16.5 Hz, 1H), 2.51 (ddd, *J* = 13.5, 10.6, 7.5 Hz, 1H), 1.99 – 1.89 (m, 1H), 1.83 (ddd, *J* = 14.0, 9.6, 4.9 Hz, 1H), 1.73 – 1.63 (m, 2H), 1.58 – 1.45 (m, 3H), 1.38 – 1.34 (m, 1H), 1.23 – 1.15 (m, 1H); $^{13}C\{^1H\}$ NMR (126 MHz, $CDCl_3$) δ 152.4, 138.9, 129.4, 128.7, 128.4, 127.5, 127.2, 126.5, 119.2, 116.7, 109.4, 105.2, 67.8, 67.0, 58.6, 53.1, 50.4, 43.3, 38.2, 35.1,

28.4, 27.8, 23.8, 19.0; HRMS-APCI (+) *m/z* calcd for $C_{26}H_{29}N_2O_2$ $[M + H]^+$: 401.2223, found 401.2219.

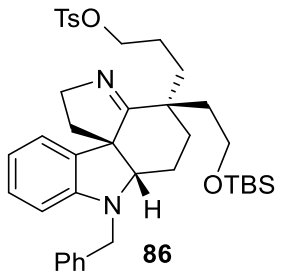

86

Imine **86**. To a Parr Reactor vessel under argon was added 2800 Ra-Ni (1.21 g, 300 wt %). A solution of tosylate **83** (403 mg, 0.59 mmol, 1.0 equiv) in MeOH (22 mL, 27 mM) was then cannulated in. The mixture was shaken in a Parr™ apparatus under hydrogen at 60 Psi pressure for 46 h. After this period, the resulting white solution mixture was filtered through Celite® and filter-cake was washed with MeOH and CH_2Cl_2 (15 mL each). Solvents were evaporated to yield imine **86** (359.5 mg, 90.8% yield). TLC: Silica (30% EtOAc:Hexanes), Rf = 0.46. ^{1}H NMR (500 MHz, $CDCl_3$) δ 7.68 (d, *J* = 8.3 Hz, 2H), 7.36 – 7.27 (m, 7H), 7.03 (td, *J* = 7.7, 1.3 Hz, 1H), 6.63 (dd, *J* = 7.3, 1.2 Hz, 1H), 6.48 (t, *J* = 5.9 Hz, 1H), 6.40 (d, *J* = 7.9 Hz, 1H), 4.48 (d, *J* = 15.5 Hz, 1H), 4.24 (d, *J* = 15.5 Hz, 1H), 3.91 (dd, *J* = 15.4, 8.5 Hz, 1H), 3.80 (m, 1H), 3.74 (m, 1H), 3.68 (m, 1H), 3.62 (td, *J* = 7.2, 3.0 Hz, 2H), 3.47 (t, *J* = 5.7 Hz, 1H), 2.45 (s, 3H), 2.19 (dt, *J* = 12.2, 6.6 Hz, 1H), 1.91 (m, 1H), 1.80 (dt, *J* = 13.9, 6.7 Hz, 1H), 1.69 (m, 2H), 1.57 (m, 2H), 1.46 (m, 2H), 1.16 (td, *J* = 13.0, 5.3 Hz, 1H), 1.04 (td, *J* = 13.1, 3.2 Hz, 1H), 0.85 (s, 9H), 0.01 (d, *J* = 1.9 Hz, 7H); ^{13}C{^{1}H} NMR (126 MHz, $CDCl_3$) δ 180.8, 149.2, 144.5, 138.4, 133.2, 132.4, 129.8, 128.7, 128.7, 127.9, 127.4, 127.3, 122.0, 117.4, 107.2, 71.6, 71.0, 61.0, 59.4, 56.9, 49.2, 43.5, 41.8, 38.6, 32.6, 31.4, 26.0, 23.7, 22.5, 21.7, 18.3, -5.3; LRMS-ESI (+) *m/z* 673.3 $[M + H]^+$.

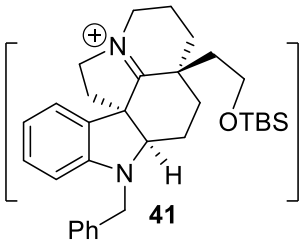

41

Iminium **41**. To a Parr reactor vessel under Argon was added 2800 Ra-Ni (51 mg, 300 wt %). A solution of tosylate **82** (17 mg, 25 μmol, 1.0 equiv) in MeOH (1 mL, 27 mM) was then

cannulated in the flask. The mixture was shaken in a Parr™ apparatus under hydrogen at 60 Psi pressure for 21 h. After this period, the resulting white solution mixture was filtered through Celite® and filter-cake was washed with MeOH and CH_2Cl_2 (10 mL each). Solvents were evaporated and the crude iminium salt **41** was used directly for the next reaction. LRMS-ESI (+) *m/z* 501.3 $[M]^+$.

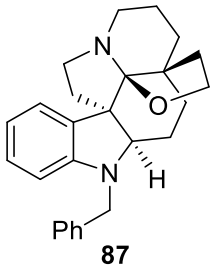

87

1-Benzyl Fendleridine **87**.[1] To a flame-dried flask under Argon equipped with a stir bar, above crude iminium salt **41** was dissolved in freshly distilled THF (0.3 mL, 0.1 M) and TBAF (1 M in THF, 30 µL, 0.03 mmol, 1.2 equiv) was added and the resulting reaction mixture was stirred for 12 h. Reaction was then quenched with H_2O (~.5 mL), extracted with EtOAc (3x), washed with brine, dried with Na_2SO_4, and concentrated. The crude mixture was purified via column chromatography over silica gel using 70% - 80% EtOAc:Hexanes as the eluent to provide benzyl derivative **87** (5.9 mg, 62% yield over 2 steps) as an off-white amorphous solid. TLC: Alumina (5% EtOAc:Hexanes), Rf = 0.50. $[\alpha]_D^{20}$ +3.0 (*c* 0.155, $CHCl_3$); ^1H NMR (400 MHz, $CDCl_3$) δ 7.36 (dd, *J* = 7.4, 1.3 Hz, 1H), 7.29 – 7.15 (m, 5H), 6.94 (td, *J* = 7.6, 1.3 Hz, 1H), 6.59 (td, *J* = 7.4, 1.1 Hz, 1H), 6.27 (dd, *J* = 7.8, 1.0 Hz, 1H), 4.34 (d, *J* = 15.4 Hz, 1H), 4.06 (d, *J* = 15.4 Hz, 1H), 3.89 – 3.75 (m, 2H), 3.22 (dd, *J* = 7.6, 4.1 Hz, 1H), 2.91 – 2.82 (m, 2H), 2.74 – 2.64 (m, 1H), 2.59 – 2.51 (m, 1H), 2.14 (ddd, *J* = 13.2, 8.9, 6.6 Hz, 1H), 1.98 – 1.84 (m, 2H), 1.77 (dd, *J* = 21.1, 10.6 Hz, 1H), 1.64 – 1.50 (m, 3H), 1.50 – 1.38 (m, 3H), 1.29 – 1.19 (m, 2H); $^{13}C\{^1H\}$ NMR (101 MHz, $CDCl_3$) δ 151.2, 139.0, 135.0, 128.6, 127.7, 127.5, 127.1, 125.9, 117.9, 106.5, 101.9, 71.5, 64.9, 57.9, 49.6, 49.2, 44.1, 38.6, 38.3, 36.9, 34.7, 27.4, 21.64, 21.56; HRMS-ESI (+) *m/z* calcd for $C_{26}H_{31}N_2O$ $[M + H]^+$: 387.2431, found 387.2429.

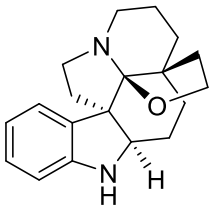

1

(+)-Fendleridine **1**.[1,2] A flame-dried round bottom flask under Argon was equipped with a stir bar and cold-finger condenser with dry ice and acetone. NH_3 was allowed to condense into the flask (1 mL) and the cold finger condenser was removed and a septum with an Argon balloon quickly replaced it. To this, small chunks of freshly cut Li (30 mg, 167 equiv) washed with hexanes were added. The solution turned dark blue. Benzyl derivative **87** (10 mg, 0.03 mmol, 1 equiv) in a mixture (10:1) of THF and *t*-BuOH (0.5 mL) was added and the reaction was allowed to stir for 2 h. Reaction was quenched with solid NH_4Cl (~100 mg, 72.3 eq) and cooling bath was removed and the reaction was warmed to 23 °C. Reaction diluted with EtOAc (1 mL), filtered through cotton plug with CH_2Cl_2 and EtOAc (5 mL each), and concentrated. The crude mixture was purified via column chromatography over alumina using 5% EtOAc:Hexanes as the eluent to provide synthetic (+)-fendleridine (**1**) as off-white amorphous solid (5.3 mg, 70%). TLC: Alumina (5% EtOAc:Hexanes), Rf = 0.13. $[\alpha]_D^{20}$ +53.7 (*c* 0.177, $CHCl_3$); ^1H NMR (800 MHz, $CDCl_3$) δ 7.45 (d, *J* = 7.5 Hz, 1H), 7.01 (t, *J* = 7.6 Hz, 1H), 6.73 (t, *J* = 7.5 Hz, 1H), 6.60 (d, *J* = 7.7 Hz, 1H), 4.03 – 3.95 (m, 2H), 3.52 (bs, 1H), 3.40 (dd, *J* = 9.5, 4.8 Hz, 1H), 3.00 (td, *J* = 8.7, 4.1 Hz, 1H), 2.92 (dt, *J* = 15.6, Hz, 1H), 2.79 (t, *J* = 11.4 Hz, 1H), 2.65 (d, *J* = 11.1 Hz, 1H), 2.24 (ddd, *J* = 13.4 8.7, 5.9 Hz, 1H), 1.92 – 1.83 (m, 2H), 1.81 (td, *J* = 12.9, 4.0 Hz, 1H), 1.78 – 1.71 (m, 2H), 1.71 – 1.59 (m, 2H), 1.51 (dt, *J* = 12.1, 3.2 Hz, 1H), 1.45 (dt, *J* = 13.8, 4.8 Hz, 1H), 1.35 (d, *J* = 13.0 Hz, 1H), 1.24 (dd, *J* = 11.9, 5.5 Hz, 1H); $^{13}C\{^1H\}$ NMR (201 MHz, $CDCl_3$) δ 150.3, 134.4, 127.3, 126.1, 119.4, 110.0, 102.1, 66.6, 64.9, 58.9, 49.3, 44.1, 39.2, 37.0, 35.8, 34.1, 27.3, 27.0, 21.5; HRMS-ESI (+) *m/z* calcd for $C_{19}H_{25}N_2O$ $[M + H]^+$: 297.1961, found 297.1964.

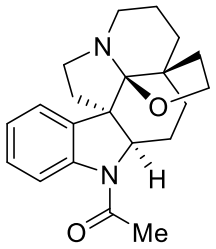

2

(+) – Acetylaspidoalbidine **2**.[1,2] To a flame-dried round bottom flask under Argon equipped with a stir bar, synthetic (+)-Fendleridine **1** (7.9 mg, 0.027 mmol, 1.0 equiv) was dissolved in CH_2Cl_2 (1 mL), was added. Pyridine (11 µL, 0.13 mmol, 5.0 equiv) and acetic anhydride (7.5 µL, 0.08 mmol, 3.0 equiv) were added sequentially. Reaction was quenched with saturated $NaHCO_3$ (~ 0.1 mL), extracted 3x with CH_2Cl_2, dried Na_2SO_4, and concentrated. The crude mixture was purified via column chromatography using 15 - 20% EtOAc:Hexanes as the eluent to provide products **(+)**-Acetylaspidoalbine **2** (rotamers) as white amorphous solid (9 mg, quantitative yield). TLC: Alumina (5% EtOAc:Hexanes), Rf = 0.08. $[\alpha]_D^{20}$ +30.2 (*c* 0.145, $CHCl_3$); ^{1}H NMR (800 MHz, $CDCl_3$) δ 8.14 (d, *J* = 8.0 Hz, 1H), 7.67 (d, *J* = 3.5 Hz, 0.3H) 7.60 (d, *J* = 7.7 Hz, 1H, minor rotamer), 7.19 (t, *J* = 7.7 Hz, 1H), 7.05 (t, *J* = 7.5 Hz, 1H), 4.42 (dd, *J* = 9.12, 4.16 Hz, minor rotamer), 4.16 (t, *J* = 8.6 Hz, 1H), 4.09 (dt, *J* = 10.5, 7.5 Hz, 1H), 3.86 (dd, *J* = 11.0, 5.2 Hz, 1H), 3.02 (td, *J* = 8.8, 4.1 Hz, 1H), 2.93 (dd, *J* = 15.7, 9.0 Hz, 1H), 2.80 (td, *J* = 11.5, 2.8 Hz, 1H), 2.65 (d, *J* = 10.7 Hz, 1H), 2.39 (s, 0.6H, minor rotamer), 2.26 (s, 2.1H), 2.10 (ddd, *J* = 14.6, 9.1, 6.1 Hz, 1H), 2.07 – 2.00 (m, 1H), 1.93 (m, 1H), 1.86 (m, 1H), 1.83 – 1.66 (m, 4H), 1.55 (dt, *J* = 12.7, 3.6 Hz, 0.8H), 1.50 (t, *J* = 13.9 Hz, .2 H, minor rotamer), 1.43 (dt, *J* = 14.0, 3.9 Hz, 1H), 1.38 (d, *J* = 12.9 Hz, 1H), 1.27 (m, 1H); ^{13}C{^{1}H} NMR (201 MHz, $CDCl_3$, major rotamer) δ 168.2, 141.2, 137.9, 127.5, 124.9, 124.8, 117.9, 102.2, 69.0, 65.1, 58.4, 49.1, 44.1, 39.8, 37.3, 34.9, 33.2, 26.6, 25.5, 23.5, 21.2; ^{13}C{^{1}H} NMR (201 MHz, $CDCl_3$, minor rotamer) δ 168.0, 140.6, 140.1, 127.1, 126.1, 124.3, 115.1, 102.5, 67.1, 65.0, 57.2, 48.9, 43.9, 39.6, 37.0, 35.2, 33.5, 26.8, 24.4, 23.8, 21.2; HRMS-ESI (+) *m/z* calcd for $C_{21}H_{27}N_2O_2$ $[M + H]^+$: 339.2067, found 339.2064.

1.7.3 Spectral Data

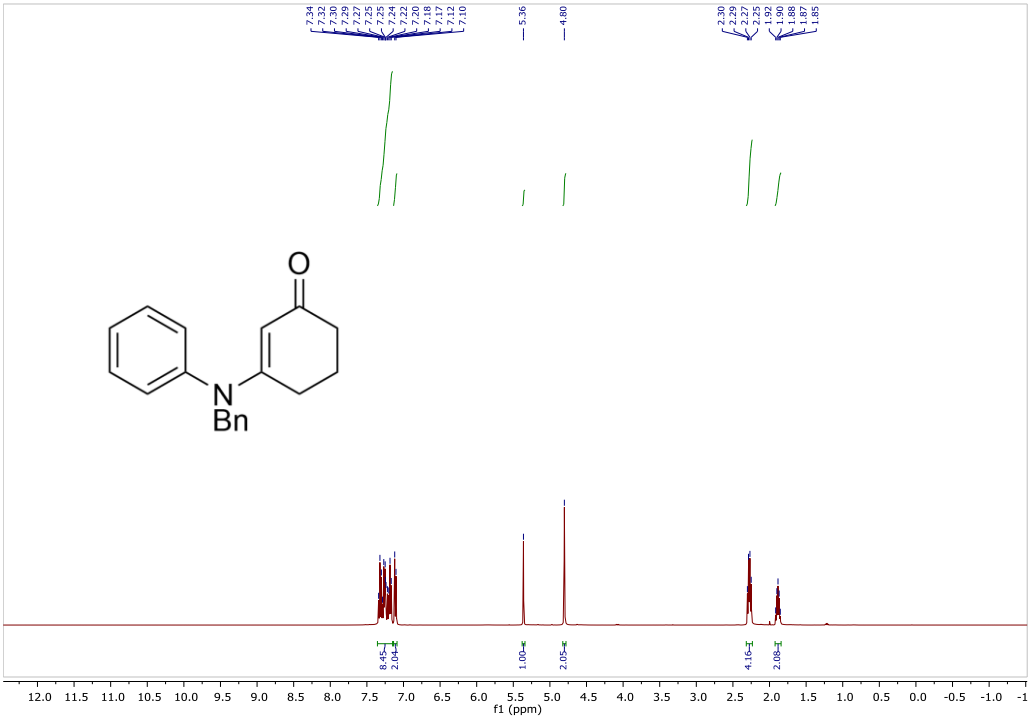

Figure 1.10 ^{1}H-NMR (400 MHz, $CDCl_3$) of Enaminone **45**

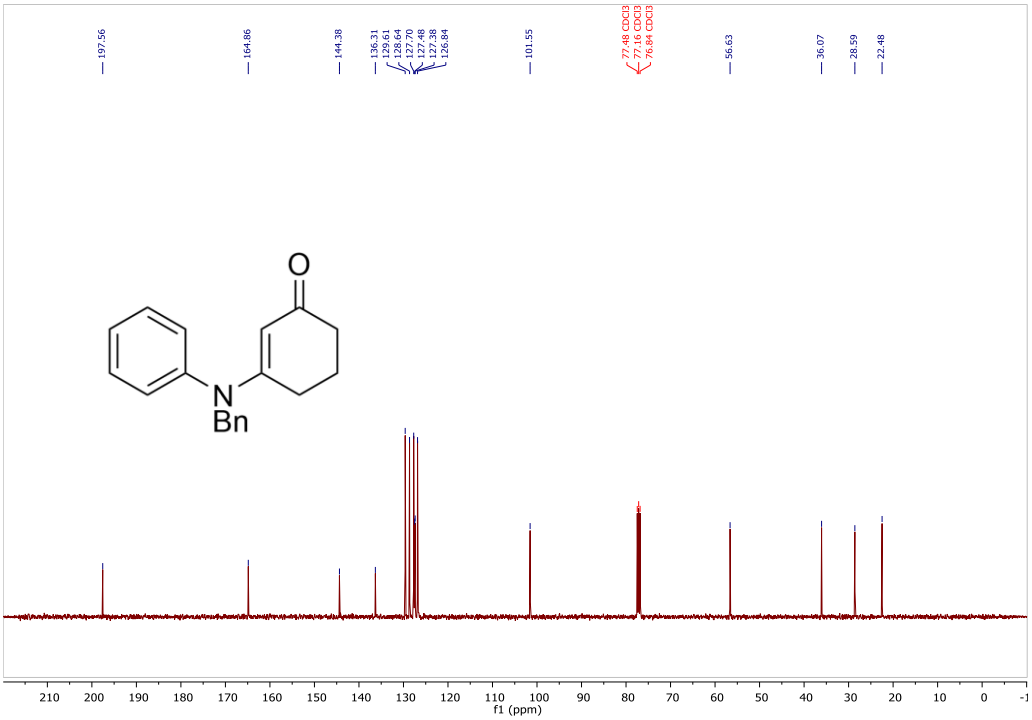

Figure 1.11 ^{13}C-NMR (100 MHz, $CDCl_3$) of Enaminone **45**

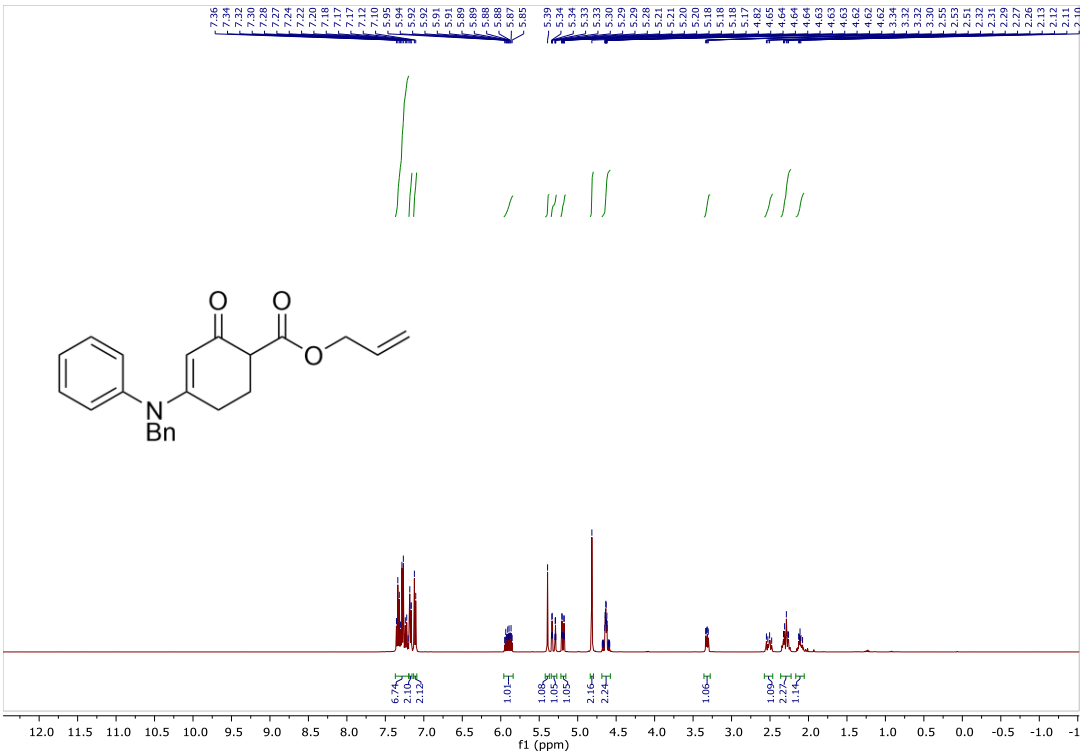

Figure 1.12 ^{1}H-NMR (400 MHz, $CDCl_3$) of Allyl Carbonate (±)-**56**

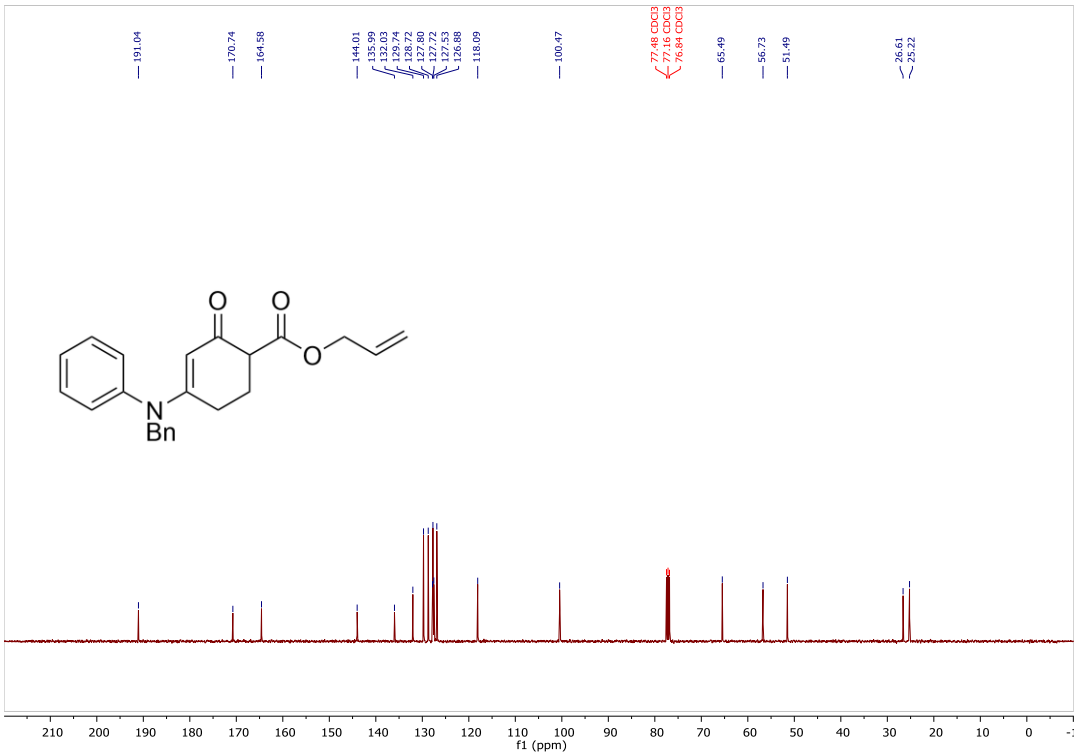

Figure 1.13 ^{13}C-NMR (100 MHz, $CDCl_3$) of Allyl Carbonate (±)-**56**

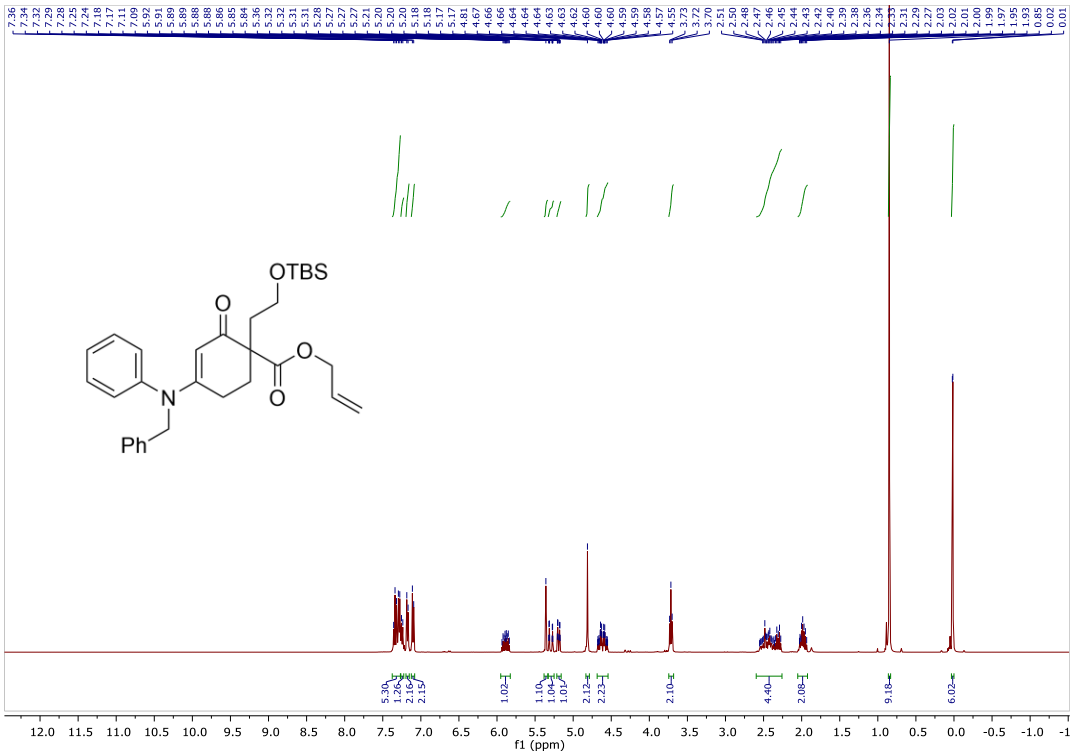

Figure 1.14 ^{1}H-NMR (400 MHz, $CDCl_3$) of Silyl Ether (±)-**58**

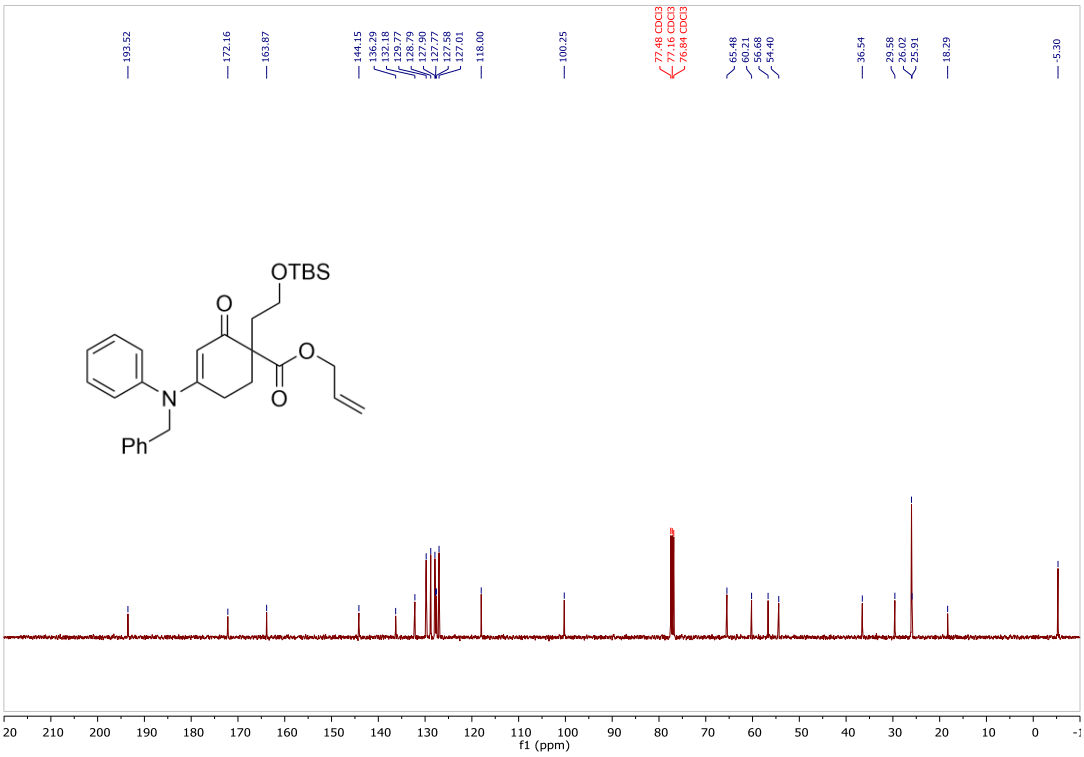

Figure 1.15 ^{13}C-NMR (100 MHz, $CDCl_3$) of Silyl Ether (±)-**58**

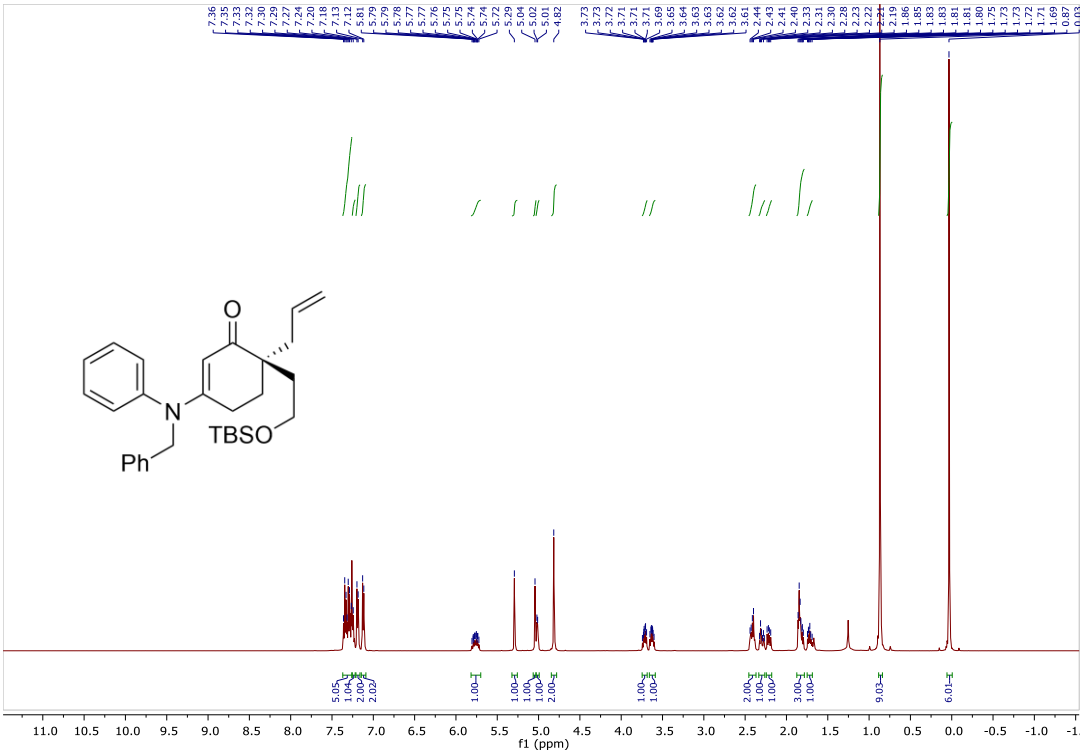

Figure 1.16 ^{1}H-NMR (500 MHz, $CDCl_3$) of Allyl **44**

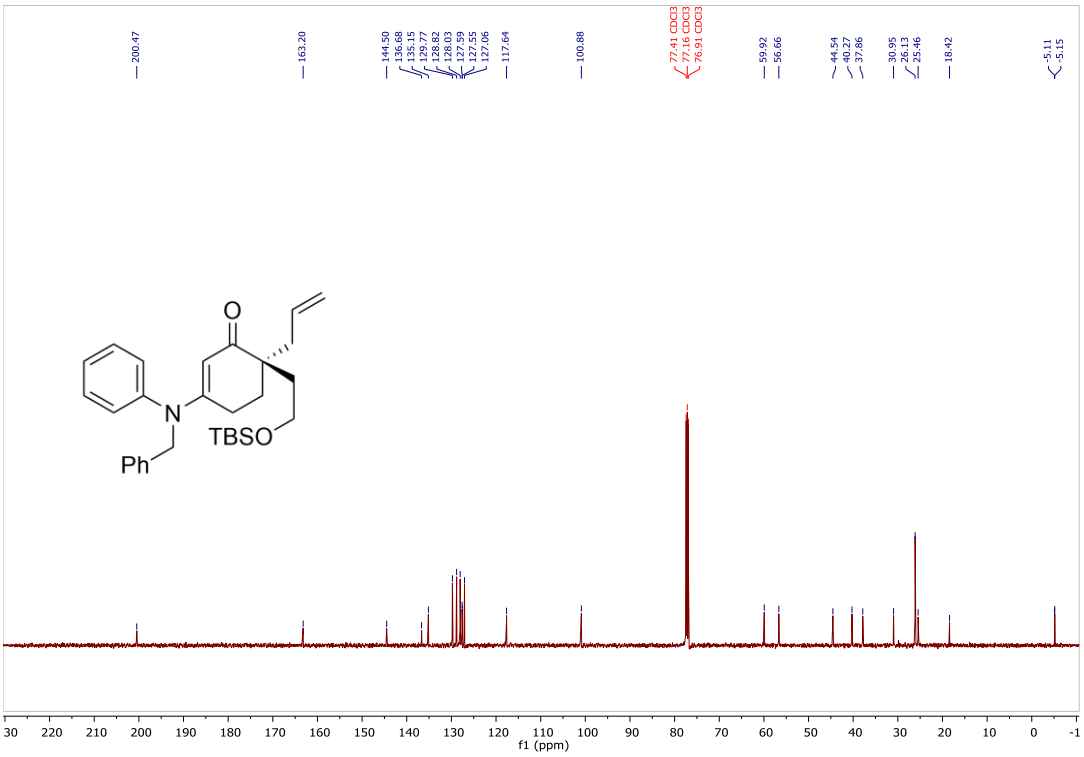

Figure 1.17 ^{13}C-NMR (125 MHz, $CDCl_3$) of Allyl **44**

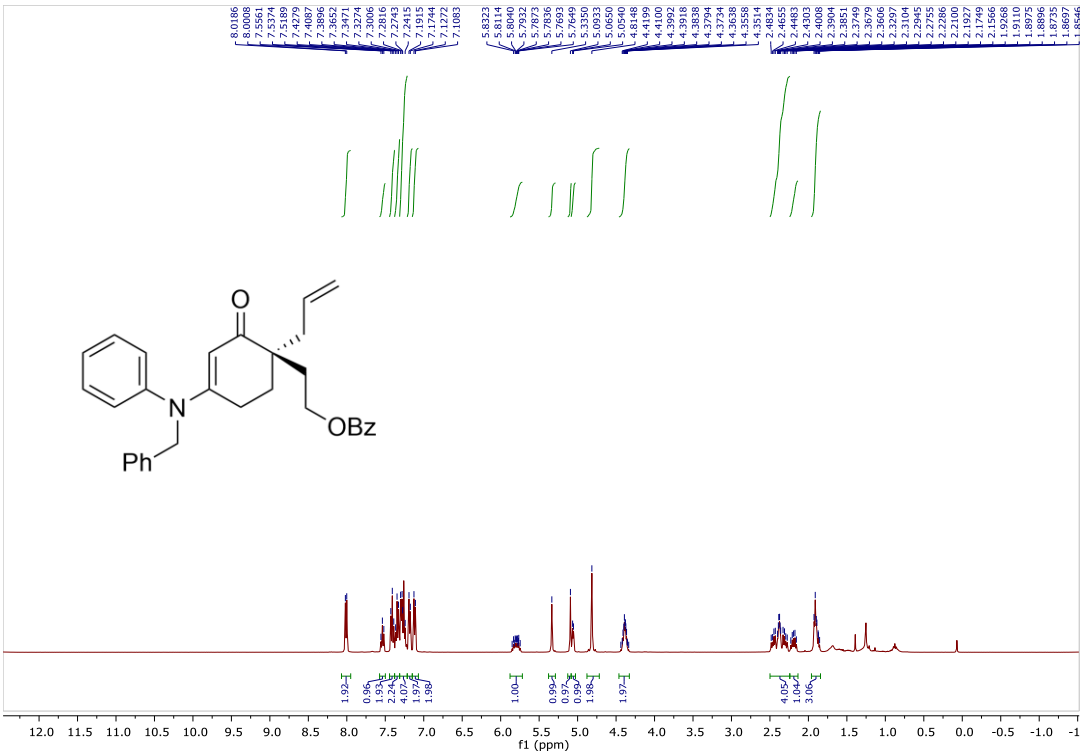

Figure 1.18 ^{1}H-NMR (400 MHz, $CDCL_3$) of Benzoate **62**

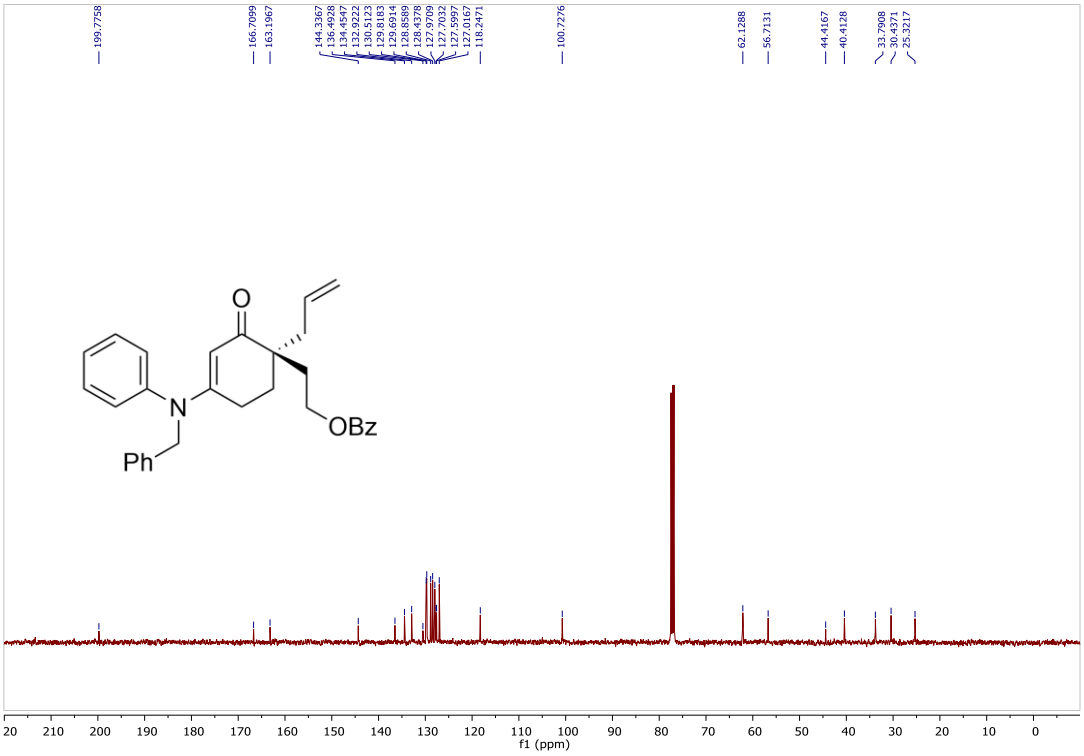

Figure 1.19 ^{13}C-NMR (100 MHz, $CDCL_3$) of Benzoate **62**

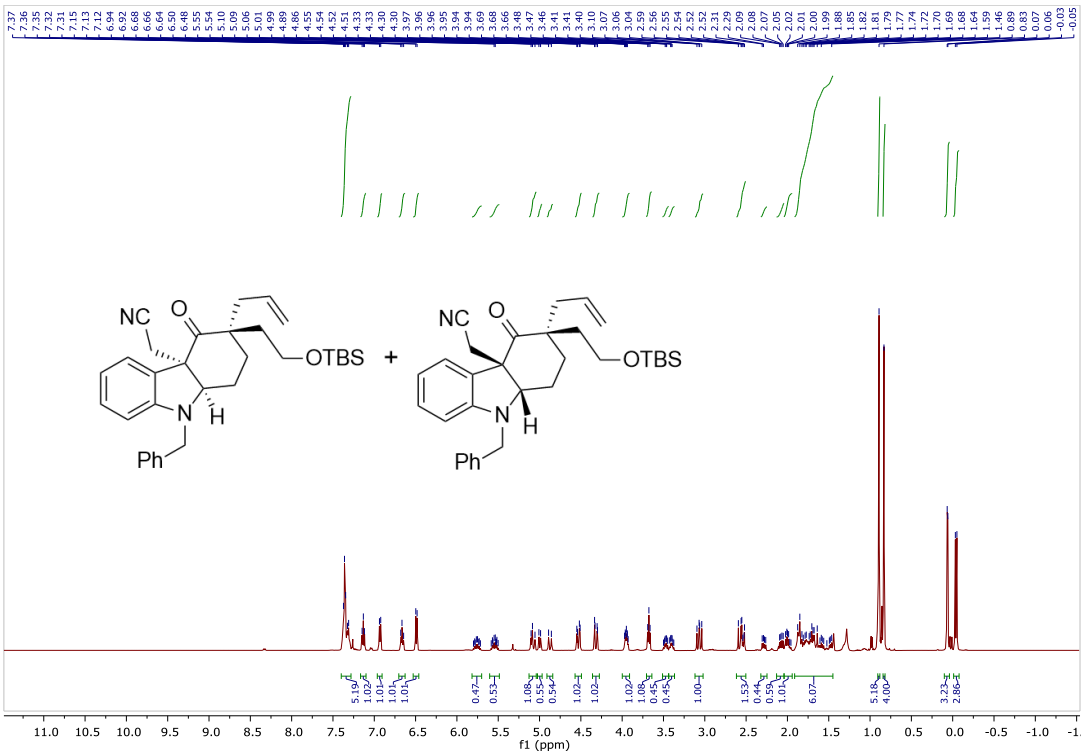

Figure 1.20 ^{1}H-NMR (500 MHz, $CDCl_3$) of Nitriles **78** & **79**

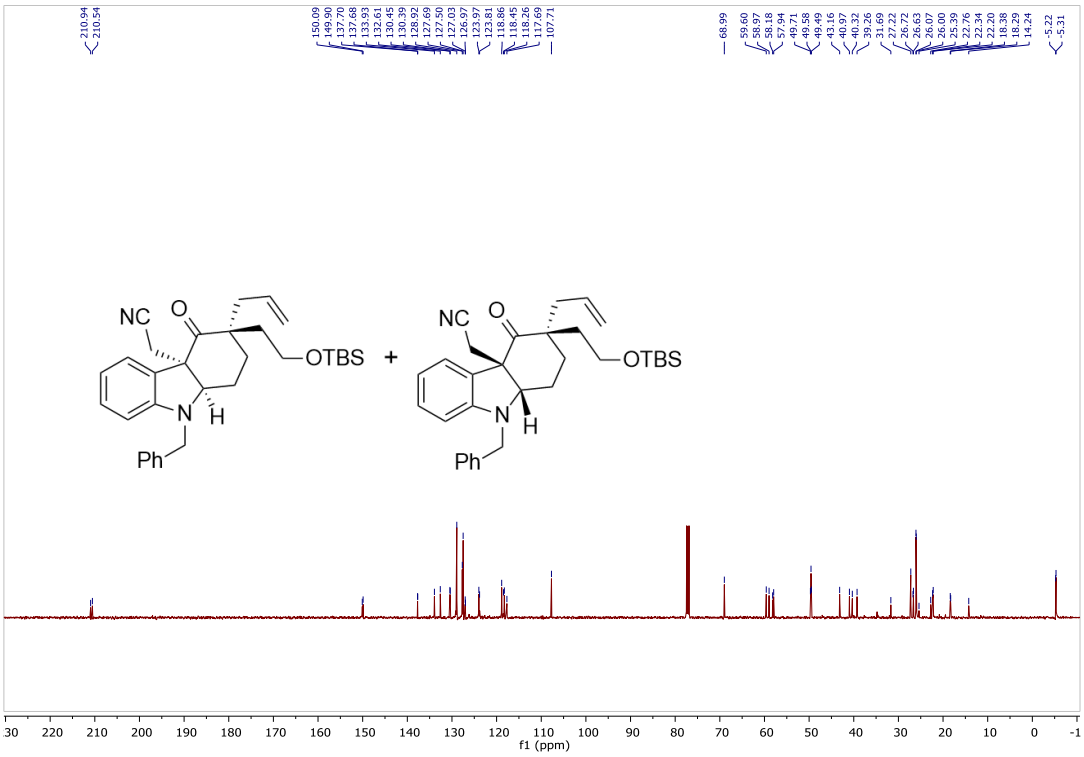

Figure 1.21 ^{13}C-NMR (125 MHz, $CDCl_3$) of Nitriles **78** & **79**

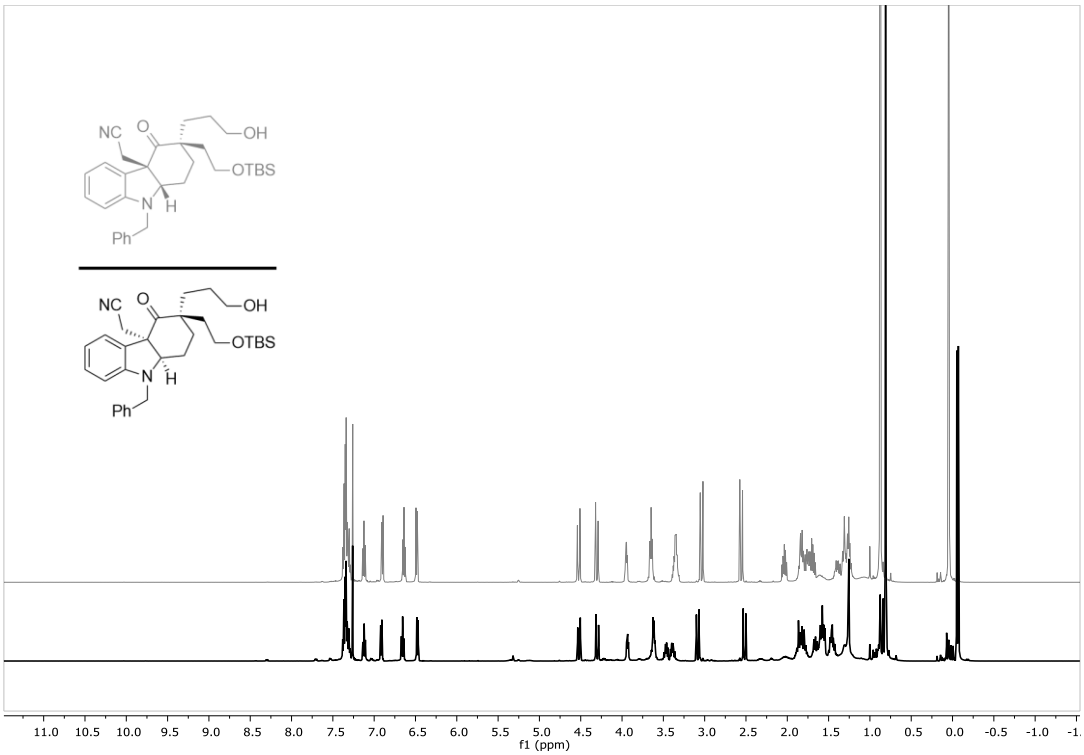

Figure 1.22 ^{1}H-NMR (500 MHz, $CDCl_3$) Comparison of Alcohols **80** & **81**

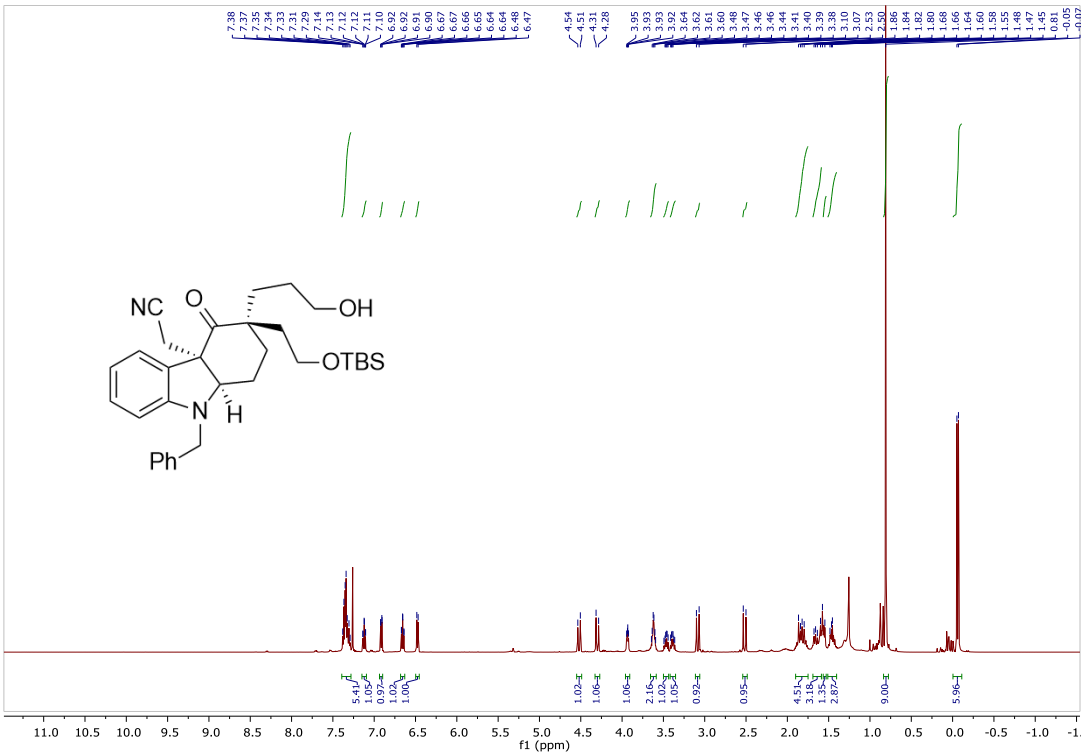

Figure 1.23 ^{1}H-NMR (500 MHz, $CDCl_3$) of Alcohol **80**

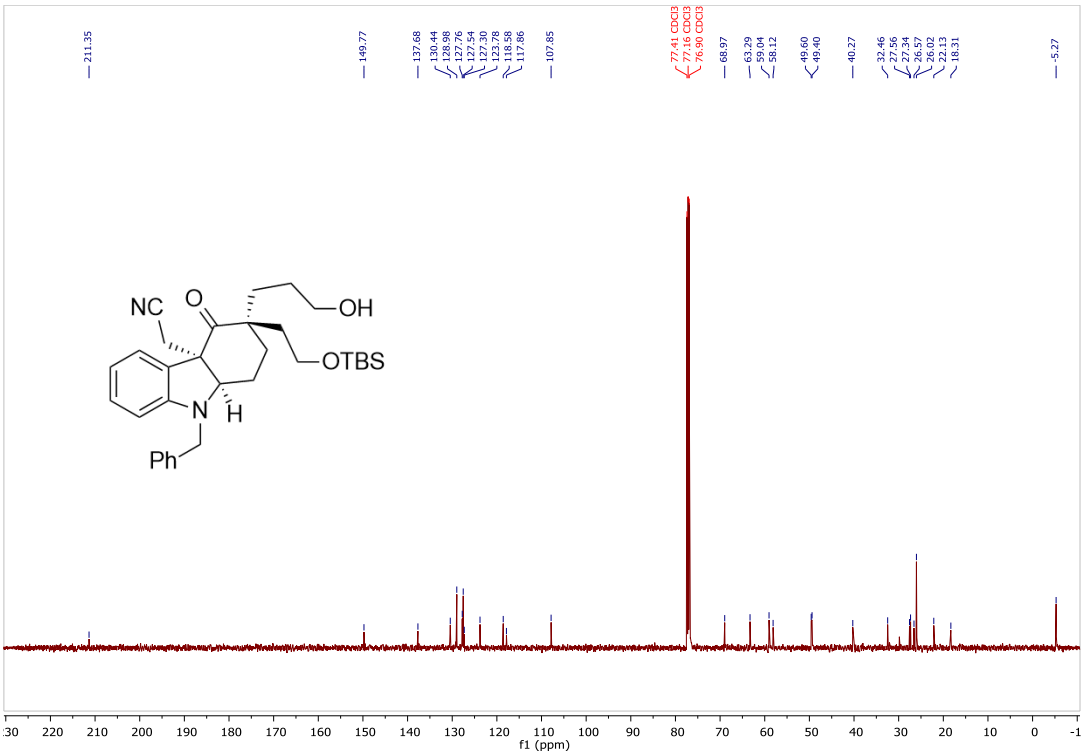

Figure 1.24 ^{13}C-NMR (125 MHz, $CDCl_3$) of Alcohol **80**

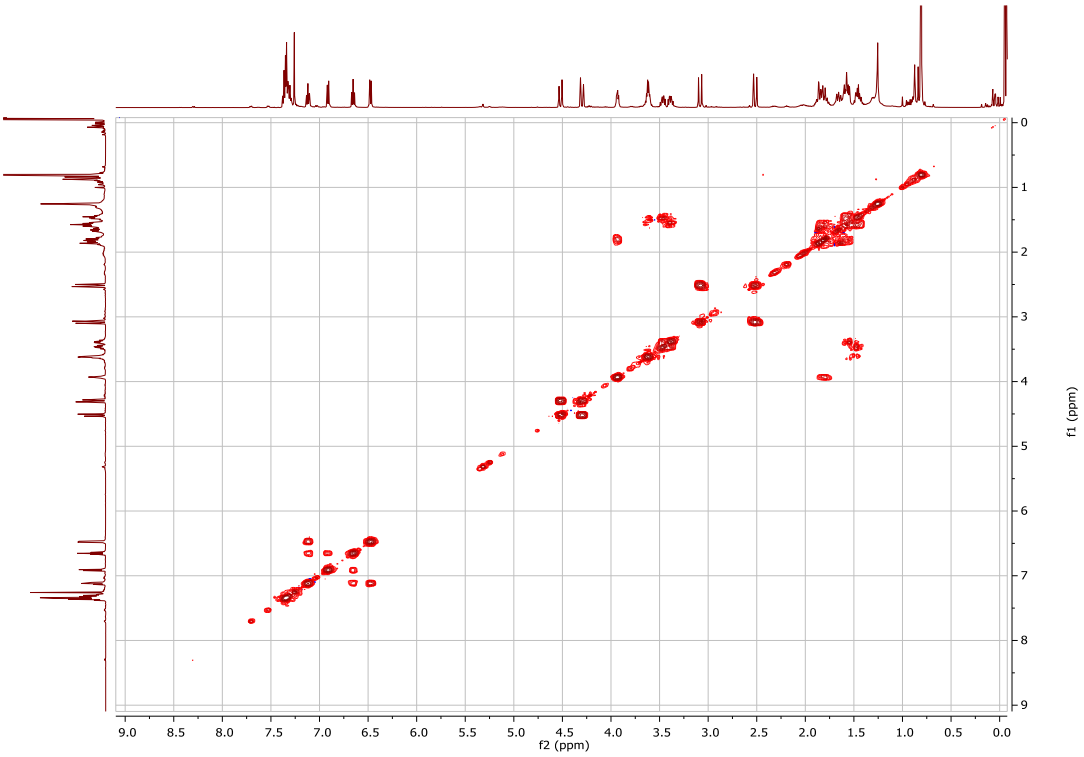

Figure 1.25 ^{1}H-^{1}H COSY NMR ($CDCl_3$) of Alcohol **80**

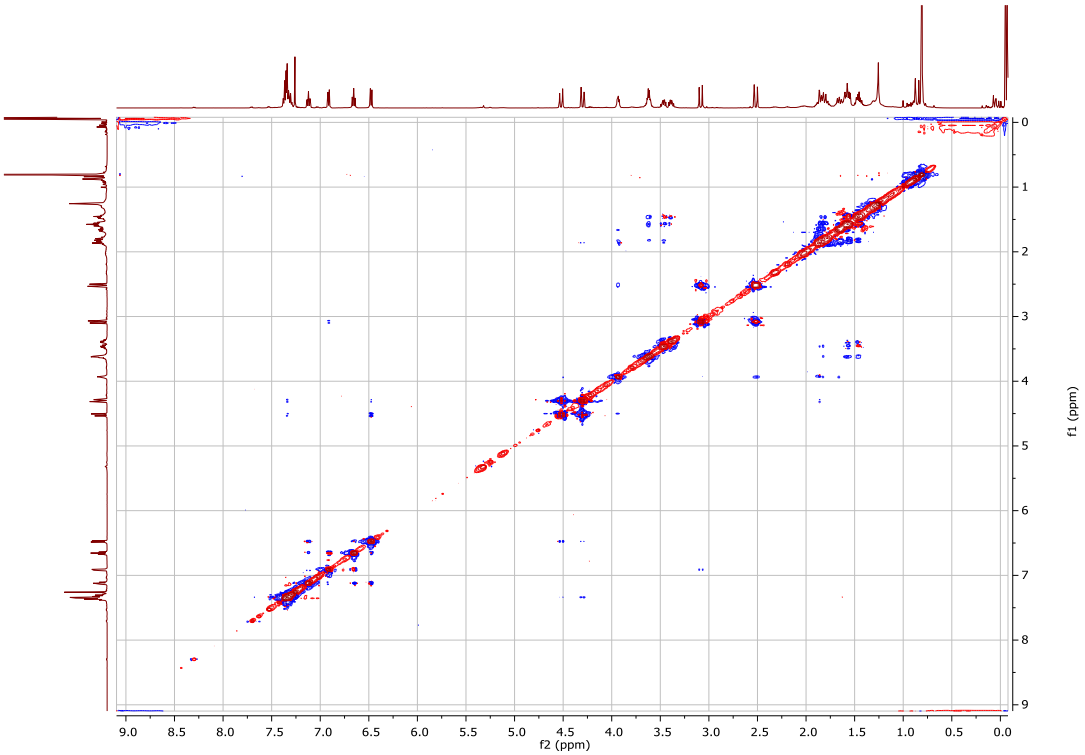

Figure 1.26 NOESY NMR ($CDCl_3$) of Alcohol **80**

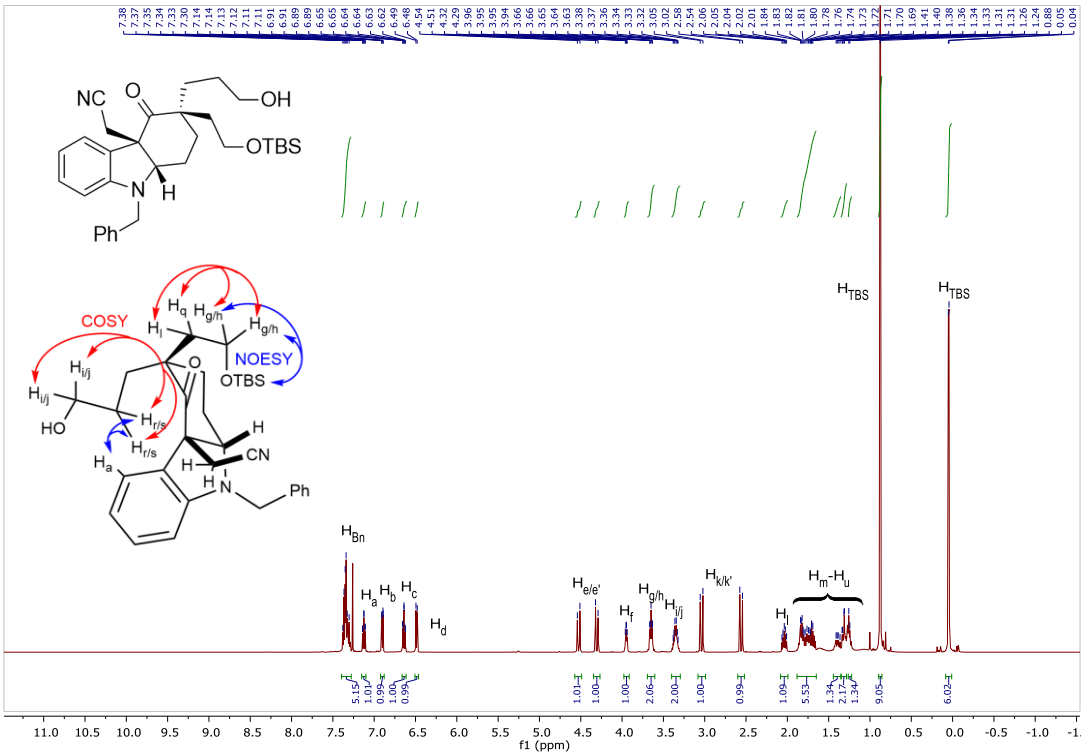

Figure 1.27 ^{1}H-NMR (500 MHz, $CDCl_3$) of Alcohol **81**

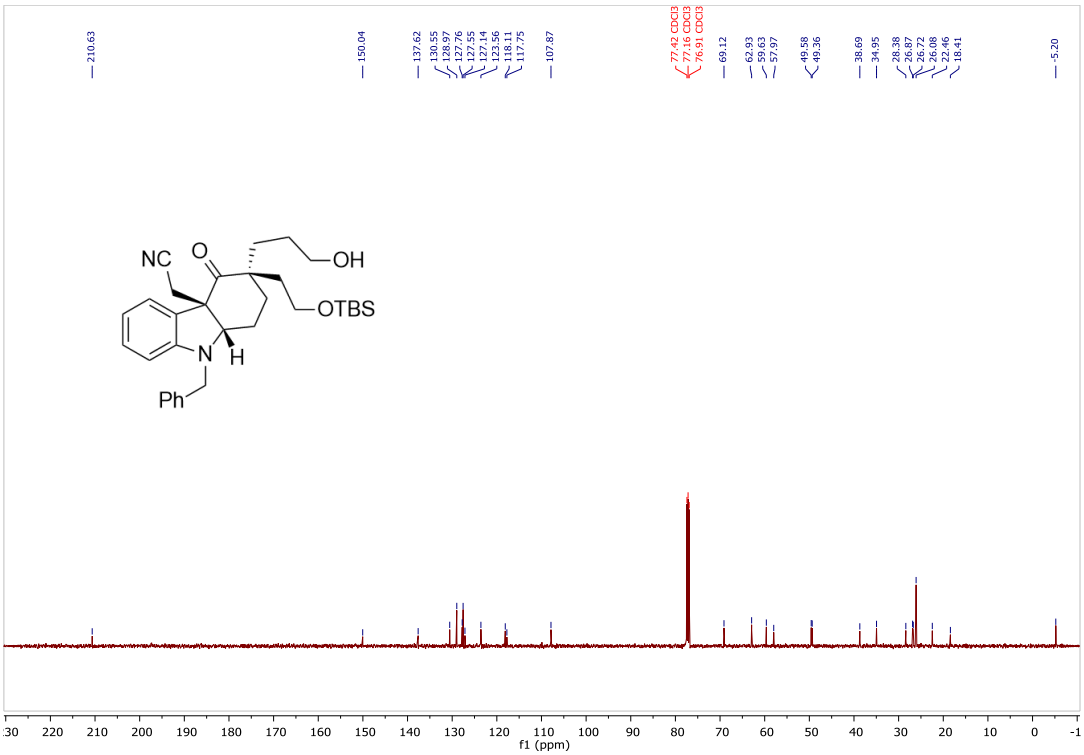

Figure 1.28 ^{13}C-NMR (125 MHz, $CDCl_3$) of Alcohol **81**

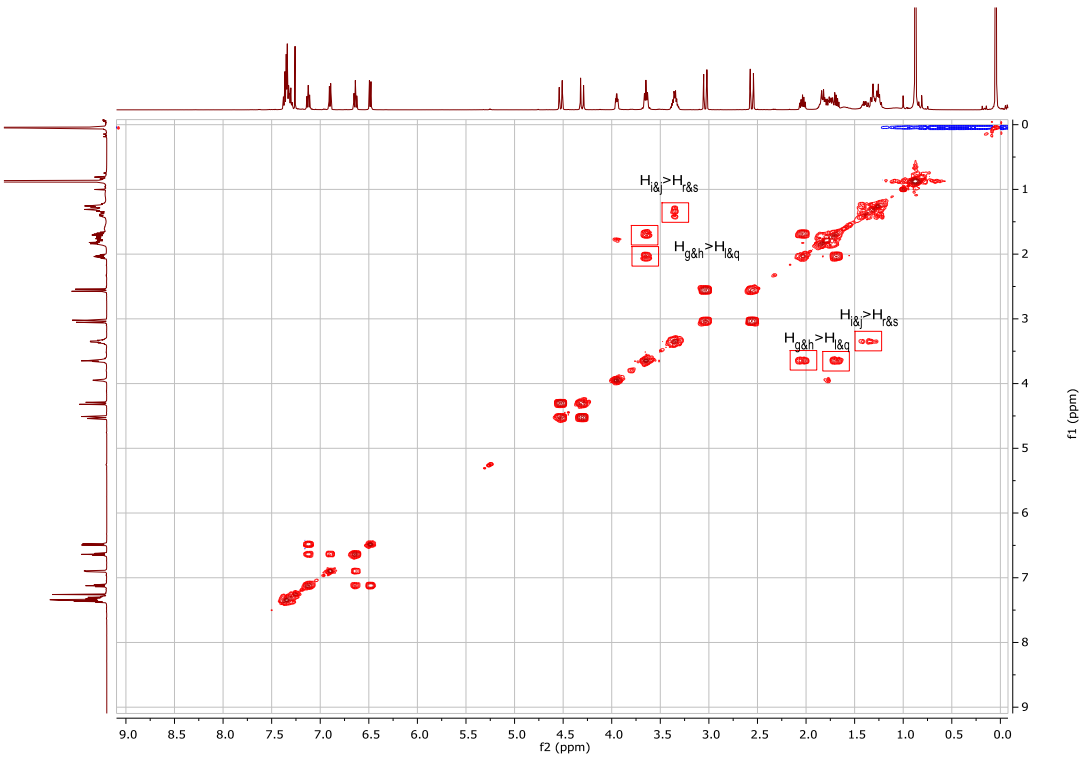

Figure 1.29 ^{1}H-^{1}H COSY NMR ($CDCl_3$) of Alcohol **81**

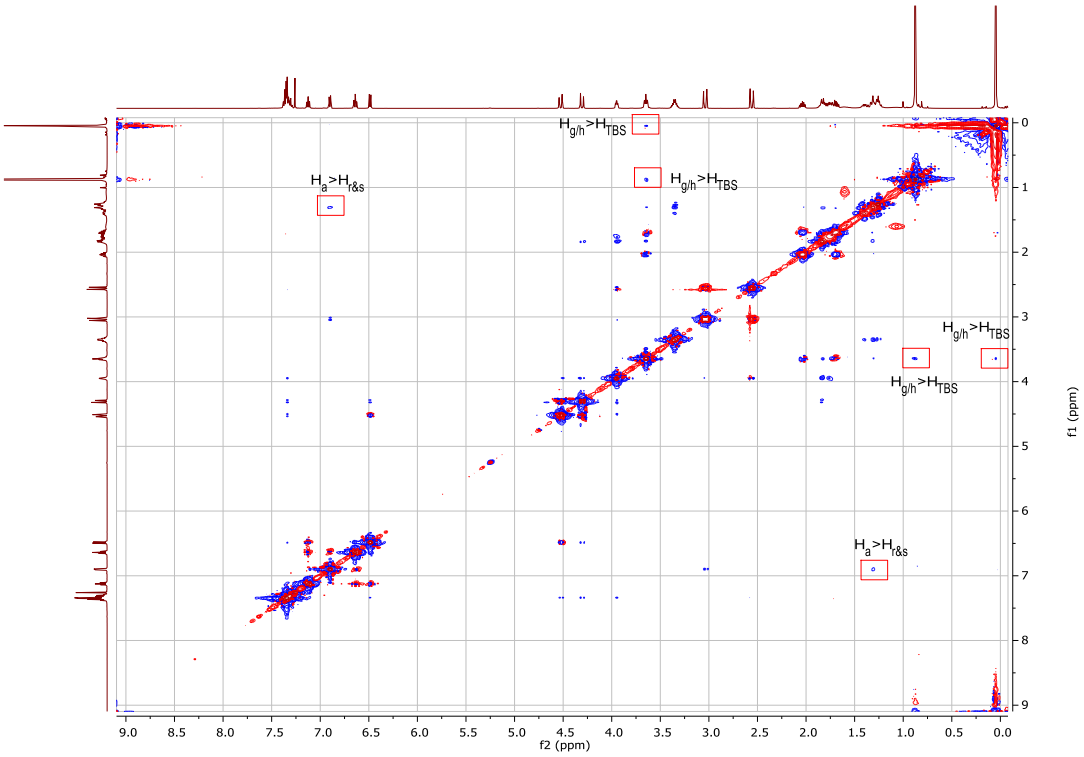

Figure 1.30 NOESY NMR ($CDCl_3$) of Alcohol **81**

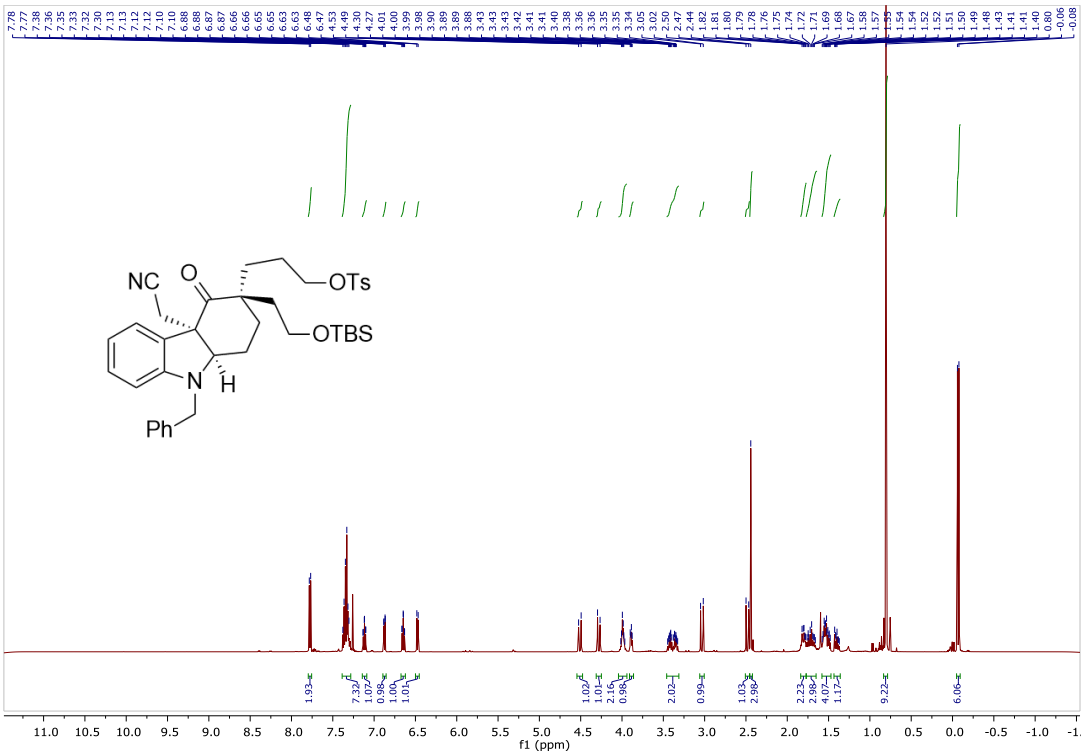

Figure 1.31 ^{1}H-NMR (500 MHz, $CDCl_3$) of Tosylate **82**

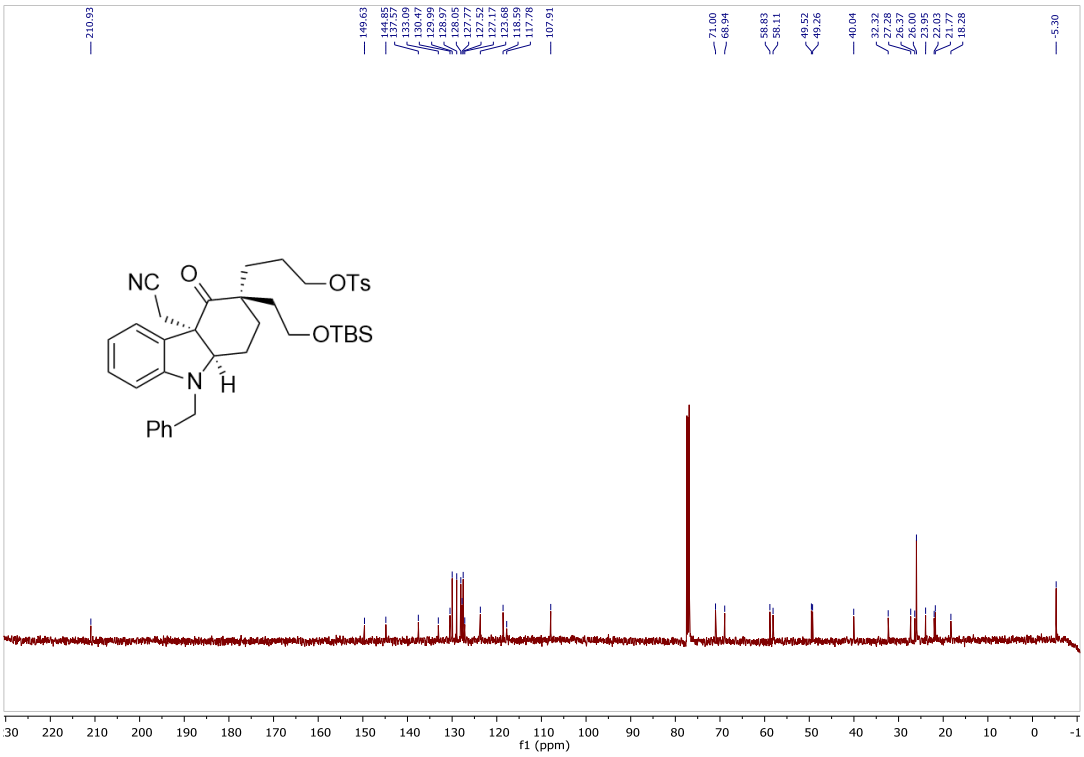

Figure 1.32 ^{13}C-NMR (125 MHz, $CDCl_3$) of Tosylate **82**

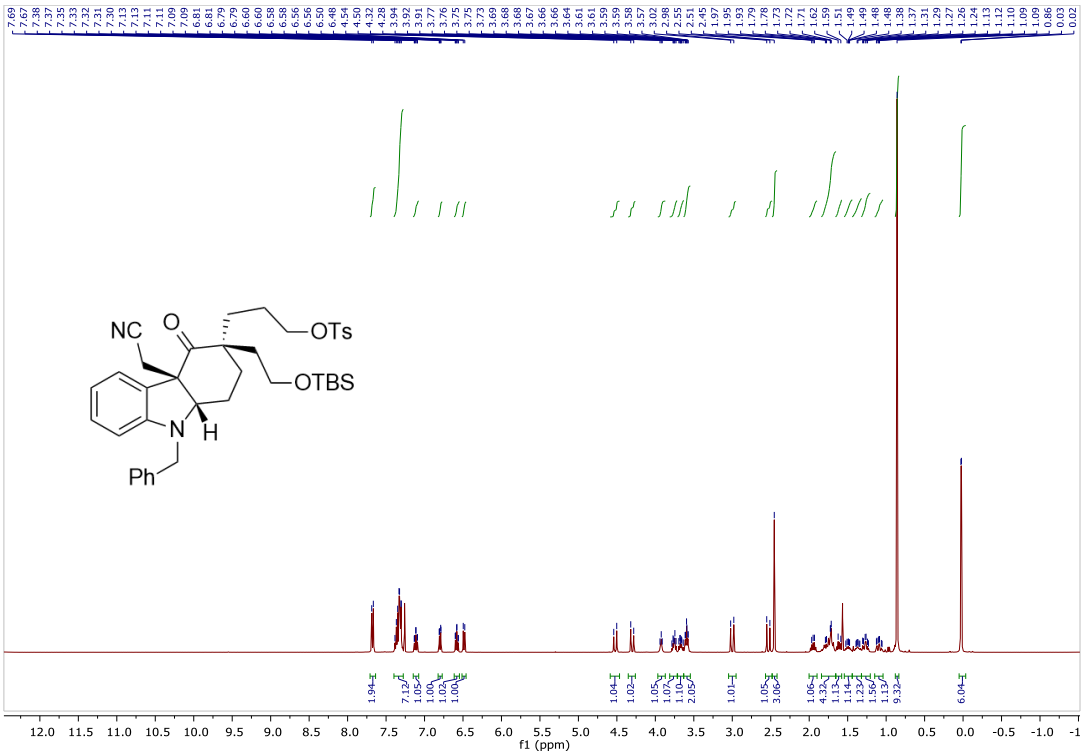

Figure 1.33 ^{1}H-NMR (400 MHz, $CDCl_3$) of Tosylate **83**

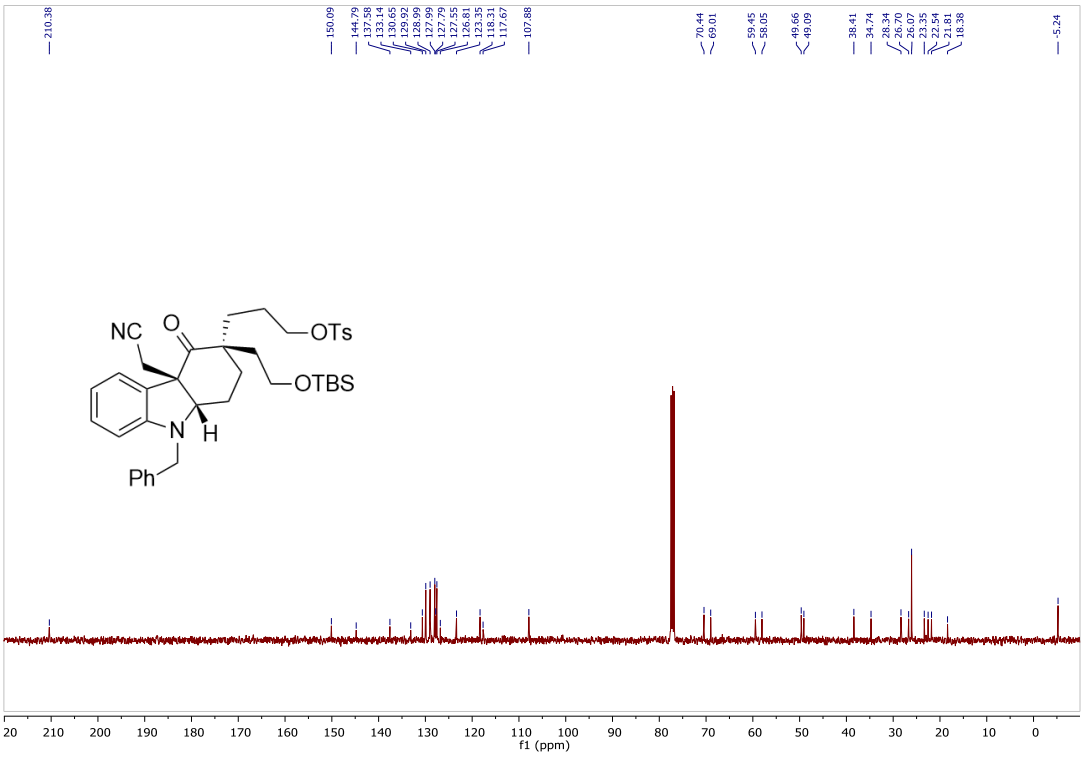

Figure 1.34 ^{13}C-NMR (100 MHz, $CDCl_3$) of Tosylate **83**

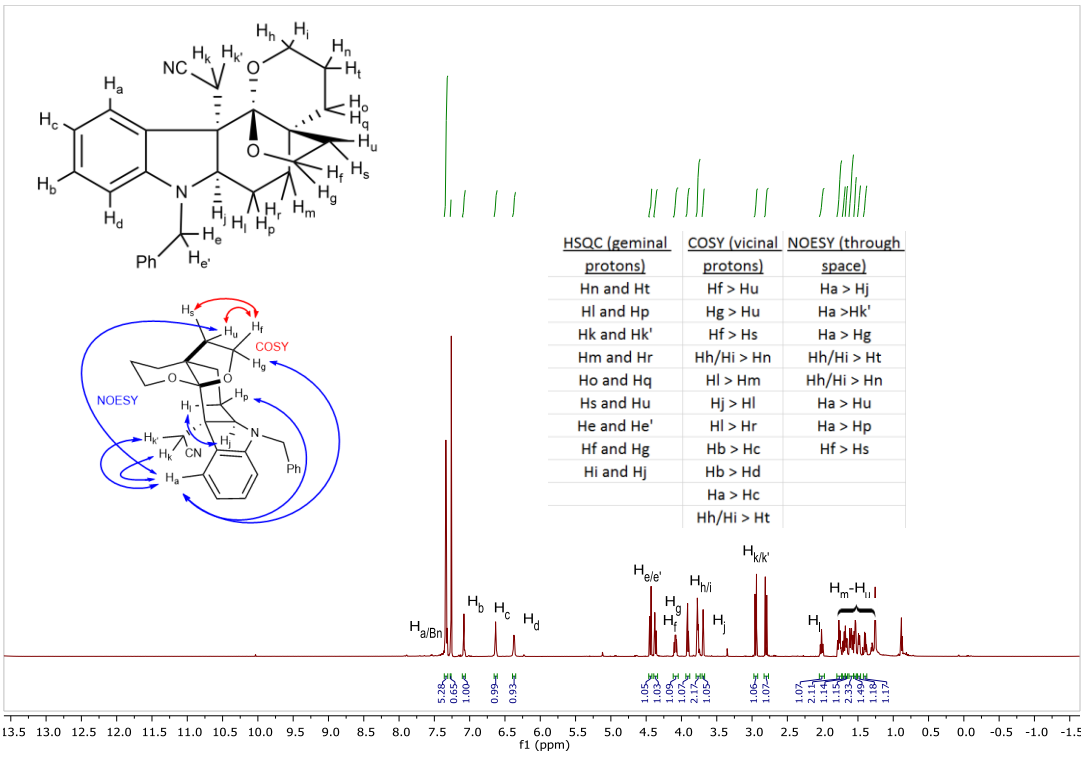

Figure 1.35 ^{1}H-NMR (400 MHz, $CDCL_3$) of Ketal **84**

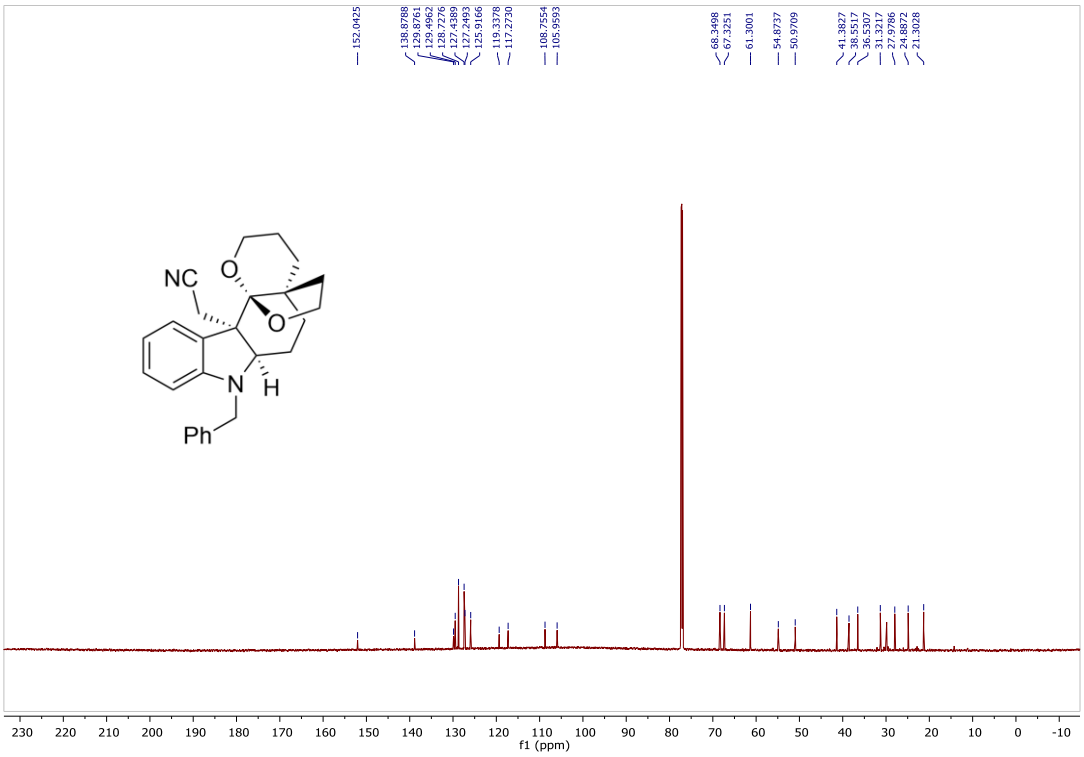

Figure 1.36 ^{13}C-NMR (100 MHz, $CDCL_3$) of Ketal **84**

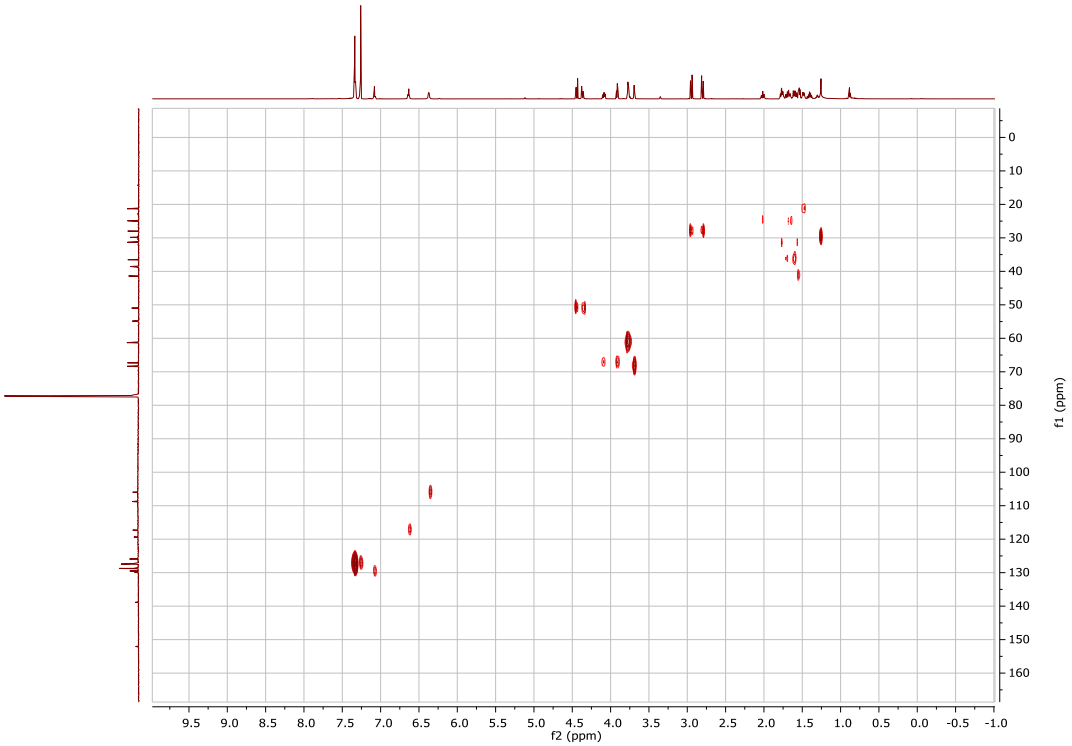

Figure 1.37 HMQC NMR ($CDCl_3$) of Ketal **84**

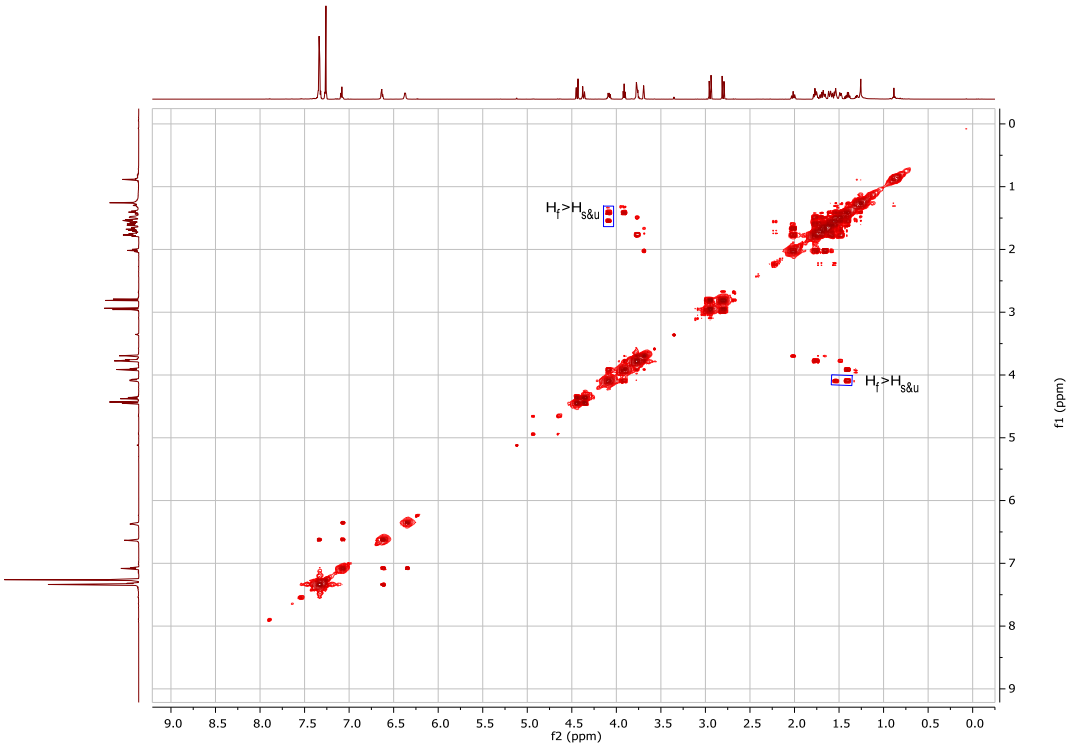

Figure 1.38 ^{1}H-^{1}H COSY NMR ($CDCl_3$) of Ketal **84**

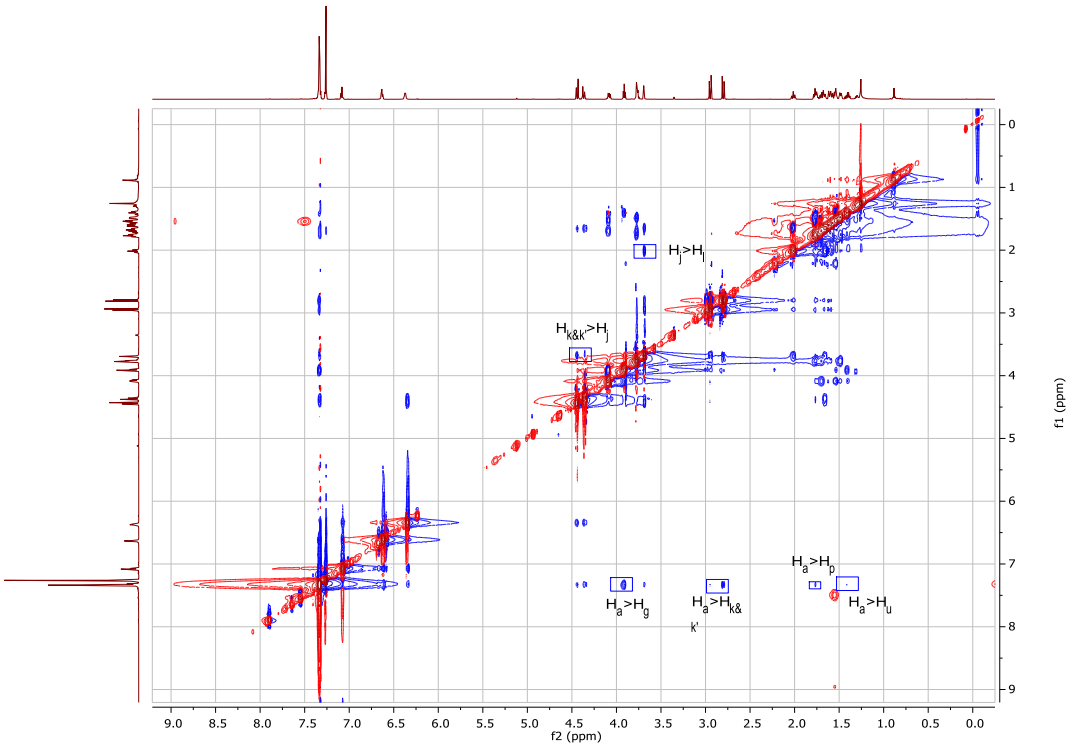

Figure 1.39 NOESY NMR ($CDCl_3$) of Ketal **84**

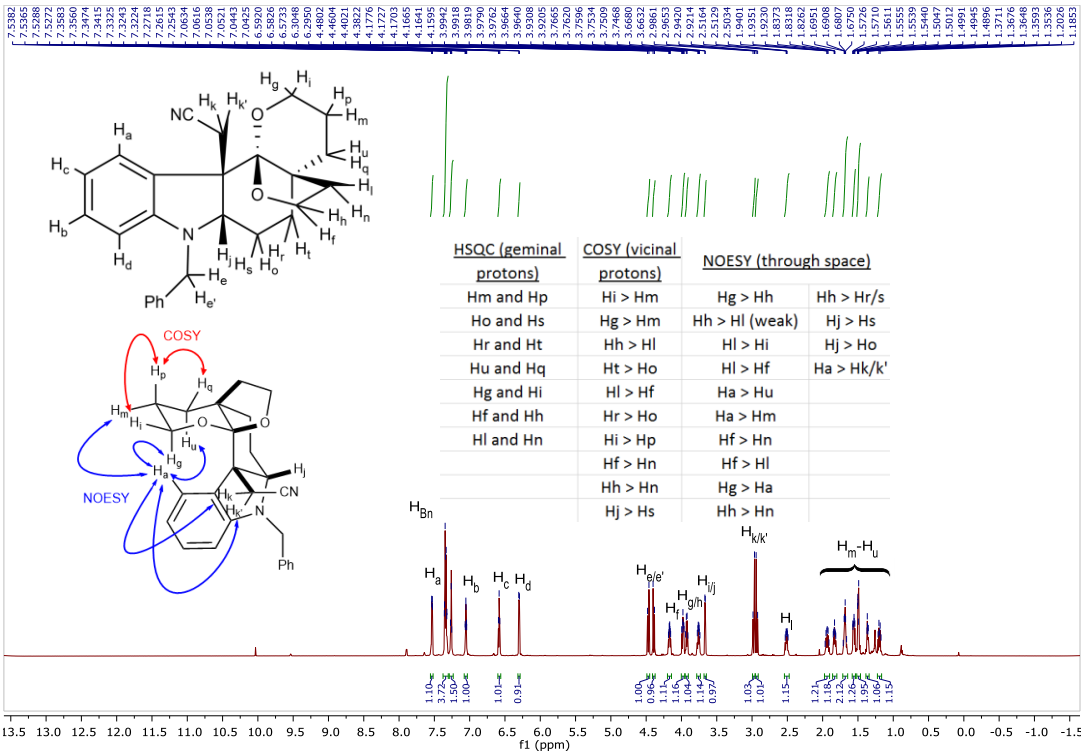

Figure 1.40 ^{1}H-NMR (500 MHz, $CDCl_3$) of Ketal **85**

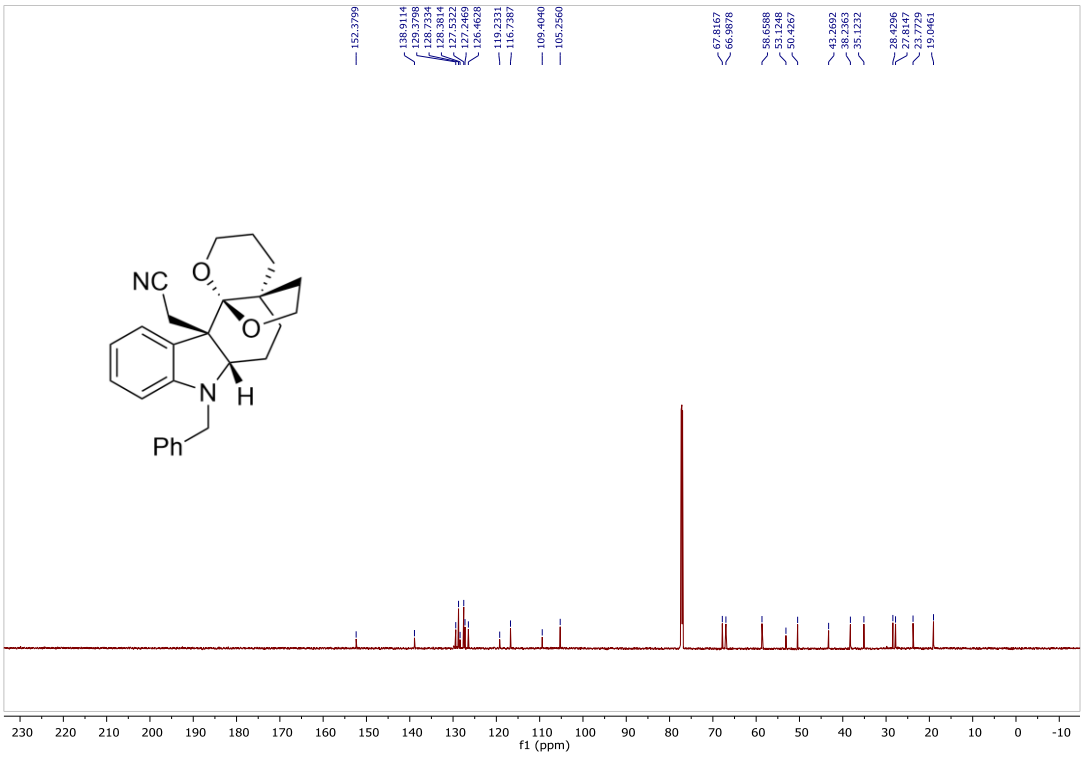

Figure 1.41 ^{13}C-NMR (125 MHz, $CDCl_3$) of Ketal **85**

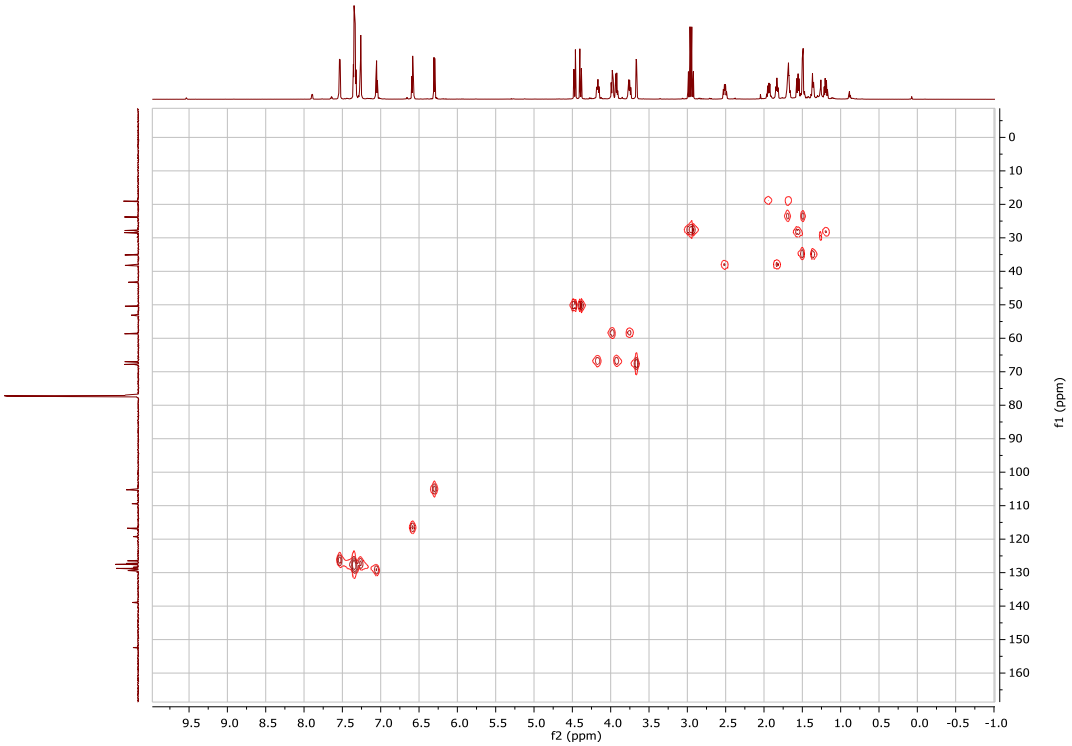

Figure 1.42 HMQC NMR ($CDCl_3$) of Ketal **85**

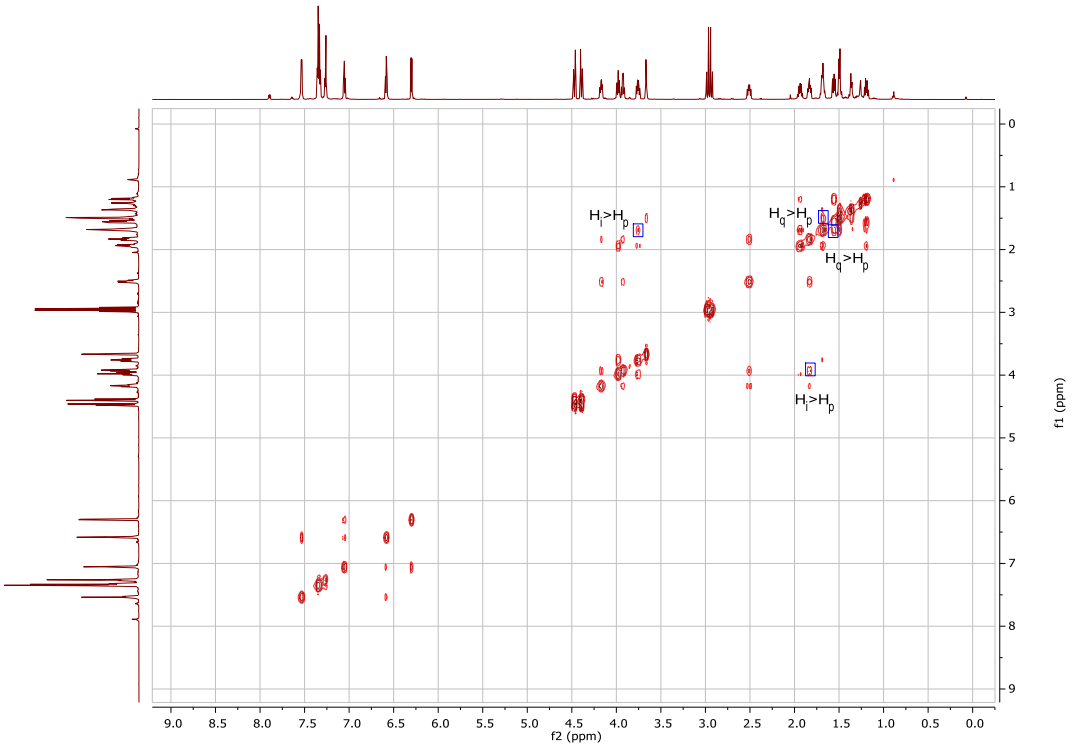

Figure 1.43 ^{1}H-^{1}H COSY NMR ($CDCl_3$) of Ketal **85**

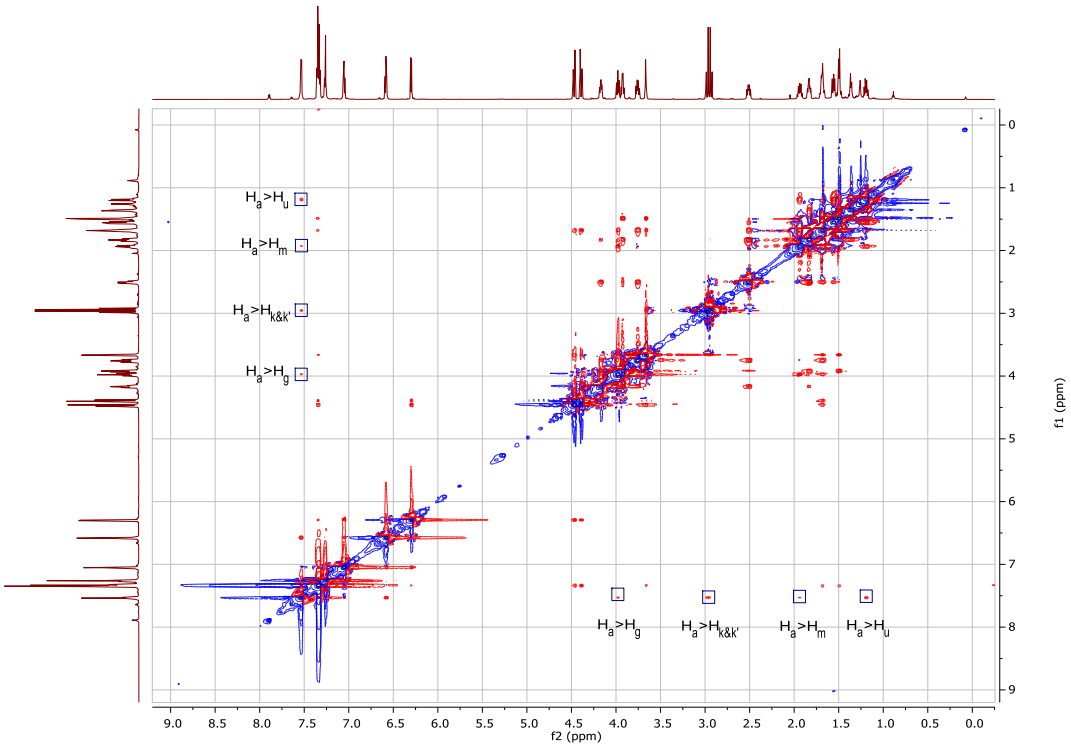

Figure 1.44 NOESY NMR ($CDCl_3$) of Ketal **85**

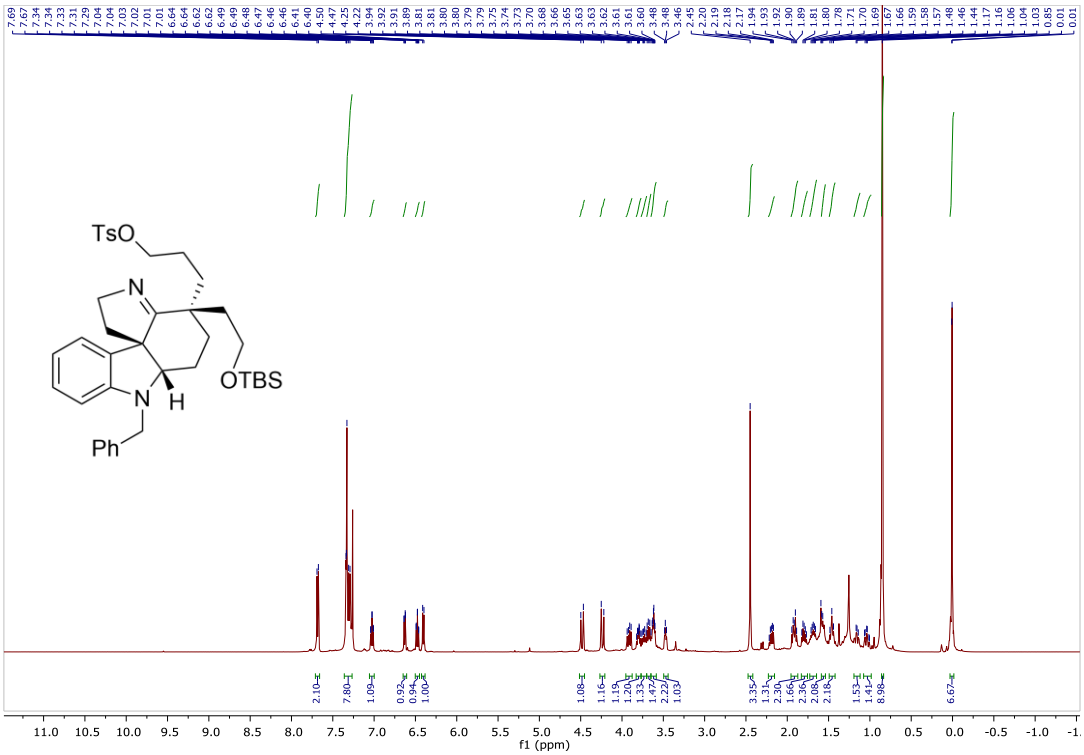

Figure 1.45 ^{1}H-NMR (500 MHz, $CDCl_3$) of Imine **86**

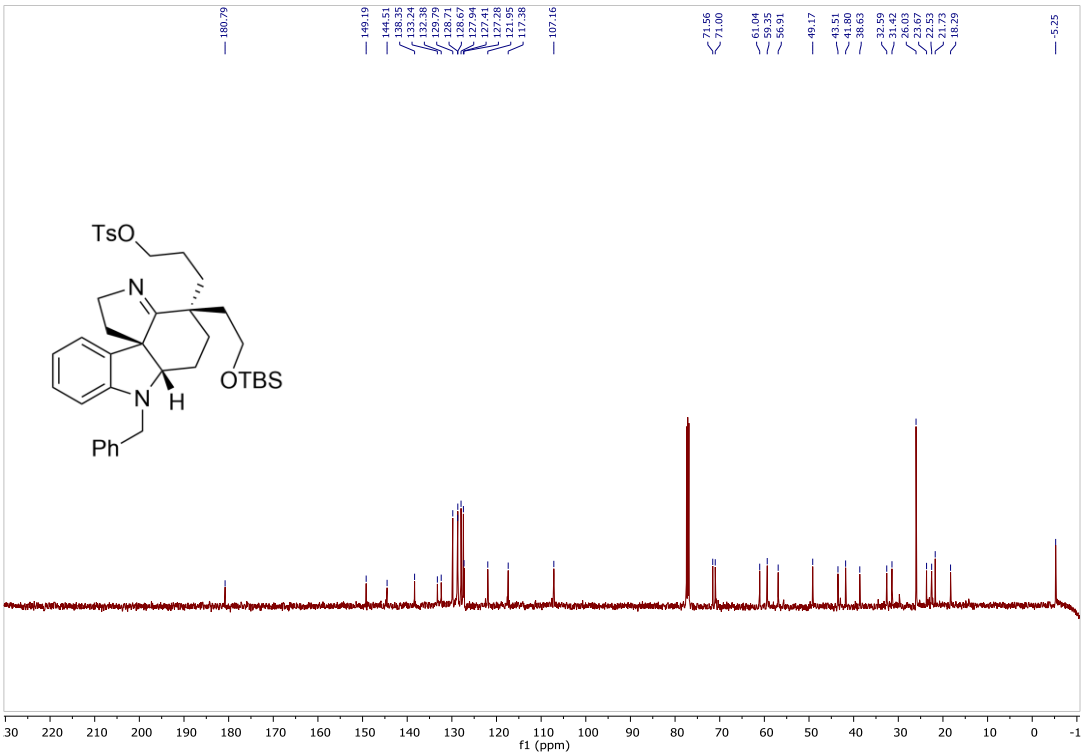

Figure 1.46 ^{13}C-NMR (125 MHz, $CDCl_3$) of Imine **86**

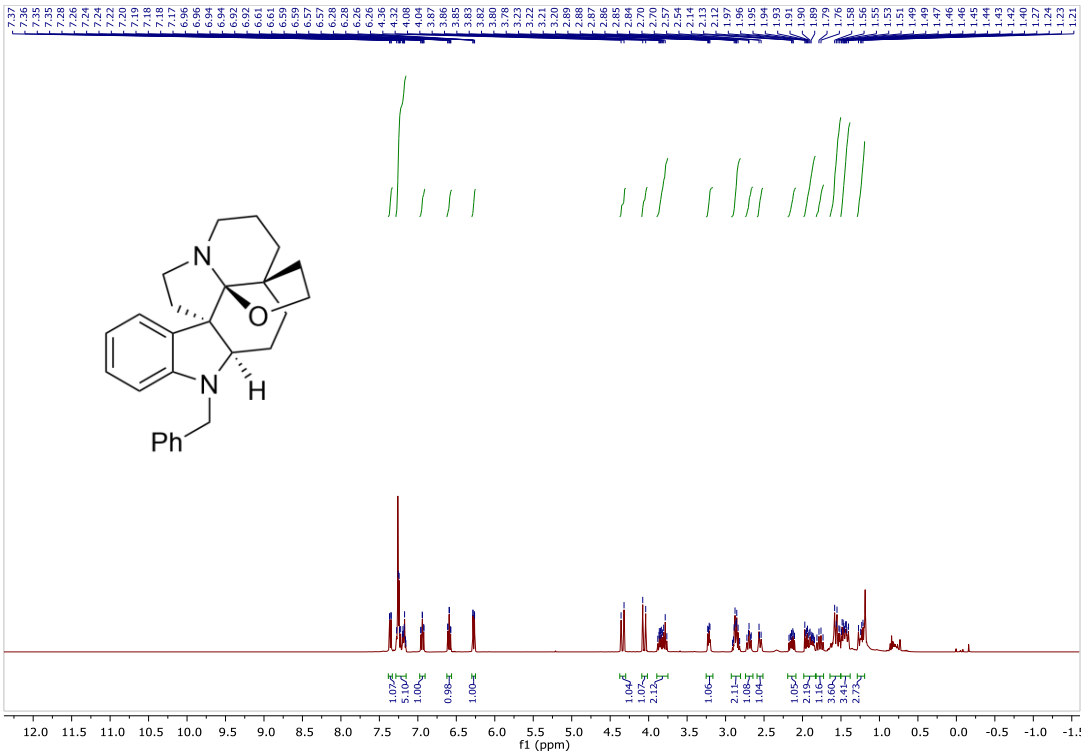

Figure 1.47 ^{1}H-NMR (400 MHz, $CDCl_3$) of Benzylated Fendleridine **87**

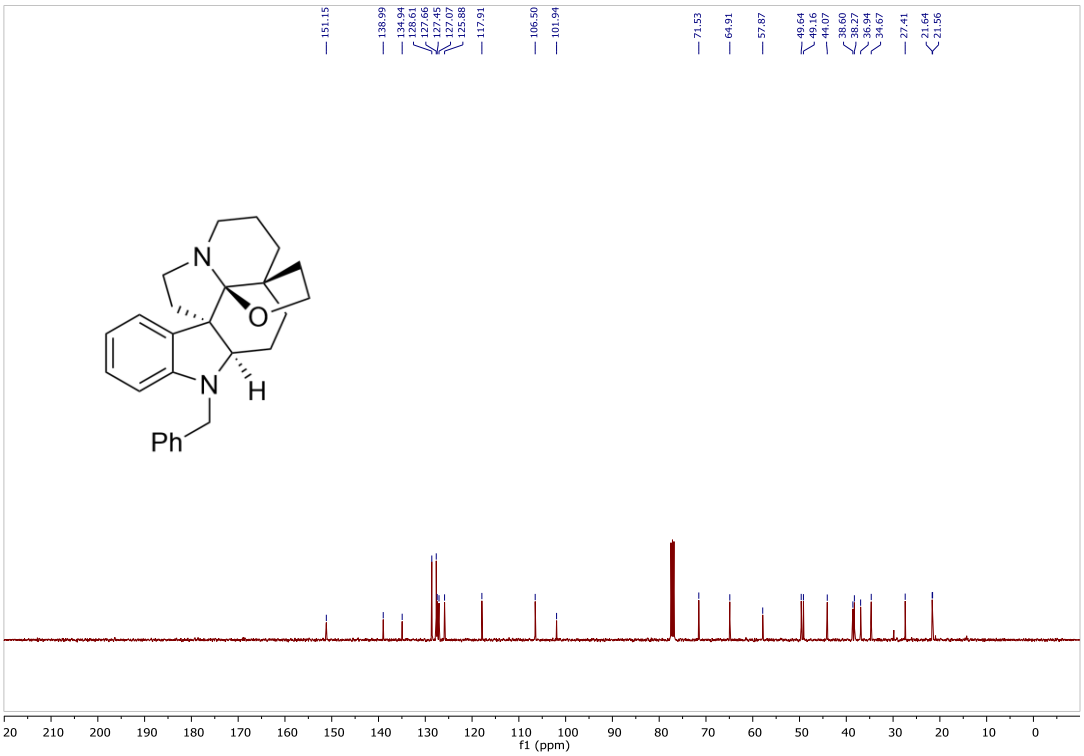

Figure 1.48 ^{13}C-NMR (100 MHz, $CDCl_3$) of Benzylated Fendleridine **87**

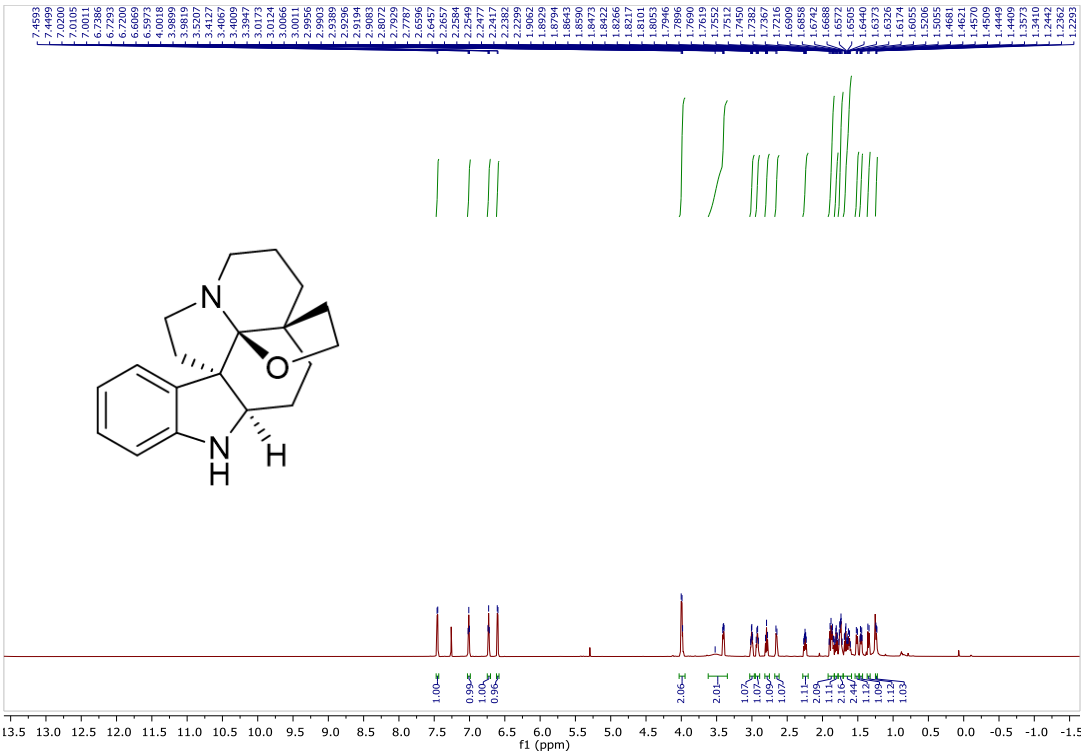

Figure 1.49 ^{1}H-NMR (800 MHz, $CDCl_3$) of **(+)**-Fendleridine **1**

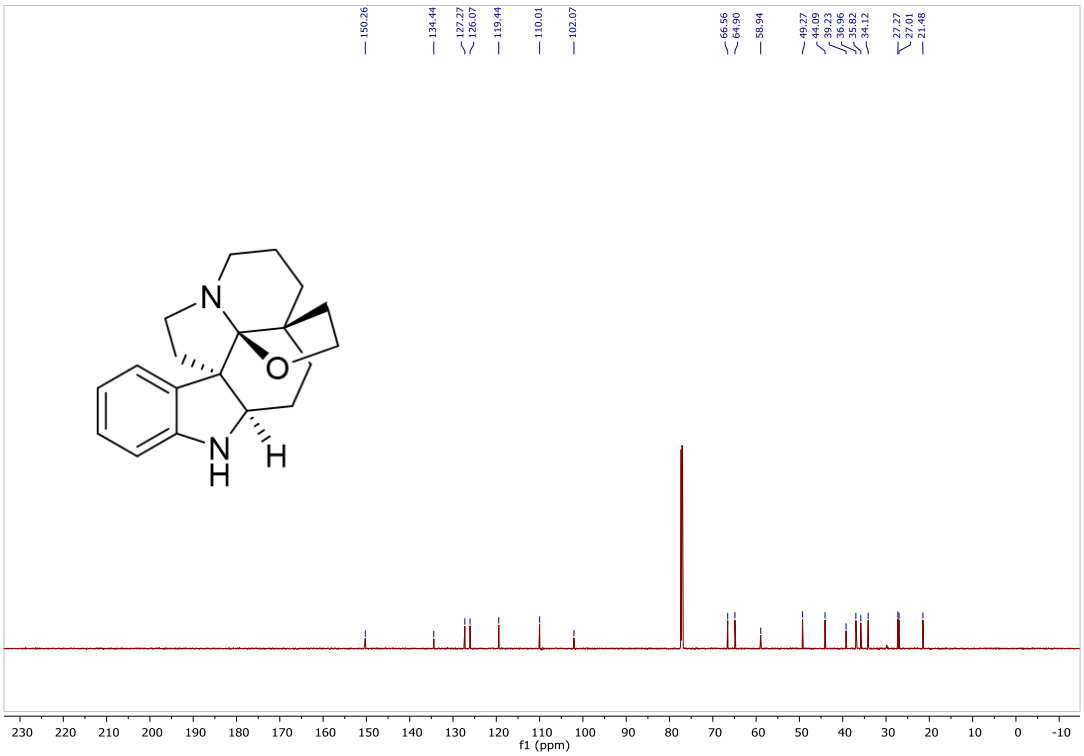

Figure 1.50 ^{13}C-NMR (200 MHz, $CDCl_3$) of **(+)**-Fendleridine **1**

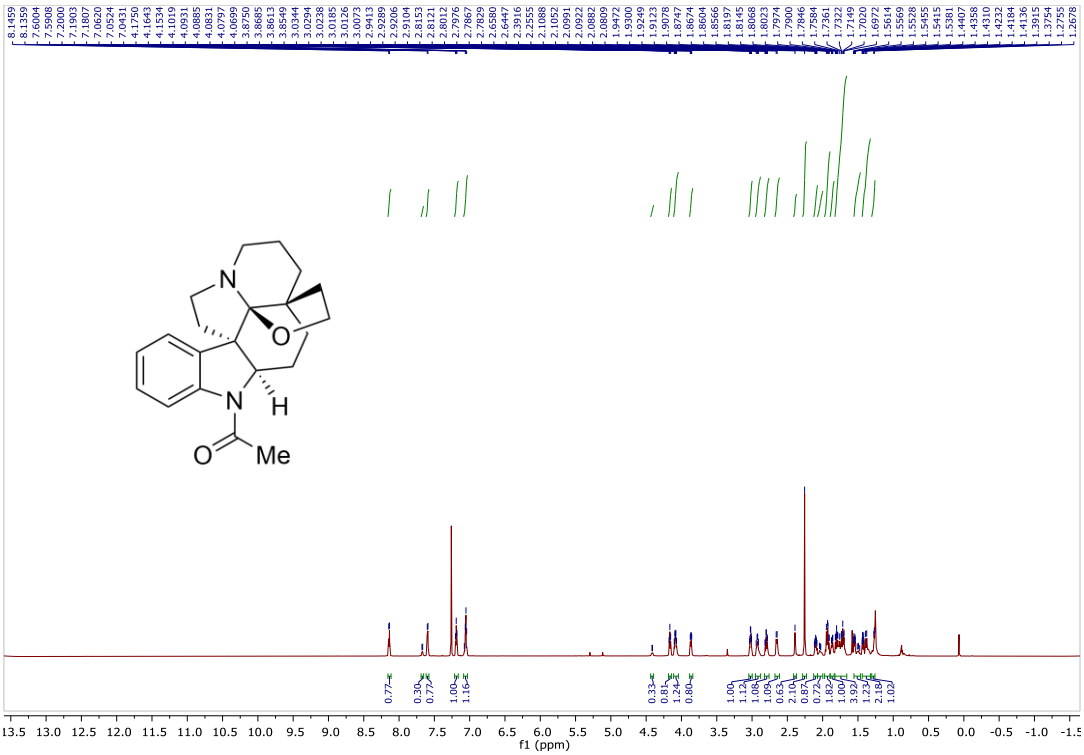

Figure 1.51 ^{1}H-NMR (800 MHz, $CDCl_3$) of **(+)**-Acetylaspidoalbidine **2**

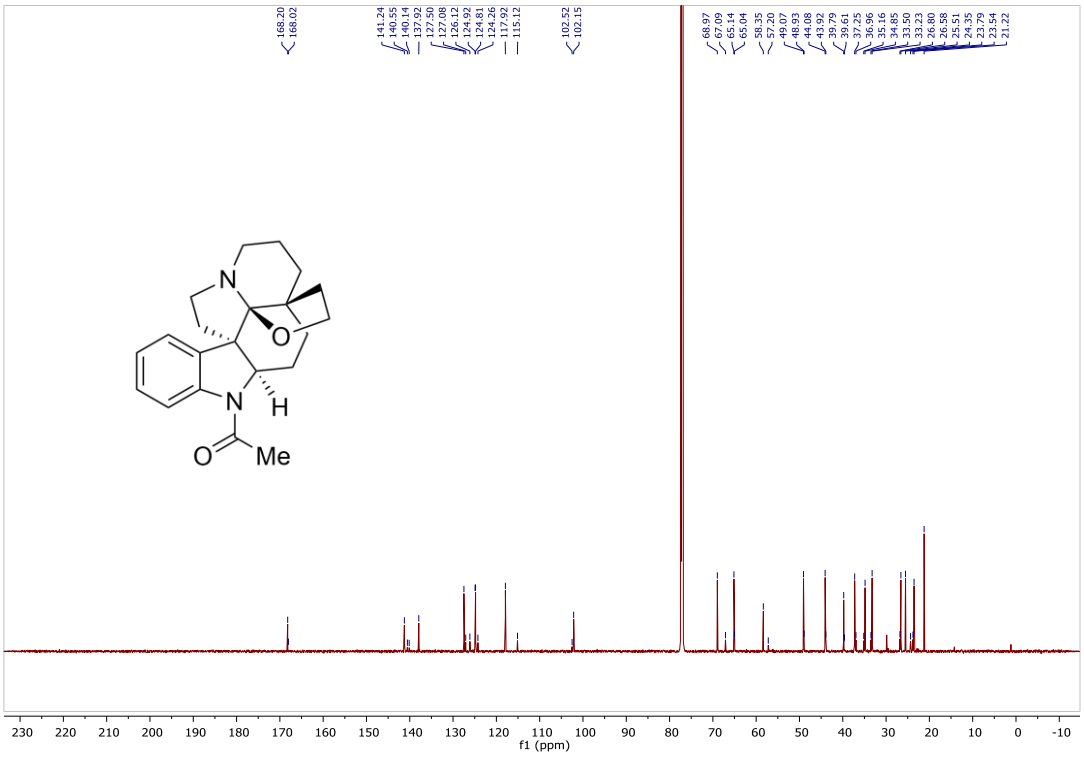

Figure 1.52 ^{13}C-NMR (200 MHz, $CDCl_3$) of **(+)**-Acetylaspidoalbidine **2**

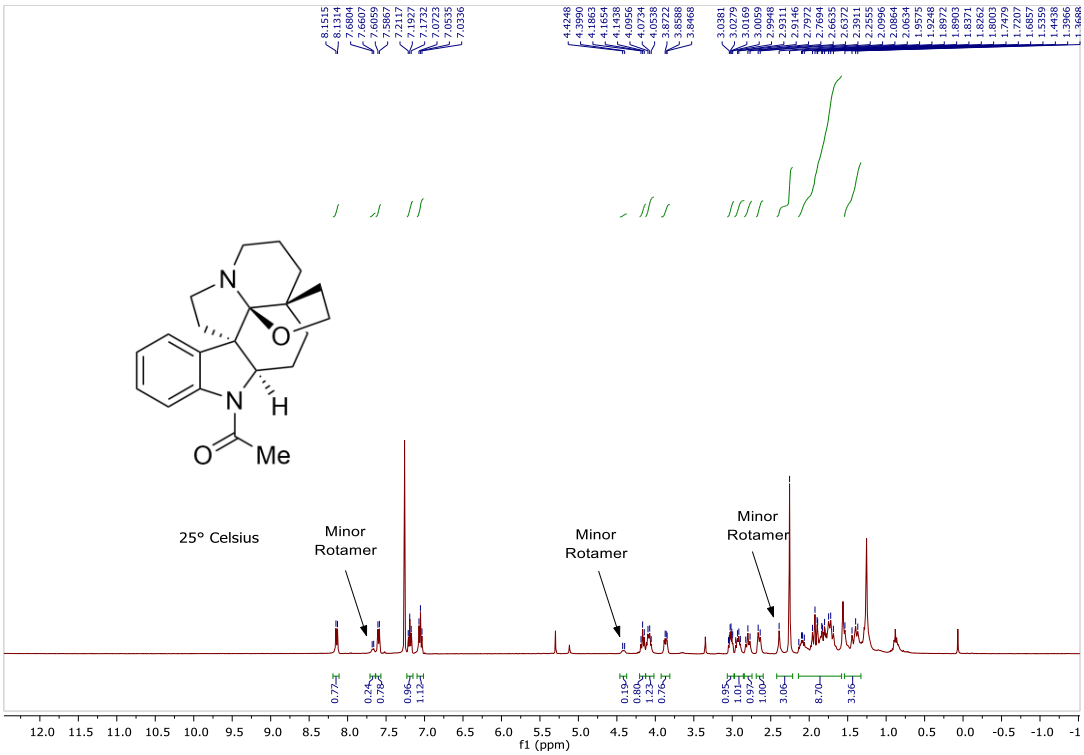

Figure 1.53 ^{1}H-NMR (400 MHz, $CDCl_3$) Experiment of **(+)**-Acetylaspidoalbidine **2** at 25°C

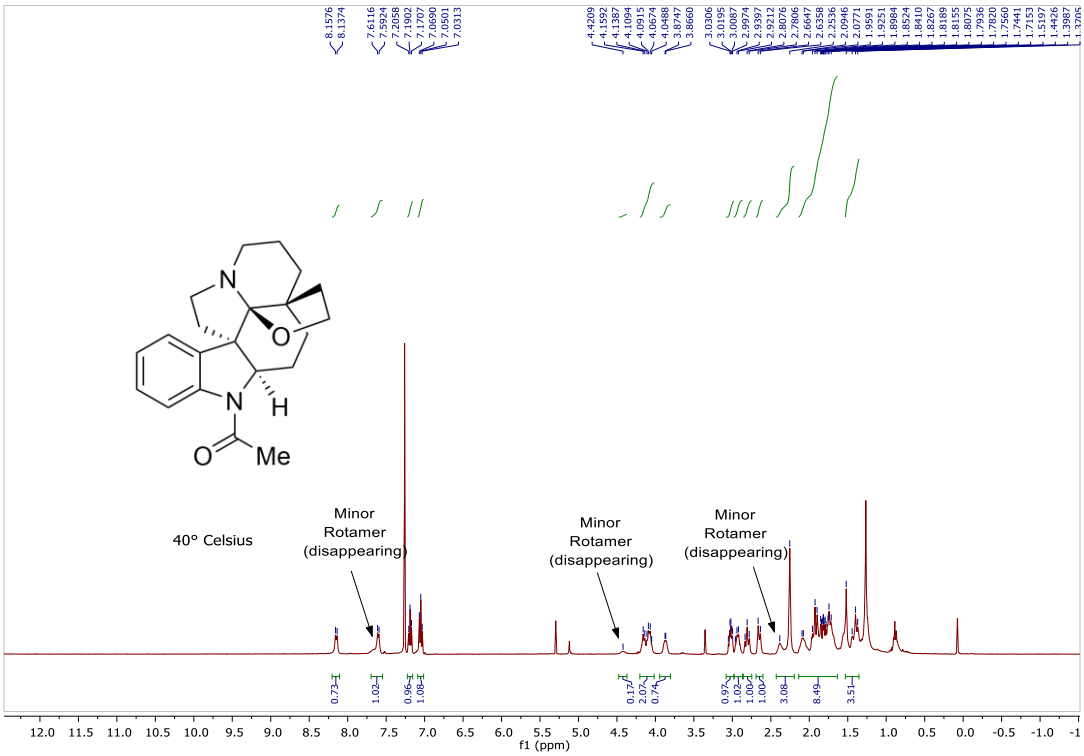

Figure 1.54 ^{1}H-NMR (400 MHz, $CDCl_3$) Experiment of **(+)**-Acetylaspidoalbidine **2** at 40°C

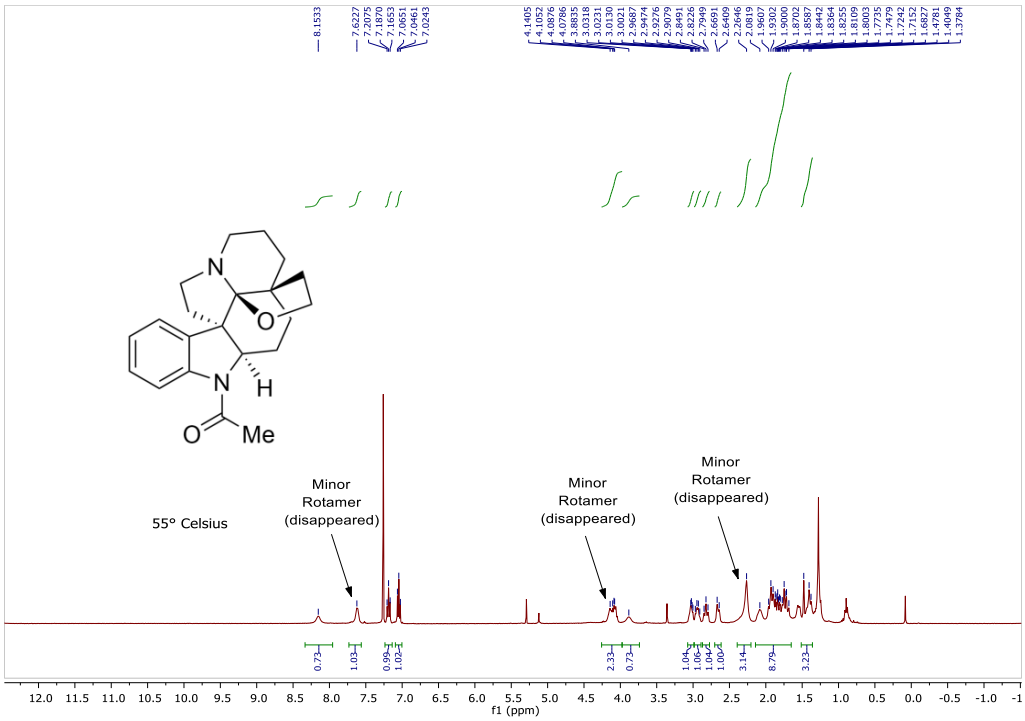

Figure 1.55 ^{1}H-NMR (400 MHz, $CDCl_3$) Experiment of **(+)**-Acetylaspidoalbidine **2** at 55°C

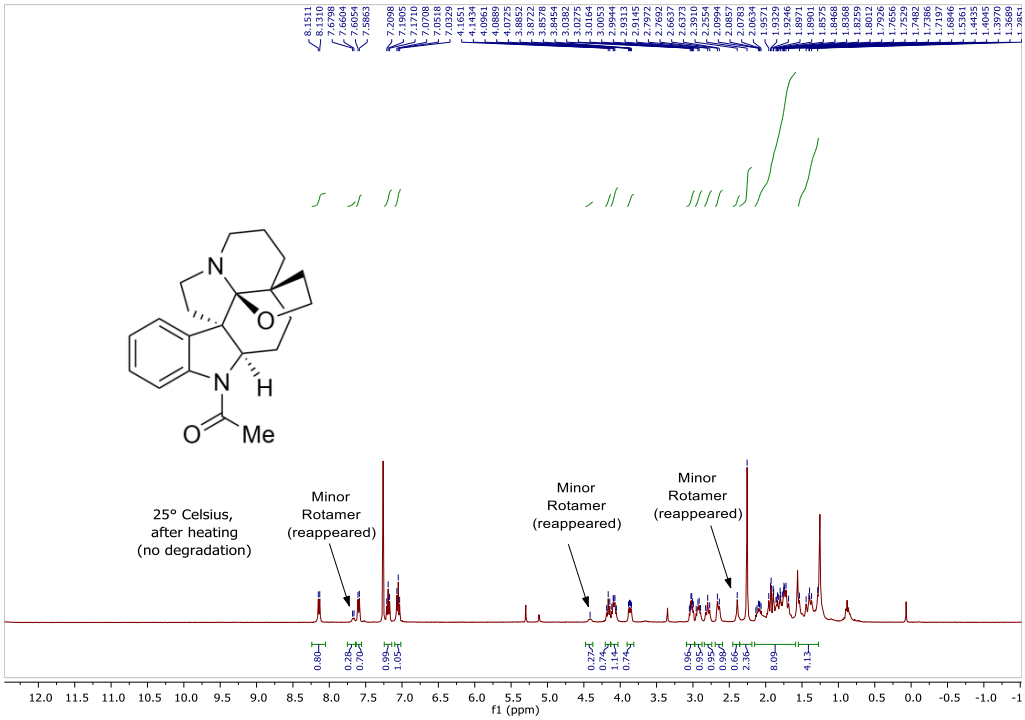

Figure 1.56 ^{1}H-NMR (400 MHz, $CDCl_3$) Experiment of **(+)**-Acetylaspidoalbidine **2** at 25°C (After cooling back down)

CHAPTER 2. A NOVEL COPPER-CATALYZED CROSS COUPLING AND ITS APPLICATION IN THE SYNTHESIS OF SPLICEOSTATIN DERIVATIVES

We developed and optimized a model substrate reaction in which we were able to cross couple an organostannyl furan with allyl bromide using catalytic amounts of CuI under ambient conditions. We then show the application of this reaction in our synthesis of the Spliceostatin and Thailanstatin (FR901464 family) THP amine core (Figure 2.1, highlighted in red). During this synthesis we also optimized the cheletropic formation of a sulfolene group to use as a novel diene protecting group utilizing non-toxic methods. Finally, we were able to undergo an optimized 4-step one-column asymmetric sequence in 60% overall yield and after two more transformations yield the formal synthesis intermediate containing 4 stereocenters as the sole isomer as detected via ^{1}H NMR. Discussion of the prior use of Cu-only catalyzed Stille reactions and their mechanism as well as brief discussion on the biological significance of Spliceostatins is also described within.

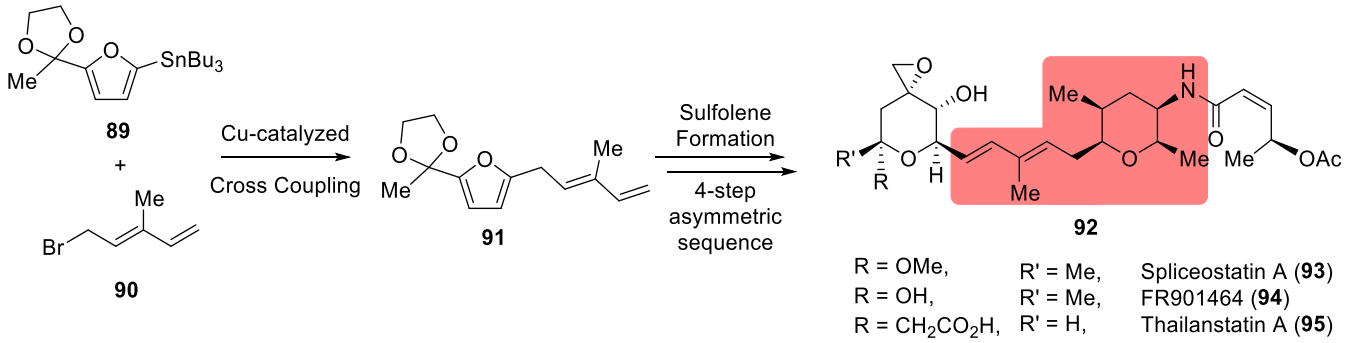

Figure 2.1 Synthesis of the Spliceostatin and Thailanstatin Tetrahydropyranyl Amine Core

2.1 Introduction

The first examples of the Stille Coupling were shown by the groups of Eaborn[39] and Kosugi-Migita.[40,41] However, the major contributions and mechanistic insight provided by Stille in 1978[42] provide reasoning for the reaction adopting his namesake (Figure 2.2). The foundation put forth by this seminal work is widely accepted to have laid the groundwork for palladium-catalyzed cross-coupling reactions, of which he would have likely shared the 2010 Nobel Prize had it not been for his untimely death at the age of 59.[43,44] The Stille cross-coupling is a widely used reaction in organic synthesis in both academia and industry, due to its broad substrate scope & ease of use.[45] Traditionally, palladium catalysts are used in the reaction. However due to the costly nature of palladium, copper catalysts have been put forth as a desirable alternative.

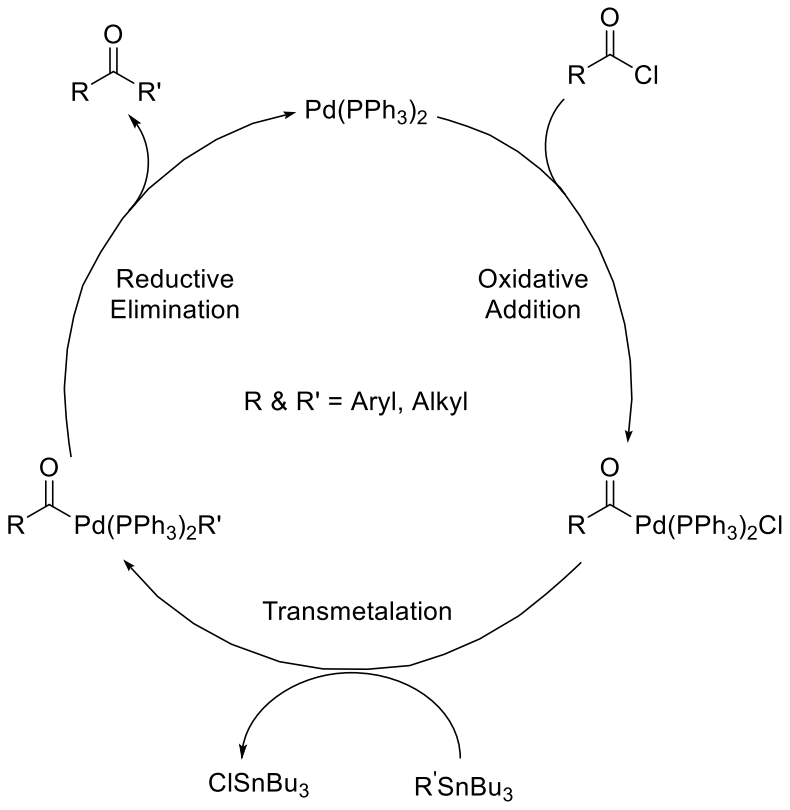

Figure 2.2 Catalytic Cycle Proposed in Stille's Seminal Work

2.2 The Copper Effect in the Stille Cross Coupling

The "Copper Effect" in the Stille coupling is a well-documented phenomenon in which copper can help improve the efficiency of otherwise sluggish palladium-catalyzed Stille reactions.[46,47] Select results from the seminal work in this area by Liebeskind and coworkers are shown in Table 2.1 below. Double the stoichiometric amount of CuI in ratio to the Pd catalyst resulted in over a 100-fold increase in rate and higher yields (entries 1 & 2). Use of less strongly chelating ligands also increased the rate dramatically (entries 3-5). It was theorized that the copper effect itself is intimately dependent on the solvent and ligands used in the Pd^{II} transitional step.

Table 2.1 Selected Results from Liebeskind "Copper Effect" Work

Entry	Ligand	Pd:L:CuI	10^5 k_{obs} (min^{-1})	HPLC Yield
1	PPh_3	1:4:0	2.66	85
2	PPh_3	1:4:2	303	>95
3	F_5C_6-PPh_2	1:4:2	401	>95
4	$AsPh_3$	1:4:0	7,210	>95
5	$AsPh_3$	1:4:2	9,640	>95

A blank experiment from this work shown in Figure 2.3 shows use of only 5 mol % CuI at extremely elevated temperatures resulted in the desired coupling, albeit in poor yield. From this, it was proposed that a copper/tin transmetallation may be occurring, thus it was theorized that copper alone may be able to catalyze the reaction in lieu of palladium.[46]

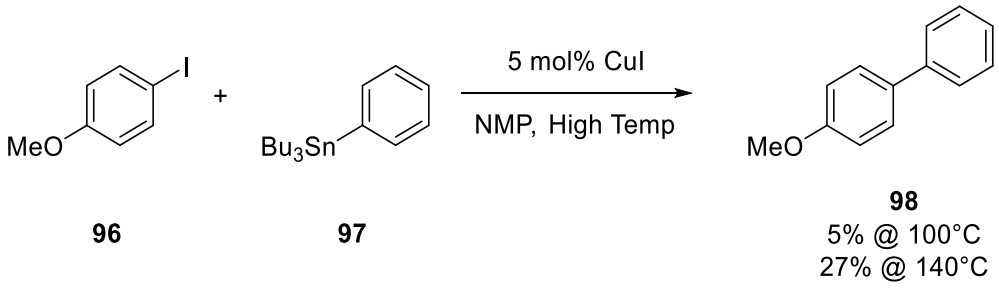

Figure 2.3 Liebeskind's Example of a Copper-only Catalyzed Stille Coupling

2.2.1 Prior Examples of Copper-only Catalyzed Stille Couplings

There are numerous instances throughout the literature reporting Cu-only catalyzed Stille cross-couplings. However, all either require stoichiometric amounts of copper, higher reaction temperatures or harsher conditions, or show difficulty with regioselectivity when the option presents itself (some results are shown in Espinet and coworkers' 2015 *ACS Catalysis* review[45]). A brief review of each of the key papers are presented below in chronological order.

In Piers and Wong's 1993 JOC publication,[48] they reported on the intramolecular cyclizations of organostannanes using CuCl to form bicyclic systems, stating that in some cases the reactions proceeded more quickly and cleanly than their Pd(0)-catalyzed counterparts. The limitations to this work were that they used stoichiometric (>2.0 equivalents) of the copper salts heating the reactions to >60°C in most cases, along with all reactions being solely intramolecular.

In Falck and coworkers' 1995 JACs publication,[49] the authors were able to perform the coupling of sp^3 centers through the use of catalytic amounts of CuCN (8 mol %). The limitations to this work include the use of sealed tube reactions and heat (typically >60°C, sometimes up to 110°C), as well as regioselectivity issues, and limited substrate scope as the reactions weren't inclined to be as efficient without use of a heteroatom such as a thioester to chelate to the tin and copper centers during the catalytic cycle (Figure 2.4). It's also worth noting that in one case they were able to get the reaction to proceed via use of no catalyst at all, although they state fresh glassware was used and no trace Pd/Cu was likely present, prompting skepticism on what was catalyzing their reaction.

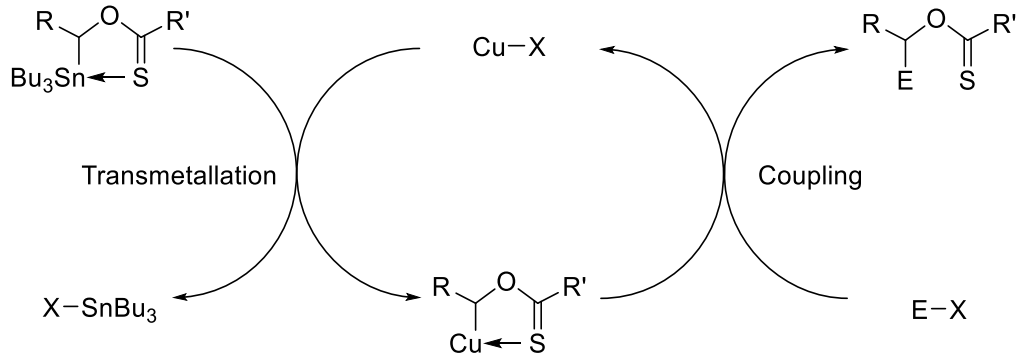

R = Alkyl, Aryl, R' = Acyl, Aryl, E = Allyl, Aryl, Acyl

Figure 2.4 Falck and coworkers' Proposed Catalytic Cycle

In Takeda and coworkers' 1995 Chem Letters publication,[50] the authors were able to show the intermolecular coupling of vinyl groups through the use of CuI. Limitations to this work include stoichiometric amounts of CuI being used (0.5-1.0), along with DMSO being indispensable as a cosolvent, and regioselectivity issues being strongly present. It's worth noting that in this paper they used Na_2CO_3 as a suppressant to help suppress the formation of the protodestannylated byproduct.

In Liebeskind and coworkers' follow-up 1996 JACs publication,[51] the authors showed the use of copper (I) thiophenecarboxylate (CuTC) to couple aryl and styryl compounds at room temperature. The limitations to this work include stoichiometric amounts of copper needed (1.5 equivalents), and that NMP was indispensable as a solvent. It's also worth noting they propose the catalytic cycle for the Sn/Cu transmetallation from their seminal work in this publication, similar to that of Figure 2.4.

In Kang and coworkers' 1997 JOC publication,[52] the authors showed the use of catalytic amounts of CuI (10 mol %) in coupling of aryl and vinyl substrates. The limitations to this work included the use of high temperatures (90-120°C) as well as NMP again being indispensable as the solvent. It's also worth noting that within this publication they screened different additives and found that NaCl addition presumably drives the reaction forward as it eliminates reversibility in the transmetallation step (discussed in Chapter 2.2.2). They also showed that $MgBr_2$ instead of CuI worked nearly as efficiently as a catalyst, providing thought that heat may be playing a larger role in the mechanism in this case.

In Nudelman and coworkers' 1999 Synlett publication,[53] the authors showed the use of catalytic amounts of CuCl (10 mol %) in the coupling of furyl and allyl substrates. The limitations to this work include the indispensable use of NMP/DMF as the solvents, HMPA as a cosolvent (which is known heavily for its toxicity) and needing to heat the reactions to 90°C to achieve their desired transformations.

In Burton and coworkers' 2005 Organic Letters publication,[54] the authors showed the use of catalytic amounts of CuI (10 mol %) in the coupling of vinyl organostannanes and acyl chlorides. The limitations to this work include substrate scope as apparent fluorinated compounds with vinyl esters *cis* to the stannane were needed, with carbonyl chelation onto the copper center occurring similarly to that of Falck's work.[49] Also, no typical vinyl or allyl couplings were shown. It's worth noting that within this publication, a supposed organocopper intermediate formed in equilibrium

from the organostannane using a stoichiometric amount of CuI and was measured via ^{19}F NMR and compared to one that was made via means of zincate formation and subsequent copper displacement (Figure 2.5). As the spectral data matched, it then became the first reported instance in which the Cu/Sn transmetallation put forth by Liebeskind and coworkers[46] was supported mechanistically.

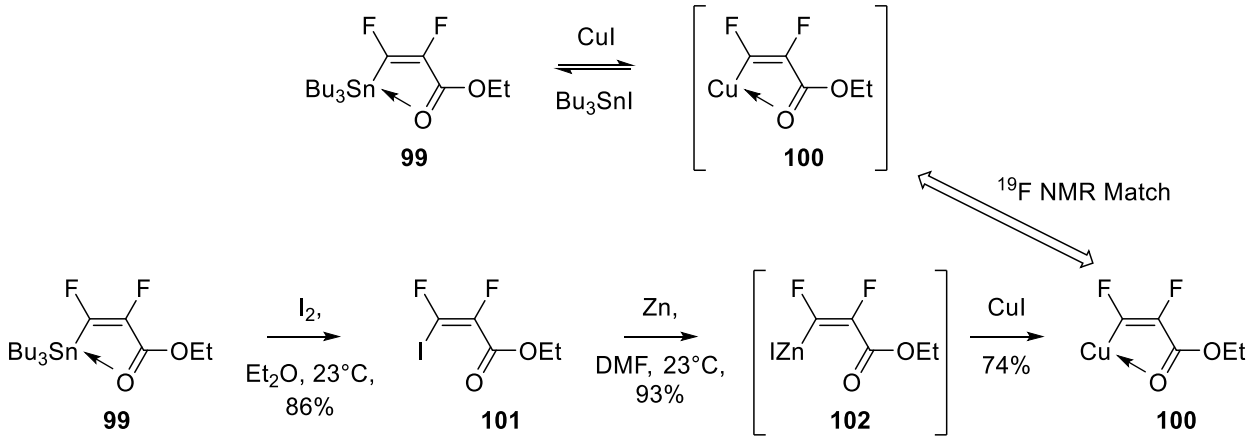

Figure 2.5 Burton and coworkers' Mechanistic Support for the Sn/Cu Transmetallation

2.2.2 Proposed Catalytic Cycle

The simplified mechanism put forth for the Pd-catalyzed Stille is shown below (Figure 2.6), yet it is worth noting that more extensive studies have been done to support whether the mechanism occurs via cyclic or open intermediates.[45] Alongside it is the "Copper Effect" proposed cocatalyzed cycle, in which copper is able to undergo the transmetallation with tin as supported,[54] and it's then theorized that the transmetallation of the palladium catalyst with the resultant organocuprate is much more facile than that of the palladium with organostannane, thus the rates of the reactions increase. Notably, copper salts have been reported to act as ligand scavengers, mitigating the retardation of free phosphines on the palladium center such as the case is with $Pd(PPh_3)_4$, and thus a possible dual role of copper salts is observed.[55]

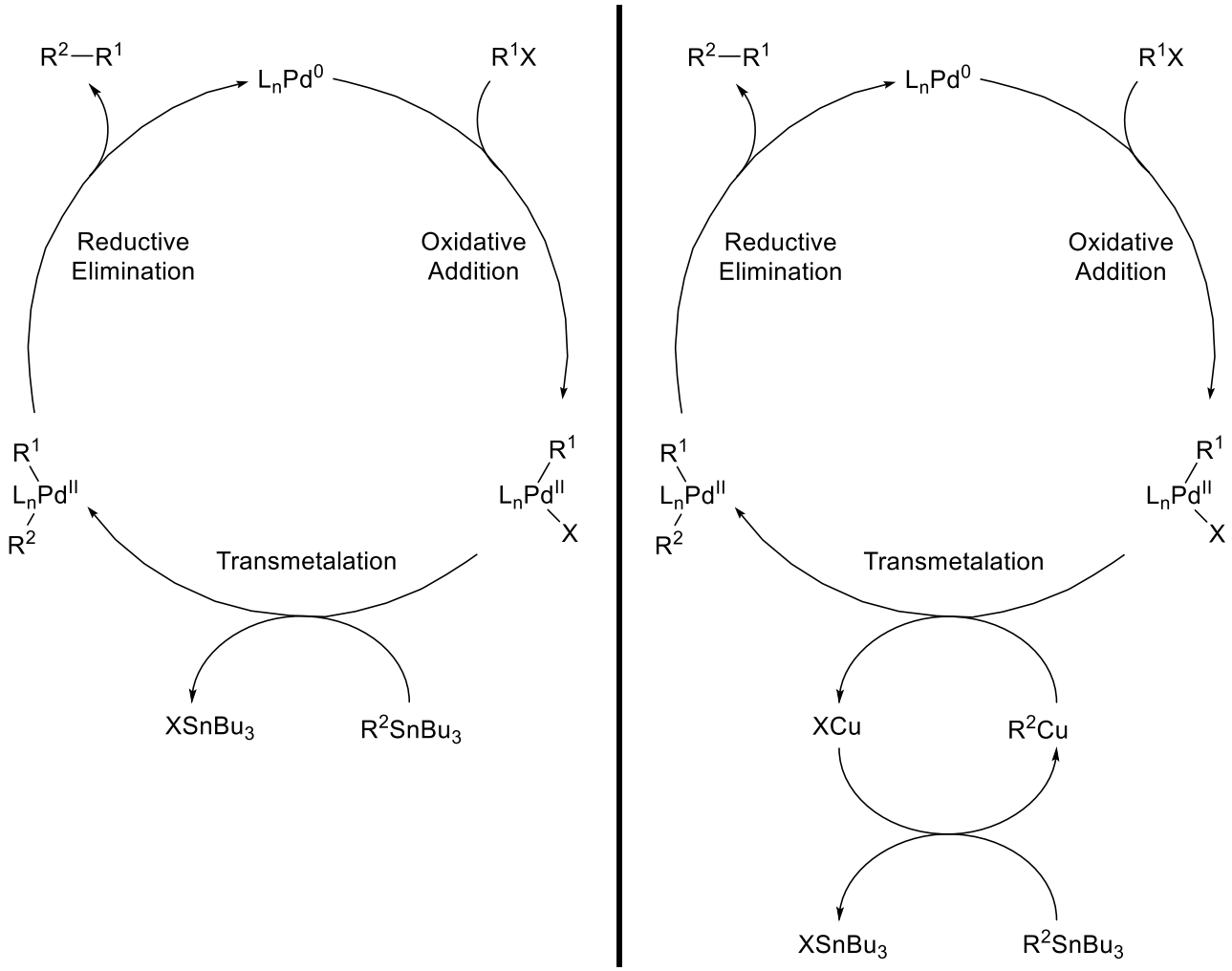

Figure 2.6 Traditional Catalytic Cycles for the Stille Coupling and the Copper-cocatalyzed Stille Coupling

The first instance of mechanistic insight into the copper-only catalyzed Stille cross coupling was done in a 2010 *Organometallics* publication by Lin and coworkers,[56] in which they performed DFT calculations with CuTC catalysts in stoichiometric amounts and observed the proposed energies. What they found was that S-coordination from the TC ligand wasn't essential, and that solvent ligation (in this case NMP) plays a very important role as the catalyst likely adopts a square-planar solvent-assisted intermediate. As supported by some prior DFT calculations,[57] the Cu(I) catalyst is likely undergoing oxidative addition to Cu(III), then reductive elimination to turn over the catalyst. The existence of Cu(III) intermediates is supported in the literature, both theoretically[58] and experimentally.[59] Based on these results, a proposed catalytic cycle is shown in Figure 2.7. Of note, in the case of the addition of a chloride/fluoride additive,[47,52,60] an off-cycle

transmetallation of the organotin halide and the respective lithium/sodium/potassium/ammonium salt can form a species that will drop out of the catalytic cycle, thus theoretically pushing forward the reaction via removal of the transmetallative reversible step. As opposed to the traditional Stille cycle, the oxidative addition and transmetallation steps are reversed in order. This is due to the likely Cu(III) square planar species not wanting to undergo transmetallation, and instead the Cu(I) organocuprate undergoing an oxidative addition instead acting as a Gilman-type intermediate.[61]

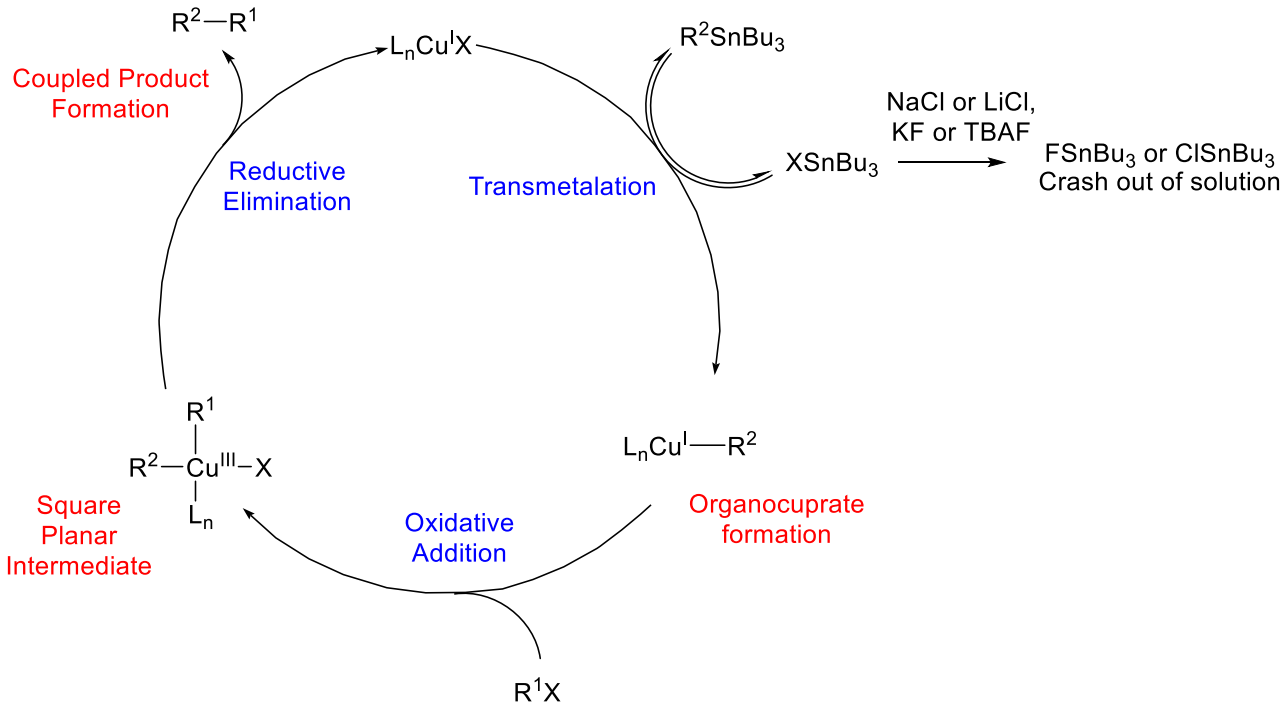

Figure 2.7 Proposed Catalytic Cycle for the Copper-Catalyzed Stille Reaction.

On a final note, one could also propose that instead of a Cu(III) center forming at all, once the organocuprate forms it could undergo simple S_N2 or S_N2' chemistry with the halide to do the alkylation instead (Figure 2.8). While this may be the case in some instances (more likely when stoichiometric amounts of copper salts are used), it could be ruled out by the presence of a homocoupled byproduct.[62] If this byproduct is seen, it would be supported that a Cu(III) intermediate is forming, as this is the only pathway in which this byproduct would form.

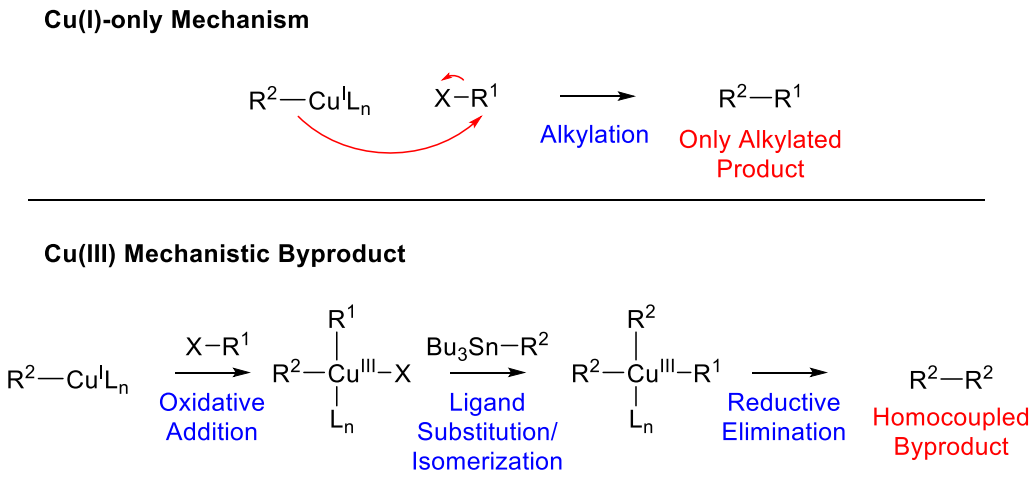

Figure 2.8 Presence of Homocoupled Product and Reasoning behind Mechanistic Differentiation

2.3 Model Substrate Optimization

Inspired by the above literature, we decided to investigate our own model substrate study on this reaction. For simplicity, we elected to use the organostannane **89** and allyl bromide **103** as they're both cheap or readily available (Scheme 2.1). With the substrates selected, we would then undergo variation of the copper(I) source, additives, and solvent choice to influence the reaction.

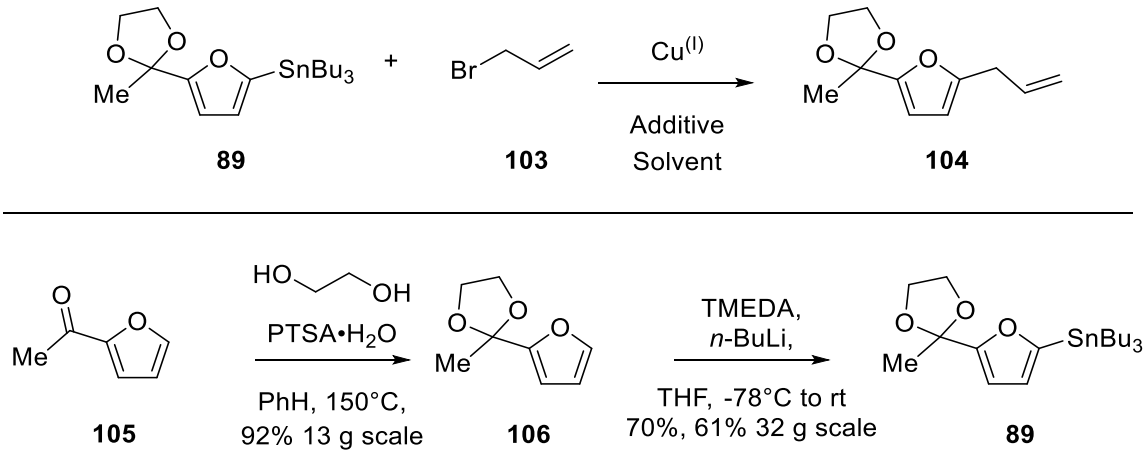

Scheme 2.1 Choice of Model Substrate Reaction and Synthesis of Organostannane **89**

89 can be made in two steps from 2-acetyl furan **105**, a highly commercially available natural product due to its likely formation during the Maillard reaction,[63] and its presence in numerous foods such as roasted sesame seeds,[64] fried beef,[65] and sweet corn products.[66] Synthesis

of the required organostannane began with protection of the carbonyl group as a dioxolane **106**, which could be achieved on a 13-gram scale using ethylene glycol in 92% yield. Gram scale stannylation could be done on the furan using TMEDA and *n*-BuLi to yield the required stannane in 70% yield. We were also pleased to see that we were able to get 61% yield when affording 32 grams of product **89** in a single pass-through. Purification of this reaction using 10% K_2CO_3:silica as the stationary phase[67] also cleanly produced the organostannane **89** with no co-elution of the $XSnBu_3$ salts and could be stored for months without degradation.

We then undertook our optimization of this reaction as shown in Table 2.2. Initial results were very promising as we were able to observe the formation of allyl dioxolane **104** in 73% yield with the use of 0.5 equivalents of copper catalyst and 0.1 equivalents of sodium carbonate as the additive (in order to suppress protodestannylation) in a DMSO:THF solvent mixture. However, the result was in a 5:1 ratio of the desired product to the undesired protodestannylated byproduct **106** (entry 1). It's worth noting that we were able to achieve this transformation at ambient temperatures without the need of any external heat added to the reaction. Flame-drying the copper catalyst beforehand and then cannulating the entire reaction to said pot only slightly increased the yield to 77% however dramatically increased the ratio of **104** to **106** to >20:1 (entry 2). A possible explanation for this is that removal of any water or adventitious acid present in the catalyst flask furthermore helps the additive suppress the formation of the undesired byproduct. Screening of CuCN, CuBr, and CuBr•DMS led to poorer yields and ratios (entries 3-5), and use of CuOAc and $Cu(MeCN)_4BF_4$ led to the mixture of the dioxolane product **104** as well as some deprotected ketone product **107**, likely due to the counter-acid in solution (entries 6-7). Finally, use of CuCl was found to give the best conversion of this reaction on the 0.5 equivalent scale (entry 8).

Table 2.2 Model Substrate Optimization

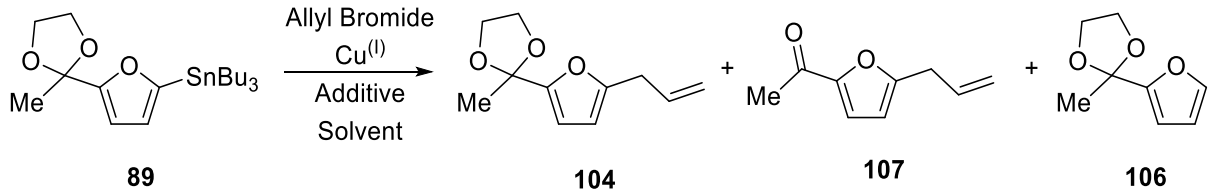

Entry	Catalyst (mol %)	Additive	Solvent	% Yield 104(107)	Ratio 104:106[a]
1	CuI (50)	Na_2CO_3	DMSO:THF 3:1	73	5:1
2[b]	CuI (50)	Na_2CO_3	DMSO:THF 3:1	77	>20:1
3	CuCN (50)	Na_2CO_3	DMSO:THF 3:1	38	10:1
4	CuBr (50)	Na_2CO_3	DMSO:THF 3:1	33	20:1
5	CuBr•DMS (50)	Na_2CO_3	DMSO:THF 3:1	53	5:1
6	CuOAc(50)	Na_2CO_3	DMSO:THF 3:1	77(14)	5:1
7	$Cu(MeCN)_4BF_4$ (50)	Na_2CO_3	DMSO:THF 3:1	17(37)	10:1
8	CuCl (50)	Na_2CO_3	DMSO:THF 3:1	82	>20:1
9	CuI (50)	Na_2CO_3	DMF	84	10:1
10	CuCl (50)	Na_2CO_3	DMF	91	ND
11	CuOAc (50)	Na_2CO_3	DMF	73	ND
12	CuOAc (50)	Na_2CO_3	DMF	0(86)[c]	ND
13	CuBr•DMS (50)	Na_2CO_3	DMF	79	ND
14	$Cu(MeCN)_4BF_4$ (5)	Na_2CO_3	DMF	87	>20:1
15	None	None	DMF	0, RSM	ND
16	CuCl (5)	None	DMF	79	>10:1
17	CuCl (5)	Cs_2CO_3	DMF	83	>20:1
18	CuCl (5)	Li_2CO_3	DMF	85	>15:1
19	CuOAc (5)	Cs_2CO_3	DMF	8(80)	>20:1
20	$(CuOTf)_2$•PhH (5)	Cs_2CO_3	DMF	0(79)	ND
21	Cu_2O (5)	Cs_2CO_3	DMF	78	ND
22	CuTC (5)	Cs_2CO_3	DMF	43	4:1
23	CuI (5)[d]	Cs_2CO_3, $NaSbF_6$	DMF	70(6)	5:1
24	CuI (5)[d]	Cs_2CO_3, $AgSbF_6$	DMF	32(33)	3:2
25	CuCl (5)	Na_2CO_3	DMF	89	>10:1
26	CuI (5)	Na_2CO_3	DMF	89	>20:1
27	CuI (5)	Cs_2CO_3	DMF	90[e]	>20:1

[a]Ratio determined via NMR [b]Flame-dried copper added last
[c]Reaction let run for several days [d]CuI 2.5 mol %, not added until later [e]Gram Scale

We were then pleased to find that the reaction gave higher yields when done in DMF as opposed to the DMSO:THF mixture (entries 9-10). Controlling reaction time with CuOAc let us

yield either solely our dioxolane product **104** (entry 11) or the deprotected ketone **107** (entry 12). It's worth noting that when solely **107** was formed, protodestannylated product **106** appeared to deprotect more slowly and thus could be recovered and reused in the synthesis above (Scheme 2.1). CuBr•DMS also gave increased yield in DMF (entry 13). We were then very pleased to observe that copper(I) catalysts were able to turnover in 5 mol % (entry 14), and further corroborated this by performing a control experiment with no catalyst nor additive in which we were able to fully recover the starting material (entry 15). To the best of our knowledge, this marks the first reported instance of an allylative copper-mediated Stille coupling using *catalytic* amounts of copper coupling under *ambient conditions*. As for why the copper (I) salts are able to catalyze this reaction it's likely due to the much lower barrier energies that are present with the sp^2 hybridized centers, as opposed to that of other sp^3 couplings. The effect of the additives on protodestannylation was then tested (entries 16-18) and it was found that Cs_2CO_3 was superior to the other carbonates presumably for its increased solubility in DMF. At these catalytic loadings, we were able to see that both CuOAc and $(CuOTf)_2$•PhH gave good yields of the deprotected product **107** (entries 19-20). Cu_2O gave fair yield of the dioxolane product **104**, however CuTC gave poor yields rather unexpectedly[51,53,56] (entries 21-22). Use of $NaSbF_6$ and $AgSbF_6$ as additives with no catalyst initially present led to no formation of product, however adding 2.5 mol % CuI after 24 hours of stirring led to mediocre yields **104** and **107** and low ratios of **104**:**106** (entries 23 and 24) furthermore corroborating the use for the presence of the catalyst. Ultimately the two best catalysts were compared, and it was observed that CuI resulted in better suppression of the formation of **106** compared to that of CuCl. (entries 25 and 26, Na_2CO_3 used as opposed to Cs_2CO_3 for comparison of **104**:**106** ratio via ^{1}H NMR). We were then able to apply our derived optimal conditions on a gram scale to afford **104** as the sole product detectable via ^{1}H NMR (entry 27). Purification of all these products were easily done using the procedure from Harrowven and coworkers.[67]

With these model substrate conditions optimized, we looked towards an application of this work. Due to our groups great interest in the synthesis of SF3B1 inhibitors as cancer therapeutics, we elected to use this methodology in the formal synthesis of FR901464 analogues.

2.4 Biological Activity of SF3B1 Inhibitors

Spliceosome is a megadalton complex of intracellular machinery within eukaryotic cells that is responsible for removal of introns and ligation of the flanking exons, or "splicing" of pre-mRNA into mature mRNA.[68,69] A very common analogy is that of a film editor that receives the full reel of film (the pre-mRNA), removes the bloopers & cuts out the extended footage (the introns) and sends off the final cut of the film to the editor (the mature mRNA). This process is vital to the gene expression of all living cells, including metastatic cells. Many cancer-associated genes involved with splicing are seen to have mutagenic alterations within.[70–72] In fact, several human genetic diseases are linked to aberrant splicing.[73] As cancer cells show very high metabolic rates in correlation to splicing, inhibition of this cellular process could halt the growth of tumor cells and thus be viewed as a potential cancer therapy. It is because of these extremely high metabolic rates that spliceosome inhibitor levels can be attenuated enough to not affect normal cells.[74] A simplified graphic for the cycle of spliceosome is shown in Figure 2.9. The pre-mRNA has flanking exons at the 5' and 3' splicing sites (ss). Within the pre-mRNA is an adenosine base that is seen as the branch point (BP) in which the intron will cyclize onto itself. This point is recognized by that of the exonic splicing enhancers (ESE's) that help provide accurate recognition of said adenosine via its proximity to the polypyrimidine tract, a sequence of pyrimidines near the 3' ss of the intron.[75] Along with the ~200 associated proteins that help catalyze spliceosome, there are 5 uridine-rich small nuclear ribonucleoproteins (snRNPs) that also help catalyze the process. Incorporation of the U1 snRNP onto the 5' ss forms complex E. U2 then attaches at the previously described branch point to form complex A, causing the helix to bulge out allowing for the subsequent intramolecular cyclization. The "tri-snRNP" composed of U4, U5, and U6 then incorporates to form complex B, which has a precatalytic and catalytic forms. Once U1 and U4 are able to dissociate, the activated form (complex B*) undergoes the first phosphodiester chemical step cleaving the bond at the 5' ss and transferring it to the 2' OH at the branch point through help of U2, forming complex C. The second step is then undergone cleaving the 3' ss and joining it to the free 3' OH created from the first reaction, linking the two exons together (complex P). At this point, the mature mRNA then dissociates and goes on to provide its role in protein synthesis and cell replication, while the remaining snRNPs dissociate from the intron and go back into the cycle.[72,76–78]

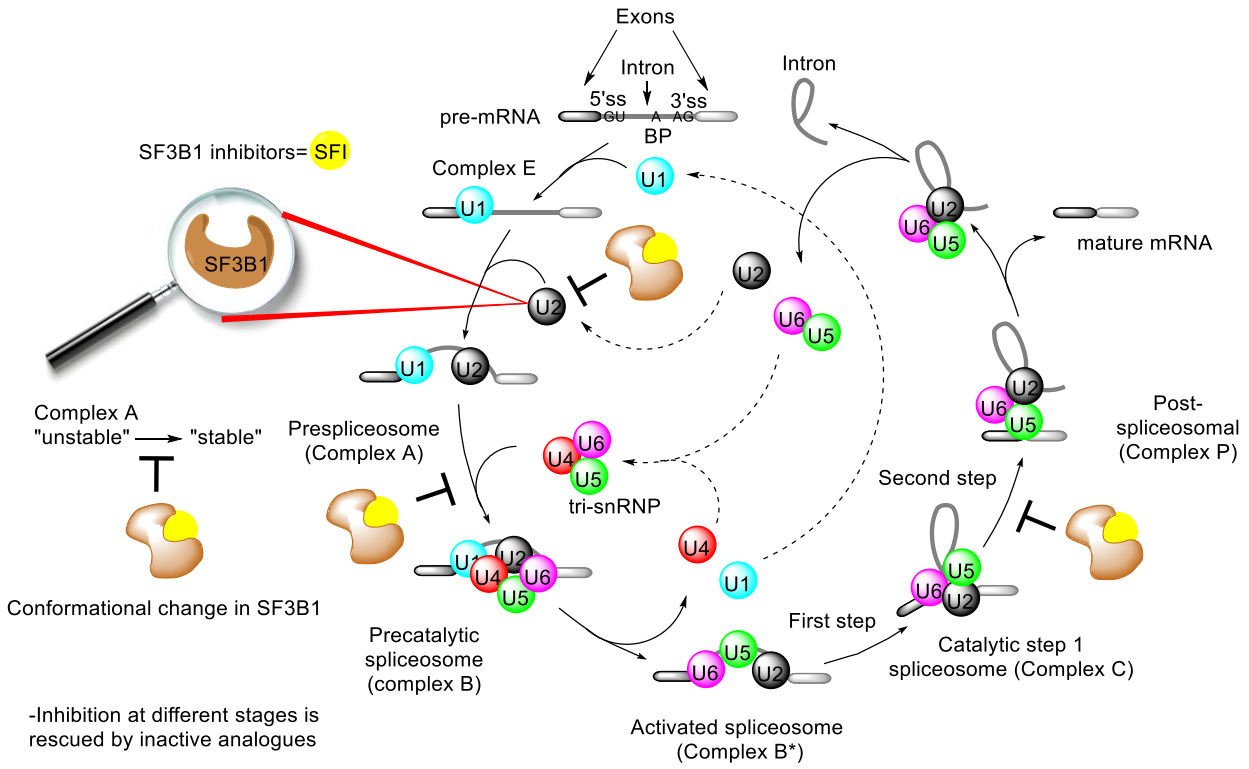

Figure 2.9 The Spliceosome Cycle

Spliceostatins and Thailanstatins (Figure 2.10) are subclass of the FR901464 family of molecules, of which the parent molecule was isolated from the fermentation broth of the bacterium Pseudomonas sp. No. 2663 by Fujisawa Pharmaceutical Co. in 1996.[79–81] This class of molecules, along with two other families (the pladienolides and GEX1 inhibitors) have been found to potently inhibit spliceosome, supported by leaked unspliced pre-mRNA observed in the cytoplasm. HeLa cell extract has become a common way to test for these inhibitors efficacy.[76] While no exact mechanism of action/active site is known, it has been found that in particular these compounds appear to be binding the SF3B1, a subset of the U2 snRNP, causing it to undergo a conformational change. This inhibition appears to affect the cycle at several different key steps, due to the importance of U2 and its role in the formation and stabilization of complex A, formation of complex B and C, and so on. During several different structure-activity relationship (SAR) studies, inactive analogues of these compounds have been made that interestingly are not only impotent but restore splicing in the cell after prior doping with the active inhibitors. It was found that cells doped with Spliceostatin A **93** could be rescued by the inactive analogues iPB **111** and iHB **112**, cells doped with Pladienolide B **109** could be rescued by the inactive analogues iSSA **108** and iHB

112, and cells doped with Herboxidiene **110** could be rescued by the inactive analogues iSSA **108** and iPB **111**. Therefore it's likely that all three inhibitor families interact with the same active site.[77] This is further supported by a point group mutation (R1074H) within SF3B1 that causes all the inhibitors to lose their respective efficacy, alluding to a possible active site/key interaction.[72]

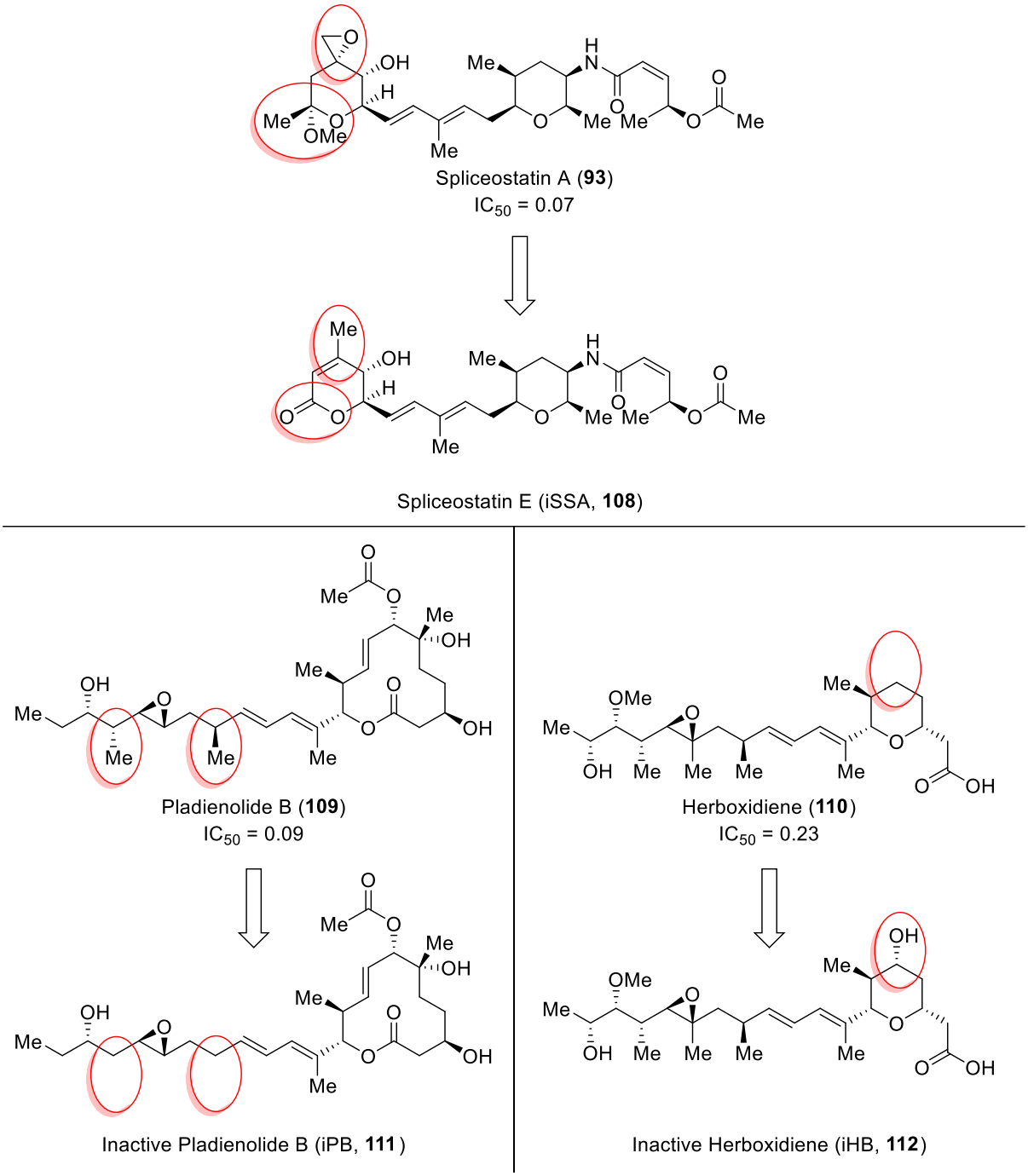

Figure 2.10 Spliceosome Inhibitors and their Inactive Analogues

2.5 Prior Syntheses of the Common Pharmacophore Tetrahydropyranal Amine

2.5.1 SAR Studies and the Significance of the THP-Diene Moieties

Owing to their insufficient quantities isolated from nature and its innate potency, the FR901464 family quickly became a synthetic target for chemists. Since the preliminary synthesis by Jacobsen and coworkers[82] (41 chemical steps, 22 LLS), the synthetic community has put forth great effort to improve said synthesis.[82–96] SAR studies has emerged as a forefront to try and increase the potency of the analogues made as well as chemically define the active site within SF3B1. Of these extensive studies, a small excerpt shows that any change in the tetrahydropyranal (THP) ring and/or the diene results in loss of activity of said analogues (Figure 2.11),[76] thus this common pharmacophore **117** seen in Spliceostatins and Thailanstatins is needed.

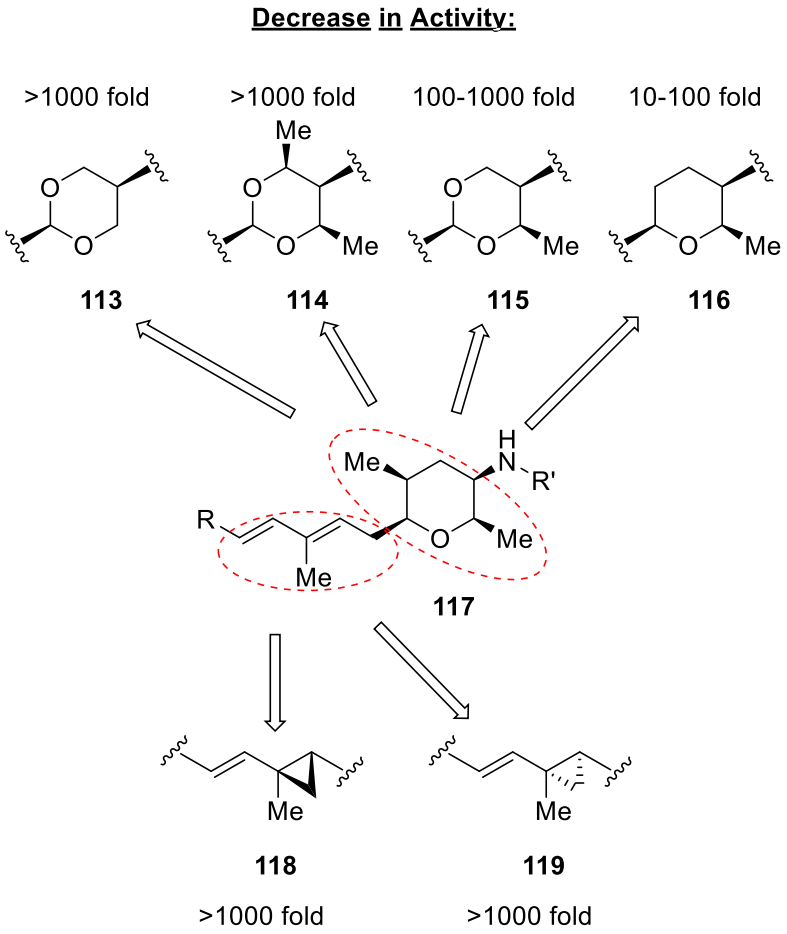

Figure 2.11 SAR Studies of the Common Pharmacophore **117** in FR901464 Analogues

2.5.2 Ghosh and Chen's 2013 Synthesis

In 2013 Ghosh and Chen put forth a synthesis that accomplished the construction of Spliceostatin A in 10 linear steps, cutting the preliminary synthesis in half.[87] Their retrosynthetic analysis of the natural products is shown in Scheme 2.2. Of note during this synthesis they synthesized the tetrahydropyranal amine **92**, highlighted in red.

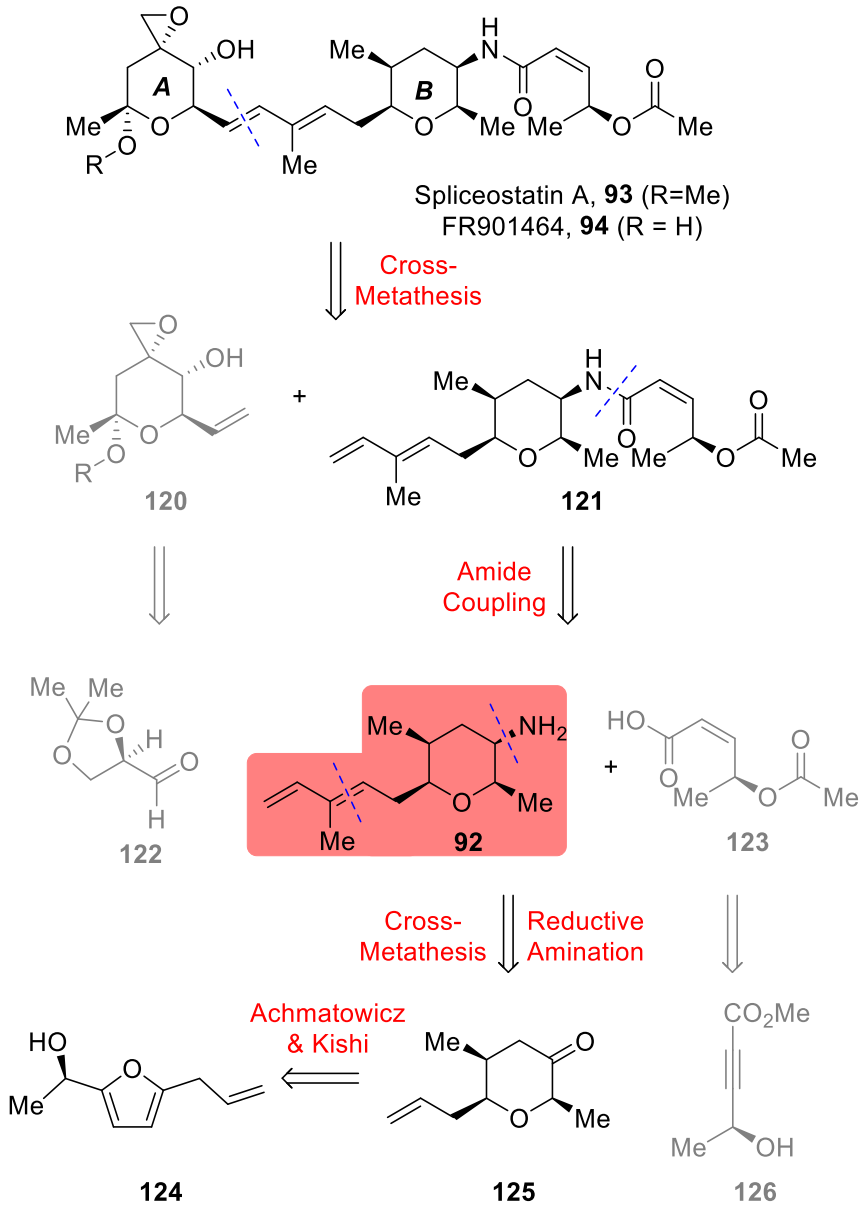

Scheme 2.2 Ghosh and Chen's Retrosynthetic Analysis of Spliceostatin A and FR901464

Retrosynthetically, they envisioned a final cross-metathesis that would couple the vinyl of ring A to the diene linker of ring B. From here, the epoxide **120** could come from aldehyde **122** after a number of transformations. Amide **121** would come from the coupling of carboxylic acid **123** and THP amine **92**, which in turn would come from ester **126** and ketone **125** respectively. Carbonyl **125** would come from the stereochemically defined alcohol **124** after an Achmatowicz followed by a Kishi reduction. In relation to the SAR studies and how THP amine **92** has been shown to be a desired intermediate in the synthesis of all FR901464 analogues, Ghosh's 2013 synthesis of THP amine **92** is described below.

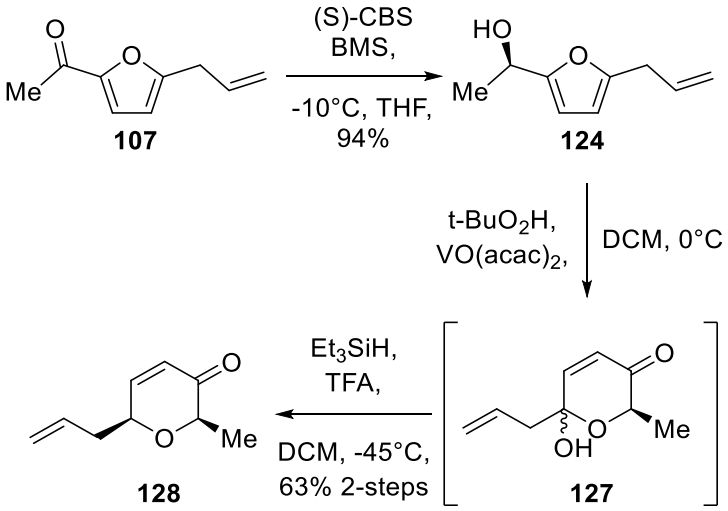

Scheme 2.3 Ghosh and Chen's Synthesis of Enone **128**

The synthesis started off with acetyl allyl furan **107,** a material that is not commercially available anymore as of this writing (however, a synthesis of it was proposed in our model substrate optimization, Chapter 2.3). CBS reduction of **107** resulted in stereochemically defined alcohol **124** in 94% yield 93% *ee* (Scheme 2.3). This material was then subjected to an Achmatowicz rearrangement using vanadyl acetylacetonate and the crude hemiacetal **127** was then reduced via a Kishi reduction using triethyl silane and TFA, resulting in the desired enone **128** in 63% over 2-steps.

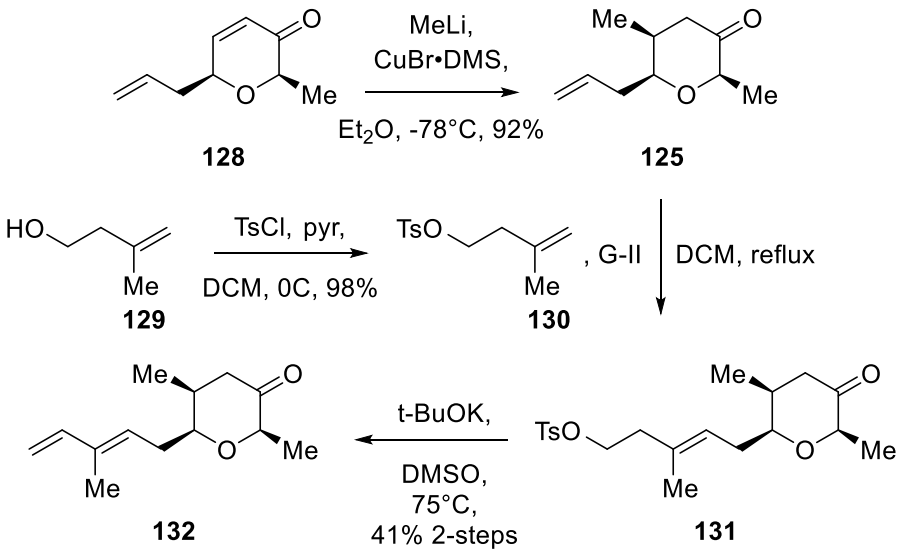

Scheme 2.4 Ghosh and Chen's Synthesis of β-methyl Ketone **132**

Enone **128** was then subjected to a stereoselective 1,4-addition to yield β-methyl ketone **125** in 92% yield, >25:1 dr via ^{1}H NMR analysis (Scheme 2.4). Meanwhile, isoprenol **129** was tosylated in near quantitative yield to afford tosylate **130**. Tosylate **130** was then coupled with β-methyl ketone **125** via Grubb's metathesis to afford olefin **131**, then subjected to β-elimination via use of potassium tert-butoxide and high heat in DMSO affording diene **132** in 41% yield over 2-steps.

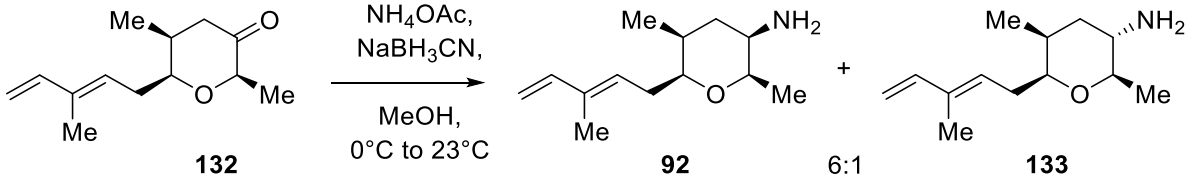

Scheme 2.5 Ghosh and Chen's Synthesis of THP amine **92**

Subjection of diene **132** to Borch reduction conditions then resulted in a 6:1 mixture of desired epimer **92** to undesired **133**, which could not be separated chromatographically and was carried on without further purification (Scheme 2.5). While this synthesis provides quick access to the THP amine core, it isn't without its limitations. These include a starting material that isn't commercially available anymore as well as a CBS reduction that requires 0.5 equivalents of the catalyst. The Achmatowicz rearrangement uses $VO(acac)_2$, which while it is relatively cheap,

much cheaper and greener methods for the rearrangement now present themselves.[97] Grubb's metathesis with use of the expensive G-II catalyst is used in the overall route twice, and a low yielding 2-step sequence is present very early on with the metathesis followed by β-elimination. Finally, poor dr at the final Borch reduction step is present and as stated the epimers aren't isolable. To this end we envision a more concise route to **92**.

2.5.3 Ghosh and Veitchegger's 2018 Synthesis

THP amine core **92** was also synthesized by Ghosh and coworkers again in 2018.[83] The retrosynthetic analysis for this synthesis is shown in Scheme 2.6. It was envisioned that THP amine **92** would come from the Borch reduction and similar methods working backward to alcohol **134**. This material would come from aldehyde **135** after multiple Wittig olefinations. In turn, aldehyde **135** would come from a Claisen rearrangement of material originating from tri-O-acetyl-D-glucal **136**, a commercially available starting material.

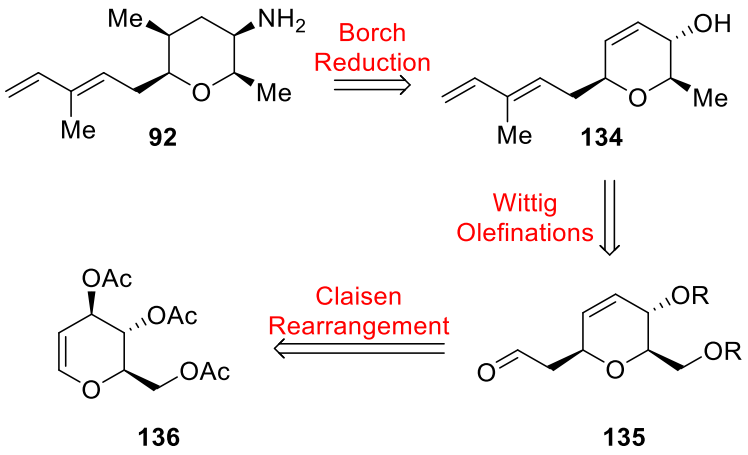

Scheme 2.6 Ghosh and Veitchegger's Retrosynthetic Analysis of THP amine **92**

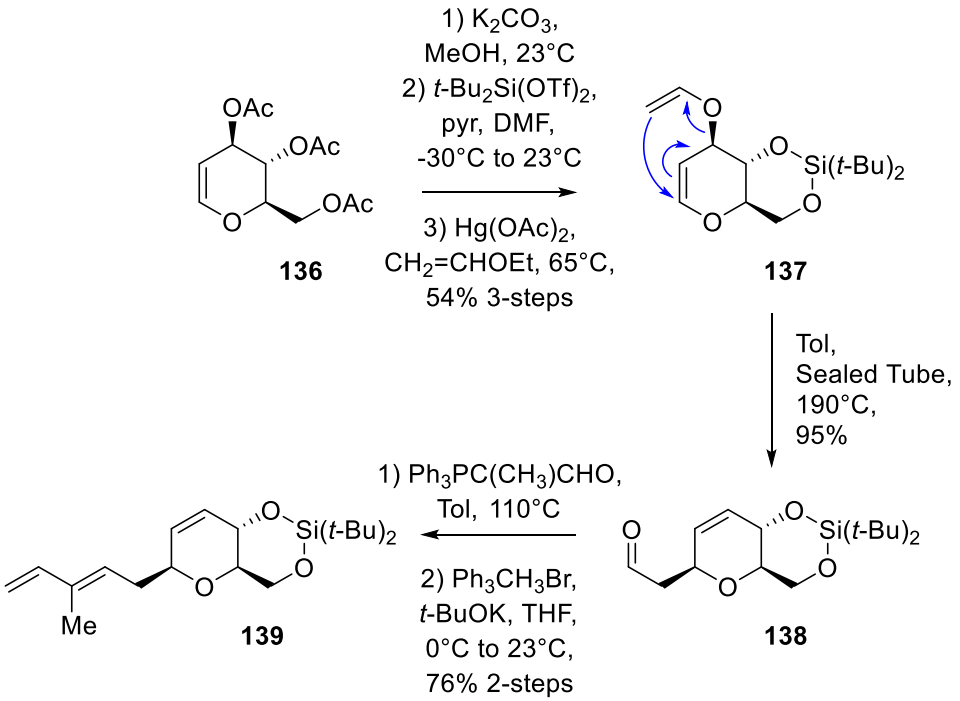

Scheme 2.7 Ghosh and Veitchegger's Synthesis of Diene **136**

Their synthesis began with the commercially available tri-O-acetyl-D-glucal **136** (Scheme 2.7). They underwent a known 3-step procedure[98,99] consisting of saponification of the triacetate, protection of the resultant 1,3-diol, and vinylation of the secondary alcohol to form **137** in 54% over 3-steps. A Claisen rearrangement could then be undergone within a sealed tube to obtain aldehyde **138** in 95% yield. With this aldehyde installed two subsequent Wittig olefinations resulted in the formation of the desired diene **139** in 76% yield over 2-steps.

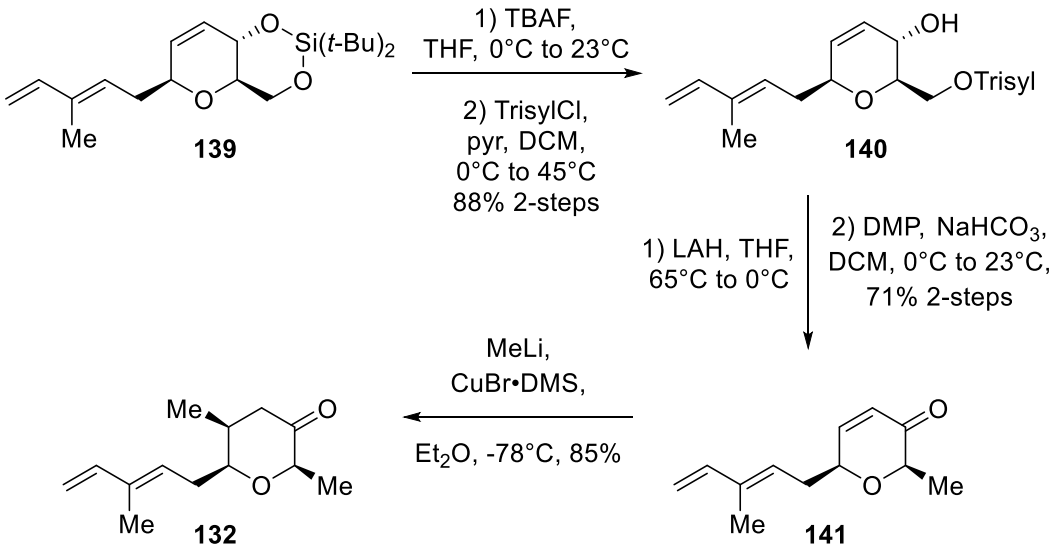

Scheme 2.8 Ghosh and Veitchegger's Synthesis of β-methyl Ketone **132**

From here, deprotection of the silyl ether resulted in the diol which could then by selectively protected with Trisyl chloride to provide the secondary alcohol **140** in 88% yield over 2-steps (Scheme 2.8).[85] LAH reduction would reduce the sulfonate off to leave the stereochemically defined methyl enol, and subsequent DMP oxidation resulted in the enone **141** in 71% yield over 2-steps. Selective 1,4-conjugate addition with use of *in-situ* formed Gilman's reagent resulted in β-methyl ketone **132** in 85% yield.

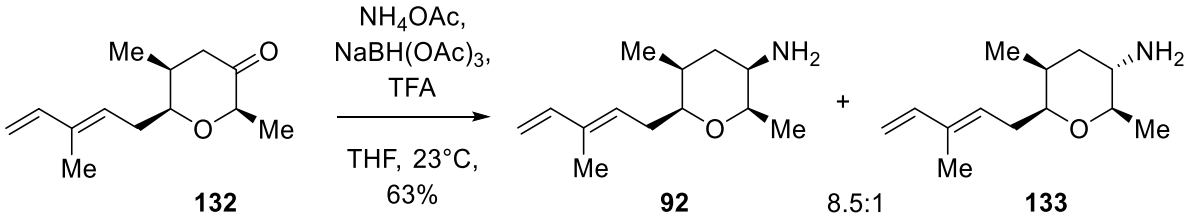

Scheme 2.9 Ghosh and Veitchegger's Synthesis of THP amine **92**

Borch-like reduction conditions now yielded the THP amine **92** and its epimer **133** in a slightly improved dr (8.5:1 via ^{1}H NMR) in 63% yield (Scheme 2.9).[100] This completed their synthesis of the intermediate **92**. The key points of this synthesis include that it can be made from cheap starting material, however the number of overall steps to **92** is thus increased. Double Wittig olefination of the material is not ideal and thus a way to install the diene in a more facile manner

is desired. Any improvements on the stereoselectivity of the reductive amination step is also desired.

Since these syntheses several FR901464 derivates have been made by the Ghosh group including the use of said THP amine, and it's presence is highly consistent in the literature.[83,84,86–88,90] Therefore, more concise efforts in the synthesis of THP amine **92** is always needed, and herein we report our synthesis of this core using our newly optimized copper catalyzed cross-coupling conditions.

2.6 Results and Discussion

2.6.1 Initial Attempt

Prior to the development of our copper-catalyzed Stille coupling conditions (Chapter 2.3), an initial route was planned towards an improved synthesis of THP amine **92**, based on a derivation of our 2013 work (Scheme 2.10).[87]

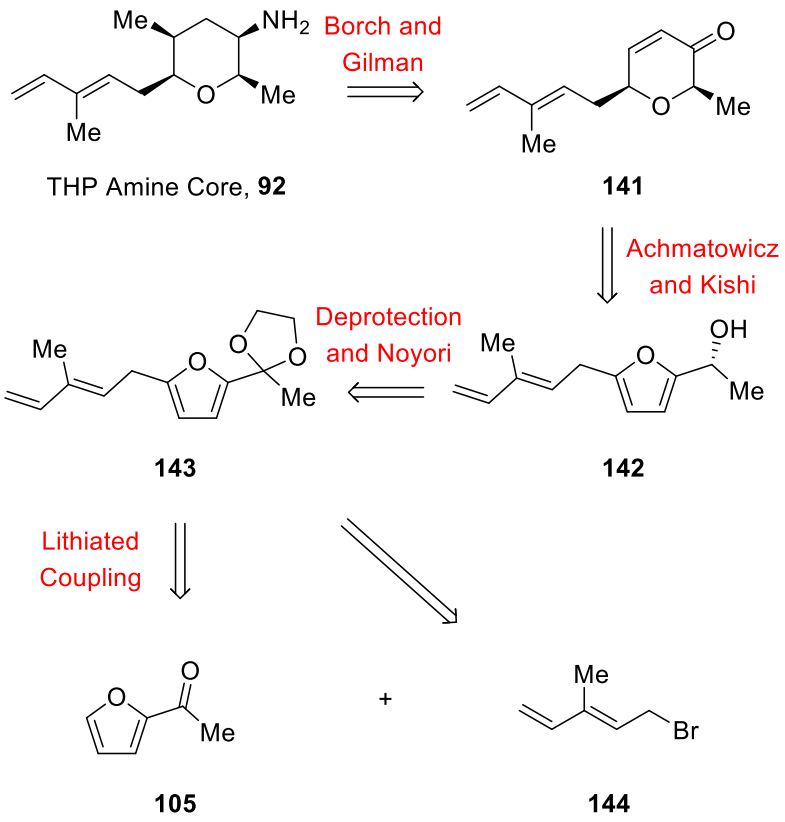

Scheme 2.10 Ghosh and Born's Attempted Retrosynthetic Analysis of THP Amine **92**

It was planned that the THP amine core **92** would come from the enone after reductive amination and 1,4-Gilman addition. The enone diene **141** would come from the stereochemically defined alcohol **142** after Achmatowicz and Kishi reductions. Alcohol **142** would come from the dioxolane diene **143**, which in turn would come from the coupling partners **105** and **144**. This route would eliminate the use of the low yielding metathesis and β-elimination steps, as well as provide a chance to improve on the stereoselectivity and employment of greener reagents over the

final steps. Notably, this route would also provide the use of 2-acetyl furan **105** as the starting material, of which we've discussed its significance in Chapter **2.3**.

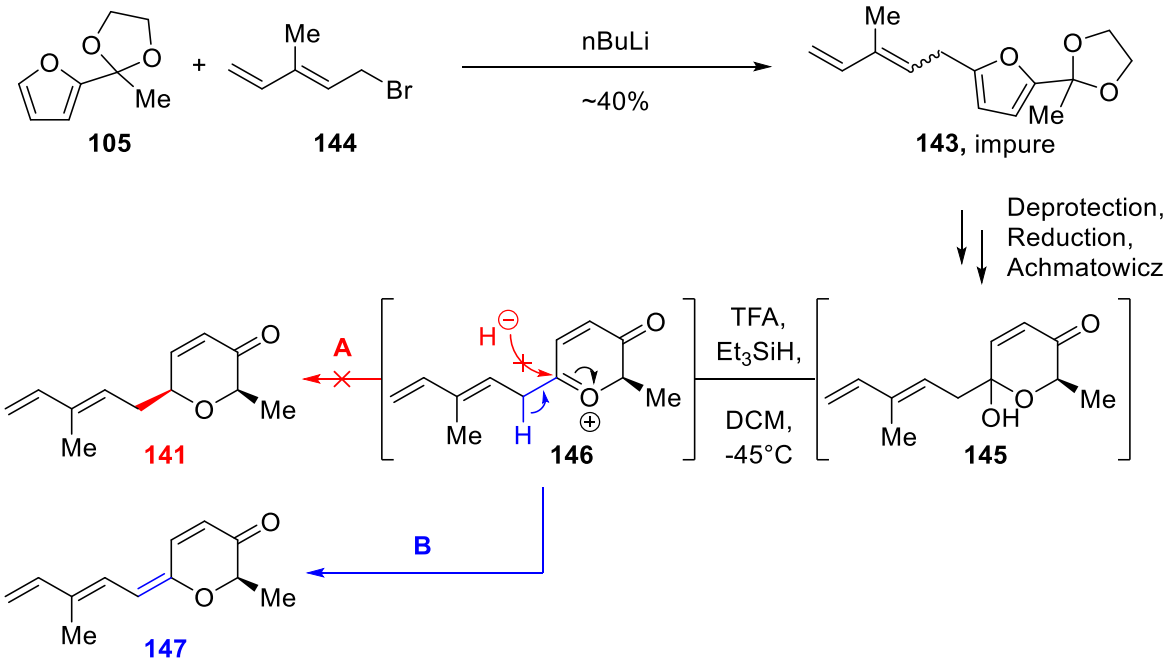

Scheme 2.11 Ghosh and Born's Initial Attempt at Enone **141**

Our initial synthesis began with the construction of dioxolane **105** and diene bromide **144** (See Chapters 2.3 and 2.6.3.1 for syntheses). Lithiated coupling of these two resulted in an optimized yield of 40% of dioxolane diene **143** as a mixture of isomers (Scheme 2.11). This yield wasn't ideal, but material was carried forward. After deprotection, reduction, and Achmatowicz rearrangement the resultant hemiacetal **145** was formed. Subjection of this to Kishi reduction however didn't result in the desired pathway A to form enone diene **141**. Instead, what was observed was that solely triene diene **147** formed instead. This likely is derived from the β-elimination that can take place to quench the *in situ* formed oxocarbenium ion (pathway B) forming an extended conjugation, instead of the 1,2-addition of the hydride to the electrophilic carbon in **146**. A modification of this route was needed to circumvent both the low yielding lithiated coupling at the beginning of the synthesis as well as protection of the diene moiety to prevent the extended conjugation that drives said β-elimination.

2.6.2 Retrosynthetic Analysis of the Tetrahydropyranyl Amine

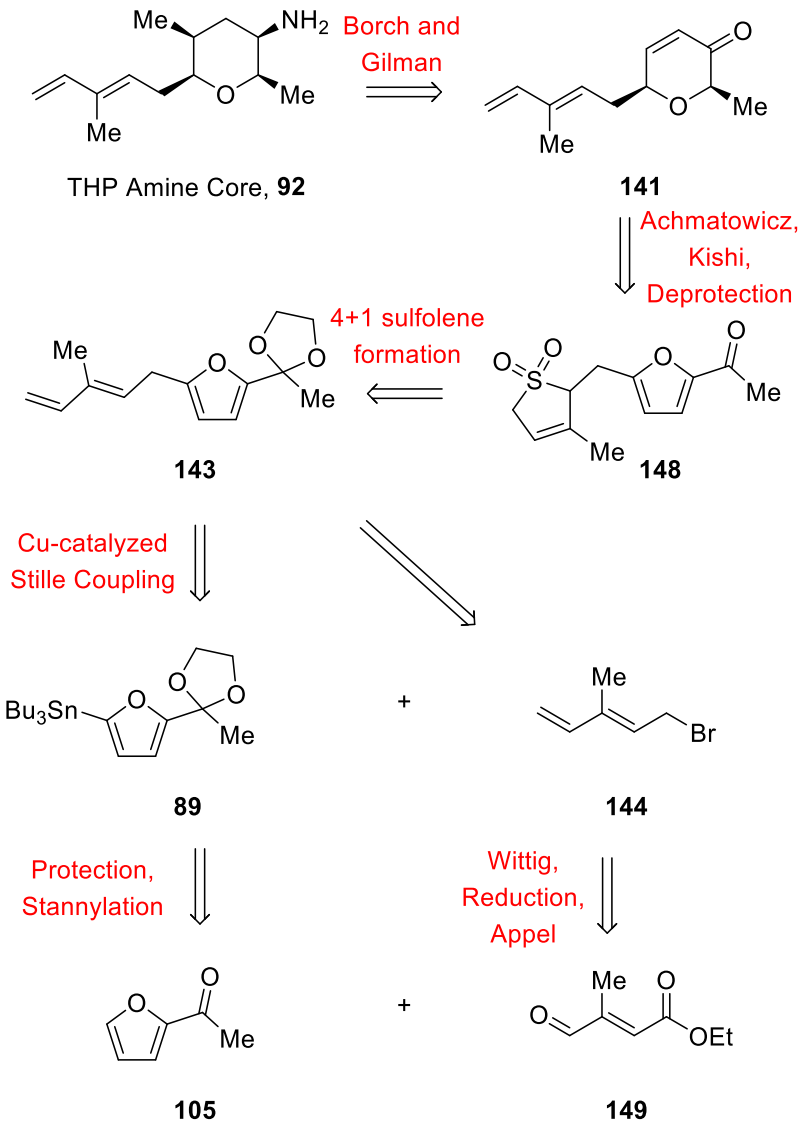

Scheme 2.12 Ghosh and Born's Retrosynthetic Analysis of THP amine **92**

We envisioned our new retrosynthesis of THP amine **92** based on these insights. Thus, amine **92** would come from the same 1,4 addition of a Gilman reagent and subsequent Borch-like reduction from the enone diene **141**. This material would come from the required Achmatowicz and Kishi reductions on the diene-protected substrate **148**, to help circumvent the formation of the triene byproduct. Sulfolene ketone **148** would be the product of a 4+1 cheletropic reaction that will be discussed (Chapter **2.6.3.5**), and dioxolane diene **143** would come from the copper-catalyzed coupling of stannane **89** and bromide **144** of which we've thoroughly optimized. These

coupling partners would come from the cheap commercially available starting materials **105** and **149**.

2.6.3 Copper-Catalyzed Cross Coupling

2.6.3.1 Synthesis of the Diene Bromide Coupling Partner

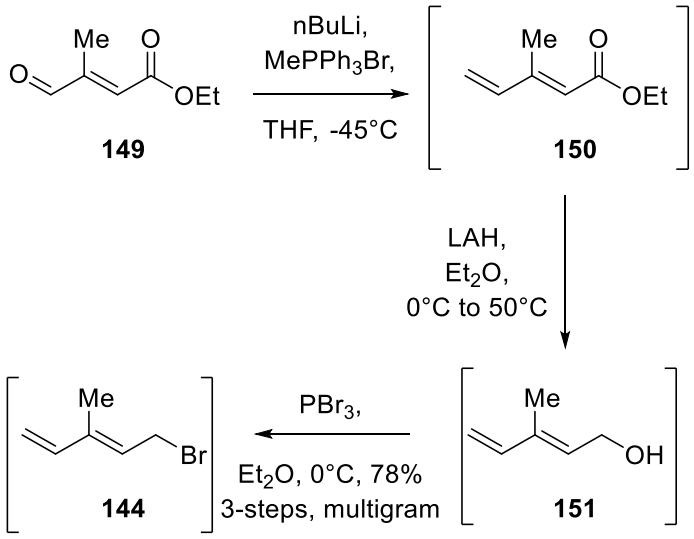

Scheme 2.13 Synthesis of Diene Bromide **144**

For the synthesis of the diene bromide coupling partner, commercially available aldehyde **149** could be Wittig olefinated to form diene ester **150** (Scheme 2.13). Reduction of this ester to the alcohol **151** using LAH and subsequent bromination of the material using tribromophosphine afforded diene bromide **144** in 78% yield over 3-steps on a multigram scale and could be used without further purification.

2.6.3.2 Characterization of the γ-Alkylated Byproduct

Initial attempts towards the synthesis of (*E*)-**143** using our model substrate copper-coupling conditions resulted in a mixture of isomers as shown by the ^{1}H NMR excerpt in Figure 2.12. The mixture consisted of the *E* & *Z* isomers of **143** (initially assigned, NOESY characterization confirmation in Scheme 2.17), unknown isomer **X**, and the protodestannylated byproduct **106** (Scheme 2.14). Characterization for identity of **X** was made by carrying forward the crude mixture and deprotecting the dioxolanes down to the respective ketones (*E*/*Z*)-**152**, **Y** (correlating isomer of **X**), & **105**. The isomers were not isolable via silica column chromatography, however 2-acetylfuran **105** was recovered and reused in the synthesis. **Y** & (*E*/*Z*)-**152** were then carried forward over the sulfolene formation step of which will be discussed later (Chapter 2.6.3.5). At this point it was observed that the *E* & *Z* isomers of **152** were converted to sulfolene **148**, whilst **Y** was left unreacted. Isomer **Y** was thus isolable and characterized to be **153** as shown, therefore retrosynthetically the structure of **X** as divinyl **154** was elucidated.

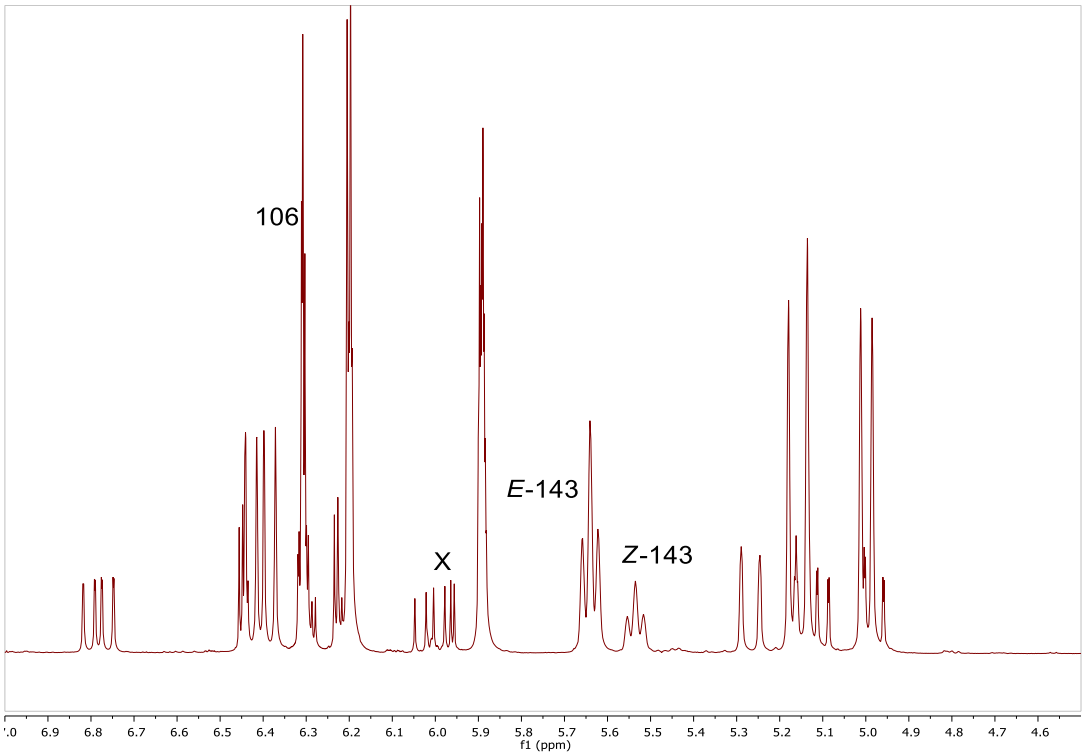

Figure 2.12 ^{1}H NMR Excerpt of Unoptimized Copper-Coupling

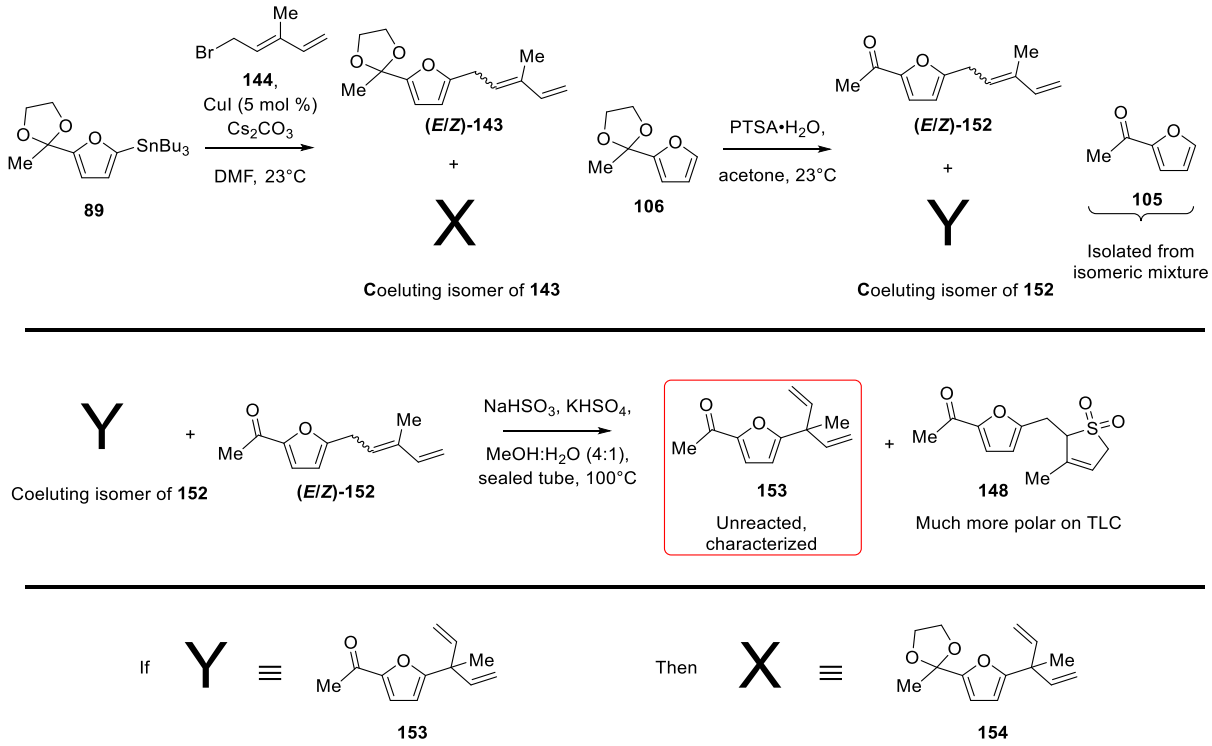

Scheme 2.14 Isolation and Characterization of Coeluting Isomer

To maximize the efficiency of this transformation, repression of the formation of the protodestannylated and isomeric materials was needed. We therefore sought to propose a pathway for the formation of these isomers and subsequently suppress it in due course.

2.6.3.3 Mechanistic Proposal for Suppression of Isomers

We then proposed a mechanism for the formation of the described isomers based on the priorly supported catalytic cycle (Figure 2.7). As π-allylcopper(III) intermediates in S_N2 and S_N2' reactions have been shown to be present in the literature,[59] it's likely that after undergoing oxidative addition our Cu(III) intermediate, with no strong ligands present, forms an η^3 allyl complexation that can lead to both the *cis*-isomerized and the γ-alkylated products in an off-cycle pathway (Scheme 2.15). Due to our extended conjugation, it could also go η^5, although no strong support for this is known as of yet.

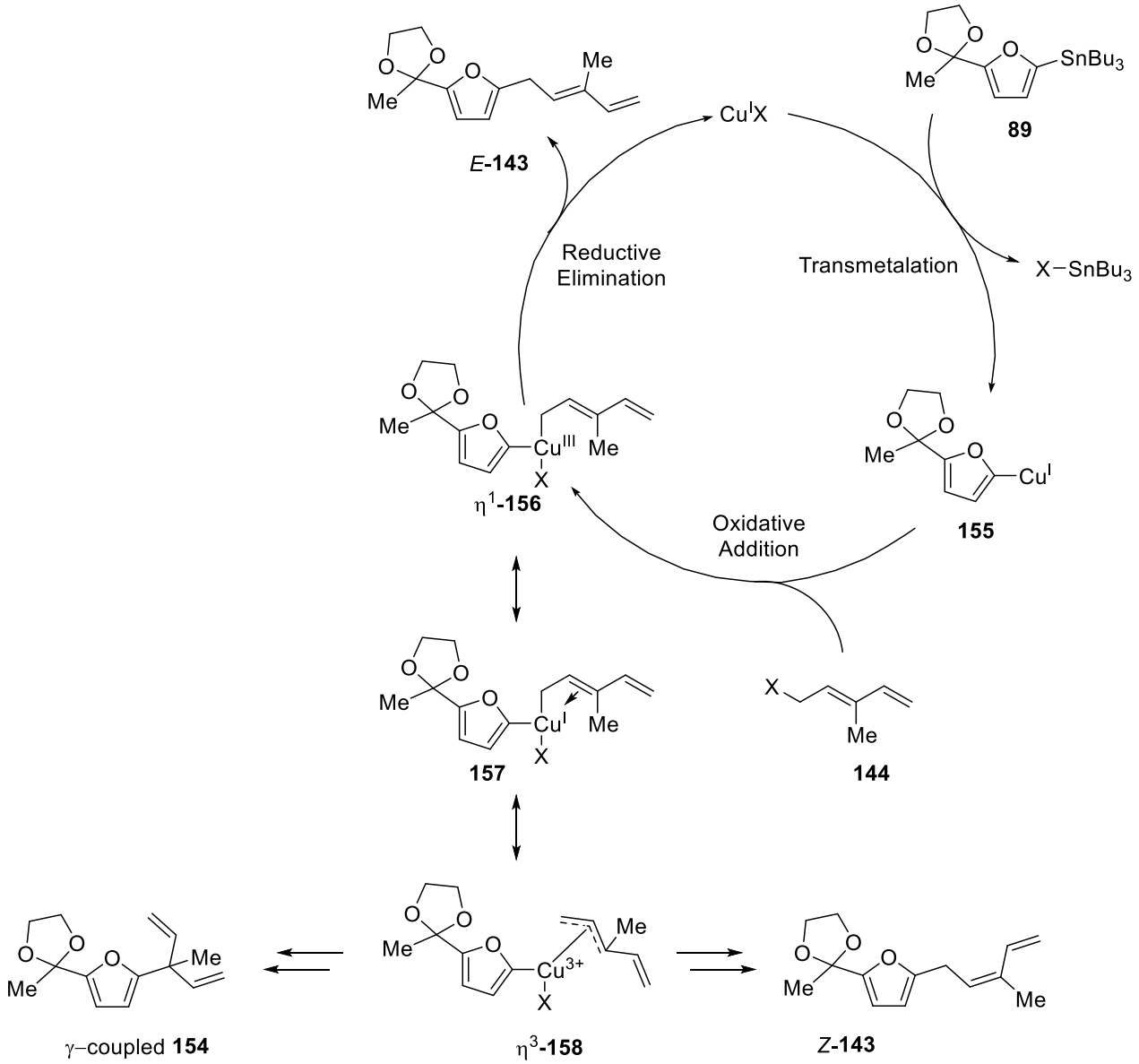

Scheme 2.15 Proposed Mechanistic Pathway for the Formation of the Undesired Isomers

Based on this hypothesis, we put forth a proposal to minimize the formation of the undesired isomers. Our proposal is that based upon careful selection of solvent, ligation could take place putting the catalyst in the square planar state resulting in less isomerization at the reductive elimination step[56,58,62] (Scheme 2.16). In other words the Cu (III) η^3 allyl complexation won't form leading to *γ*-alkylated nor *Z*-isomerized products **154** & (*Z*)-**143**.

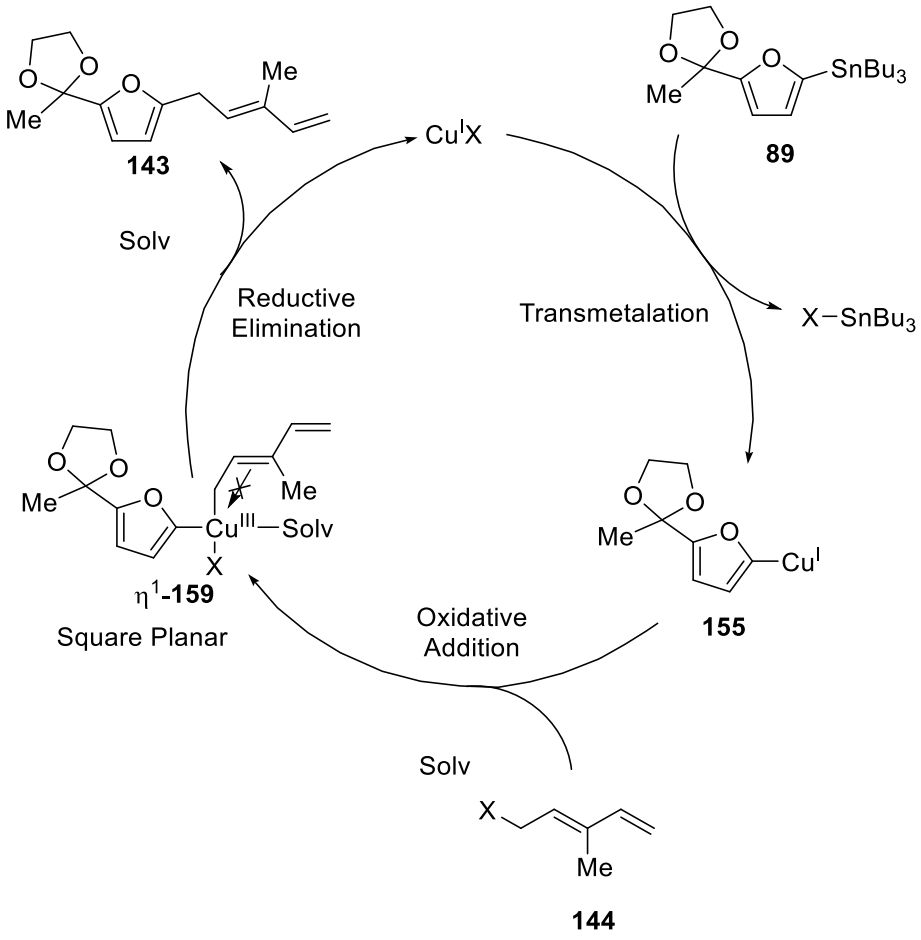

Scheme 2.16 Proposed Mechanistic Pathway for the Suppression of the Undesired Isomers

2.6.3.4 Optimization of the Cross Coupling

Table 2.3 Optimization of the Coupling for the Formation of (*E*)-**143**

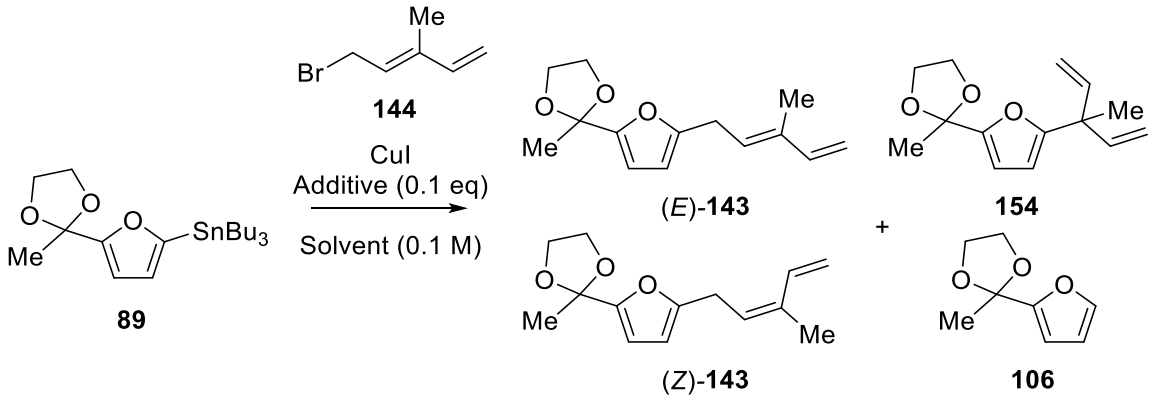

Entry	mol % CuI	Additive	Solvent	% Yield (BRSM)	Ratio (*E*)-143:(*Z*)-143:154:106[a]
1	50	Na_2CO_3	DMSO:THF(3:1)	84	10:1:1:1
2	50	Na_2CO_3	NMP	0	N/A
3	50	$NaHCO_3$	DMSO:THF(3:1)	77	20:1:1:2
4	20	Na_2CO_3	DMSO:THF(3:1)	76	20:3:1:1
5	5	Cs_2CO_3[b]	THF:H_2O (3:1)	27	>20:1:1:20
6	1[c]	Na_2CO_3	DMF	48	10:4:3:5
7	1	Cs_2CO_3	DMF	57[d]	10:8:4:4
8	5	$NaHCO_3$	DMF	73	20:4:1:11
9	5	Cs_2CO_3	DMF	72	5:2:1:2
10	5	Cs_2CO_3	DMF[e]	72	10:3:2:4
11	5[f]	Cs_2CO_3	DMF	77	10:4:1:4
12	5	Cs_2CO_3	DMSO:THF(3:1)	69[g]	>20:8:2:1
13	5	Cs_2CO_3	THF	63(87)	>20:1:1:2
14	5	Cs_2CO_3[b]	DMF:THF (1:3)	90	>20:1:1:4
15	5	Cs_2CO_3[b], TBAF	DMF:THF (1:1)	65	20:7:6:4
16	5	Cs_2CO_3[b], CsF	DMF:MeCN (1:1)	76(90)	10:4:2:1
17	5	Cs_2CO_3[b], LiCl	MeCN:THF (1:1)	37	20:3:3:16
18	5	Cs_2CO_3[b], NaCl	MeCN	89	>20:1:1:2
19	5	Cs_2CO_3[b]	MeCN	85[h]	>20:1:1:1

[a]Determined by HNMR [b]>0.1equiv carbonate used [c]CuCl used

[d]Gram scale, yield of ketone over two steps, no purification after coupling [e]freshly bubbled solv
[f]CuI added last [g]ketone product formed [h]decagram scale, yield of ketone over two steps

With this mechanistic insight in mind, we began our optimization of the copper coupling (Table 2.3). Initial attempt to couple **89** and **144** using 50 mol % CuI, 0.1 equivalents Na_2CO_3, in a DMSO:THF mixture resulted in 84% yield of a mixture of the *trans*, *cis*, gamma alkylated, and protodestannylated products as discussed before (entry 1). NMP was then attempted as it is a common solvent choice used in Stille couplings due to its likely catalyst ligation[46,51,53,56] In our attempt however, it provided no conversion at all (entry 2). Either use of sodium bicarbonate as the suppressant or lower catalytic loading resulted in decreased yield but increased ratio of the desired product as seen in entries 3 and 4. Replacement of DMSO with water as the cosolvent had a detrimental effect, yielding a low amount of the mixture of products as well as a roughly 1:1 ratio of the desired product (*E*)-**143** to the protodestannylated material **106** (entry 5). It was at this point that we had begun our model substrate optimization as seen in Chapter 2.3 and thus we elected to use DMF as the solvent in hopes of improving the proposed ligation. 1 mol % catalyst loading led to poorer yields of **143** or the ketone **152** after further transformations (entries 6 & 7). $NaHCO_3$ again as the additive appeared less suppressive than Cs_2CO_3, and freshly bubbling the solvent beforehand only very slightly increased the desired ratios (entries 8-10). Changing the order of addition as done in the prior optimization led to a slight increase in yield again but similar ratios of the products (entry 11). Use of the DMSO:THF solvent system at this stage resulted in coupling followed by dioxolane deprotection but a decrease in the ratio of *E*/*Z*-isomers (entry 12), while solely THF was found to work well as a solvent resulting in great ratios of the isomers however the reaction wouldn't go to completion (entry 13).

Based on these results a mixture of DMF and THF (3:1) was then tested and allowed for the reaction to go to 90% yield in great ratios of the isomers, albeit the ratio of (*E*)-**143** to the protodestannylated **106** was 5:1, even with additional carbonate added (entry 14). A similar solvent mixture was tried again employing the use of TBAF as an additive to drive forward the reaction,[47,60] (see Chapter 2.2.2 for discussion) however it resulted in poorer yields and ratios (entry 15). In a similar fashion CsF was used in a DMF:MeCN mixture and the reaction was found to not go to completion after 6 days and resulted in a poor ratio of isomers and moderate yield (entry 16). LiCl was then tested in a mixture of MeCN:THF and gave even lower yields (entry

17). Based upon these solvent mixtures affording detrimental yields, solely MeCN as the solvent was screened with the use of NaCl as the additive (entry 18). We were pleased to find that once the reaction was complete via TLC analysis simply concentrating down the reaction mixture under reduced pressure and purifying it using Harrowven's procedure[67] allowed for 89% isolated yield of the sole desired isomer (*E*)-**143** on a multigram scale as the major product. It was then observed that MeCN without any additive gave the best yields and ratios for the formation of (*E*)-**143**, and we were able to deprotect the dioxolane to yield ketone (*E*)-**152** over 2-steps in 85% yield starting with nearly a gram of **89** (entry 19 and Scheme 2.17), and the reaction conditions were reproducible on a decagram scale. With ketone **152** in hand, we were able to characterize that we did indeed have the *trans*-isomer in hand via use of 2D NMR. Comparatively, our confirmation for the *cis*-**152** was done by carrying forward one of our crude unoptimized copper-couplings over the same deprotection step. While *Z*-**152** was not isolable from the rest of the mixture, NOESY interactions of the suspected isomer's key signals were still present, corroborating its stereochemistry.

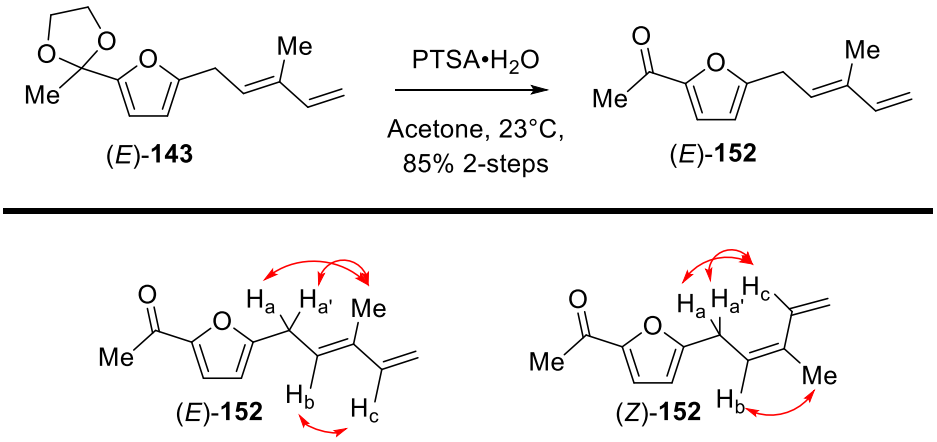

Scheme 2.17 Synthesis of Ketone **152** and NOESY Confirmation of *trans* and *cis*-Isomers

A comparison of the ^{1}H NMRs of the products under non-optimized and optimized conditions are shown below in Figure 2.13. As it can be seen, the isomers suppression is virtually non-existent. The only peak seen outside of the desired product is that of the protodestannylated material **106** and is only observed due to that peak correlating to an integration of two protons (as opposed to the peaks on either side of it correlating to one proton in the product).

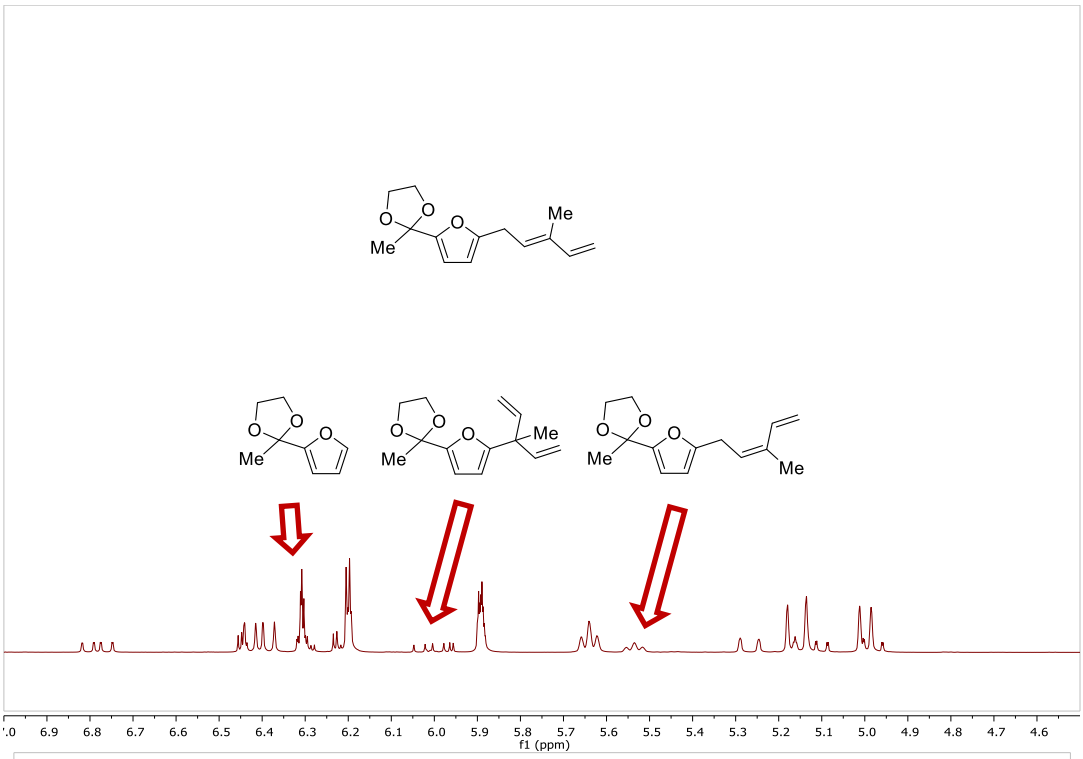

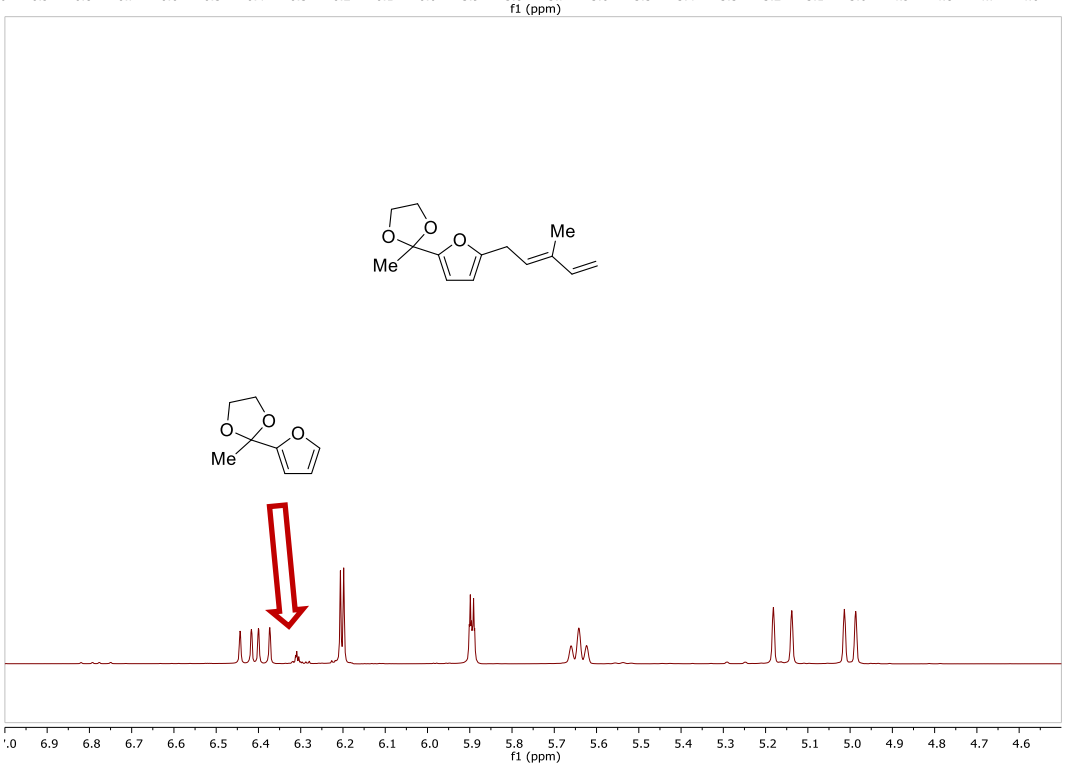

Figure 2.13 ^{1}H NMR Comparison of Product Mixture Before and After Optimization

2.6.3.5 Mechanistic Experiments for the Optimized Copper-Coupling

To further corroborate the robustness of copper in these transformations and support the presence of the Cu(III) intermediate, three more experiments were done (Scheme 2.18). To rule out that the mechanism occurs via a radical pathway, the common radical scavenger TEMPO was added to the optimized conditions (first entry) and it was seen that the reaction still occurred yielding 68% dioxolane **143** and 20% ketone **152**. An experiment with solely a palladium (0) catalyst was then set up (second entry) and it was seen that very complex mixtures with trace amounts of the desired products were produced, instead yielding the homocoupled byproduct **161** as the major product in 21% yield. Attempting to set up this same reaction, this time adding CuI last to try and invoke the "Copper Effect" still yielded these same complex mixtures, with **161** as the major product again in 34% yield. The presence of this homocoupled product (discussed priorly in Figure 2.8) is also observed in several of our prior optimization reactions in trace amounts when using only Cu(I). This byproduct along with the radical experiment support that the reaction occurs via the Cu(III) intermediate, and shows the substantial use of cheap copper salts as the catalysts and provide great alternatives as opposed to traditional Pd-catalysts in this transformation.

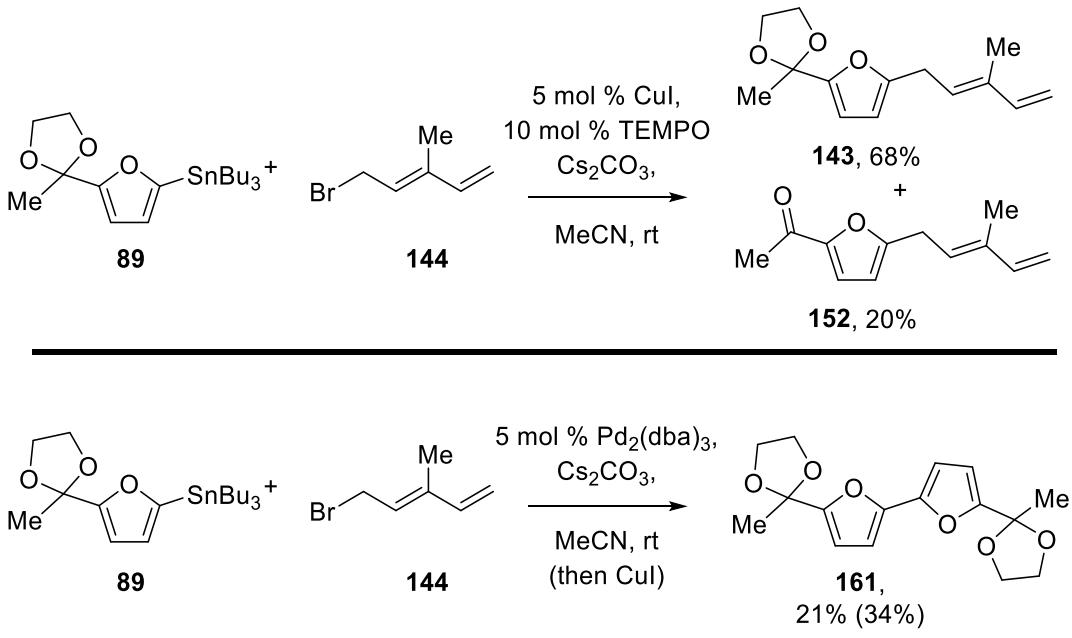

Scheme 2.18 Mechanistic Experiments for the Copper-Catalyzed Reactions

2.6.4 Sulfolene's Use as a Novel Protecting Group for Dienes

2.6.4.1 Circumventing Enone Triene Formation

With the coupled diene **143** now in hand, we turned our attention towards the synthesis of enone **141** shown in our prior work.[83] To help fight the resulting conjugation of the enone triene byproduct **147** (Scheme 2.19), we decided to protect the diene **143** via a cheletropic reaction. After a few planned steps this would result in the intermediate oxocarbenium ion **162**, that should now favor the 1,2 addition during the Kishi reduction as opposed to the β-elimination, resulting in enone **163**, which could then be deprotected via a retro 4+1 forming the desired enone **141**.

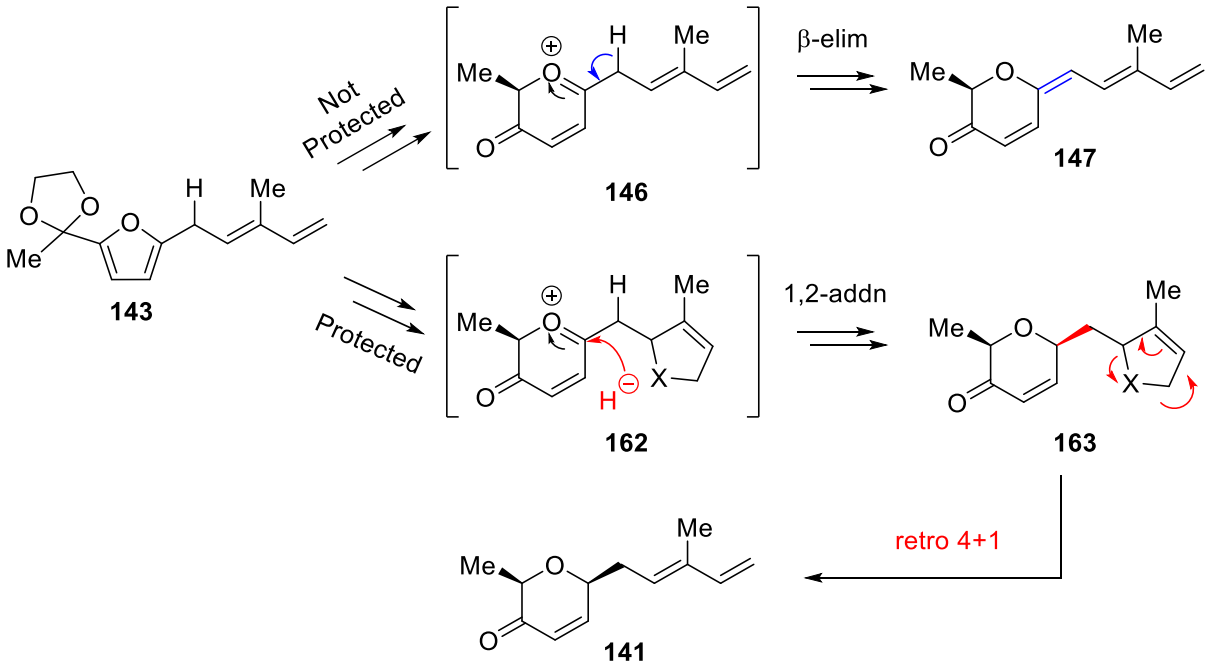

Scheme 2.19 Proposed Route to Circumvent Formation of Enone Triene **147**

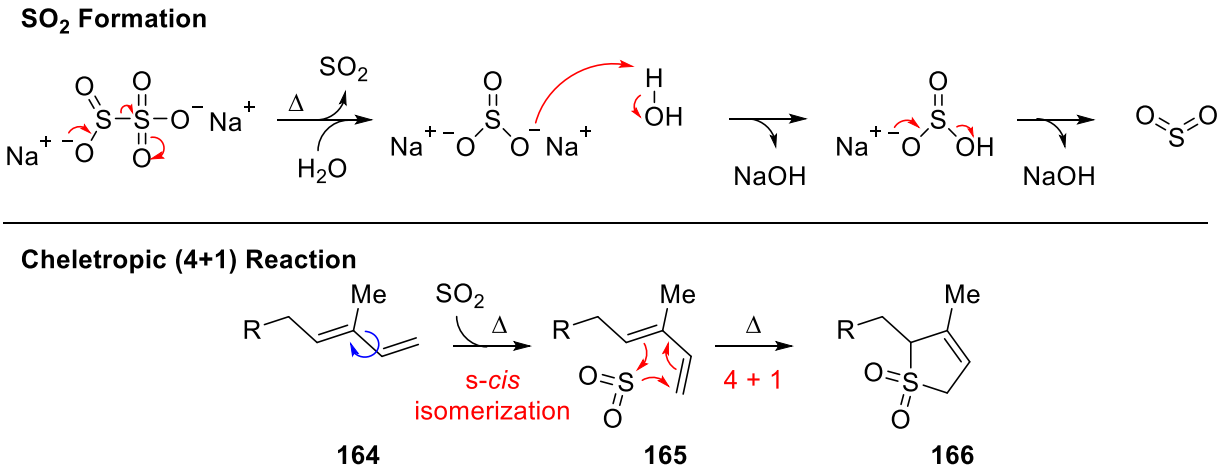

Figure 2.14 Sulfur Dioxide Formation and Subsequent 4+1

Inspired by the literature on pericyclic reactions,[101] we elected to use sulfolene as our novel protecting group due to its ability to undergo a retro 4+1 with heat, attributing to its facile removal when needed. Traditional formation of sulfolenes however are done by bubbling toxic SO_2 gas through a solution, making it difficult and dangerous to handle. Recently Larionov and coworkers[102] were able to circumvent this through the use $Na_2S_2O_5$ as an easy to handle solid to form the gas *in situ* upon heating and addition to water. A mechanism for the formation of the SO_2 gas is shown in Figure 2.14, in which two equivalents of the gas are made from every equivalent of the solid used. Isomerization of a diene **164** under heat will occur to form the s-*cis* isomer **165** that's geometrically available to undergo said 4+1, forming the desired sulfolene **166**.

2.6.4.2 Optimization of the Sulfolene Formation

To this end, we optimized the 4+1 reaction with our diene substrates **143** and **152** (Table 2.4). Starting off the optimization, we explored the use **143** as the starting material, with HFIP and water as the solvent system, sealing the reaction and heating it to 100°C as shown in the literature.[102] While they reported good to great yields (60-90%), we found very poor conversion with our substrate (entry 1). Diluting the reaction and using the ketone **152** instead decreased the yields (entry 2). We then screened using crude product **143** of the prior copper-catalyzed reaction and found those yields to be insufficient as well (entries 3-5). Thus we explored using pure dioxolane furyl diene **143** as the starting material for the reaction and observed that varying the SO_2 source, concentration, nor equivalences of the reagents used had a significant impact on the yield (entries 6-12). Instead, we tried the reactions with the ketone furyl diene **152** as the starting material. Again, similar trends were seen, even with varying the temperature as well, and it was observed that running the reaction at ambient temperature using HCl to try and promote the cheletropic reaction instead degraded the starting material (Entries 13-23).

Table 2.4 Optimization of Sulfolene Formation

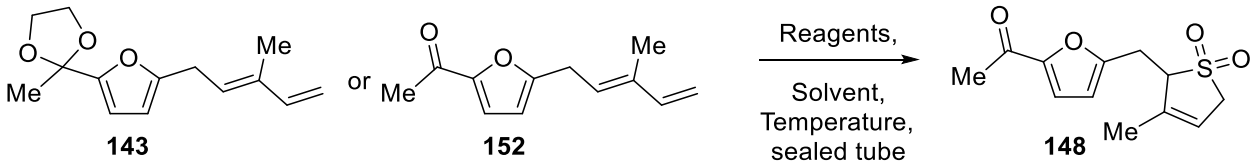

Entry	SM	Temp	Reagents (equiv)	Solvent (M)	% Yield (BRSM)
1	143	100	$Na_2S_2O_5$ (5)	HFIP:H_2O (4:1) **0.4** M	21
2	152	100	$Na_2S_2O_5$ (5)	HFIP:H_2O (4:1) **0.2** M	6
3	143[a]	100	$Na_2S_2O_5$ (5) $KHSO_4$ (2)	MeOH/H_2O (4:1) **0.4** M	7-18
4	143[a]	100	$Na_2S_2O_5$ (5) $KHSO_4$ (2)	MeOH/H_2O (4:1) **0.28** M	8
5	143[a]	100	$Na_2S_2O_5$ (5) $KHSO_4$ (2)	MeOH/H_2O (4:1) **0.1** M	11-17
6	143	100	$Na_2S_2O_5$ (**4.6**) $KHSO_4$ (**2.8**)	MeOH/H_2O (4:1) 0.1 M	29
7	143	100	$Na_2S_2O_5$ (5) $KHSO_4$ (**2**)	MeOH/H_2O (4:1) 0.4 M	13-48
8	143	100	$Na_2S_2O_5$ (5) $KHSO_4$ (**3**)	MeOH/H_2O (4:1) 0.4 M	6
9	143	100	$Na_2S_2O_5$ (**5**) $KHSO_4$ (**2**)	MeOH/H_2O (4:1) 0.**1** M	36
10	143	100	$Na_2S_2O_5$ (**6**) $KHSO_4$ (**3**)	MeOH/H_2O (4:1) 0.**2** M	20
11	143	100	$Na_2S_2O_5$ (**10**) $KHSO_4$ (**4**)	MeOH/H_2O (4:1) 0.**4** M	20
12	143	100	**$NaHSO_3$** (5) $KHSO_4$ (2)	MeOH/H_2O (4:1) 0.4 M	10
13	152	**50**	$Na_2S_2O_5$ (5) $KHSO_4$ (2)	MeOH/H_2O (4:1) 0.4 M	14
14	152	**80**	$Na_2S_2O_5$ (5) $KHSO_4$ (2)	MeOH/H_2O (**4:1**) 0.4 M	32

Table 2.4 Continued

Entry	SM	Temp	Reagents (equiv)	Solvent (M)	% Yield (BRSM)
15	152	**80**	$Na_2S_2O_5$ (5) $KHSO_4$ (2)	MeOH/H_2O (**1:1**) 0.4 M	18
16	152	100	$Na_2S_2O_5$ (**7**) $KHSO_4$ (2)	MeOH/H_2O (4:1) 0.3 M	24
17	152	100	$Na_2S_2O_5$ (**10**) $KHSO_4$ (2)	MeOH/H_2O (4:1) 0.2 M	22
18	152	100	**$NaHSO_3$** (5) $KHSO_4$ (2)	MeOH/H_2O (4:1) **0.4** M	19
19	152	100	**$NaHSO_3$** (**5**) $KHSO_4$ (2)	MeOH/H_2O (4:1) **0.2** M	18
20	152	100	**$NaHSO_3$** (**10**) $KHSO_4$ (2)	MeOH/H_2O (4:1) 0.2 M	38(58)
21	152	**23**	$Na_2S_2O_5$ (5) $KHSO_4$ (2)	MeCN/**HCl** (1:1) 0.05 M	trace
22	152	**23**	$Na_2S_2O_5$ (5) $KHSO_4$ (2)	THF/**HCl** (1:1) 0.05 M	RSM (52%)
23	152	**23**	$Na_2S_2O_5$ (**10**) $KHSO_4$ (2)	THF/**H_2O** (1:1) 0.4 M	trace
24	152	100	$Na_2S_2O_5$ (5) $KHSO_4$ (2)	MeCN/H_2O (1:1) 0.2 M	24(32)
25	152	100	**$NaHSO_3$** (5) $KHSO_4$ (2)	MeCN/H_2O (1:1) 0.2 M	trace
26	152	100	$Na_2S_2O_5$ (5) $KHSO_4$ (2)	**EtOH**/H_2O (1:1) 0.2 M	7
27	152	100	$Na_2S_2O_5$ (5) $KHSO_4$ (2)	**THF**/H_2O (1:1) 0.2 M	10(22)
28	152	100	$Na_2S_2O_5$ (5) $KHSO_4$ (2)	**IPA**/H_2O (1:1) 0.2 M	29(79)
29	152	100	$Na_2S_2O_5$ (5) $KHSO_4$ (2)	**Acetone**/H_2O (1:1) 0.2 M	7(13)
30	152	100	$Na_2S_2O_5$ (5) $KHSO_4$ (2)	**n-propanol**/H_2O (1:1) 0.2 M	29(44)
31	152	100	$Na_2S_2O_5$ (5) $KHSO_4$ (2)	**1,4-Diox**/H_2O (1:1) 0.2 M	40(60)
32	152	100	$Na_2S_2O_5$ (5) $KHSO_4$ (2)	1,4-Diox/H_2O (1:1) **0.4** M	31(40)
33	152	100	$Na_2S_2O_5$ (**10**) $KHSO_4$ (2)	1,4-Diox/H_2O (1:1) 0.2 M	29(40)
34	152	**80**	$Na_2S_2O_5$ (5) $KHSO_4$ (2)	1,4-Diox/H_2O (1:1) 0.2 M	15(89)
35	152	**120**	$Na_2S_2O_5$ (5) $KHSO_4$ (2)	1,4-Diox/H_2O (1:1) 0.2 M	27(40)
36	152	100	$NaHSO_3$ (**5**) $KHSO_4$ (**2**)	1,4-Diox/H_2O (1:1) 0.2 M	30(95)
37	152	100	$NaHSO_3$ (**10**) $KHSO_4$ (**4**)	1,4-Diox/H_2O (1:1) 0.2 M	53(89)
38	152	100	$NaHSO_3$ (**15**) $KHSO_4$ (**6**)	1,4-Diox/H_2O (1:1) 0.2 M	62(99)
39	**143**	100	$NaHSO_3$ (15) $KHSO_4$ (6)	1,4-Diox/H_2O (1:1) 0.2 M	60(71)
40	**143**	100	$NaHSO_3$ (20) $KHSO_4$ (8)	1,4-Diox/H_2O (1:1) 0.2 M	61(79)

[a]Carried forward crude from coupling

Finally, variance in organic co-solvent was done and more significant changes were seen (entries 21-31). EtOH gave very little conversion. Acetone, THF, and *n*-propanol also resulted in poorer yields of **148**, although we were able to recover some unreacted ketone **152**. Isopropanol and 1,4-Dioxane were both observed to allow for further recovery of **152**, and therefore 1,4-Dioxane was chosen as the co-solvent due to its inherent slightly higher yield of sulfolene **148** (entry 31). Attempts to concentrate the reaction, increase the equivalences of sodium metabisulfite used, or raise and lower the reaction temperature showed decreased efficiency of the reaction (entries 32-35). We were pleased to find that changing the SO_2 source to that of sodium bisulfite ($NaHSO_3$) showed great yields based on recovered starting material, slowly increasing the base

yield of ketone **148** as equivalences of the reagents were increased (entries 36-38). Finally, it was shown that no need for a prior deprotection of the coupled product (*E*)-**143** was needed, and the deprotection/protection steps could be done in one reaction pot to yield sulfolene **148** in 61% yield, 79% BRSM (entries 39 and 40).

2.6.5 Four-Step Asymmetric Sequence and Optimization

With the sulfolene formation now accomplished, we turned our attention toward the synthesis of enone **141**. We found that we were able to circumvent the use of 0.5 equivalents of CBS as shown in prior syntheses[87] and instead use 1 mol % of Noyori catalyst with *in situ* formed H_2 gas[103] to asymmetrically reduce the ketone in **148**, which resulted quantitatively in the alcohol **167**. The catalytic cycle for this transformation is shown in Figure 2.15. RuCl[(R,R)-TsDPEN](mesitylene) **I** first undergoes solvation and loss of its chlorine ligand to form it's $16e^-$ cationic species **II**, which upon dissociation of the solvent and incorporation of hydrogen gas it forms reversibly the η^2-H_2 complex **III**. The H_2 gas is formed via deprotonation of formic acid with triethylamine which leads to spontaneous decarboxylation. Finally, deprotonation of **III** with the chloride anion in a reversible fashion leads to the active catalytic hydride species **IV**,[104] which upon coordination to our substrate **148** via hydrogen-bond formation of the free secondary amine and carbonyl will lead to selective reduction from the *si* face,[105] and upon HCl incorporation will reform our catalyst **I** and the chiral product **167**.

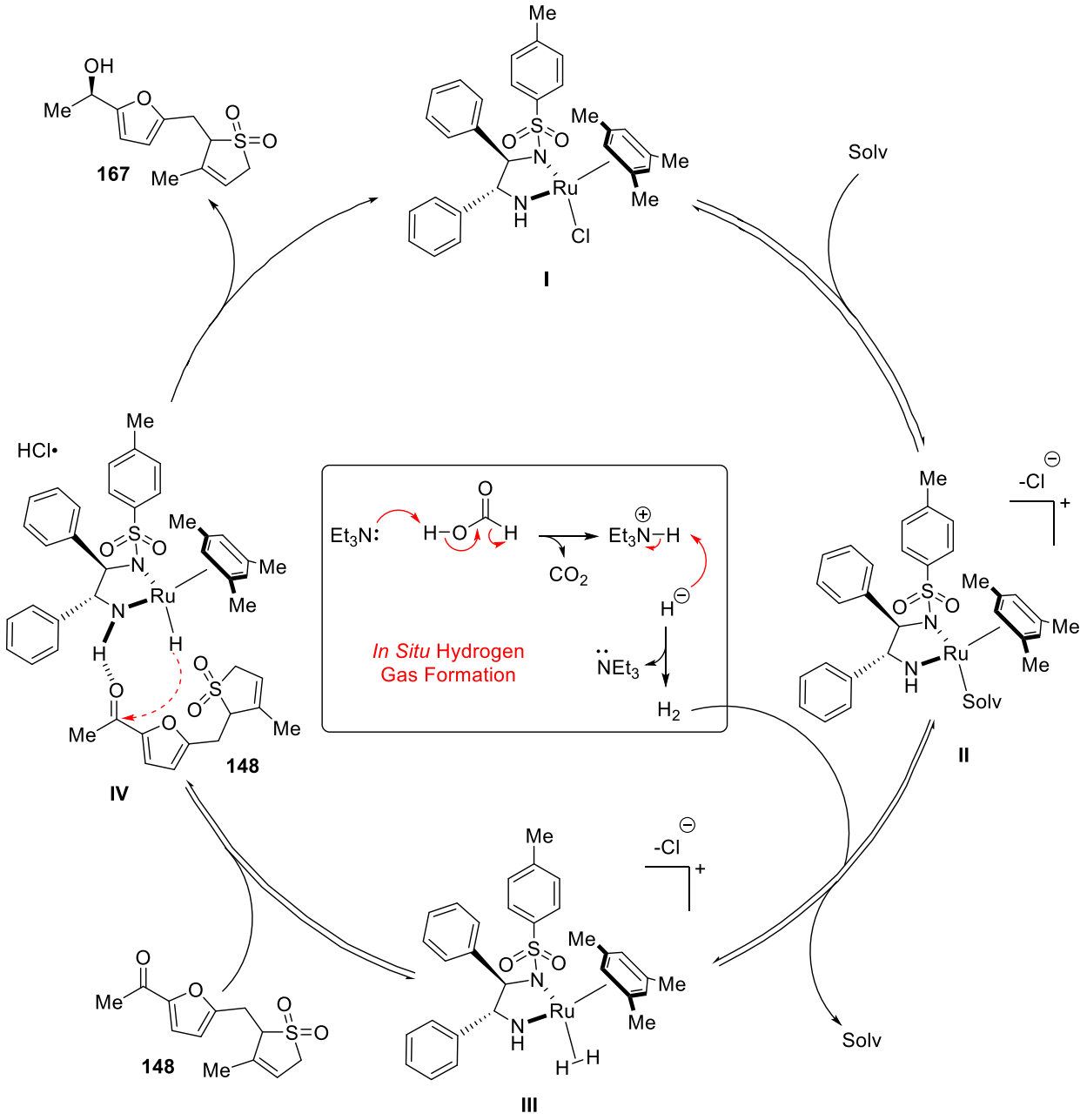

Figure 2.15 Catalytic Cycle for the Noyori Asymmetric Hydrogenation

During our synthesis, it was found that **167** degraded to uncharacterizable byproducts upon isolation in a manner of hours. The crude product was thus carried forward into the Achmatowicz step, resulting in the hemiketal **168** (Table 2.5). Of note, we were able to circumvent the use of $VO(acac)_2$ as well at this point and use a much greener and commercially available method.[97] This hemiketal material, as expected, was not isolable and the crude product immediately was used again in the next step. After carrying out the Kishi reduction and then removing the sulfolene via

a retro 4+1 to reform the diene in **141**, we noticed that a small amount of **147** was still forming in a 10:1 ratio, in 28% yield over the 4 steps (entry 1). As for why a small amount of triene still forms, results yet remain unclear. It's likely that the sulfolene group appears to be deprotecting a small amount during this multistep sequence, and then undergoing the β-elimination as before. To improve on the ratio and overall yield of this sequence, we carried out another small optimization, this time of the Kishi reduction step. We lowered the equivalents of the Lewis acid and Et_3SiH, obtaining enone **141** as the sole product via NMR and in similar yield (entry 2). Warming the reaction to 0°C resulted in full degradation of the starting material, and use of a Brønsted acid at -45°C in lieu of a Lewis Acid resulted in 33% yield but a 2:1 mixture of **141**:**147** (entries 3 and 4). Letting the reaction warm only slightly as well as increasing the number of equivalents of Et_3SiH decreased the yield, however maintained the great selectivity (entry 5). At this point, it was decided to do a head to head comparison of the Brønsted and Lewis acids and let the reaction run for several hours at -78°C. It was seen that TFA resulted in only enone triene **147** forming, whilst BF_3•Et_2O achieved the transformation in great yield (60%) of **141** over 4 steps and good ratio (>10:1, entries 6 & 7).

Table 2.5 Four Step Sequence and Optimization of the Kishi Reduction

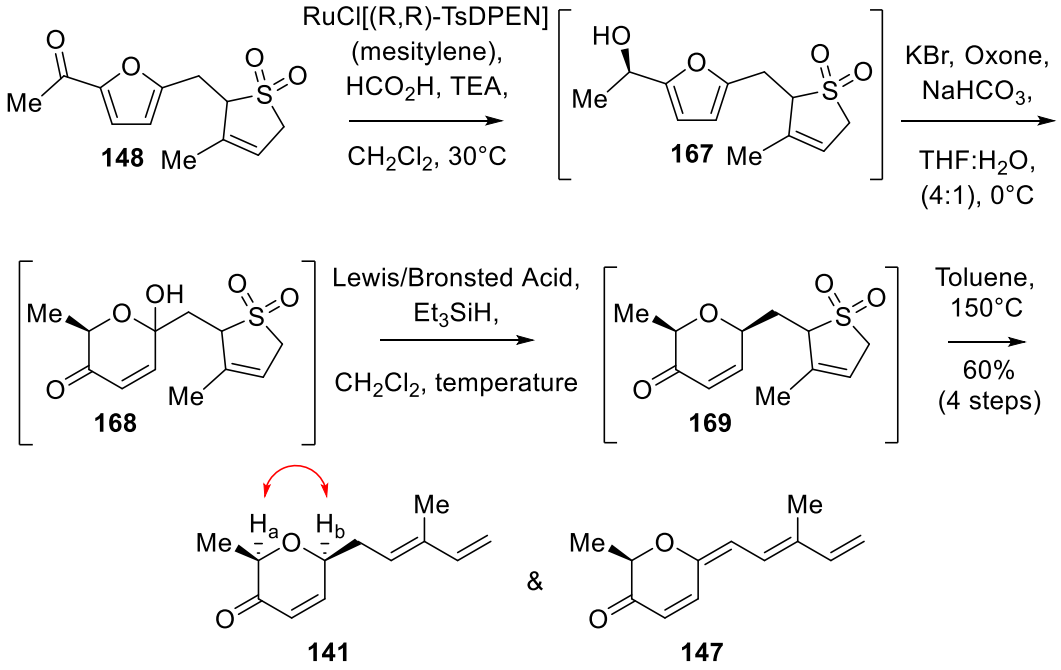

Entry	Acid (eq) Et_3SiH (eq)	Temp	Yield (4 steps)	Ratio 141:147[a]
1	$BF_3.Et_2O$ (2), (2.5)	-78°C	28%	10:1
2	$BF_3.Et_2O$ (1.2), (1.2)	-78°C	24%	>20:1
3	$BF_3.Et_2O$ (3), (3)	-78°C to 0°C	degraded	ND
4	TFA (15), (10)	-45°C	33%	2:1
5	$BF_3.Et_2O$ (5), (5)	-60°C to -45°C	20%	>20:1
6	TFA (2), (6)	-78°C[b]	ND	1:>20
7	$BF_3.Et_2O$ (2), (6)	-78°C[b]	60%	>10:1

[a]Ratio determined via ^1H NMR

As only one diastereomer was detectable via ^1H NMR, a proposed transition state for this observation is presented in Figure 2.16. Attack of the hydride to the bottom face (**170**) results in the more stable half chair in which the bulky sulfolene moiety rests pseudo-equatorial (**172**) Approach of the reductant to the top face as shown in **171** is hindered due to the up-facing methyl group, and would result in a pseudo-axial sulfolene moiety (**173**). We were able to support the *cis* relationship via 2D NMR correlation of H_a and H_b in enone **174**, and determine its *ee* to be >98% via chiral HPLC coming from the desymmetrization at the Noyori reduction step (Figure 2.17). To the best of the authors knowledge this is the first instance of sulfolene's use as a diene protecting group.

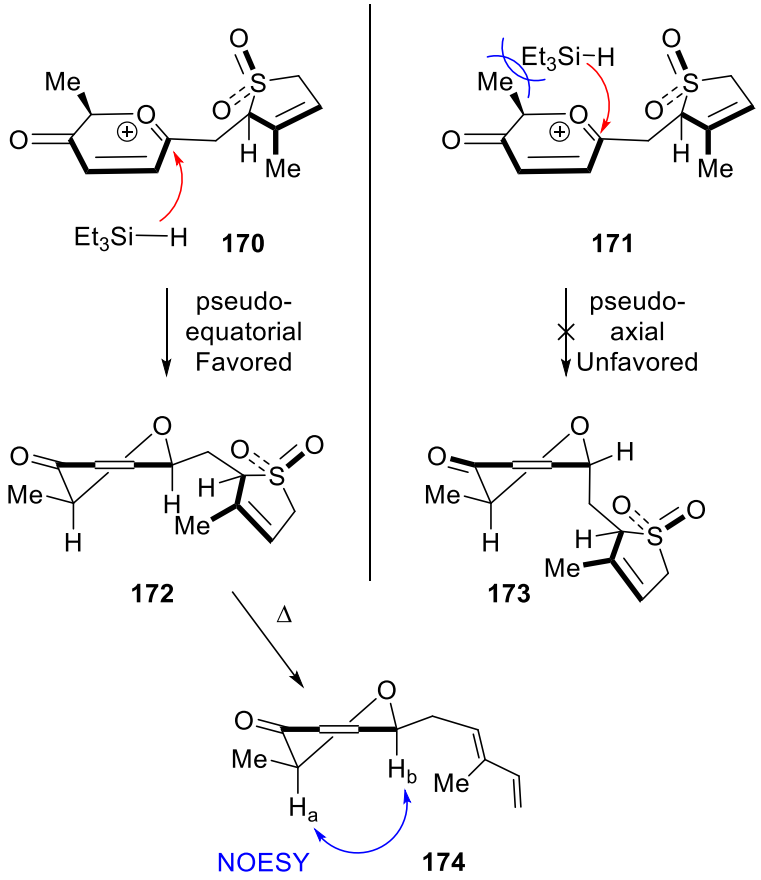

Figure 2.16 Proposed Transition State for the Diastereoselectivity of the Kishi Reduction and NOESY Interaction Observed

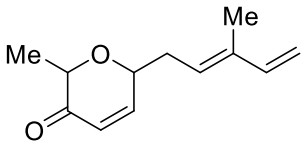

(±)-141

0.281% *ee*

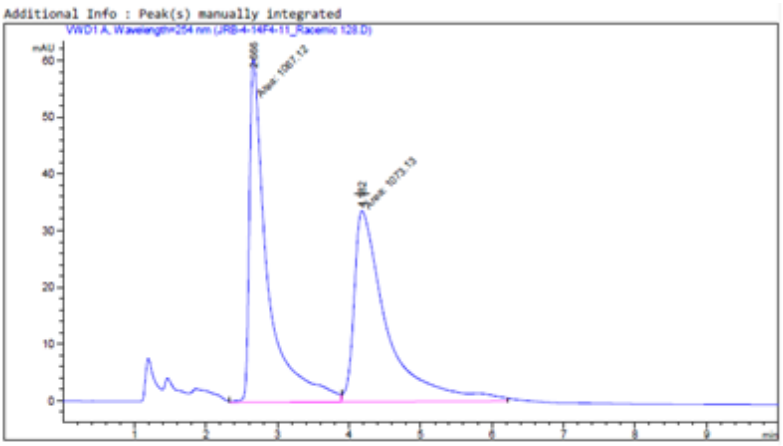

Sample Info : CHIRALPAK AY-3
1% IPA:Hexanes w/ 0.1% TFA Additive
Sample Dissolved1.5mg/mL in 10% IPA/HX
2.5 mL/min
254 nm
5 uL inj.

Signal 1: VWD1 A, Wavelength=254 nm

Peak #	RetTime [min]	Type	Width [min]	Area [mAU*s]	Height [mAU]	Area %
1	2.666	MF	0.2932	1067.11511	60.65258	49.8595
2	4.182	FM	0.5308	1073.12976	33.69788	50.1405

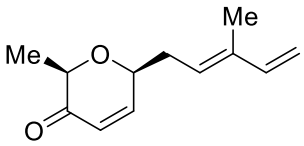

(+)-141

>98% *ee*

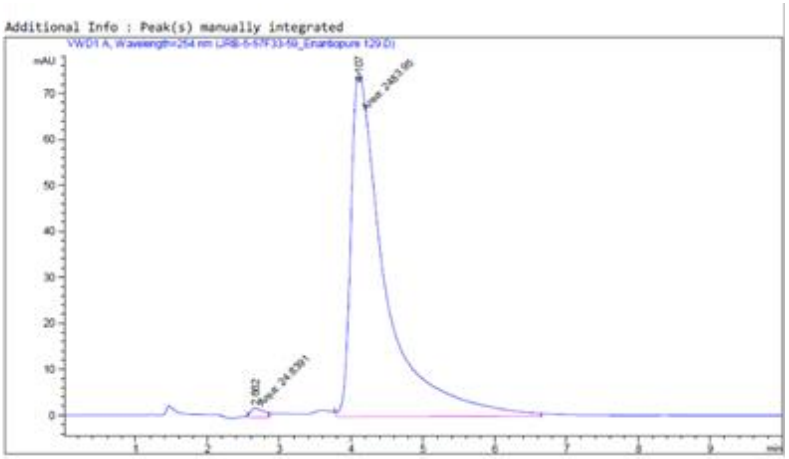

Sample Info : CHIRALPAK AY-3
1% IPA:Hexanes w/ 0.1% TFA Additive
Sample Dissolved1.5mg/mL in 10% IPA/HX
2.5 mL/min
254 nm
5 uL inj.

Signal 1: VWD1 A, Wavelength=254 nm

Peak #	RetTime [min]	Type	Width [min]	Area [mAU*s]	Height [mAU]	Area %
1	2.662	MF	0.2140	24.83908	1.93458	0.9901
2	4.107	FM	0.5532	2483.94556	74.83511	99.0099

Figure 2.17 HPLC Traces of **141** and After the Four Step Asymmetric Sequence

2.6.6 Synthesis of Tetrahydropyranyl Amine

With the construction of enone **141** now completed we've synthesized the common intermediate from our prior work,[83] and we're two steps away from the THP amine **92**. In previous work it was shown that Gilman formation using CuBr•DMS gave a 10:1 diastereomeric ratio. We were able to improve on this by using flame-dried CuI, forming the Gilman reagent at 0°C, then cannulating **141** to this solution at -78°C. This resulted in 91% yield of the desired product as the sole isomer as detected by ^{1}H NMR (Scheme 2.20). The stereoselectivity in the Michael addition is the result of chelation by the Gilman reagent to the top face inserting the methyl group in an axial fashion (intermediate **175**), which would otherwise be unfavored.[58,106] An excerpt of the spectral comparison of this isomer to another ^{1}H NMR showing a 2:3 dr ratio (undesired epimer the major product) of the same molecule is shown in Figure 2.18.

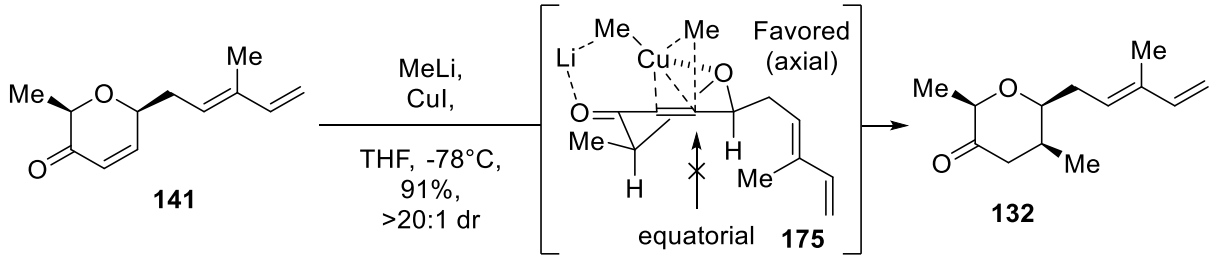

Scheme 2.20 Synthesis of β-methyl Ketone **132** and Proposed Intermediate

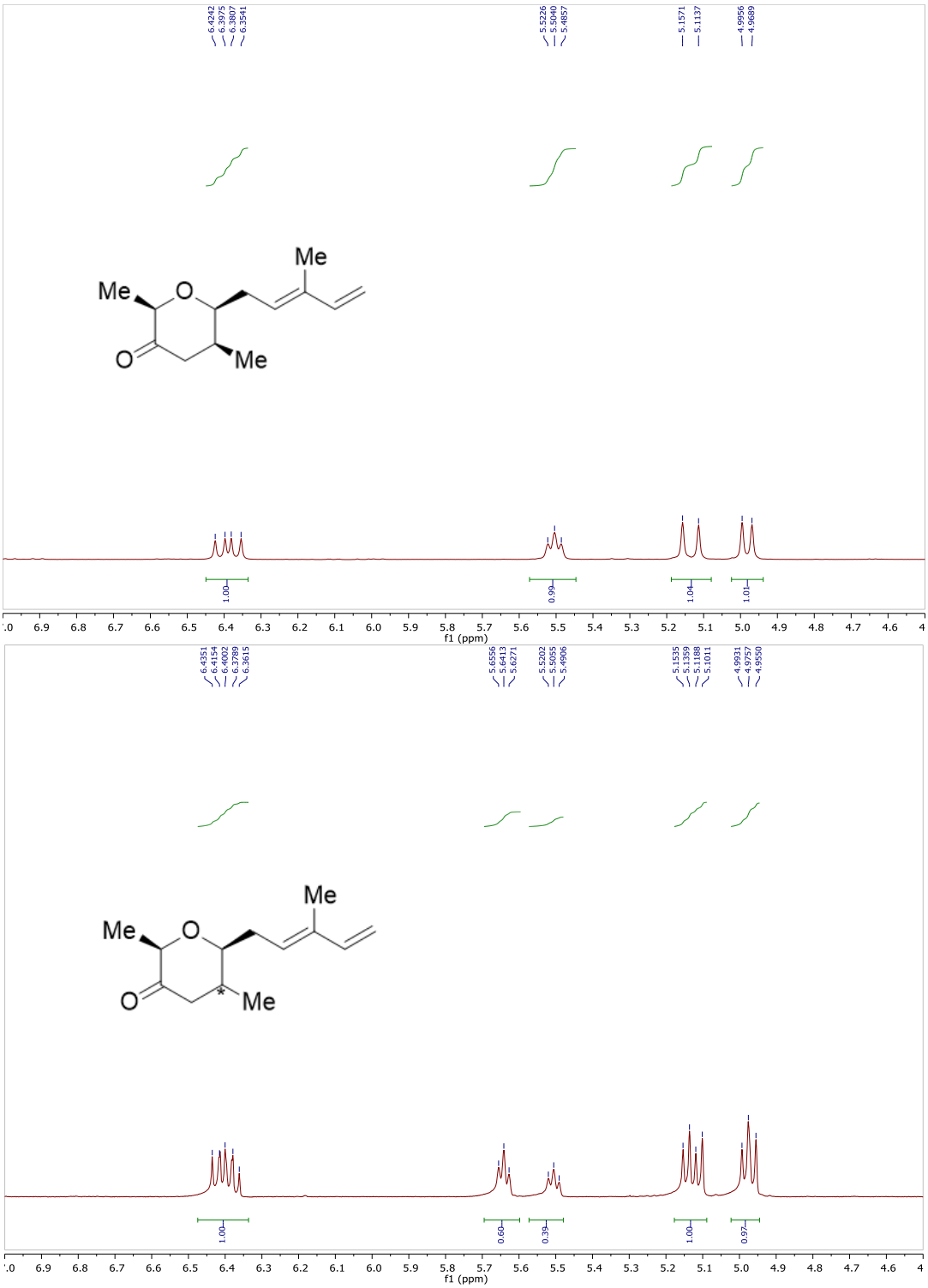

Figure 2.18 ^{1}H NMR Comparisons of β-methyl Ketones when Gilman Chelation Does and Doesn't Occur

With the β-methyl ketone in hand the last step to undergo is the stereoselective reductive amination. In the past we've shown this reduction to occur in 63% yield and up to an 8.5:1 dr. This stereoselectivity likely comes from the iminium ion being attacked from the equatorial position as opposed to the axial attack as the methyl group on the top blocks the face (**176**, Scheme 2.21)[100]. We were able to improve upon this by cooling the reaction to 0°C and letting it warm slowly to ambient temperature, resulting in one isomer detectable via NMR and in 82% yield.

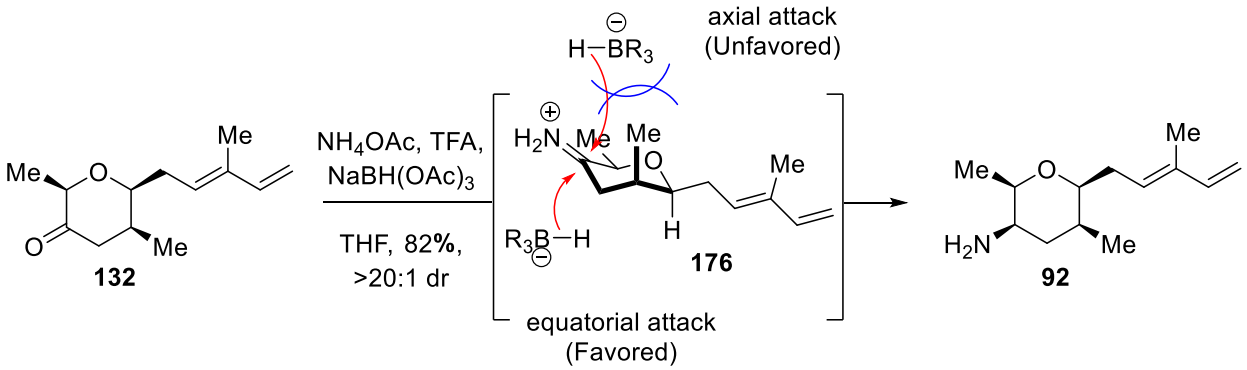

Scheme 2.21 Synthesis of the Tetrahydropyranal Amine **92**

2.7 Conclusion

In conclusion, we developed a novel copper-catalyzed Stille cross-coupling reaction between a stannyl furan and allyl bromides. This reaction is the first shown to be able to occur in the absence of palladium with catalytic (5 mol %) amounts of copper salts under ambient conditions and without the need for any external ligands or otherwise intramolecular chelation to undergo the transformation. We were able to apply this coupling in a multigram scale in our new concise formal synthesis of FR901464 derivatives. During said synthesis, we optimized the coupling in order to significantly improve the stereo- and regioselectivity, created and optimized the use of a novel diene protecting group to avoid the formation of an undesired triene moiety, constructed and optimized an asymmetric 4-step one column sequence, and improved upon prior steps to increase the stereoselectivity in the synthesis of the THP amine core. This core's stereochemistry and connectivity has been shown to be vital via past SAR studies and has been used several times in the synthesis of FR901464 analogues, achieving the final compounds in only two to three more linear steps (Figure 2.19).[83,84,86–88,90] Notably, the 4 chiral centers present in the THP amine are all constructed from that of the extremely prevalent natural product 2-acetyl furan, found in a grand variety of foods.[63–66,107]

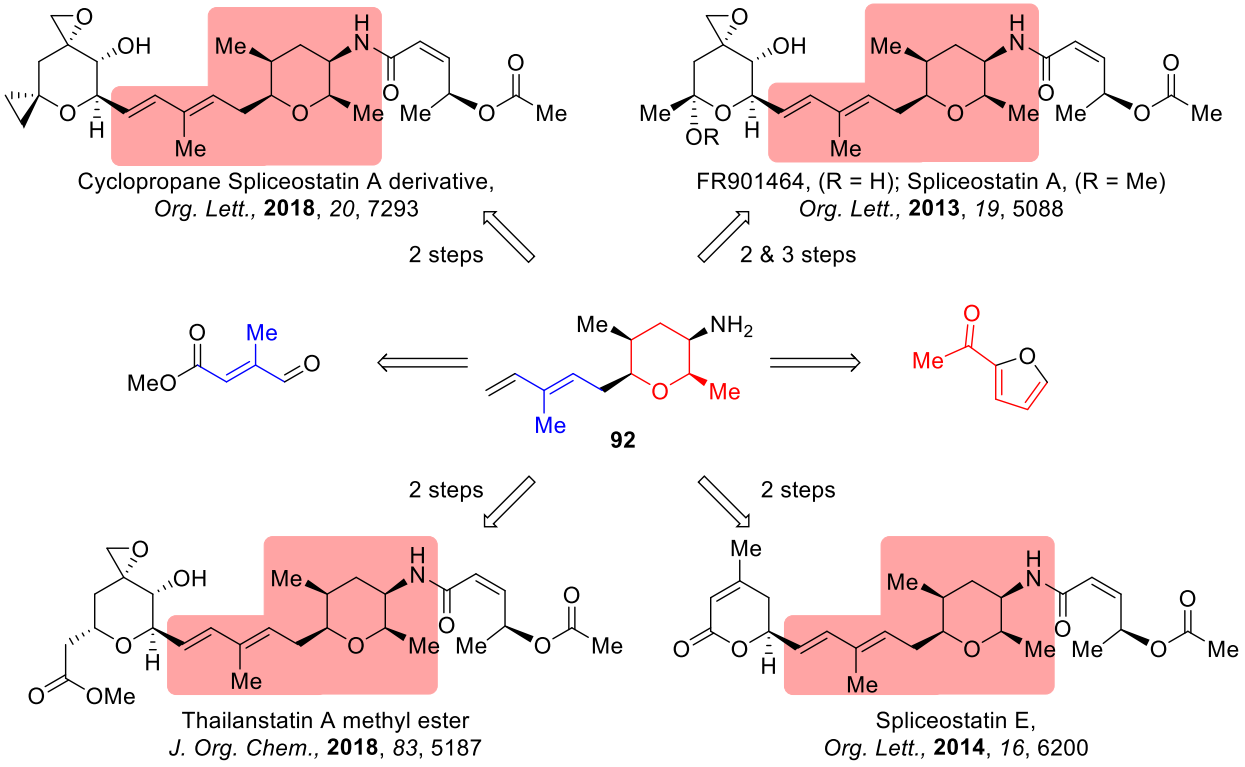

Figure 2.19 THP Amine's Presence in the Literature

2.8 Experimental Conditions

2.8.1 General Experimental Methods

All chemical and reagents were purchased from commercial suppliers and used without further purification unless otherwise noted. Tetrahydrofuran was distilled from Na/Benzophenone prior to use. All reactions were performed in oven-dried round-bottom flasks followed by flame-drying under vacuum in the case of moisture-sensitive reactions. The flasks were fitted with rubber septa and kept under a positive pressure of argon. Cannula were used in the transfer of moisture-sensitive liquids. Heated reactions were ran using an oil bath on a hot plate equipped with a temperature probe. TLC analysis was conducted using glass-backed thin-layer silica gel chromatography plates (60 Å, 250 μm thickness, F-254 indicator). Flash chromatography was done using a 230−400 mesh, a 60 Å pore diameter silica gel. Organic solutions were concentrated at 30−35 °C on rotary evaporators capable of achieving a minimum pressure of ∼25 Torr and further concentrated on a Hi-vacuum pump capable of achieving a minimum pressure of ∼4 Torr. ^{1}H NMR spectra were recorded on 400, 500, and 800 MHz spectrometers. ^{13}C NMR spectra were recorded at 100, 125, and 200 MHz on the respective NMRs. Chemical shifts are reported in parts per million and referenced to the deuterated residual solvent peak ($CDCl_3$, 7.26 ppm for ^{1}H and 77.16 ppm for ^{13}C). NMR data are reported as δ value (chemical shift), J-value (Hz), and integration, where s = singlet, bs = broad singlet, d = doublet, t = triplet, q = quartet, p = quintet, m = multiplet, dd = doublet doublets, and so on. Optical rotations were recorded on a digital polarimeter. Low resolution mass spectra (LRMS) spectra were recorded using a quadrupole LCMS under positive electrospray ionization (ESI+). High-resolution mass spectrometry (HRMS) spectra were recorded at the Purdue University Department of Chemistry Mass Spectrometry Center. These experiments were performed under ESI+ and positive atmospheric pressure chemical ionization (APCI+) conditions using an Orbitrap XL Instrument.

2.8.2 Experimental Procedures

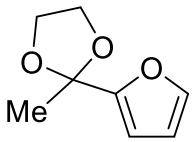

106

Furyl Dioxolane **106**.[108] To a one-neck oven dried 500 mL round bottom flask equipped with a Dean-Stark apparatus and reflux condenser 2-acetyl furan **105** (10 g, 91 mmol, 1.0 equiv) was added followed by benzene (PhH, 181 mL, 0.5 M). To this, ethylene glycol (7.6 mL, 136 mmol, 1.5 equiv) and p-Toluenesulfonic acid monohydrate (PTSA•H_2O, 863 mg, 4.5 mmol, 5 mol %) were added sequentially and the reaction was refluxed at 150°C in order to remove water. Reaction mixture turned gold after several hours, and overnight developed a dark maroon color. Once reaction appeared to be complete via TLC analysis (75 hours), flask was cooled to ambient temperature, quenched 1 M NaOH (200 mL), extracted with ethyl acetate three times, dried with Na_2SO_4, and concentrated under reduced pressure. The crude mixture was purified via silica column chromatography using 10% ethyl acetate:hexanes as the eluent. Furyl dioxolane **106** was isolated as a brown liquid (12.8 g, 92%). TLC: silica gel (10% ethyl acetate:hexanes) R_f = 0.39. ^{1}H NMR (400 MHz, $CDCl_3$) δ 7.37 (t, *J* = 1.3 Hz, 1H), 6.32-6.30 (m, 2H), 4.07 – 3.99 (m, 4H), 1.74 (s, 3H). $^{13}C\{^1H\}$ NMR (100 MHz, $CDCl_3$) δ 154.6, 142.5, 110.0, 106.6, 104.9, 65.3, 24.5.

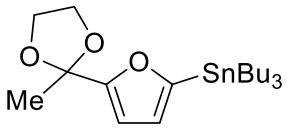

89

Furyl Organostannyl Dioxolane **89**. To a two-neck oven dried 1 L round bottom flask furyl dioxolane **106** (12.9 g, 117 mmol, 1.0 equiv) was dissolved in freshly distilled tetrahydrofuran (THF, 195 mL) followed by tetramethylethylenediamine (TMEDA, 40 mL, 269 mmol, 2.3 equiv) and cooled to -78°C. *n*-Butyl Lithium (1.6 M in hexanes, 95 mL, 152 mmol, 1.3 equiv) was added slowly, changing the color of the reaction from gold to orange then dark green. The flask was let warm to a range of -40°C to -20°C for a duration 2.5 hours. At this time the flask was cooled back to -78°C. In a separate flask tributyltin chloride ($ClSnBu_3$, 41.3 mL, 152 mmol, 1.3 equiv) in freshly distilled THF (195 mL) was cooled to -78°C as well and cannulated into the reaction flask

at the same temperature. Receiving flask went from brown with a golden fringe to orange. The reaction was let warm slowly to ambient temperature over the course of 20 hours. The dark orange solution was quenched with saturated $NaHCO_3$ (300 mL), extracted with diethyl ether three times, washed with brine, dried over Na_2SO_4, and concentrated under reduced pressure. The crude material was purified via column chromatography using Harrowven and coworkers procedure[67] (10% K_2CO_3:silica stationary phase), and with a 2-10% ethyl acetate:hexanes gradient. Furyl organostannyl dioxolane **89** was isolated as a brown oil (31.9 g, 61%). TLC: silica gel (20% ethyl acetate:hexanes) R_f = 0.47 ^{1}H NMR (500 MHz, $CDCl_3$) δ 6.44 (d, *J* = 3.1 Hz, 1H), 6.30 (d, *J* = 3.1 Hz, 1H), 4.06 – 4.00 (m, 4H), 1.75 (s, 3H), 1.59 – 1.53 (m, 6H), 1.35 – 1.30 (m, 6H), 1.14 – 1.00 (m, 6H), 0.89 (t, *J* = 7.3 Hz, 9H). $^{13}C\{^1H\}$ NMR (200 MHz, $CDCl_3$) δ 161.2, 159.2, 121.7, 106.3, 105.1, 65.2, 29.1, 27.3, 24.4, 13.8, 10.3.

General Procedure for Cu-Catalyzed Cross Coupling of model substrate*

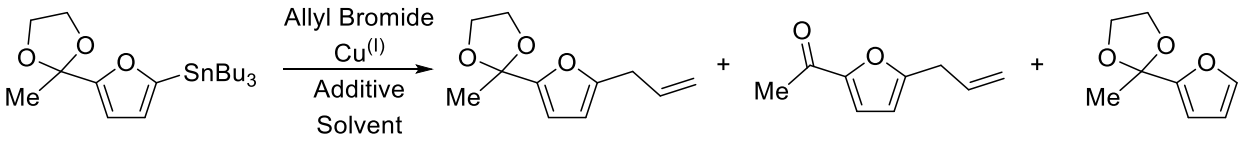

89 **104** **107** **106**

To a two-neck oven dried round bottom flask containing furyl organostannyl dioxolane **89** (1.0 equiv) and solvent (0.1 molar), additive (0.1 equiv) and Cu^{I} catalyst (5 – 50 mol %) was added. Allyl bromide (2.0 equiv) was then added neat. Once reaction appears complete via TLC analysis (3-120 hours depending on desired product and scale of reaction), saturated KF (0.1 Molar) was added and let stir for a few minutes. The quenched reaction was then diluted with ethyl acetate, extracted three times with said solvent, washed with brine/saturated LiCl, dried with Na_2SO_4, and concentrated under reduced pressure. The crude material was then passed through a 10% K_2CO_3:Silica plug,[67] using 10% ethyl acetate:hexanes as the eluent. Allyl furyl dioxolane **104** and protodestannylated byproduct **106** coeluted and thus ratios were calculated via ^{1}H NMR. Allyl furyl ketone **107** was isolable, if formed. The same stationary phase for the plug could be used several times before needing to be replaced due to decreased flow & blockage. *In the case a change of addition was indicated, **89** was dissolved in the solvent followed by the additive and the bromide. In a separate flask CuI was then flame-dried under vacuum to form a canary yellow color, then cooled under Argon and the reaction flask was cannulated to the copper flask and let stir. Equivalences, workup, and purification all remained the same.

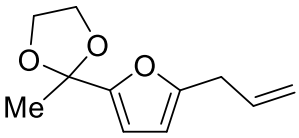

104

Allyl Furyl Dioxolane **104**. TLC: silica gel (10% ethyl acetate:hexanes) R_f = 0.40 ^{1}H NMR (400 MHz, $CDCl_3$) δ 6.21 (d, *J* = 3.1 Hz, 1H), 5.97 – 5.87 (m, 2H), 5.16 – 5.08 (m, 2H), 4.05 – 3.98 (m, 4H), 3.38 (dq, *J* = 6.6, 1.4 Hz, 2H), 1.72 (s, 3H). ^{13}C{^{1}H} NMR (100 MHz, $CDCl_3$) δ 154.1, 153.1, 133.8, 117.1, 107.3, 105.9, 104.9, 65.2, 32.8, 24.5. LRMS-ESI (+) *m/z*: 195.1 $[M + H]^+$.

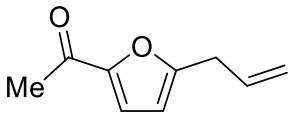

107

Allyl Furyl Ketone **107**. TLC: silica gel (10% ethyl acetate:hexanes) R_f = 0.24 ^{1}H NMR (400 MHz, $CDCl_3$) δ 7.11 (d, *J* = 3.5 Hz, 1H), 6.19 (d, *J* = 3.5 Hz, 1H), 5.93 (ddt, *J* = 16.8, 10.1, 6.7 Hz, 1H), 5.22 – 5.16 (m, 2H), 3.47 (d, *J* = 6.7 Hz, 2H), 2.43 (s, 3H). $^{13}C\{^1H\}$ NMR (100 MHz, $CDCl_3$) δ 186.4, 159.6, 151.9, 132.4, 119.2, 118.3, 108.8, 33.0, 25.9. LRMS-ESI (+) *m/z*: 151.1 $[M + H]^+$.

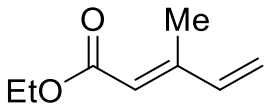

150

Diene Ester **150**.[109] To a two-neck oven dried 500 mL round bottom flask $MePPh_3Br$ (8.4 g, 23.5 mmol, 1.07 equiv) was added with a stirbar and stirred under vacuum while heating the flask to 110°C overnight. The flask was cooled under Argon then freshly distilled tetrahydrofuran (THF, 157 mL, 0.14 M) was added followed by *n*-butyllithium (*n*-BuLi, 1.6 M in hexanes, 15 mL, 24 mmol, 1.1 equiv) at -78°C. Solution went from white slurry to golden. Flask was then allowed to warm to 0°C over the course of an hour, and then re-cooled to -45°C and Ethyl-3-methyl-4-oxocronate **149** (3 mL, 22 mmol, 1.0 equiv) was added slowly. Reaction went from golden orange to pink. After two hours, reaction was pulled from -45°C bath and quenched H_20 (150 mL), turning purple. The crude mixture was extracted three times with diethyl ether, then concentrated under reduced pressure on ice due to product volatility. The crude mixture was purified via a short silica plug with 5% diethyl ether:hexanes as the eluent. Diene ester **150** was isolated as a clear liquid. The product was taken on without any further purification. TLC: silica gel (10% ethyl acetate:hexanes) R_f = 0.24 ^{1}H NMR (400 MHz, $CDCl_3$) δ 6.40 (ddd, *J* = 17.4, 10.6, 0.8 Hz, 1H), 5.79 (s, 1H), 5.61 (d, *J* = 17.4 Hz, 1H), 5.38 (d, *J* = 10.6 Hz, 1H), 4.18 (q, *J* = 7.1 Hz, 2H), 2.27 (d, *J* = 1.2 Hz, 3H), 1.28 (t, *J* = 7.2 Hz, 3H). $^{13}C\{^1H\}$ NMR (126 MHz, $CDCl_3$) δ 167.1, 152.1, 140.3, 120.2, 119.5, 60.0, 14.5, 13.2.

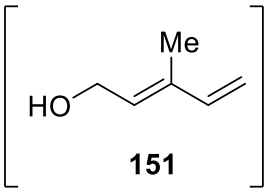

151

Diene Alcohol **151**. To a two-neck oven dried 500 mL round bottom flask lithium aluminum hydride (LAH, 1 g, 27 mmol, 1.5 equiv) was added to diethyl ether (135 mL). In a separate flask, diene ester **150** (2.5 g, 18 mmol, 1.0 equiv) was dissolved in diethyl ether (Et_2O, 43 mL) and cannulated to the flask containing LAH at 0°C. The reaction was removed from the ice bath, equipped with a reflux condenser, and heated to reflux (50°C) for 2 hours. The reaction was then cooled to 0°C again, quenched with ice and cold water slowly (100 mL) then 10% H_2SO_4 (100 mL). Reaction was then extracted with diethyl ether three times, dried over Na_2SO_4, and

concentrated under reduced pressure on ice to yield diene alcohol **151** as a colorless liquid (1.7 g, 97% yield, 78% over two steps). TLC: silica gel (10% ethyl acetate:hexanes) R_f = 0.09 ^{1}H NMR (500 MHz, Chloroform-*d*) δ 6.39 (ddd, *J* = 17.4, 10.7, 0.7 Hz, 1H), 5.68 (t, *J* = 7.0 Hz, 1H), 5.22 (d, *J* = 17.4 Hz, 1H), 5.07 (d, *J* = 10.7 Hz, 1H), 4.30 (d, *J* = 6.8 Hz, 2H), 1.79 (d, *J* = 1.1 Hz, 3H), 1.33 (bs, 1H). ^{13}C{^{1}H} NMR (125 MHz, $CDCl_3$) δ 140.8, 136.5, 130.5, 113.3, 59.5, 12.0.

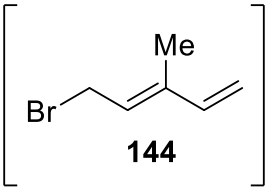

144

Diene Bromide **144**. To a one-neck oven dried 250 mL round bottom flask diene alcohol **151** was dissolved in diethyl ether (Et_2O, 94 mL, 0.27 M) and cooled to 0°C. Tribromophosphine (1.3 mL, 13.9 mmol, 0.55 equiv) was added (fuming occurred) and the reaction was let stir for 1.5 hours at 0°C. Reaction was then quenched with brine (100 mL), brought to ambient temperature, and extracted with ether three times. The organic layer was dried over Na_2SO_4 and concentrated under reduced pressure on ice. The crude material was then diluted with cold hexanes and filtered through a cotton plug to remove majority of the phosphine oxide, and concentrated again under reduced pressure on ice to yield diene bromide **144** as a yellow liquid (4 g, >99%), and was used without further purification. TLC: silica gel (10% ethyl acetate:hexanes) R_f = 0.66, clearly degrading on silica. ^{1}H NMR (400 MHz, $CDCl_3$) δ 6.38 (ddd, *J* = 17.4, 10.7, 0.7 Hz, 1H), 5.78 (t, *J* = 8.9 Hz, 1H), 5.30 (d, *J* = 17.4 Hz, 1H), 5.12 (d, *J* = 10.7 Hz, 1H), 4.13 (d, *J* = 8.6 Hz, 2H), 1.85 (d, *J* = 1.3 Hz, 3H). ^{13}C{^{1}H} NMR (100 MHz, $CDCl_3$) δ 140.2, 139.9, 126.8, 114.9, 29.0, 11.6.

Formation of Dioxolane Diene

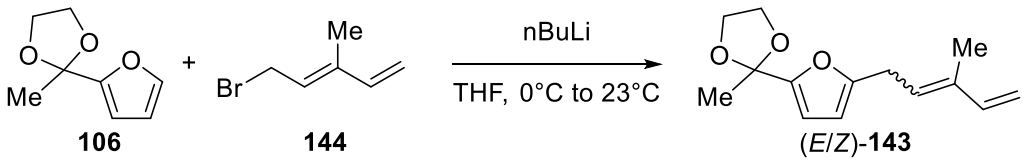

106 **144** (*E*/*Z*)-**143**

Initial attempts: To a two-neck oven dried 10 mL round bottom flask Furyl dioxolane **106** (81 mg, 0.53 mmol, 1.0 equiv) was dissolved in freshly distilled tetrahydrofuran (THF, 2.5 mL). To this, *n*-butyllithium (*n*-BuLi , 1.6 M, 0.5 mL, 0.79 mmol, 1.5 equiv) was added at 0°C. The reaction turned teal, then greener and finally yellow as it warmed to ambient temperature. After 50 minutes the reaction was cooled back to 0°C and a solution of diene bromide **144** (127 mg, 0.79 mmol, 1.5 equiv) in 2.5 mL THF was cannulated in. After 2.5 hours, the reaction was quenched with saturated NH_4Cl (5 mL), extracted three times with ethyl acetate, washed with brine, dried with Na_2SO_4, and concentrated under reduced pressure. The crude material was purified via silica column chromatography using 3-5% ethyl acetate:hexanes as the gradient. Dioxolane furyl diene **143** was isolated as a clear yellow liquid (54 mg, 44% yield, mixture of isomers).

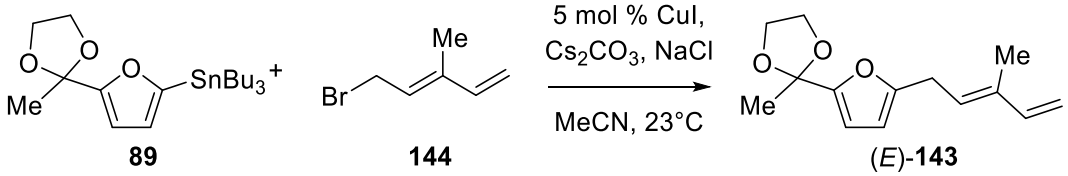

89 **144** (*E*)-**143**

Optimized Copper Coupling: To a two-neck oven dried 500 mL round bottom flask stannane **89** (7.34 g, 16.6 mmol, 1.0 equiv) was dissolved in acetonitrile (MeCN, 125 mL). To this, Cs_2CO_3 (1.0 g, 3.3 mmol, 0.2 equiv) was added. Diene bromide **144** (4.0 g, 25 mmol, 1.5 equiv) in 41 mL MeCN was then cannulated to the reaction mixture, then copper (I) iodide (CuI , 158 mg, 0.8 mmol, 5 mol %) and NaCl (1.0 g, 18 mmol, 1.1 equiv) was added and reaction let stir. After the reaction appeared complete via TLC analysis (24-96 hours depending scale of reaction), it was concentrated down under reduced pressure. The crude material was purified via column chromatography using Harrowven and coworkers procedure[67] (10% K_2CO_3:silica stationary phase), and with a 1-20% ethyl acetate:hexanes gradient. Dioxolane furyl diene (*E*)-**143** was isolated as yellow liquid (3.42 g, 88% yield).

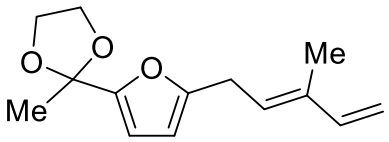

(*E*)-**143**

Dioxolane Furyl Diene **143**. TLC: silica gel (10% ethyl acetate:hexanes) R_f = 0.39 ^{1}H NMR (400 MHz, $CDCl_3$) δ 6.41 (ddd, *J* = 17.4, 10.7, 0.7 Hz, 1H), 6.20 (d, *J* = 3.1 Hz, 1H), 5.89 (dt, *J* = 3.1, 1.0 Hz, 1H), 5.64 (t, *J* = 7.3 Hz, 1H), 5.16 (d, *J* = 17.4 Hz, 1H), 5.00 (d, *J* = 10.7 Hz, 1H), 4.05 – 4.00 (m, 4H), 3.48 (d, *J* = 7.4 Hz, 2H), 1.80 (d, *J* = 1.1 Hz, 3H), 1.72 (s, 3H). ^{13}C NMR (100 MHz, $CDCl_3$) δ 154.3, 153.0, 141.1, 136.1, 127.0, 111.9, 107.3, 105.5, 104.8, 65.2, 27.4, 24.4, 11.9. HRMS-APCI (+) m/z: calcd for $C_{14}H_{19}O_3$ $[M + H]^+$, 235.1329; found, 235.1332.

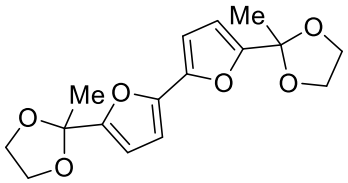

161

Furyl Dioxolane Dimer **161**. TLC: silica gel (10% ethyl acetate:hexanes) R_f = 0.09 ^{1}H NMR (400 MHz, $CDCl_3$) δ 6.48 (d, J = 3.3 Hz, 1H), 6.36 (d, J = 3.3 Hz, 1H), 4.08 – 4.01 (m, 4H), 1.76 (s, 3H). ^{13}C{^{1}H} NMR (100 MHz, $CDCl_3$) δ 153.85, 146.28, 108.40, 105.74, 104.81, 65.29, 24.57. LRMS-ESI (+) *m/z*: 307.1 $[M + H]^+$.

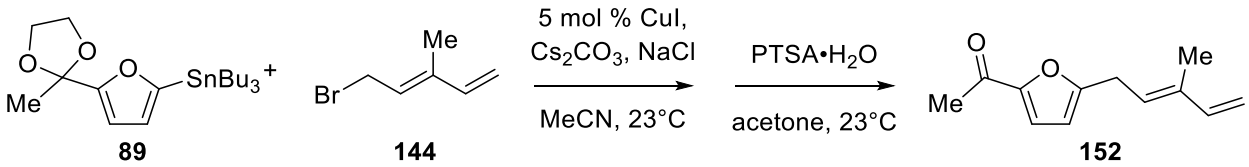

89 **144** **152**

2-Step Copper Coupling and Deprotection: To a two-neck oven dried 100 mL round bottom flask furyl organostannyl dioxolane **89** (970 mg, 2.2 mmol, 1.0 equiv) was dissolved in acetonitrile (MeCN, 15 mL). To this, Cs_2CO_3 (143 mg, 0.4 mmol, 0.2 equiv) was added. Diene bromide **144** (705 mg, 4.4 mmol, 2.0 equiv) in 7 mL MeCN was then cannulated to the reaction mixture, then copper (I) iodide (CuI, 21 mg, 0.1 mmol, 5 mol %) was added and reaction let stir. After the reaction appeared complete via TLC analysis (24-96 hours depending on scale of reaction), it was concentrated down under reduced pressure, taken back up in ethyl acetate (20 mL), brine (10 mL), and water (10 mL). It was extracted three times with ethyl acetate, then the organic layers were washed with brine, dried with Na_2SO_4, and concentrated under reduced pressure. The crude material was purified via column chromatography using Harrowven and coworkers procedure[67] (10% K_2CO_3:silica stationary phase), and with 10% ethyl acetate:hexanes as the eluent. The fractions containing dioxolane furyl diene (*E*)-**143** were concentrated under reduced pressure and carried on to the next step (479 mg, 94%).

To a one-neck oven-dried 50 mL round bottom flask dioxolane furyl diene (*E*)-**143** (479 mg, 2.0 mmol, 1.0 equiv) was dissolved in acetone (25 mL, 0.08 M), and p-Toluenesulfonic acid monohydrate (430 mg, 2.2 mmol, 1.1 equiv) was added. Reaction went from yellow to a greenish-gold color. After the reaction appeared complete via TLC analysis (2 hours), it was concentrated down under reduced pressure and purified via silica column chromatography using 5% ethyl acetate:hexanes as the eluent. Ketone furyl diene **152** was isolated as a yellow oil (349 mg, 90%, 85% over two steps).

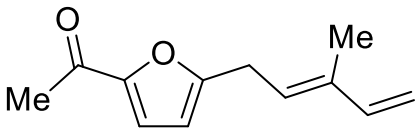

(*E*)-**152**

Ketone Furyl Diene (*E*)-**152**. TLC: silica gel (20% ethyl acetate:hexanes) R_f = 0.24 ^{1}H NMR (400 MHz, $CDCl_3$) δ 7.09 (d, *J* = 3.5 Hz, 1H), 6.39 (ddd, *J* = 17.4, 10.7, 0.7 Hz, 1H), 6.15 (dt, *J* = 3.5, 1.0 Hz, 1H), 5.63 (dddd, *J* = 7.4, 6.8, 1.4, 0.7 Hz, 1H), 5.18 (d, *J* = 17.2 Hz, 1H), 5.02

(d, *J* = 10.7 Hz, 1H), 3.55 (d, *J* = 7.4 Hz, 2H), 2.42 (s, 3H), 1.80 (s, 3H). $^{13}C\{^{1}H\}$ NMR (100 MHz, $CDCl_3$) δ 186.2, 159.8, 151.8, 140.7, 137.0, 125.2, 119.2, 112.6, 108.5, 27.7, 25.8, 12.0. HRMS-ESI (+) m/z: calcd for $C_{12}H_{14}O_2Na$ $[M + Na]^+$, 213.0886; found, 213.0885

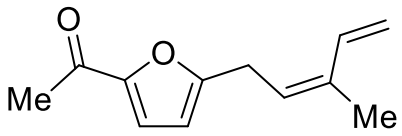

(*Z*)-**152**

Ketone Furyl Diene (*Z*)-**152**. Part of mixture of isomers, only ^{1}H NMR shifts could be determined. TLC: silica gel (20% ethyl acetate:hexanes) R_f = 0.24 ^{1}H NMR (400 MHz, $CDCl_3$) δ 7.12 -7.09 (m, 1H), 6.76 (ddd, J = 17.2, 10.8, 0.9 Hz, 1H), 6.17-6.15 (m, 1H), 5.54 (t, J = 7.6 Hz, 1H), 5.35 – 5.28 (m, 1H), 5.22 – 5.15 (m, 1H), 3.62-3.58 (m, 2H), 2.49 (s, 3H), 1.88 (d, J = 1.3 Hz, 3H). LRMS-ESI (+) *m/z*: 191.1 $[M + H]^+$.

General Procedure for 1+4 chelatropic sulfolene formation of 143 and 152

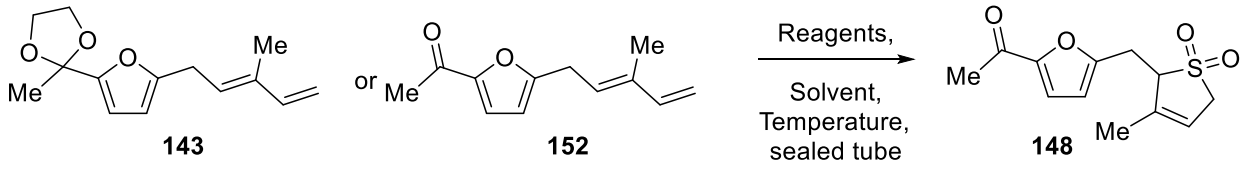

143 152 148

A thick-walled sealed tube reaction vessel was fitted with a stir bar and septa. The apparatus was flame-dried under vacuum then cooled under argon. Solvents were pre-bubbled with argon for at least ten minutes beforehand, and then starting material (either dioxolane furyl diene **143** or ketone furyl diene **152**, 1.0 equiv) in a one-neck oven dried round bottom flask was dissolved in the freshly bubbled solvent (0.1-0.4 Molar) and cannulated to the sealed tube. The reagents (2-15 equiv, $KHSO_4$ added first if used) were then added to the reaction vessel and the tube was sealed and heated to the desired temperature. After 24 hours, the vessel was cooled down to 0°C and opened. If TLC analysis showed reaction still in progress it was resealed and heated back up until reaction either complete or if TLC analysis showed no further progression. Reaction would then be diluted with ethyl acetate (0.1 M) and H_2O (0.1M) and extracted with ethyl acetate four times. Organic layers were then washed with brine, dried with Na_2SO_4, and concentrated under reduced pressure. The crude material was purified via silica gel column chromatography using 10-70% ethyl acetate:hexanes as the gradient to recover any unreacted ketone furyl diene **152** and sulfolene ketone **148** as clear yellow oils. Sulfolene ketone **148** would solidify to a yellow white solid (6-62%, 6->99% BRSM) once concentrated under reduced pressure with diethyl ether three times iteratively.

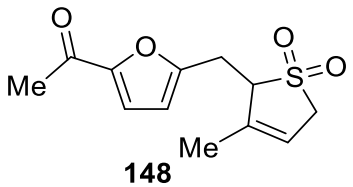

148

Sulfolene Ketone **148**. TLC: silica gel (60% ethyl acetate:hexanes) R_f = 0.24 ^{1}H NMR (400 MHz, $CDCl_3$) δ 7.11 (d, *J* = 3.5 Hz, 1H), 6.45 (dt, *J* = 3.5, 0.8 Hz, 1H), 5.70 (tt, *J* = 3.1, 1.6 Hz, 1H), 3.94 – 3.85 (m, 1H), 3.77 – 3.61 (m, 2H), 3.35 – 3.19 (m, 2H), 2.43 (s, 3H), 1.85 – 1.83 (m, 3H). $^{13}C\{^1H\}$ NMR (100 MHz, $CDCl_3$) δ 186.2, 155.5, 152.2, 137.6, 119.1, 118.4, 111.2,

65.5, 55.9, 26.9, 26.0, 18.2. HRMS-ESI (+) m/z: calcd for $C_{12}H_{14}O_4SNa$ $[M + Na]^+$, 277.0505; found, 277.0502

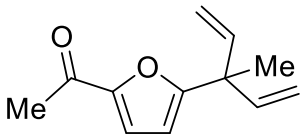

153

Divinyl Ketone **153**. See chapter **2.6.3.2** and **2.6.3.3** for discussion on the formation, isolation, and characterization of this substrate. TLC: silica gel (20% ethyl acetate:hexanes) R_f = 0.24. ^{1}H NMR (800 MHz, $CDCl_3$) δ 7.11 (d, *J* = 3.5 Hz, 1H), 6.22 (d, *J* = 3.5 Hz, 1H), 6.04 (dd, *J* = 17.4, 10.5 Hz, 2H), 5.18 (d, *J* = 10.5 Hz, 2H), 5.04 (d, *J* = 17.4 Hz, 2H), 2.44 (s, 3H), 1.54 (s, 3H). $^{13}C\{^1H\}$ NMR (200 MHz, $CDCl_3$) δ 186.7, 163.8, 152.3, 141.6, 118.3, 114.7, 108.6, 46.1, 26.0, 23.5. LRMS-ESI (+) *m/z*: 191.1 $[M + H]^+$.

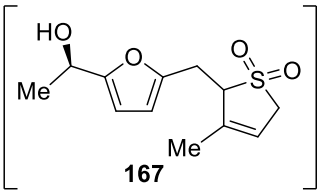

167

Sulfolene Alcohol **167**. To a one-neck oven dried 10 mL round bottom flask equipped with a reflux condenser ketone sulfolene **148** (80 mg, 0.31 mmol, 1.0 equiv) was dissolved in dichloromethane (DCM, 3.1 mL, 0.1 M). Triethylamine (TEA, 329 µL, 2.4 mmol, 7.5 equiv) and formic acid (HCO_2H, 89µL, 2.4 mmol, 7.5 equiv) were added sequentially and evolution of H_2 gas was observed. [N-[(1R,2R)-2-(Amino-κN)-1,2- diphenylethyl]-4-methylbenzenesulfonamidato-κN]chloro [(1,2,3,4,5,6-η)-1,3,5-trimethylbenzene]-ruthenium (RuCl[(R,R)-TsDPEN](mesitylene), 2 mg, 0.003 mmol, 1 mol %) was added last, and the reaction was heated to reflux (30°C). After reaction appeared complete TLC analysis (24-48 hours), solution was cooled and concentrated down under reduced pressure and passed through 10% K_2CO_3:Silica plug, using 65% ethyl acetate:hexanes as the eluent. Solution was concentrated down under reduced pressure again, and the crude material taken on immediately to the next reaction.*

*Note: When doing any transfers of the crude mixture ethyl acetate was found to be a necessity. If crude came into contact with dichloromethane or deuterated chloroform for the NMR analysis it appeared to degrade very quickly afterwards before next reaction could be set up. NMR data was able to be quickly taken a single time however sample degraded before material could be recovered and used in next step (Figure 2.49 and Figure 2.50). The use of a 10% K_2CO_3:Silica plug appeared to less degrade **167** as opposed to tradition silica and celite plugs. HRMS data was able to be taken as well. TLC: silica gel (60% ethyl acetate:hexanes) R_f = 0.22. ^{1}H NMR (400 MHz, $CDCl_3$) δ 6.16 – 6.12 (m, 2H), 5.66 (bs, 1H), 4.81 (q, *J* = 6.6 Hz, 1H), 3.82 (t, *J* = 6.4 Hz, 1H), 3.72 – 3.58 (m, 2H), 3.29 -3.07 (m, 2H), 2.14 (bs, 1H), 1.79 (bs, 3H), 1.50 (d, *J* = 6.6 Hz, 3H). ^{13}C{^{1}H} NMR (100 MHz, $CDCl_3$) δ (157.1, 157.0), (149.7, 149.6), 138.4, 118.0, (108.7, 108.7), (106.3, 106.2), (65.9, 65.8), (63.7, 63.6), 55.7, 26.9, (21.4, 21.3), 18.3. HRMS-ESI (+) m/z: calcd for $C_{12}H_{16}O_4SNa$ $[M + Na]^+$, 279.0662; found, 279.0665

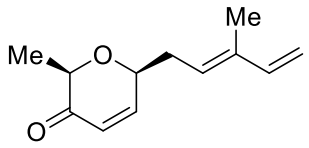

141

Enone Diene **141**. To a one-neck oven dried 10 mL round bottom flask crude alcohol sulfolene **167** (80.6 mg assumed, 0.31 mmol, 1.0 equiv) was dissolved in a tetrahydrofuran:H_2O mixture (2.5 mL:0.6mL, 0.1M) and cooled to 0°C. Potassium bromide (KBr, 3.7 mg, 0.03 mmol, 0.1 equiv), sodium bicarbonate ($NaHCO_3$, 13 mg, 0.16 mmol, 0.5 equiv), and oxone (213 mg, 0.35 mmol, 1.1 equiv) were added sequentially and the reaction let stir at 0°C for 1.5 hours. After the reaction was observed to be complete via TLC analysis, it was quenched with saturated $NaHCO_3$ (3 mL), extracted three times with ethyl acetate, washed with brine, dried with Na_2SO_4, and concentrated under reduced pressure. The crude material was taken on immediately to the next reaction. TLC: silica gel (60% ethyl acetate:hexanes) R_f = 0.30.

To a one-neck oven dried 10 mL round bottom flask crude hemiacetal (42.8 mg, 0.16 mmol, 1.0 equiv) was dissolved in dichloromethane (DCM, 1.6 mL, 0.1M) and cooled to -78°C. To this, triethylsilane (Et_3SiH, 151 µL, 0.94 mmol, 6.0 equiv), and boron trifluoride etherate (BF_3•Et_2O, 39 µL, 0.31 mmol, 2.0 equiv) were added sequentially, and let stir at this temperature for at least 7 hours. The reaction would turn a dark orange gold or orange pink color. The reaction was then pulled from the -78°C bath and quenched slowly with the addition of saturated $NaHCO_3$ (2 mL, bubbled violently). The organic layer was then extracted with DCM five times, dried Na_2SO_4, and concentrated under reduced pressure. The crude material was taken on immediately to the next reaction. TLC*: silica gel (60% ethyl acetate:hexanes) R_f = 0.54. *NOTE: TLC analysis during reaction appears to not be reliable as it shows full conversion almost immediately, but if worked up TLC of crude material then shows starting material (almost no conversion). This is likely due to reaction occurring in spotter as transferred from flask to spotting on TLC. It was found that letting the reaction run for several hours instead and then working it up showed full conversion via crude TLC.

To a one-neck oven dried 50 mL round bottom flask equipped with a reflux condenser the crude sulfolene enone (40 mg assumed, 0.16 mmol, 1.0 equiv) was dissolved in toluene (15.7 mL, 0.01 M) and heated to reflux (150°C). After reaction appeared complete via TLC analysis (3 hours), flask was cooled to ambient temperature and concentrated under reduced pressure. The

crude material was then purified via 10% K_2CO_3:silica chromatography[67] using 1-10% ethyl acetate:hexanes as the gradient. Enone diene **141** was isolated as a yellow oil (18 mg, 60% over four steps, >10:1 ratio of **141:147,** >98% *ee*). TLC: silica gel (10% ethyl acetate:hexanes) R_f = 0.20. $[\alpha]_D^{20}$ +76.2 (*c* 0.362, $CHCl_3$); ^1H NMR (400 MHz, $CDCl_3$) δ 6.90 (d, *J* = 10.3 Hz, 1H), 6.39 (dd, *J* = 17.3, 10.6 Hz, 1H), 6.10 (d, *J* = 10.2 Hz, 1H), 5.55 (t, *J* = 7.1 Hz, 1H), 5.16 (d, *J* = 17.4 Hz, 1H), 5.01 (d, *J* = 10.7 Hz, 1H), 4.41 (t, *J* = 6.4 Hz, 1H), 4.09 (q, *J* = 6.5 Hz, 1H), 2.60 – 2.50 (m, 2H), 1.78 (s, 3H), 1.39 (d, *J* = 6.6 Hz, 3H). $^{13}C\{^1H\}$ NMR (100 MHz, $CDCl_3$) δ 197.1, 150.8, 141.0, 137.2, 127.0, 126.2, 112.1, 77.3, 74.0, 33.8, 15.6, 12.2. HRMS-ESI (+) m/z: calcd for $C_{12}H_{17}O_2$ $[M + H]^+$,193.1223; found, 193.1227

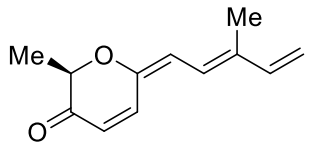

147

Enone Triene **147**. See chapter **2.6.1** for discussion on the formation, isolation, and characterization of this substrate. TLC: silica gel (10% ethyl acetate:hexanes) R_f = 0.21. ^{1}H NMR (800 MHz, $CDCl_3$) δ 6.98 (d, *J* = 9.8 Hz, 1H), 6.57 – 6.51 (m, 2H), 6.02 (d, *J* = 12.0 Hz, 1H), 5.98 (d, *J* = 9.8 Hz, 1H), 5.33 (d, *J* = 17.3 Hz, 1H), 5.16 (d, *J* = 10.6 Hz, 1H), 4.64 (q, *J* = 7.0 Hz, 1H), 1.92 (d, *J* = 1.3 Hz, 3H), 1.49 (d, *J* = 6.9 Hz, 3H). ^{13}C{^{1}H} NMR (200 MHz, $CDCl_3$) δ 195.3, 147.3, 141.3, 141.1, 139.3, 124.9, 121.5, 116.0, 114.7, 78.0, 18.2, 12.4. LRMS-ESI (+) *m/z*: 191.1 $[M + H]^+$.

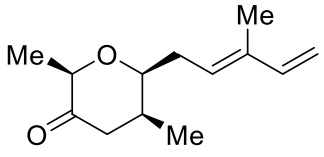

132

β-Methyl Ketone **132**. To a one-neck oven dried 10 mL round bottom flask copper (I) iodide (CuI, 108 mg, 0.56 mmol, 3.0 equiv) was flame-dried under vacuum until a canary yellow color, then cooled under argon. Diethyl ether (Et_2O, 1.0 mL) was then added, the solution was cooled to 0°C, and methyl lithium (MeLi, 3.1 M in diethyl ether, 371 µL, 1.15 mmol, 6.1 equiv) was added and let stir at 0°C for 30 minutes. Reaction went from a yellow color to orange then clear. In a separate flask, enone diene **141** (12 mg, 0.06 mmol, 1.0 equiv) was dissolved in Et_2O (1.35 mL) and cooled to -78°C. The solution of the starting material was then cannulated to the *in situ* formed Gilman reagent at -78°C and let stir. Reaction went from a yellow to orange yellow color and eventually grew darker over time. Hours later it developed a dark brown-green color. After reaction appeared complete via TLC analysis (5 hours), it was pulled from the bath and quenched slowly with H_2O (2.5 mL) and brought to ambient temperature. The crude mixture was extracted with ethyl acetate three times, washed with brine, dried with Na_2SO_4, and concentrated under reduced pressure. The crude material was purified via silica column chromatography using 5% ethyl acetate:hexanes as the eluent. β-methyl ketone **132** was isolated as a clear yellow oil (34.5 mg, 91%). TLC: silica gel (10% ethyl acetate:hexanes) R_f = 0.36. $[\alpha]_D^{20}$ -19.6 (*c* 0.467,

$CHCl_3$); ^{1}H NMR ^{1}H NMR (400 MHz, $CDCl_3$) δ 6.39 (dd, *J* = 17.4, 10.7 Hz, 1H), 5.50 (t, *J* = 7.4 Hz, 1H), 5.14 (d, *J* = 17.3 Hz, 1H), 4.98 (d, *J* = 10.7 Hz, 1H), 3.96 (q, *J* = 6.5 Hz, 1H), 3.90 (td, *J* = 7.0, 1.7 Hz, 1H), 2.64 (dd, *J* = 15.2, 6.1 Hz, 1H), 2.48 (dt, *J* = 14.0, 6.7 Hz, 1H), 2.38 – 2.25 (m, 3H), 1.78 (s, 3H), 1.28 (d, *J* = 6.5 Hz, 3H), 0.98 (d, *J* = 7.0 Hz, 3H). ^{13}C{^{1}H} NMR (200 MHz, $CDCl_3$) δ 208.9, 141.3, 136.1, 128.1, 111.6, 79.7, 78.9, 46.9, 35.1, 31.6, 15.2, 13.3, 12.1. LRMS-ESI (+) *m/z*: 209.1 $[M + H]^+$.[83]

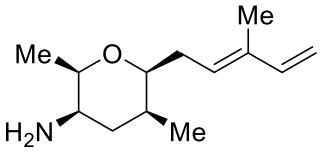

92

THP Amine **92**. To an oven-dried 10 mL round bottom flask β-methyl ketone **132** (30 mg, 0.14, 1.0 equiv) was dissolved in tetrahydrofuran (THF, 2.88 mL, 0.05 M) and cooled to 0°C. Ammonium acetate (NH_4OAc, 222 mg, 2.88 mmol, 20 equiv), sodium triacetoxy borohydride ($NaBH(OAc)_3$, 152.6 mg, 0.72 mmol, 5.0 equiv), and trifluoracetic acid (TFA, 11 µL, 0.14 mmol, 1.0 equiv) were added sequentially and reaction was let warm slowly to ambient temperature. Fuming and bubbling were observed upon addition of reagents. After TLC analysis indicated the reaction was complete (44 hours), it was quenched with saturated $NaHCO_3$ (3.0 mL), extracted with ethyl acetate three times, washed with brine, dried with Na_2SO_4, and concentrated under reduced pressure. The crude material was purified via silica column chromatography using 10% MeOH:DCM as the eluent to yield amine **92** as a clear goo (24.8 mg, 82% yield) as the sole isomer as detectable via ^{1}H NMR. TLC: silica gel (5% methanol:dichloromethane) R_f = 0.07 $[\alpha]_D^{20}$ –4.0 (*c* 0.708, $CHCl_3$); ^{1}H NMR (400 MHz, $CDCl_3$) δ 6.36 (dd, J = 17.4, 10.7 Hz, 1H), 6.05 (bs, 2H), 5.44 (t, J = 7.2 Hz, 1H), 5.10 (d, J = 17.3 Hz, 1H), 4.94 (d, J = 10.7 Hz, 1H), 3.62 (bs, 1H), 3.52 – 3.44 (m, 1H), 3.09 (bs, 1H), 2.40 (dt, J = 14.2, 6.7 Hz, 1H), 2.24 (dt, J = 15.1, 7.5 Hz, 1H), 2.15 (d, J = 14.7 Hz, 1H), 2.02 – 2.00 (m, 1H), 1.80 - 1.72 (m, 4H), 1.26 (d, J = 6.6 Hz, 3H), 1.12 (d, J = 7.4 Hz, 3H). ^{13}C NMR (100 MHz, $CDCl_3$) δ 141.5, 135.8, 128.3, 111.2, 80.9,75.1, 49.3, 35.6, 31.9, 28.6, 17.8, 14.5, 12.1. LRMS-ESI (+) *m/z*: 210.1 $[M + H]^+$.[83]

2.8.3 Spectral Data

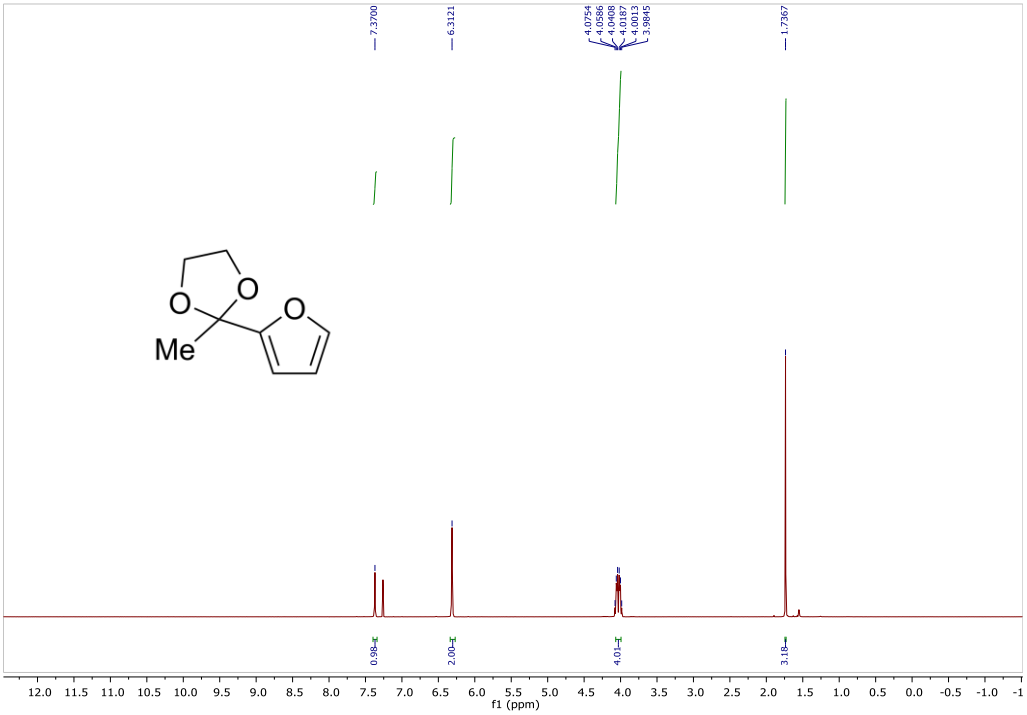

Figure 2.20 ^{1}H-NMR (400 MHz, $CDCl_3$) of Furyl Dioxolane **106**

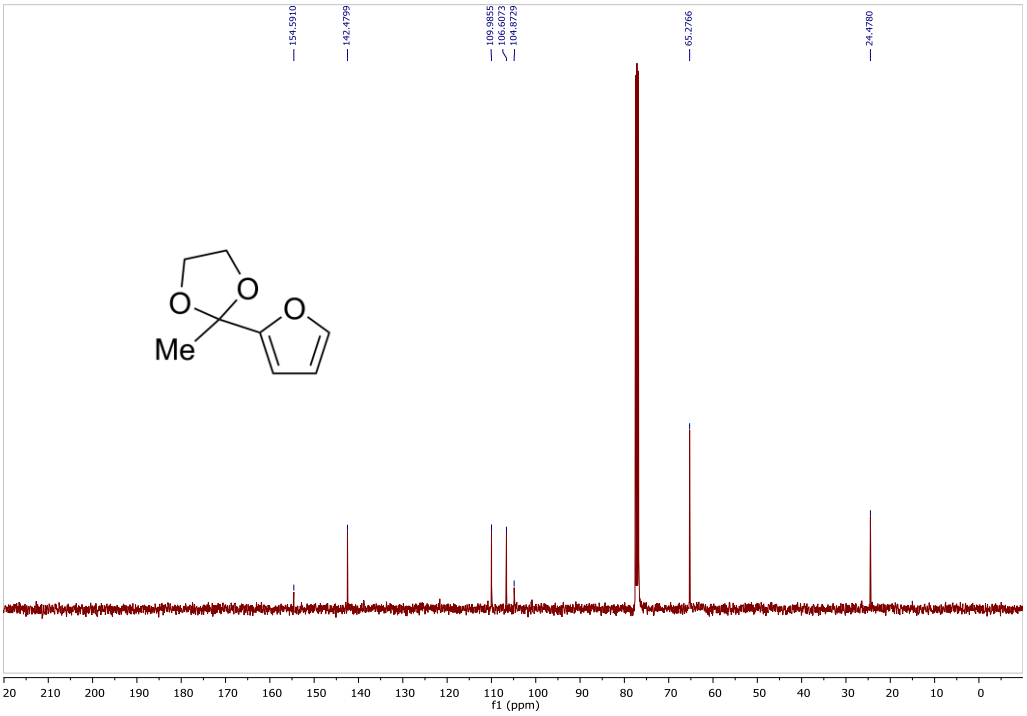

Figure 2.21 ^{13}C-NMR (100 MHz, $CDCl_3$) of Furyl Dioxolane **106**

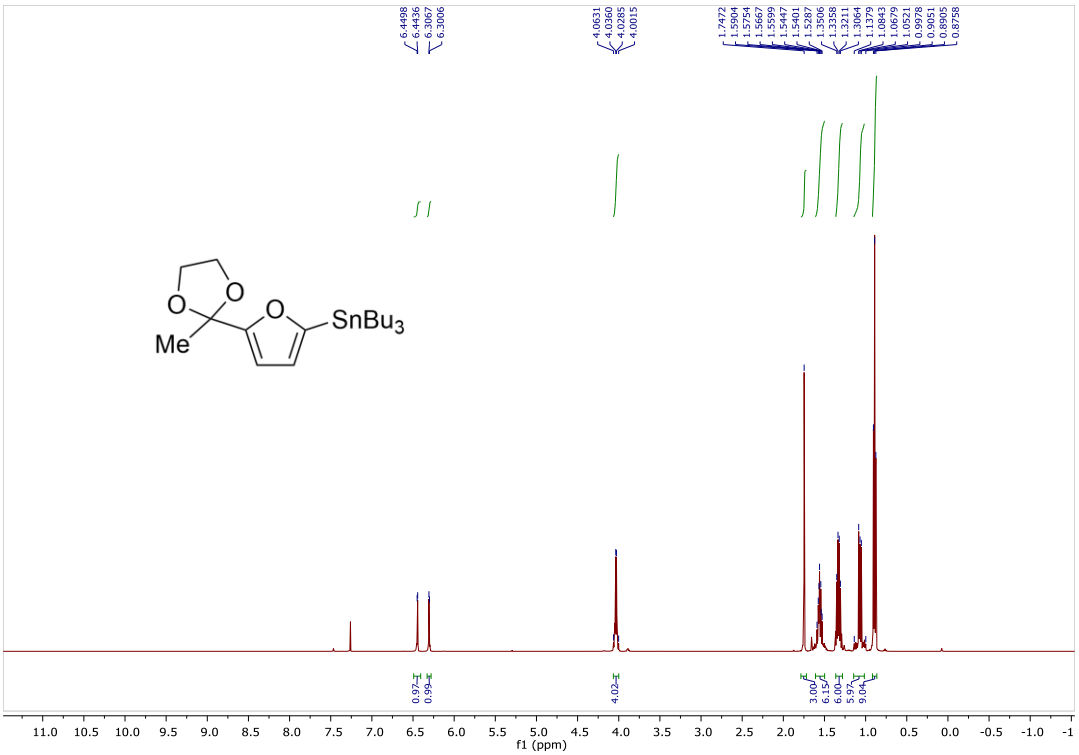

Figure 2.22 ^{1}H-NMR (500 MHz, $CDCl_3$) of Furyl Organostannyl Dioxolane **89**

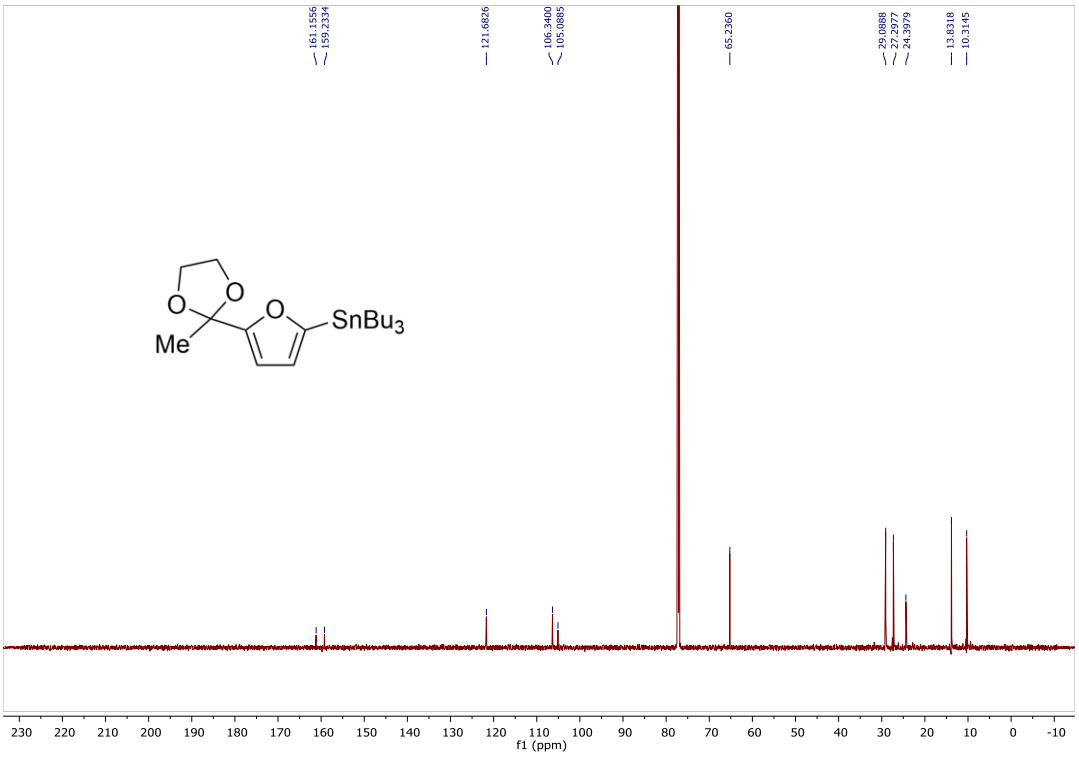

Figure 2.23 ^{13}C-NMR (125 MHz, $CDCl_3$) of Furyl Organostannyl Dioxolane **89**

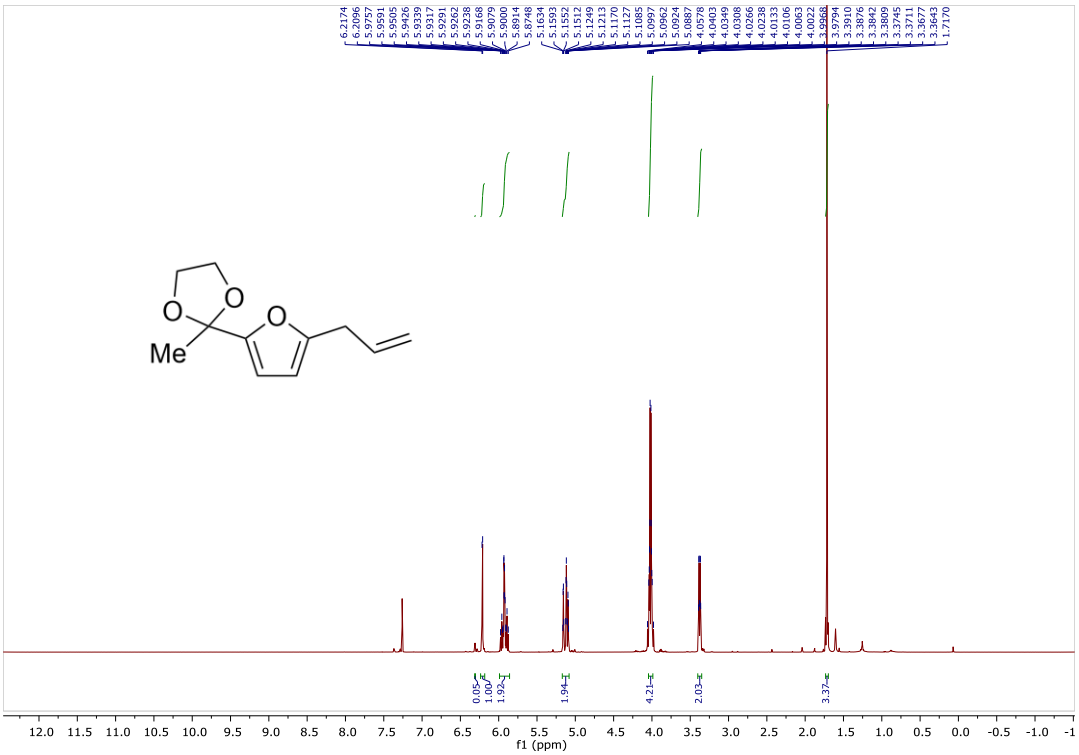

Figure 2.24 ^{1}H-NMR (400 MHz, $CDCl_3$) of Ally Furyl Dioxolane **104**

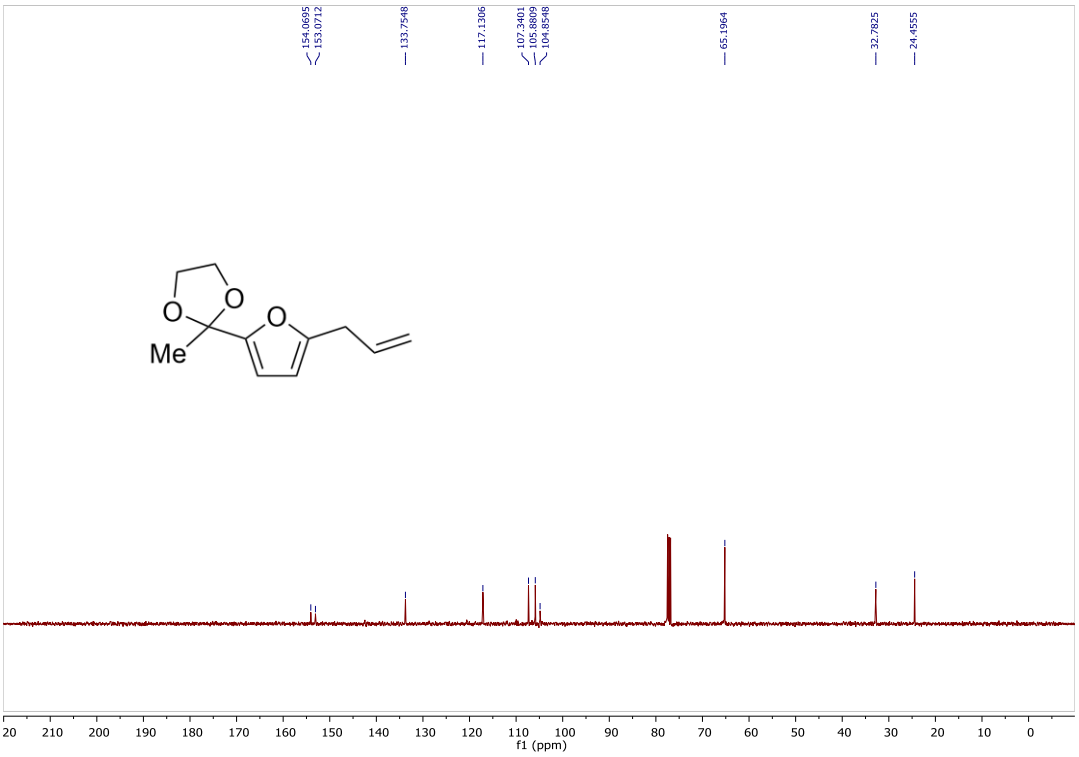

Figure 2.25 ^{13}C-NMR (100 MHz, $CDCl_3$) of Ally Furyl Dioxolane **104**

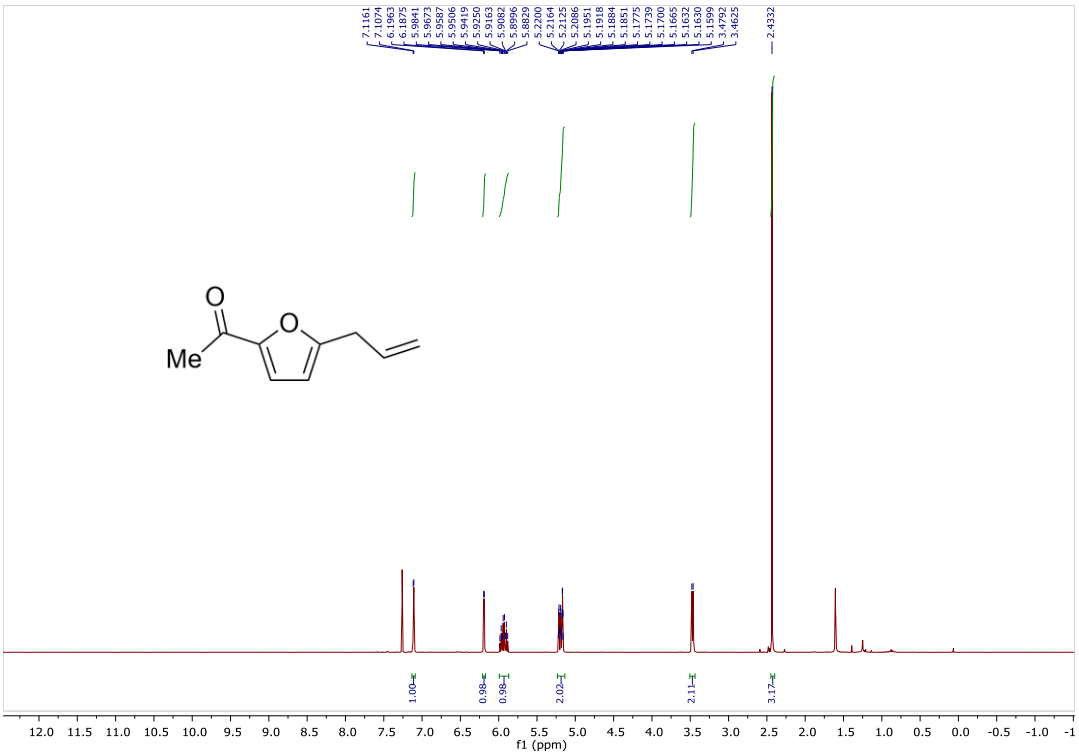

Figure 2.26 ^{1}H-NMR (400 MHz, $CDCl_3$) of Ally Furyl Ketone **107**

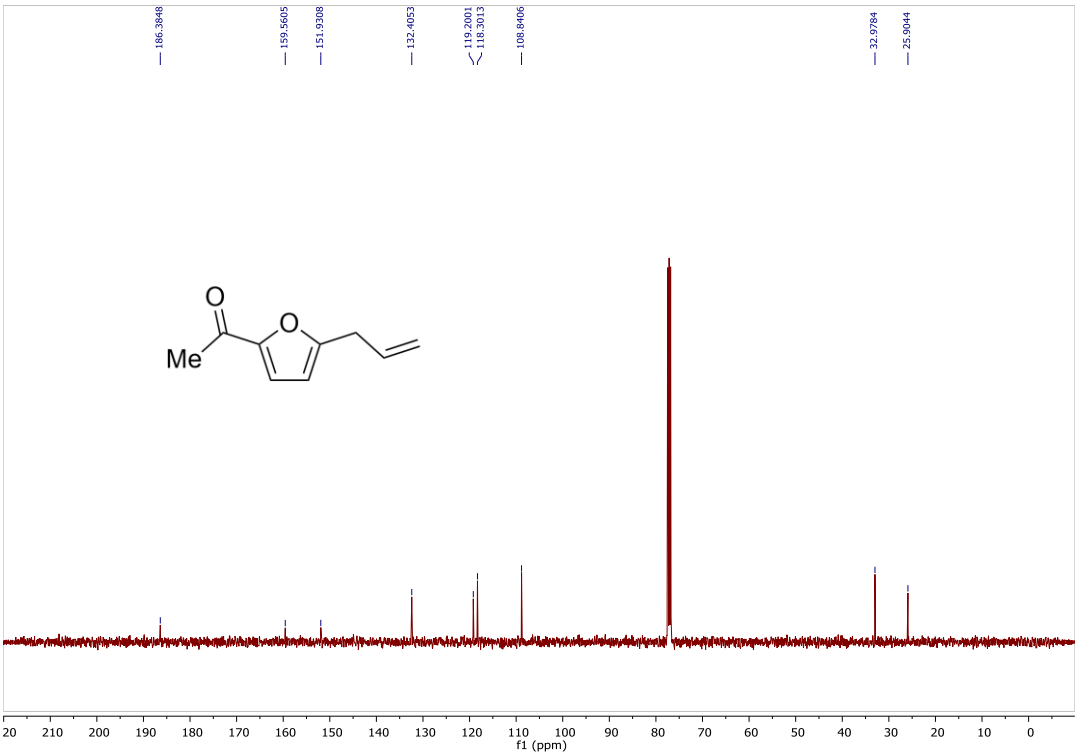

Figure 2.27 ^{13}C-NMR (100 MHz, $CDCl_3$) of Ally Furyl Ketone **107**

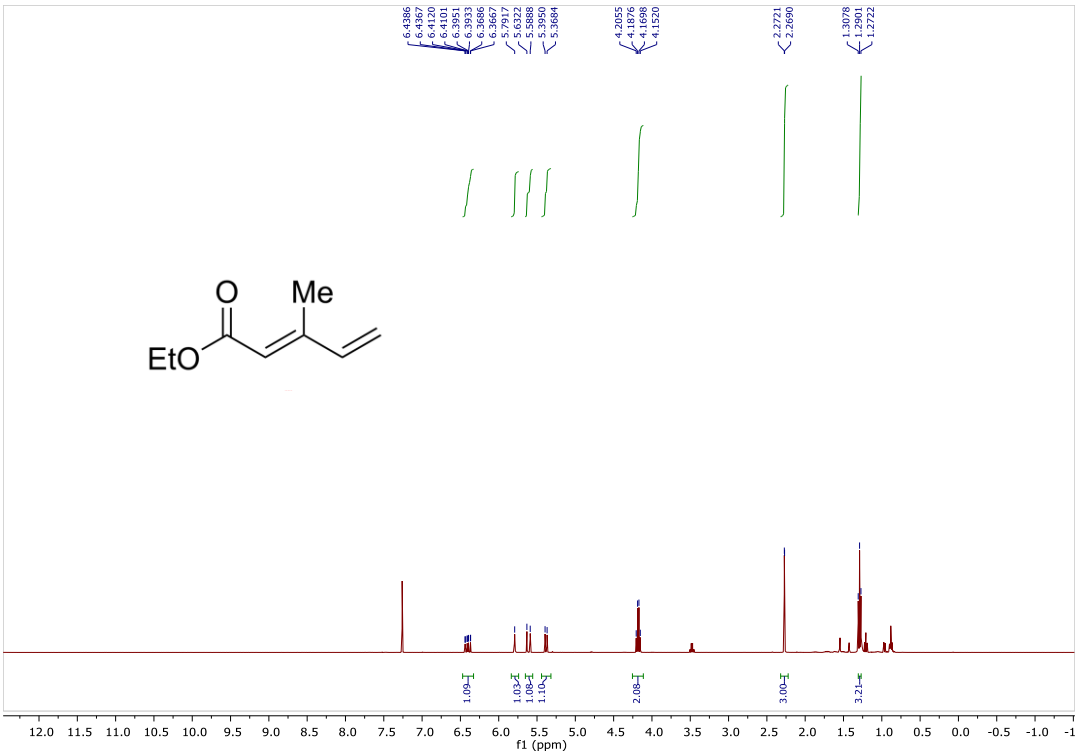

Figure 2.28 ^{1}H-NMR (400 MHz, $CDCl_3$) of Diene Ester **150**

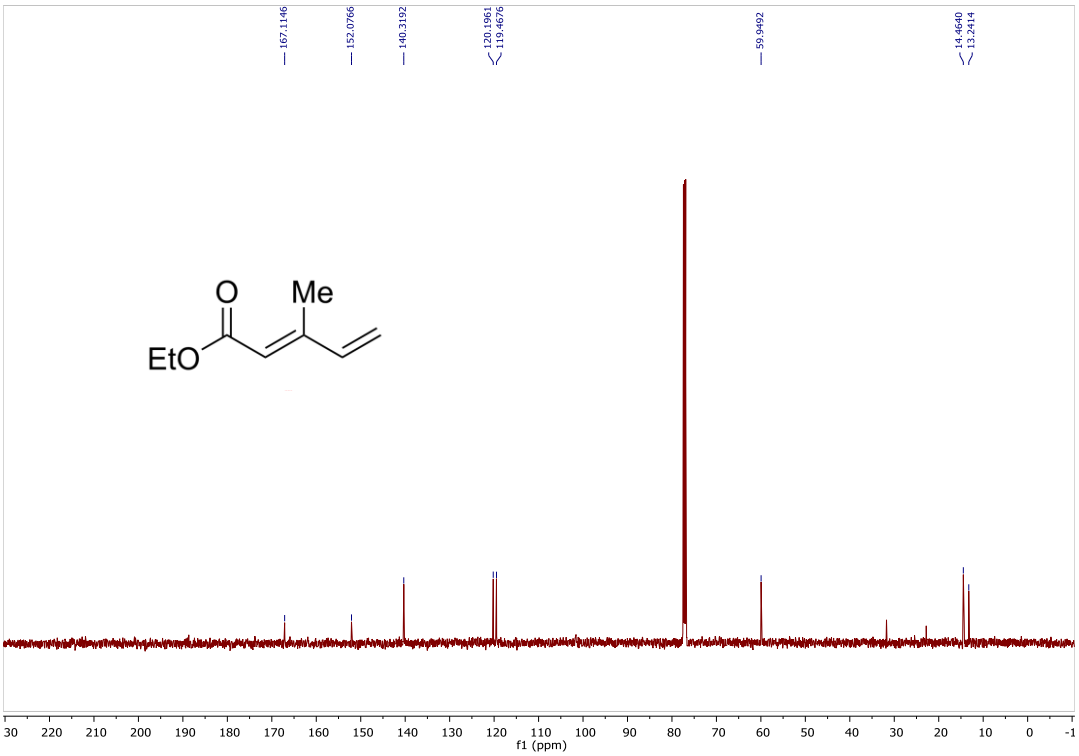

Figure 2.29 ^{13}C-NMR (100 MHz, $CDCl_3$) of Ally Furyl Ketone **150**

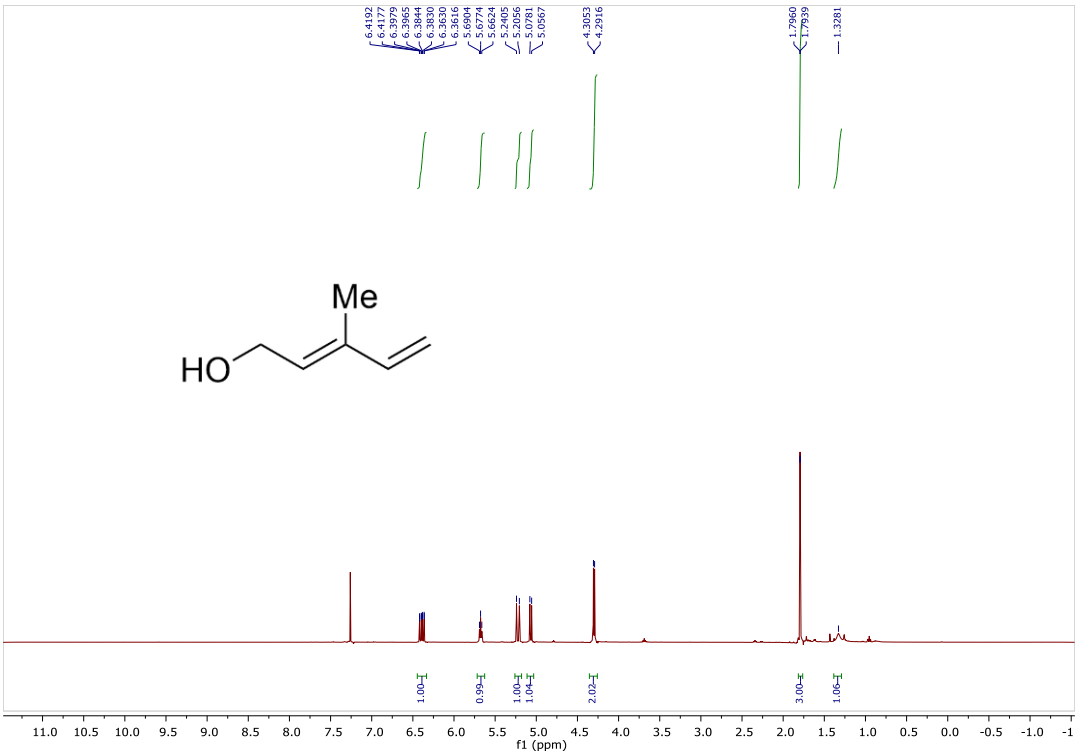

Figure 2.30 ^{1}H-NMR (500 MHz, $CDCl_3$) of Diene Alcohol **151**

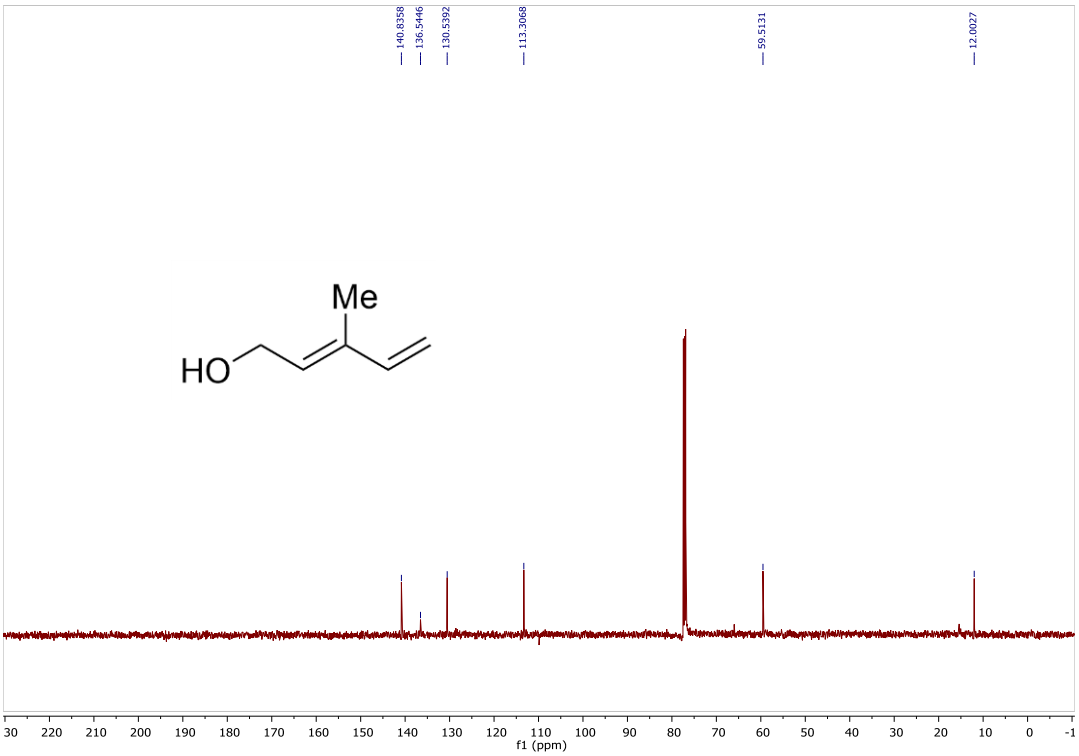

Figure 2.31 ^{13}C-NMR (125 MHz, $CDCl_3$) of Diene Alcohol **151**

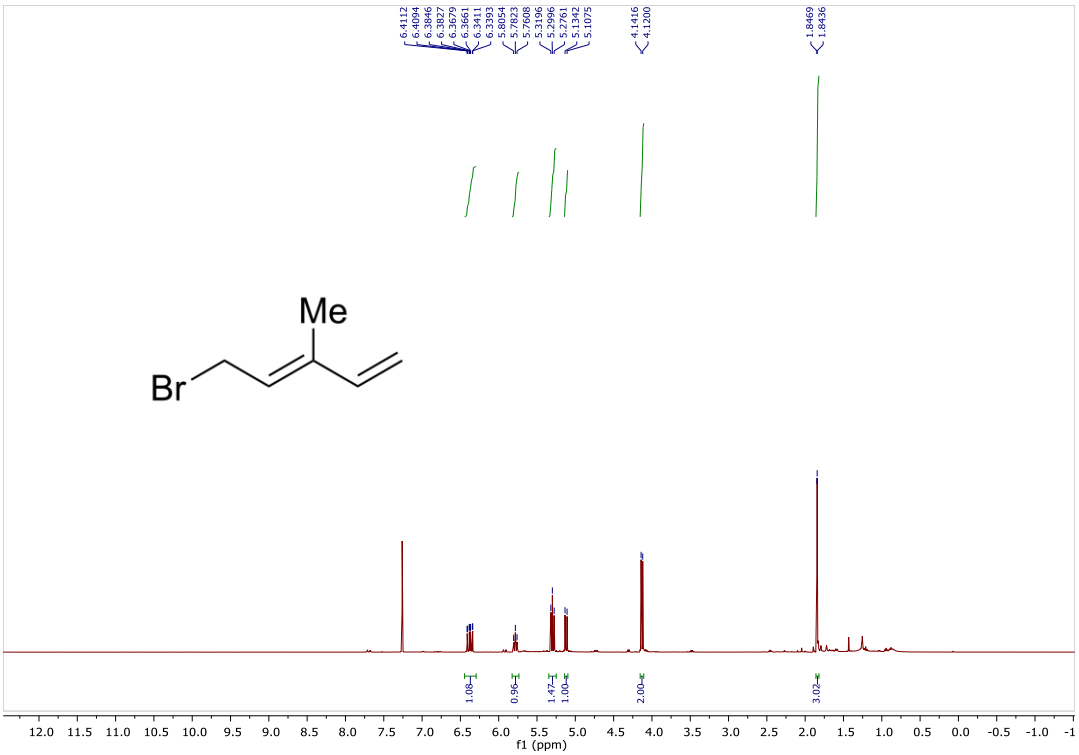

Figure 2.32 ^{1}H-NMR (400 MHz, $CDCl_3$) of Diene Bromide **144**

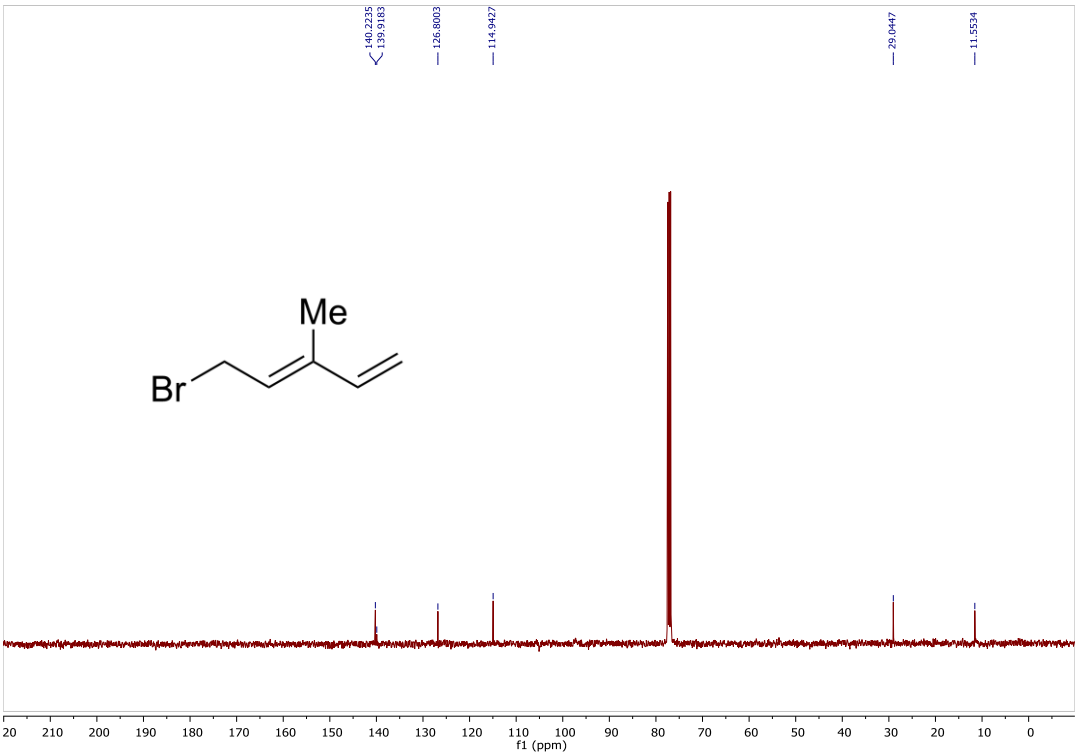

Figure 2.33 ^{13}C-NMR (100 MHz, $CDCl_3$) of Diene Bromide **144**

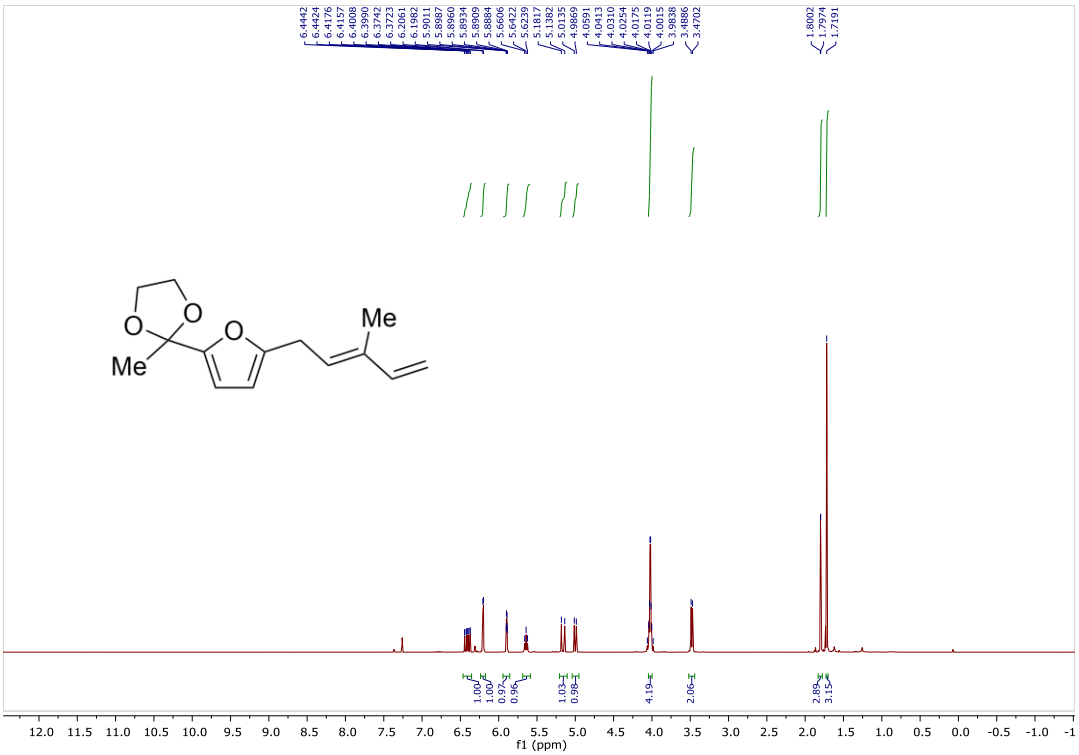

Figure 2.34 ^{1}H-NMR (400 MHz, $CDCl_3$) of Dioxolane Furyl Diene **143**

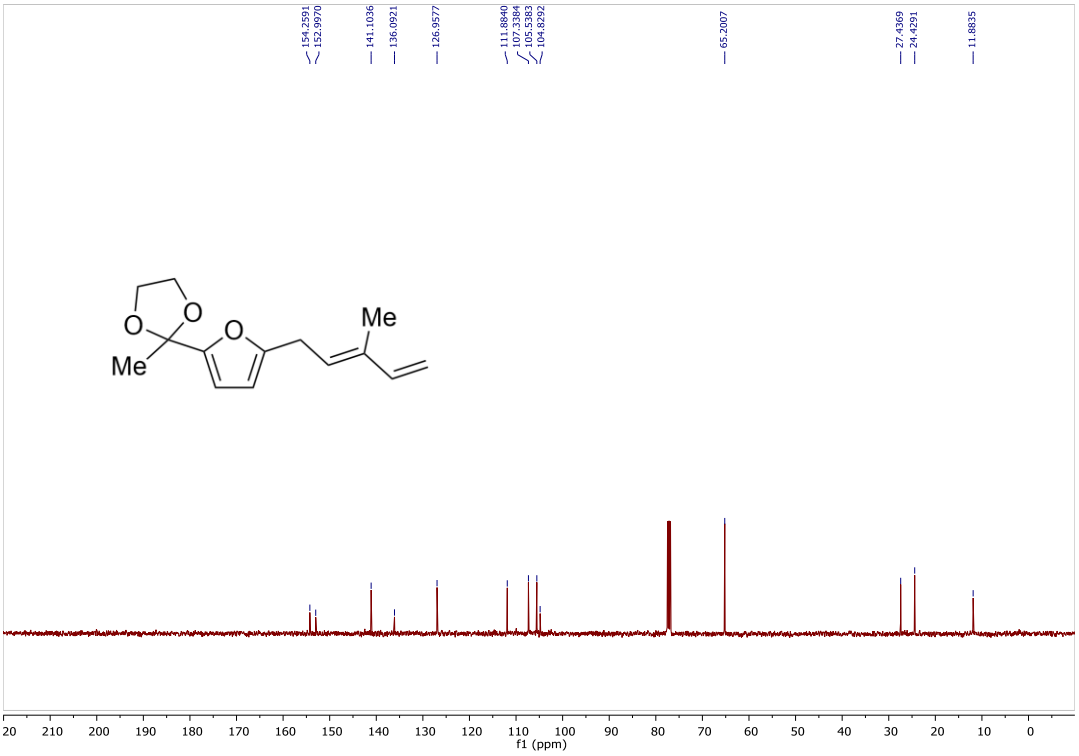

Figure 2.35 ^{13}C-NMR (100 MHz, $CDCl_3$) of Dioxolane Furyl Diene **143**

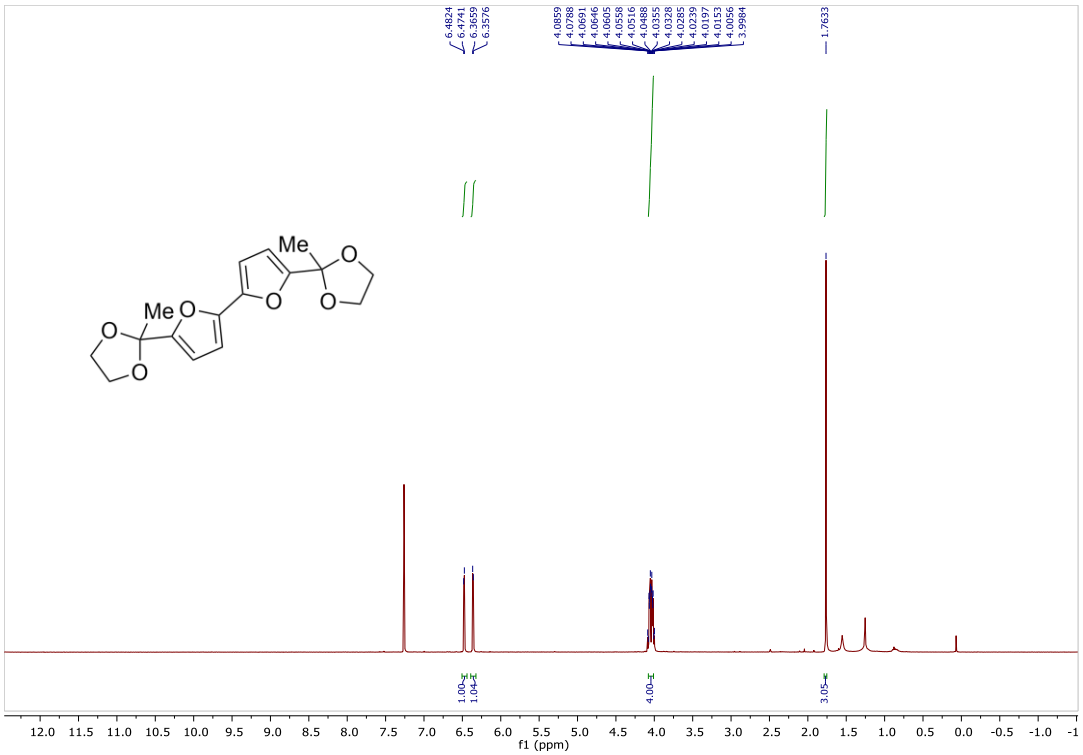

Figure 2.36 ^{1}H-NMR (400 MHz, $CDCl_3$) of Furyl Dioxolane Dimer **161**

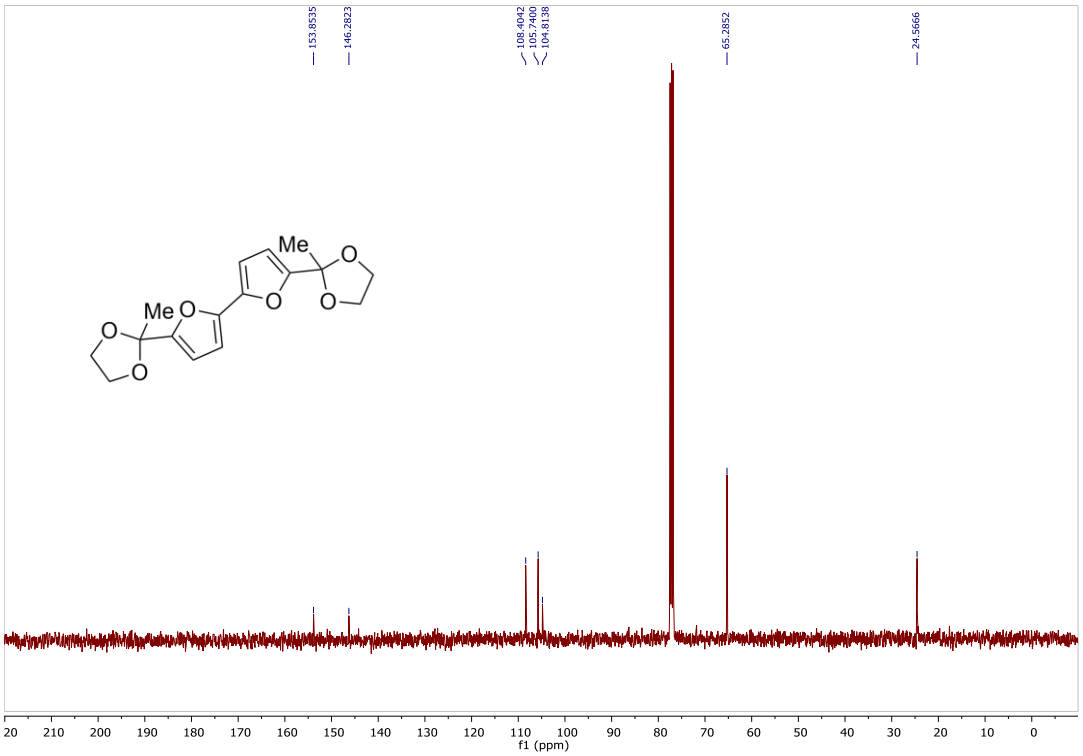

Figure 2.37 ^{13}C-NMR (100 MHz, $CDCl_3$) of Furyl Dioxolane Dimer **161**

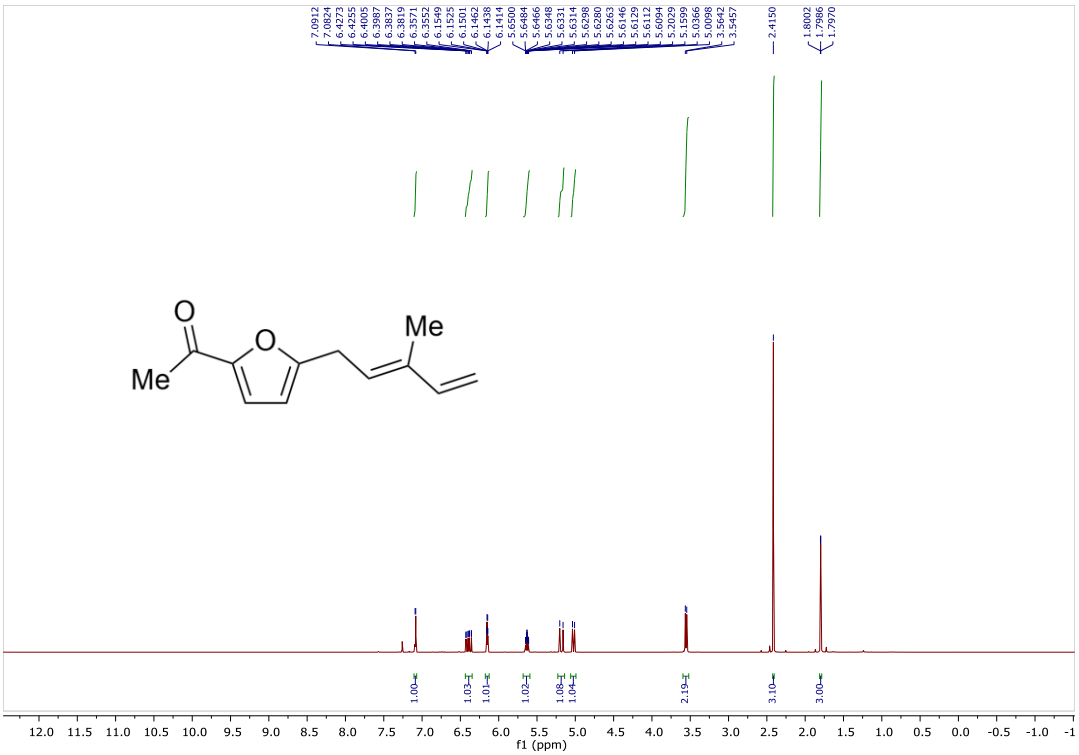

Figure 2.38 ^{1}H-NMR (400 MHz, $CDCl_3$) of *trans*-Ketone Furyl Diene **152**

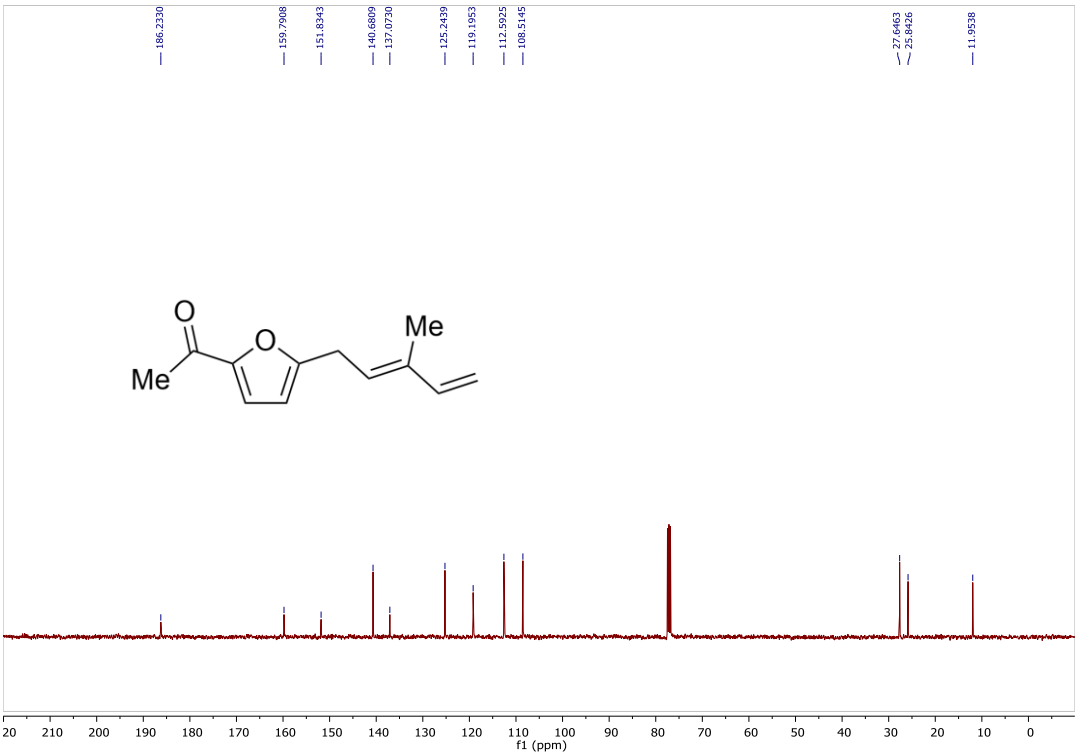

Figure 2.39 ^{13}C-NMR (100 MHz, $CDCl_3$) of *trans*-Ketone Furyl Diene **152**

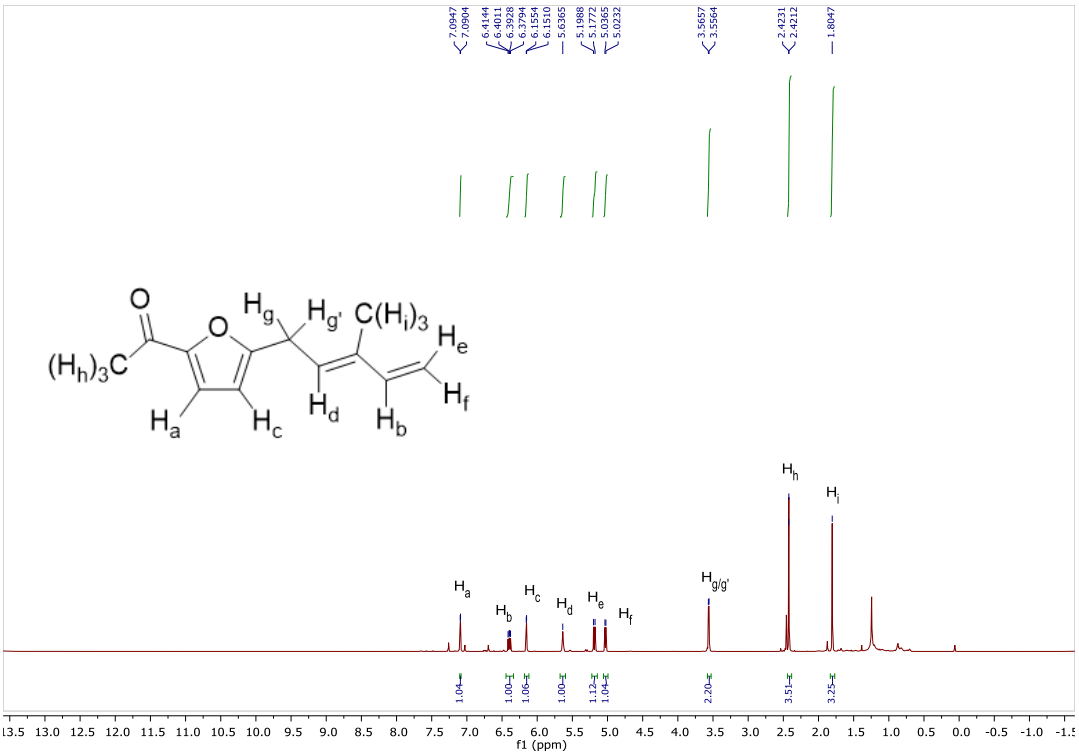

Figure 2.40 Assigned ^{1}H-NMR (800 MHz, $CDCl_3$) of *trans*-Ketone Furyl Diene **152**

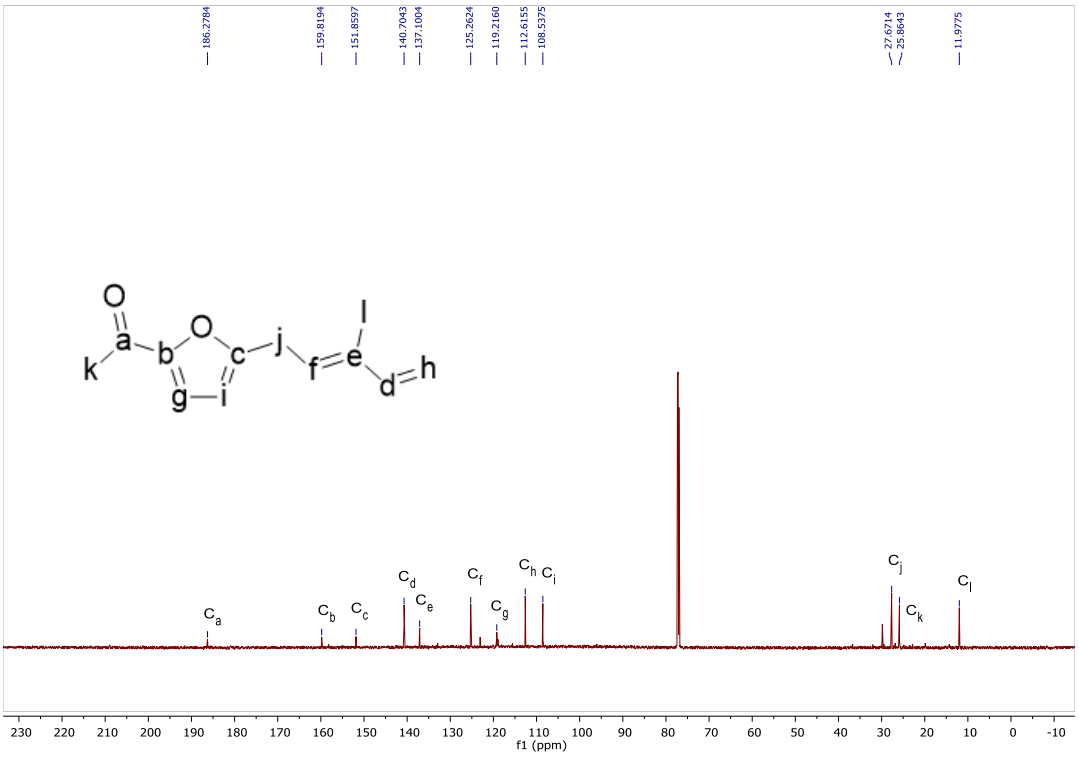

Figure 2.41 Assigned ^{13}C-NMR (200 MHz, $CDCl_3$) of *trans*-Ketone Furyl Diene **152**

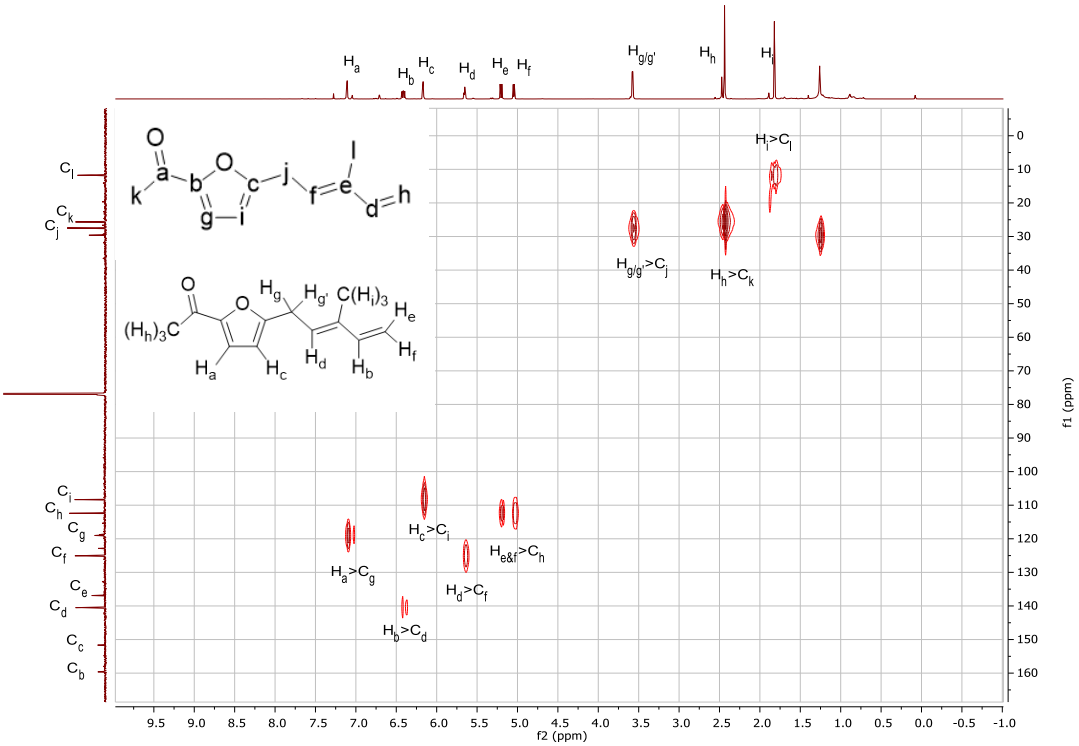

Figure 2.42 HMQC NMR ($CDCl_3$) of *trans*-Ketone Furyl Diene **152**

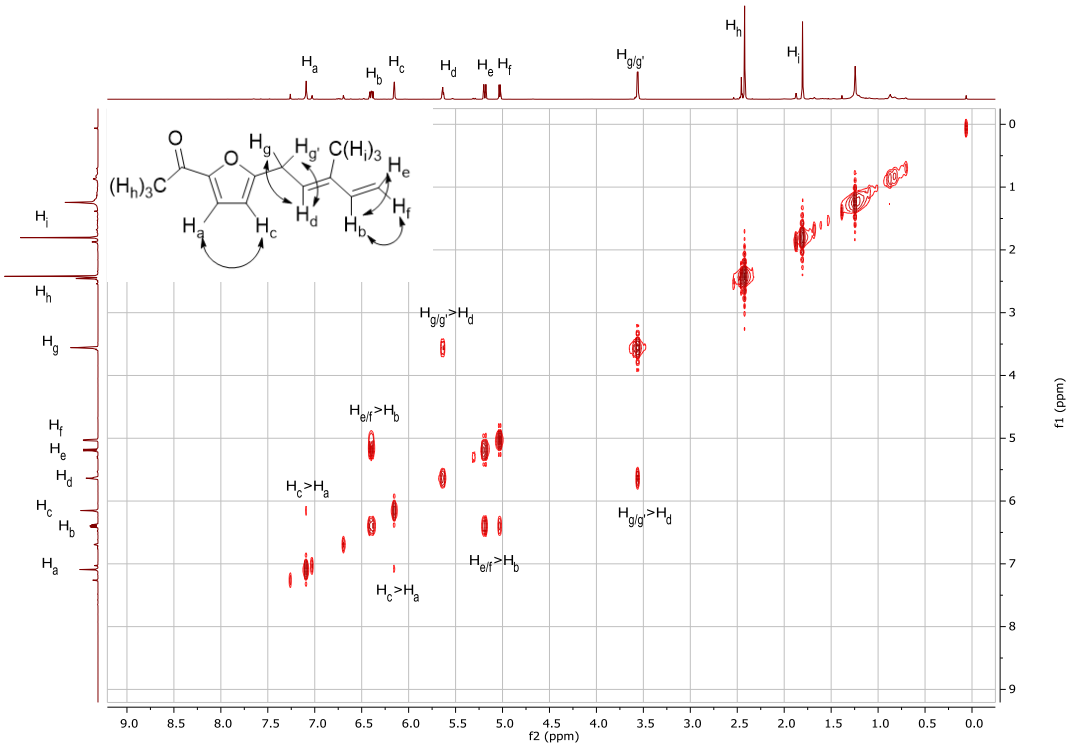

Figure 2.43 ^1H-^1H COSY NMR ($CDCl_3$) of *trans*-Ketone Furyl Diene **152**

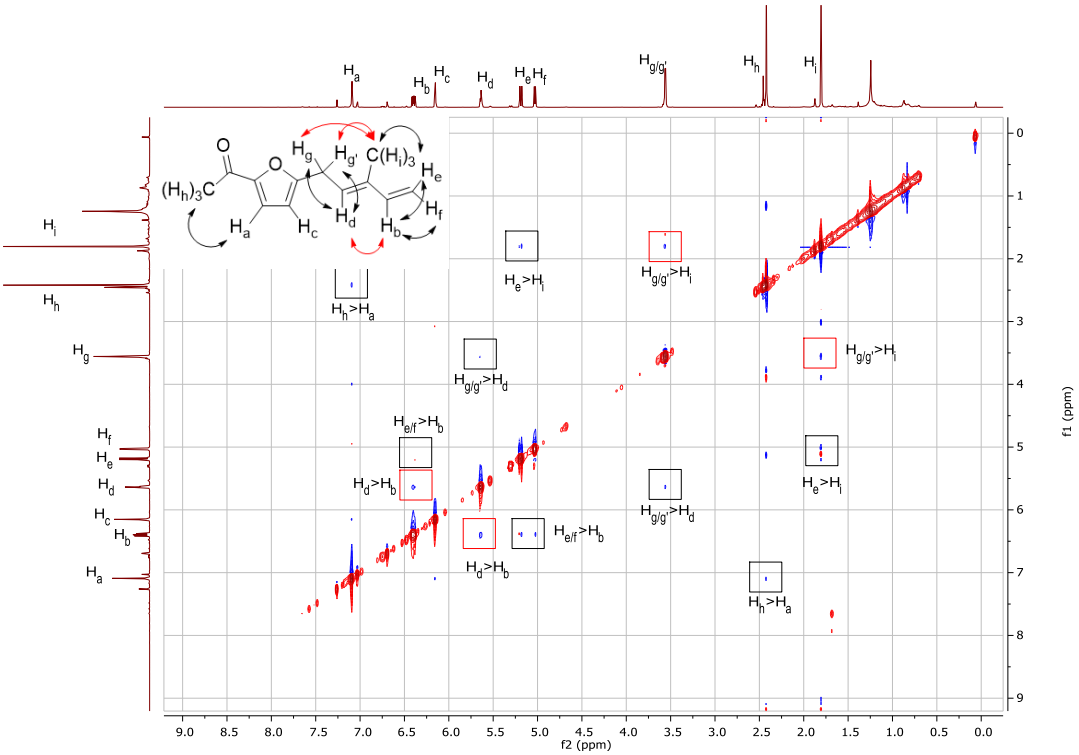

Figure 2.44 NOESY NMR ($CDCl_3$) of *trans*-Ketone Furyl Diene **152**

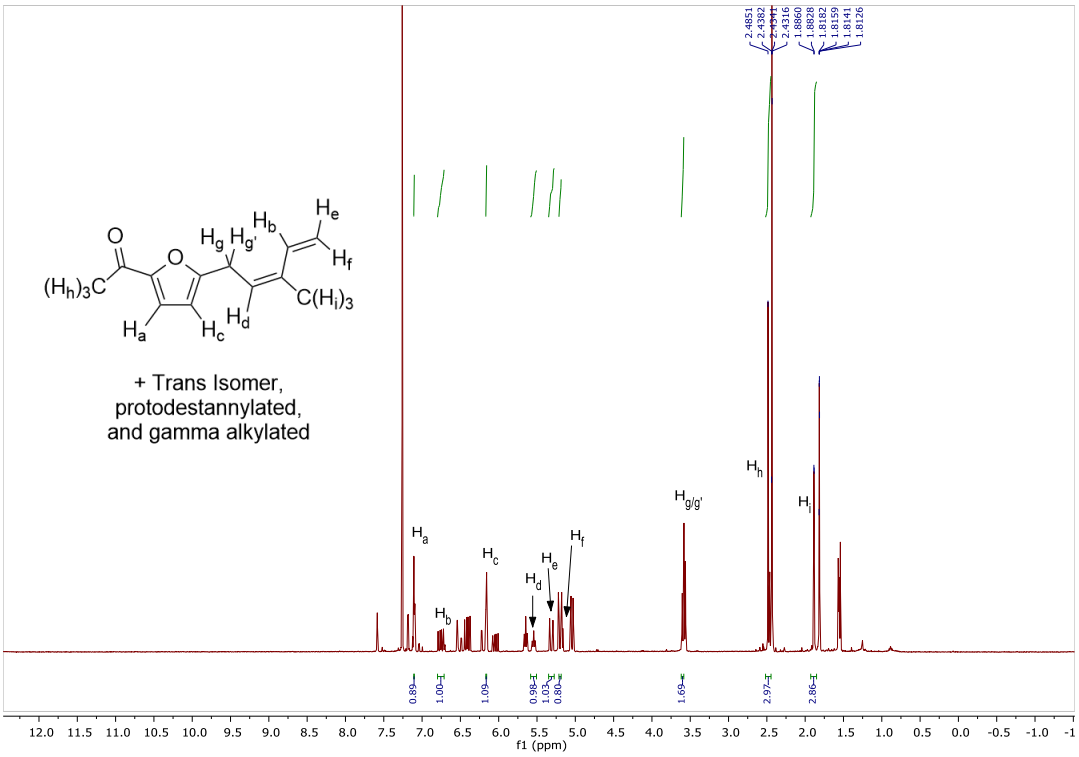

Figure 2.45 ^{1}H-NMR (400 MHz, $CDCl_3$) of *cis*-Ketone Furyl Diene **152** in Crude Mixture

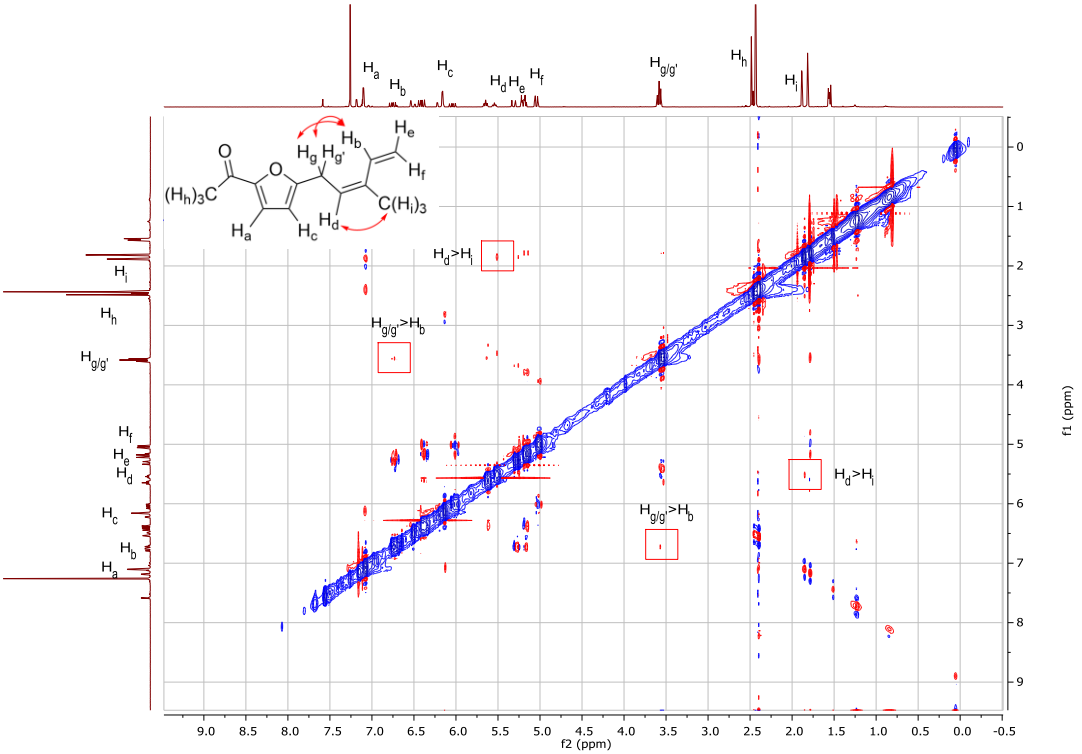

Figure 2.46 NOESY NMR ($CDCl_3$) of *cis*-Ketone Furyl Diene **152** in Crude Mixture

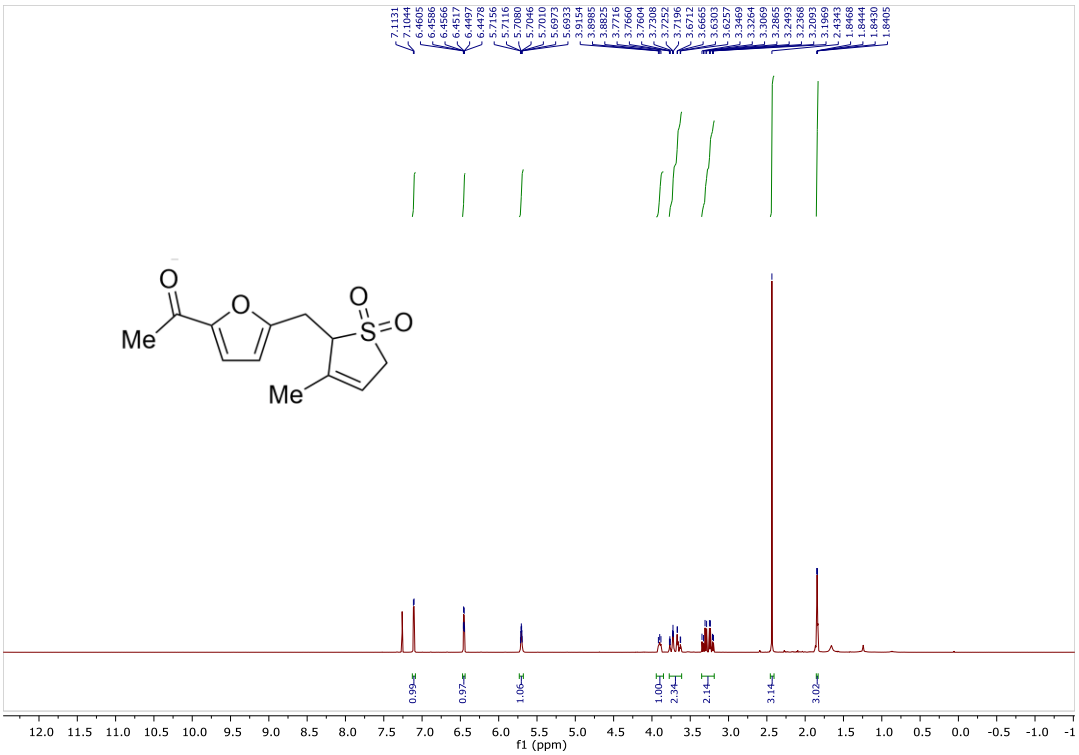

Figure 2.47 ^{1}H-NMR (400 MHz, $CDCl_3$) of Sulfolene Ketone **148**

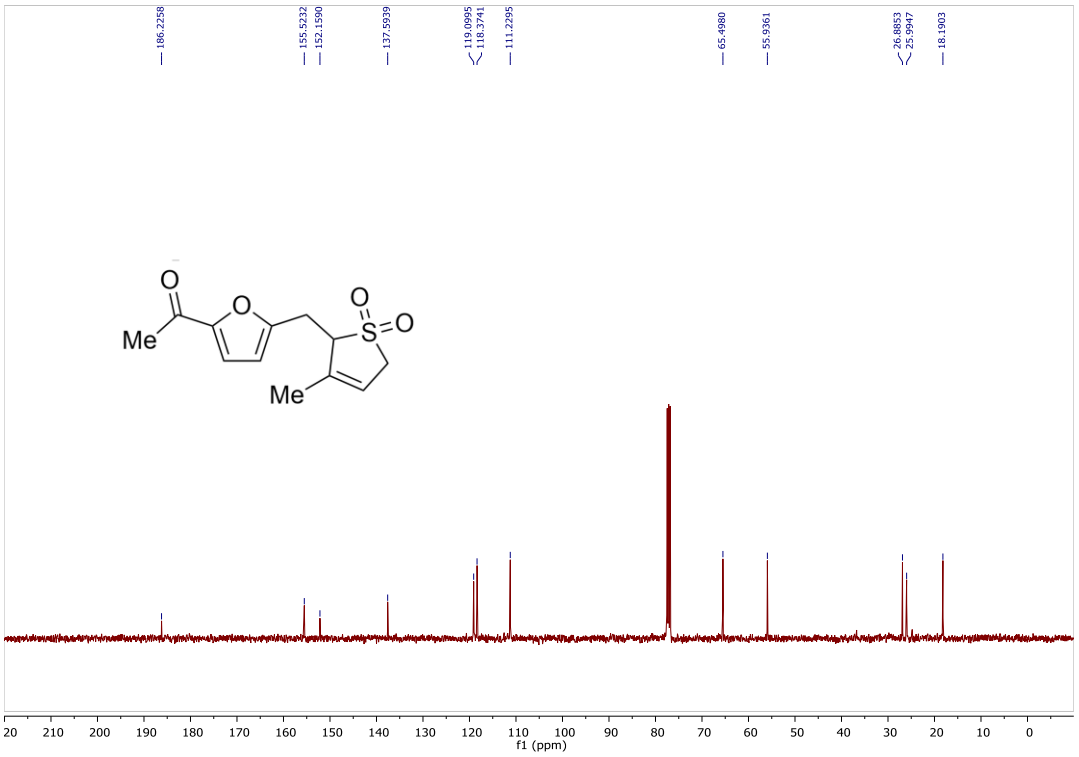

Figure 2.48 ^{13}C-NMR (100 MHz, $CDCl_3$) of Sulfolene Ketone **148**

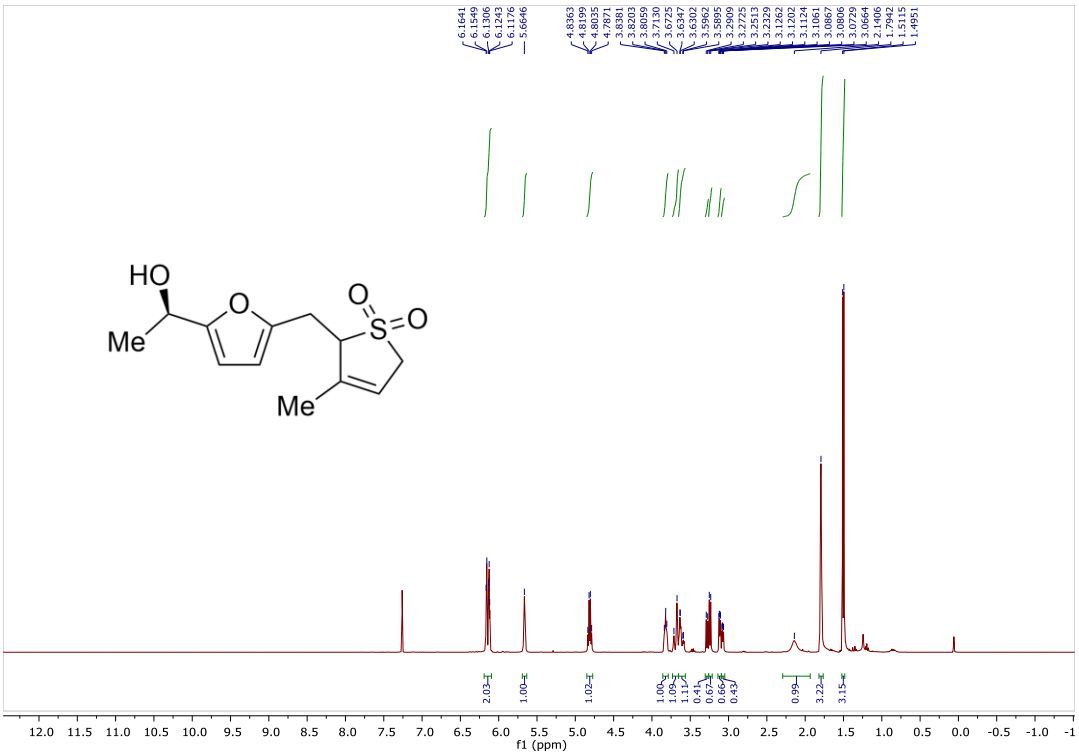

Figure 2.49 ^{1}H-NMR (400 MHz, $CDCl_3$) of Sulfolene Alcohol **167**

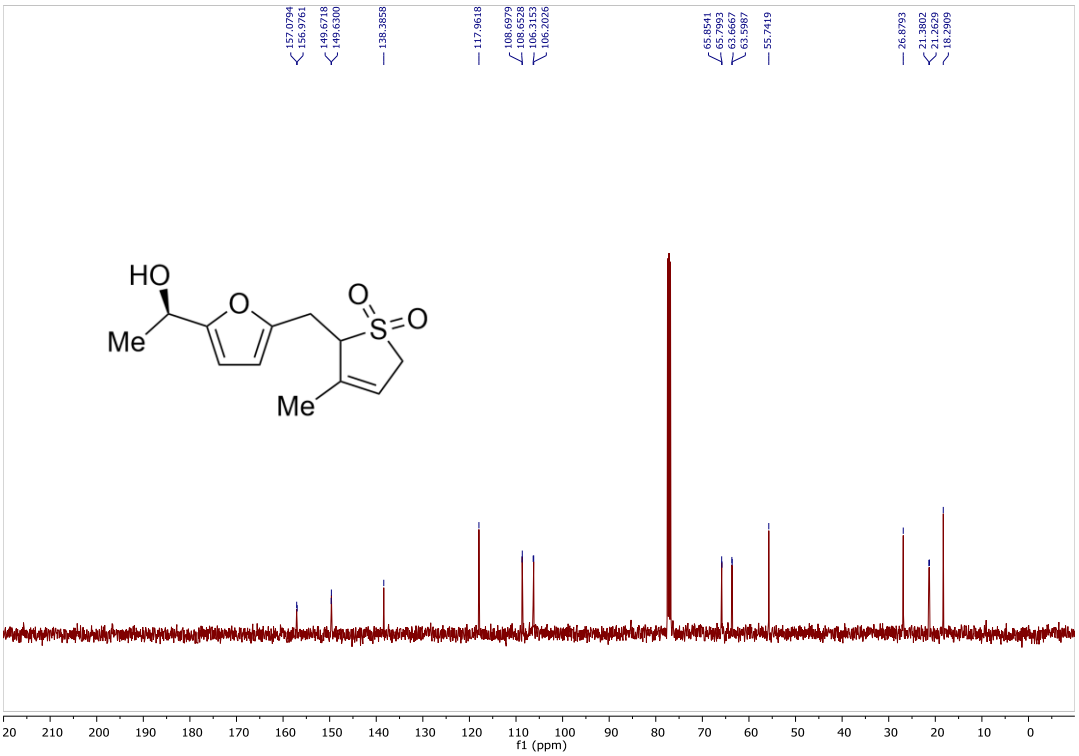

Figure 2.50 ^{13}C-NMR (100 MHz, $CDCl_3$) of Sulfolene Alcohol **167**

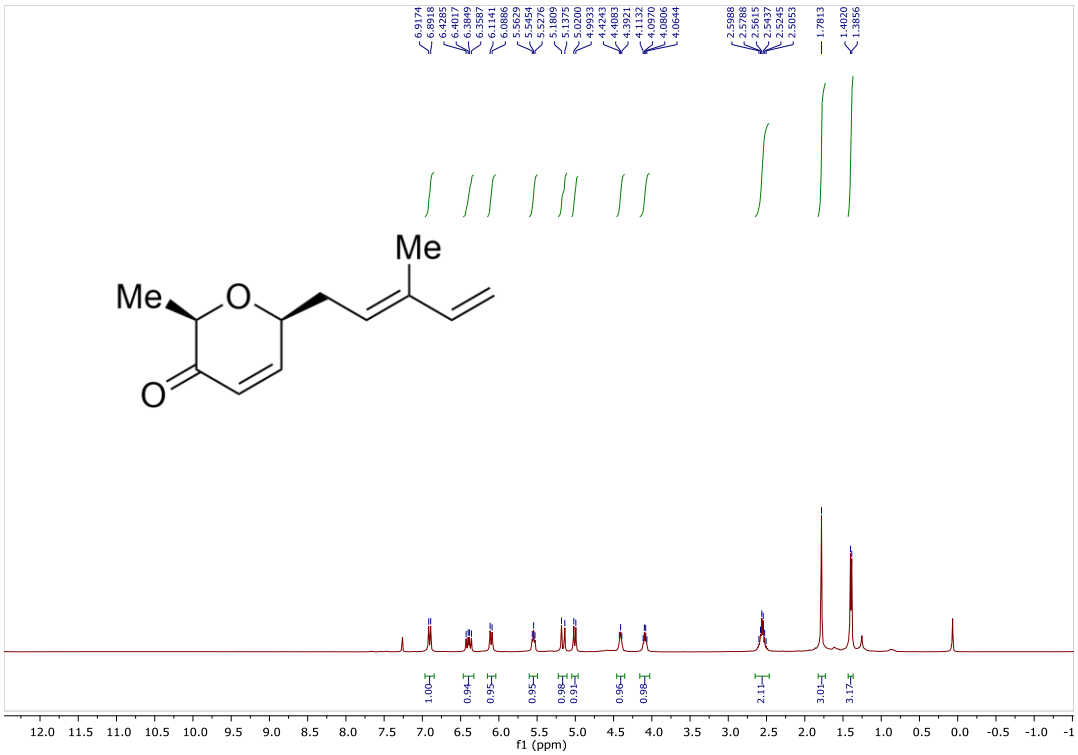

Figure 2.51 ^{1}H-NMR (400 MHz, $CDCl_3$) of Enone Diene **141**

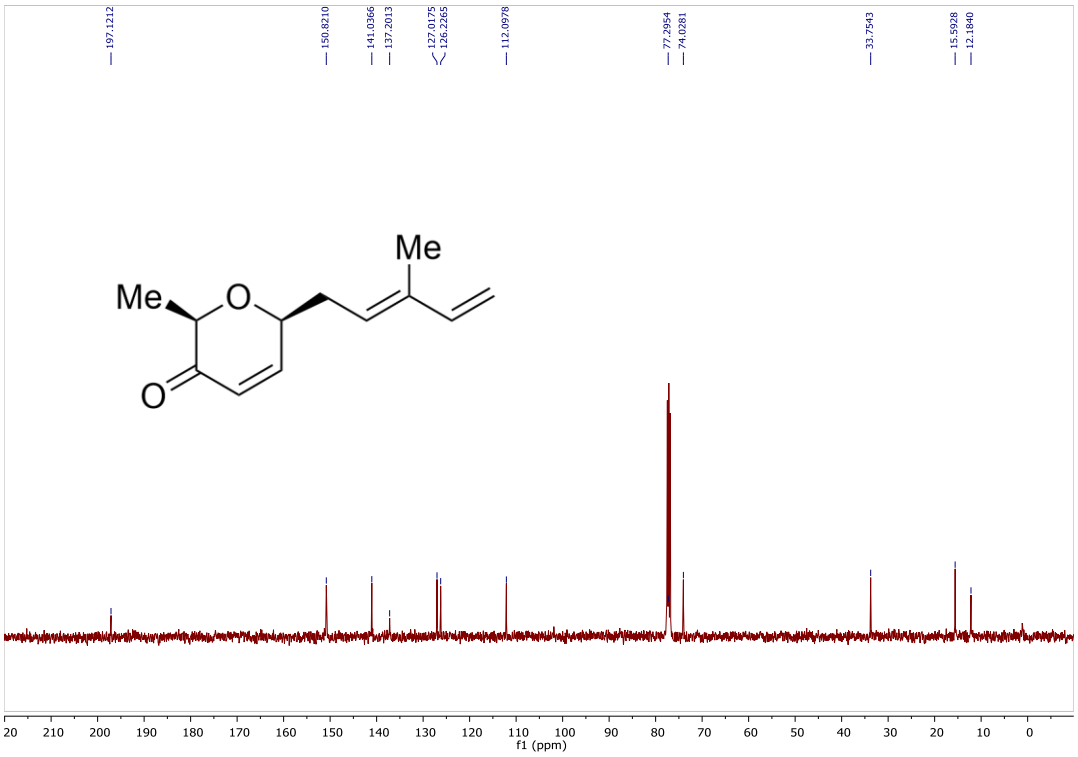

Figure 2.52 ^{13}C-NMR (100 MHz, $CDCl_3$) of Enone Diene **141**

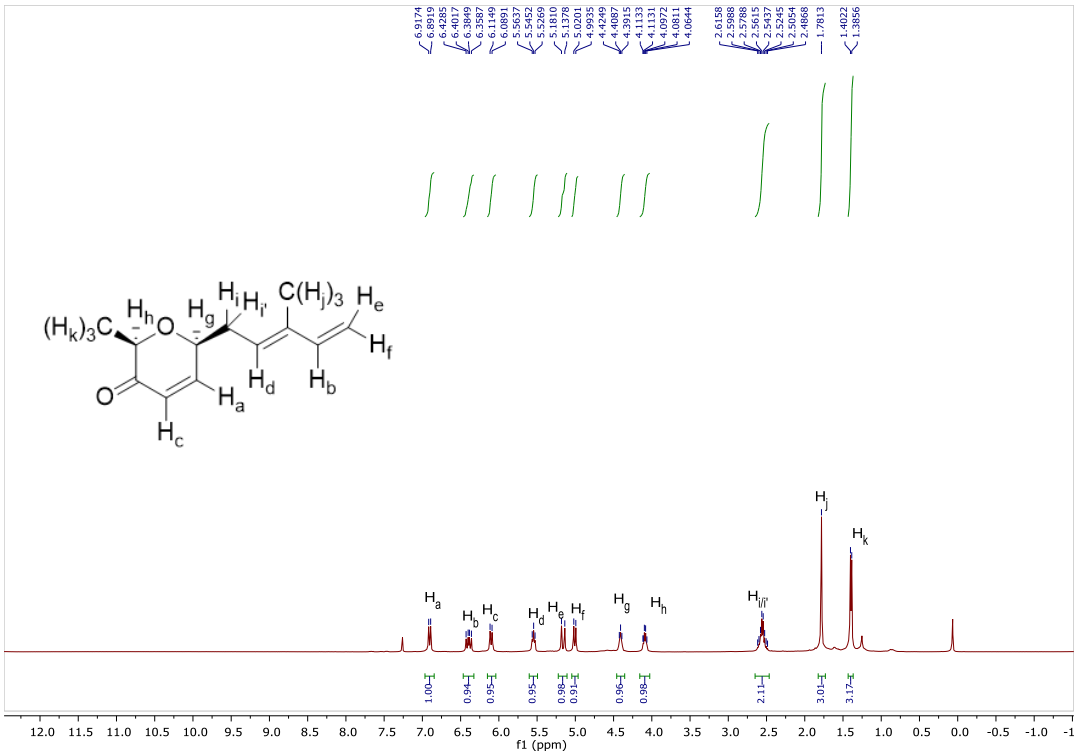

Figure 2.53 Assigned ^{1}H-NMR (800 MHz, $CDCl_3$) of Enone Diene **141**

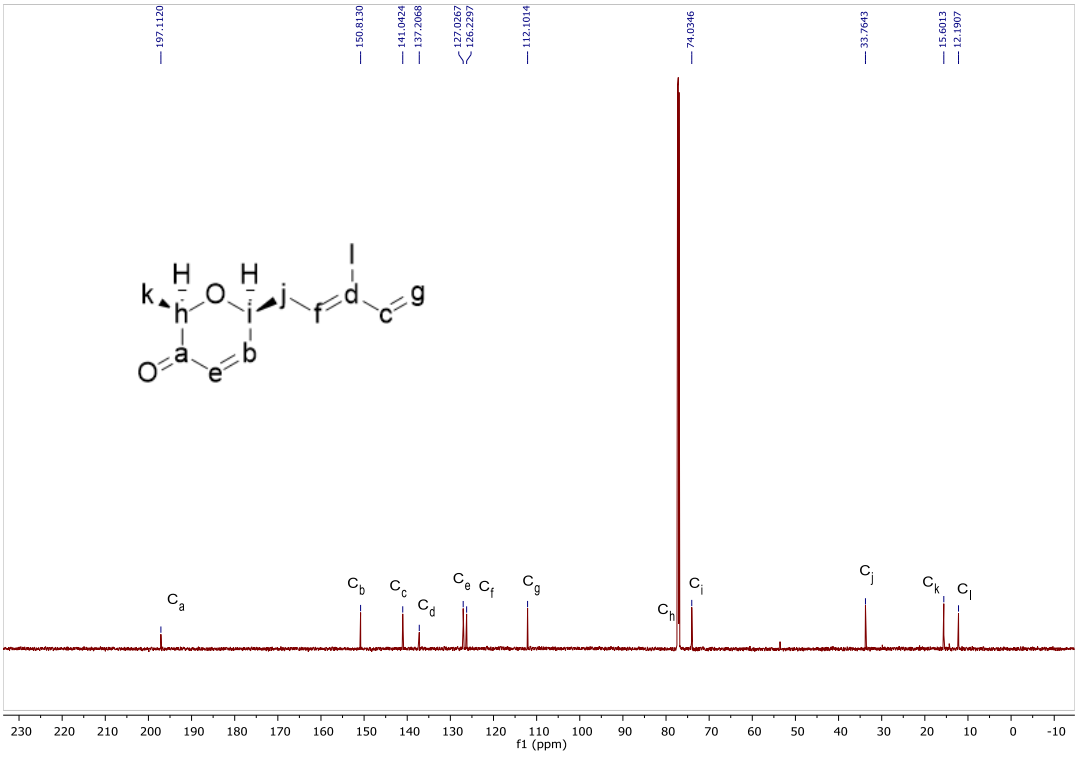

Figure 2.54 Assigned ^{13}C-NMR (200 MHz, $CDCl_3$) of Enone Diene **141**

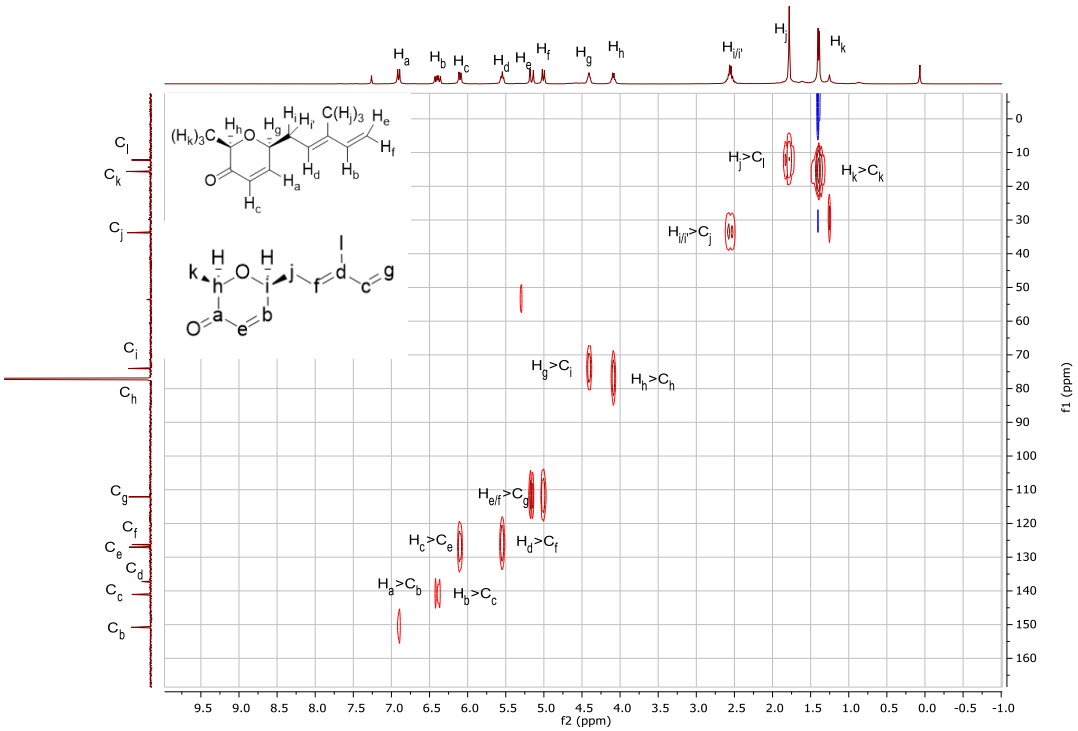

Figure 2.55 HMQC NMR ($CDCl_3$) of Enone Diene **141**

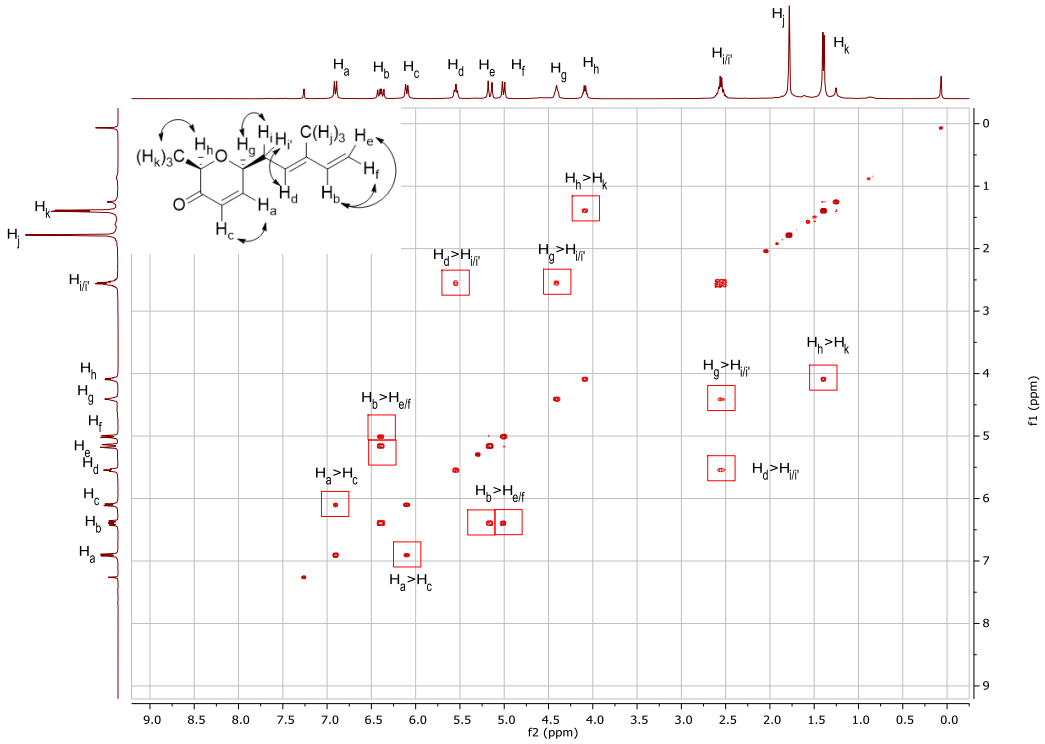

Figure 2.56 ^{1}H-^{1}H COSY NMR ($CDCl_3$) of Enone Diene **141**

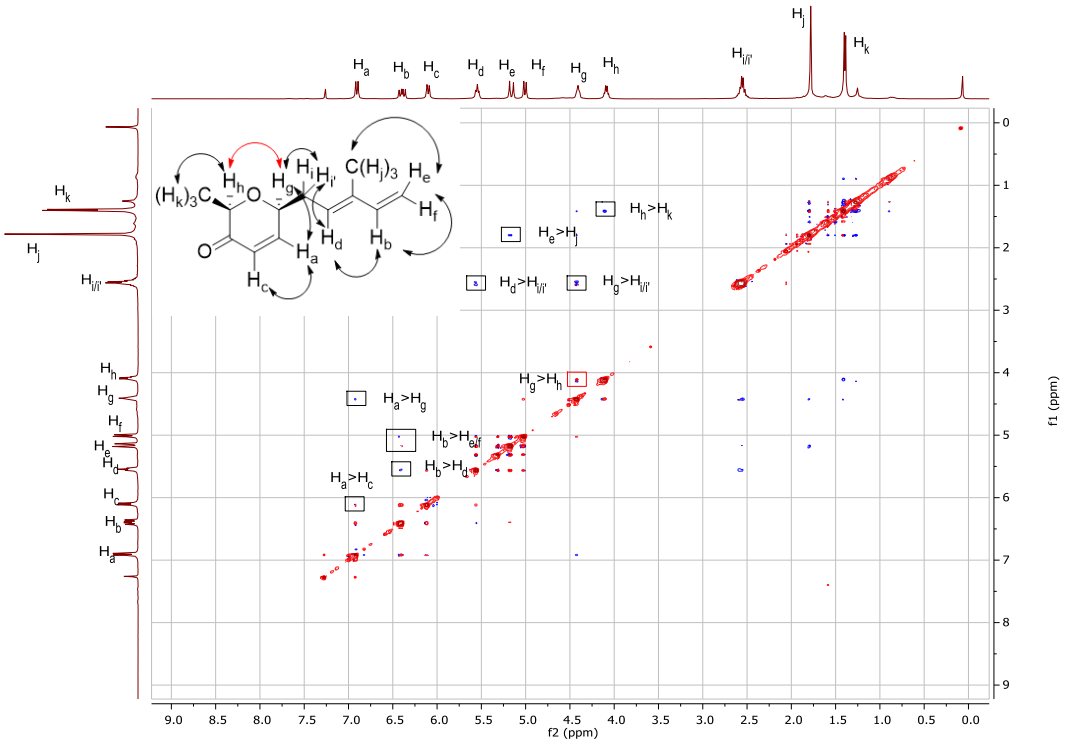

Figure 2.57 NOESY NMR ($CDCl_3$) of Enone Diene **141**

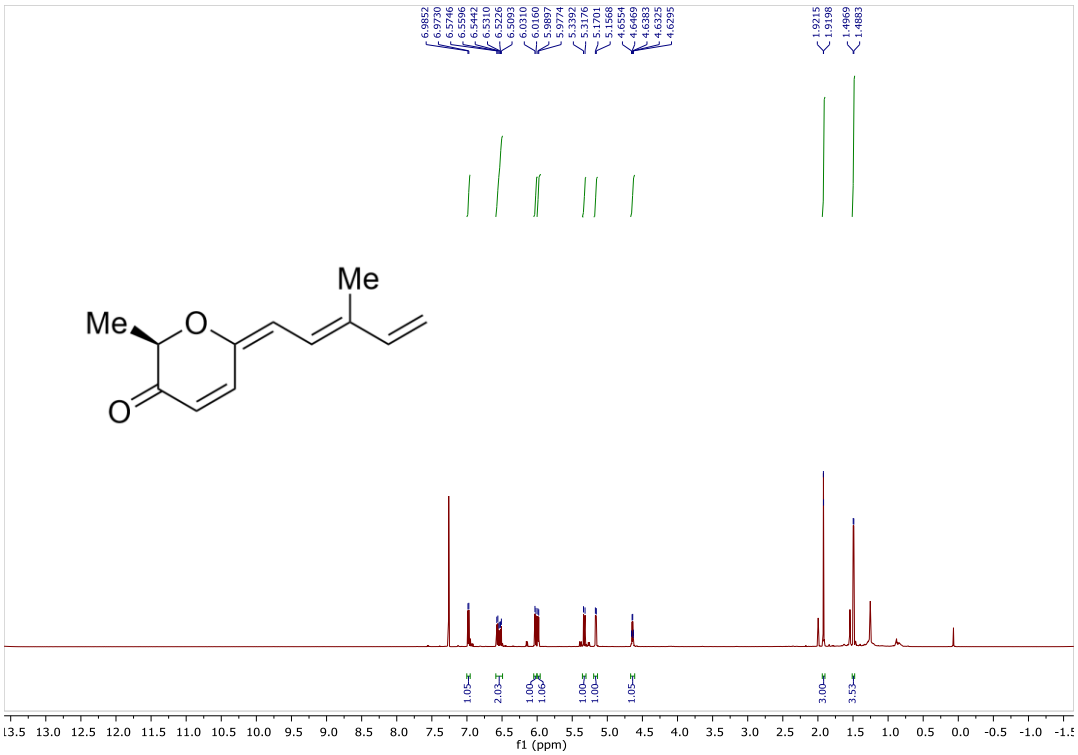

Figure 2.58 ^{1}H-NMR (800 MHz, $CDCl_3$) of Enone Triene **147**

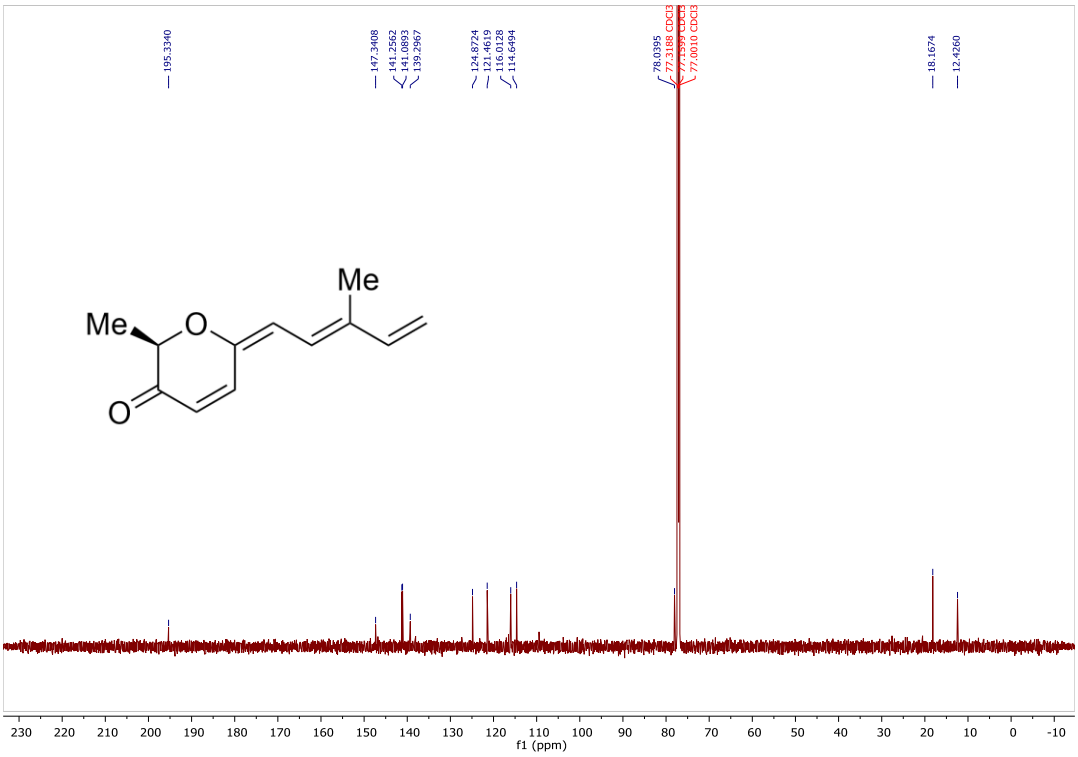

Figure 2.59 ^{13}C-NMR (200 MHz, $CDCl_3$) of Enone Triene **147**

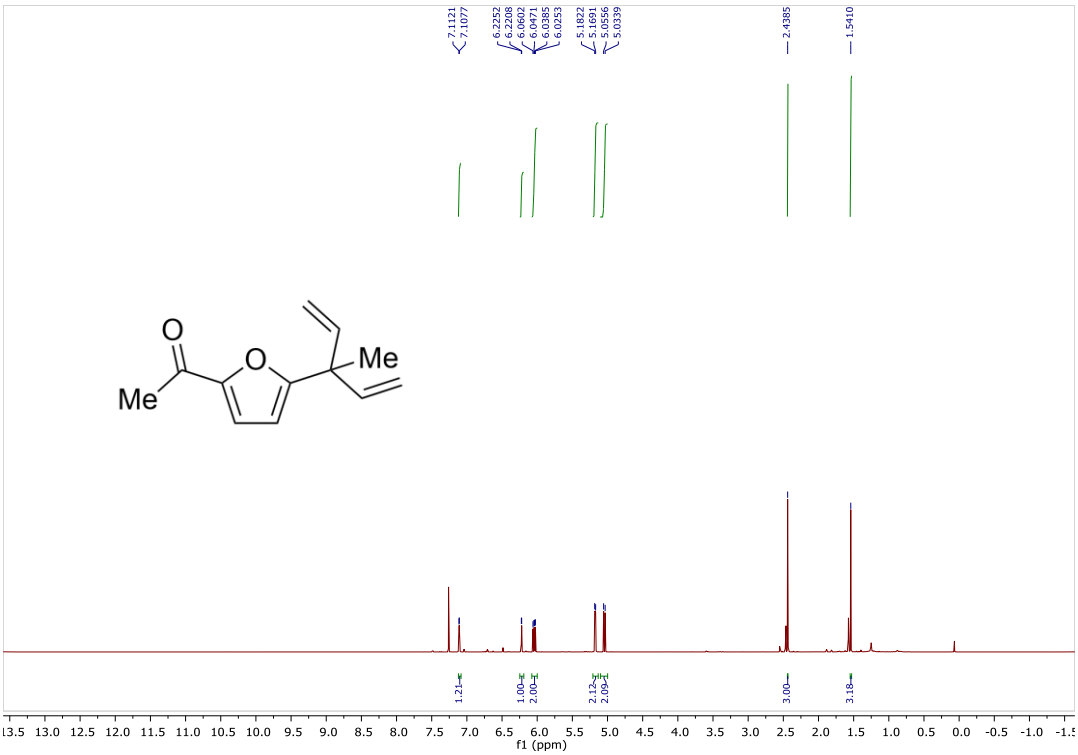

Figure 2.60 ^{1}H-NMR (800 MHz, $CDCl_3$) of Divinyl Ketone **153**

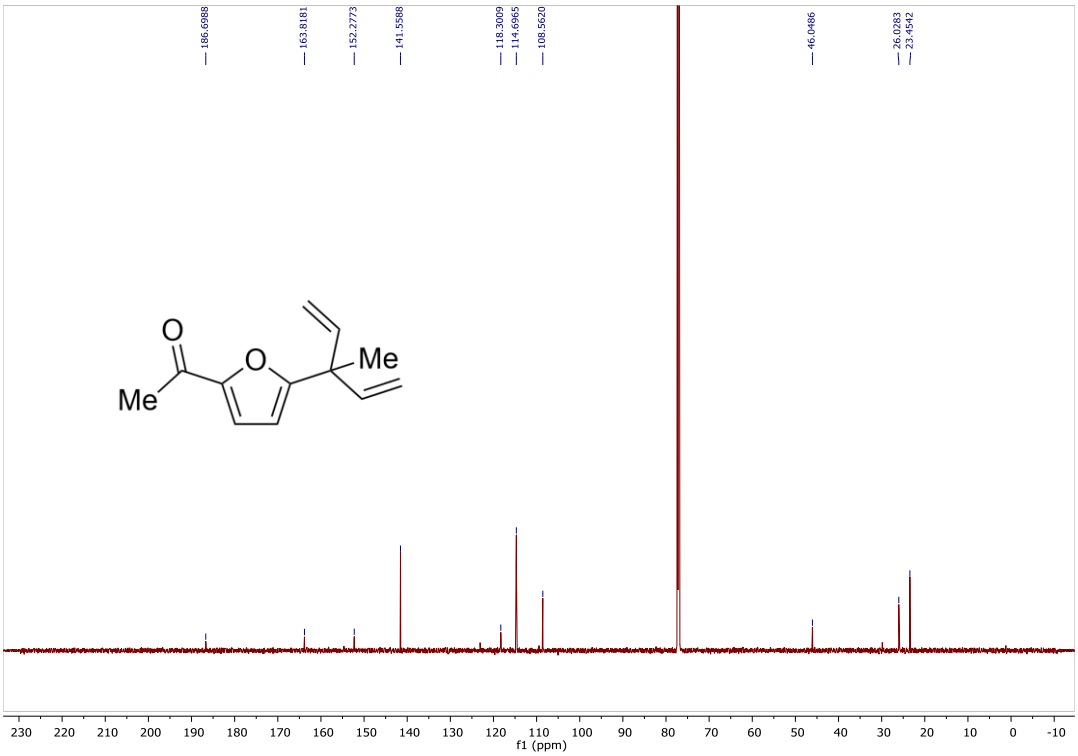

Figure 2.61 ^{13}C-NMR (200 MHz, $CDCl_3$) of Divinyl Ketone **153**

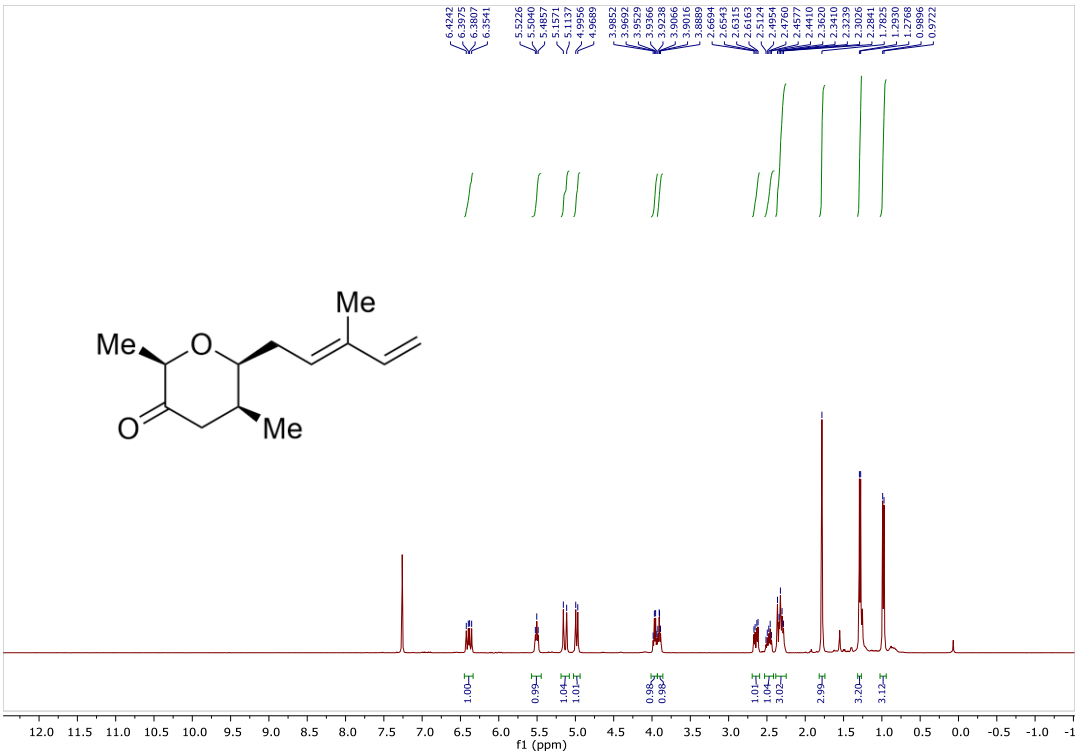

Figure 2.62 ^{1}H-NMR (400 MHz, $CDCl_3$) of β-Methyl Ketone **132**

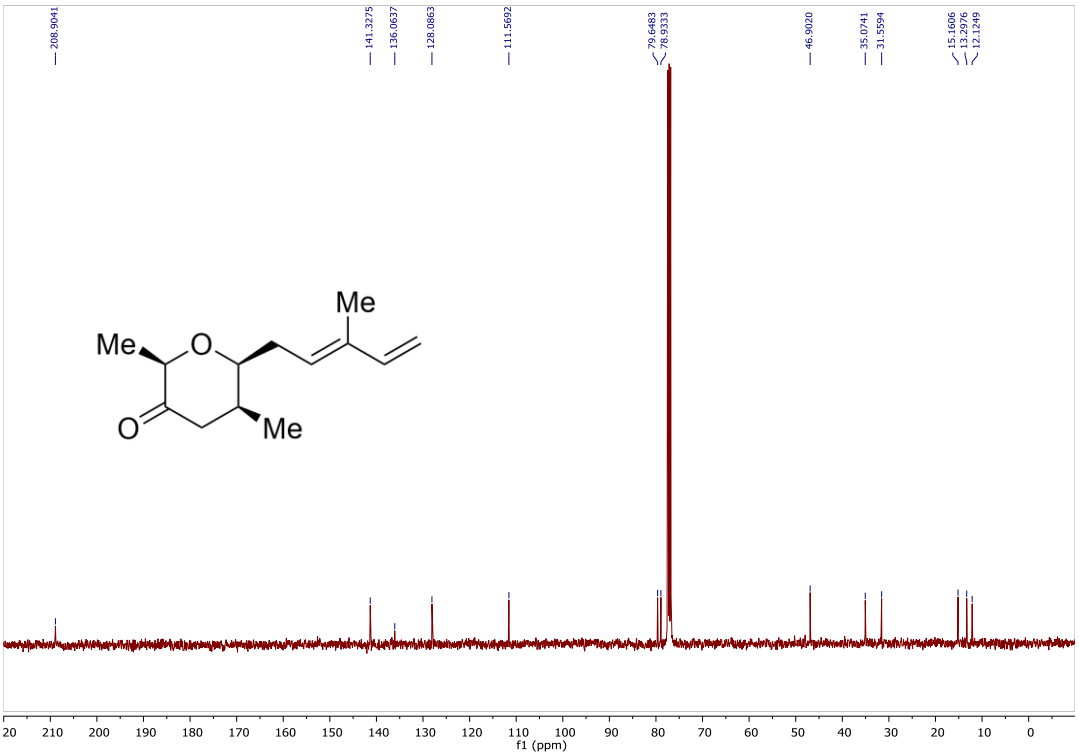

Figure 2.63 ^{13}C-NMR (100 MHz, $CDCl_3$) of β-Methyl Ketone **132**

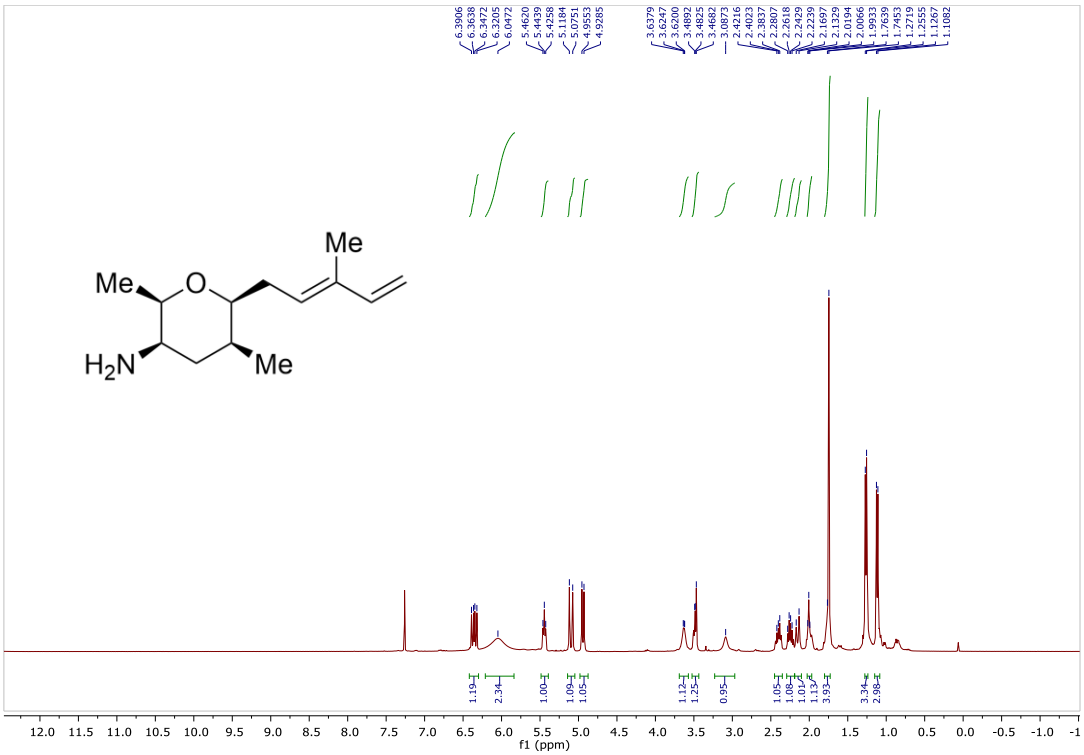

Figure 2.64 ^{1}H-NMR (400 MHz, $CDCl_3$) of THP Amine **92**

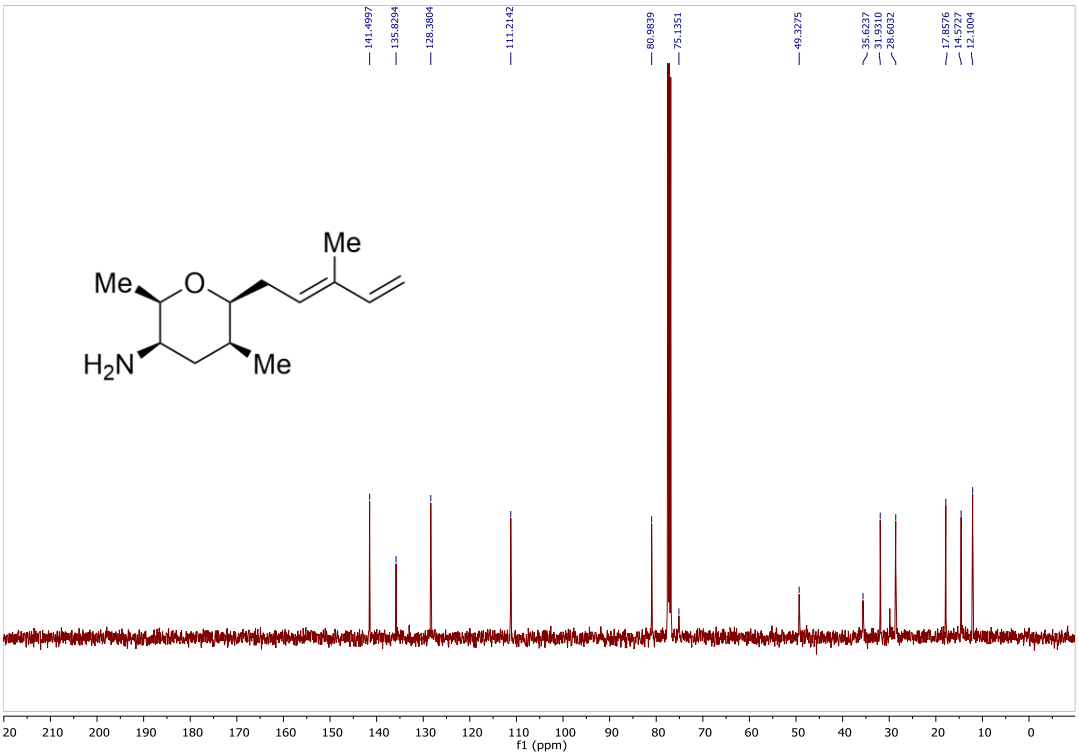

Figure 2.65 ^{13}C-NMR (100 MHz, $CDCl_3$) of THP Amine **92**

REFERENCES

(1) Campbell, E. L.; Zuhl, A. M.; Liu, C. M.; Boger, D. L. Total Synthesis of (+)-Fendleridine (Aspidoalbidine) and (+)-1-Acetylaspidoalbidine. *J. Am. Chem. Soc.* **2010**, *132* (9), 3009–3012. https://doi.org/10.1021/ja908819q.

(2) White, K. L.; Movassaghi, M. Concise Total Syntheses of (+)-Haplocidine and (+)-Haplocine via Late-Stage Oxidation of (+)-Fendleridine Derivatives. *J. Am. Chem. Soc.* **2016**, *138* (35), 11383–11389. https://doi.org/10.1021/jacs.6b07623.

(3) Saxton, J. E. Chapter 9 Synthesis of the Aspidosperma Alkaloids. In *The Alkaloids: Chemistry and Biology*; Cordell, G. A., Ed.; Academic Press, 1998; Vol. 50, pp 343–376. https://doi.org/10.1016/S1099-4831(08)60047-4.

(4) Saxton, J. E. Chapter 1 - Alkaloids of the Aspidospermine Group. In *The Alkaloids: Chemistry and Biology*; Cordell, G. A., Ed.; Academic Press, 1998; Vol. 51, pp 1–197. https://doi.org/10.1016/S0099-9598(08)60005-X.

(5) Kozmin, S. A.; Iwama, T.; Huang, Y.; Rawal, V. H. An Efficient Approach to Aspidosperma Alkaloids via [4 + 2] Cycloadditions of Aminosiloxydienes: Stereocontrolled Total Synthesis of (±)-Tabersonine. Gram-Scale Catalytic Asymmetric Syntheses of (+)-Tabersonine and (+)-16-Methoxytabersonine. Asymmetric Syntheses of (+)-Aspidospermidine and (−)-Quebrachamine. *J. Am. Chem. Soc.* **2002**, *124* (17), 4628–4641. https://doi.org/10.1021/ja017863s.

(6) Saxton, J. E. Chapter 18 Alkaloids of Haplophyton Cimicidum. In *The Alkaloids: Chemistry and Physiology*; Elsevier, 1965; Vol. 8, pp 673–678. https://doi.org/10.1016/S1876-0813(08)60057-3.

(7) Aquino, P. G. V.; Aquino, T. M. de; Alexandre-Moreira, M. S.; OliveiraSantos, B. V. de; Santana, A. E. G.; deAraújo-Júnior, J. X. Aspidosperma Terpenoid Alkaloids — Biosynthetic Origin, Chemical Synthesis and Importance. *Phytochem. - Isol. Characterisation Role Hum. Health* **2015**. https://doi.org/10.5772/59758.

(8) Tanaka, J. C. A.; Silva, C. C. da; Oliveira, A. J. B. de; Nakamura, C. V.; Dias Filho, B. P. Antibacterial Activity of Indole Alkaloids from Aspidosperma Ramiflorum. *Braz. J. Med. Biol. Res.* **2006**, *39* (3), 387–391. https://doi.org/10.1590/S0100-879X2006000300009.

(9) Lobert, S.; Vulevic, B.; Correia, J. J. Interaction of Vinca Alkaloids with Tubulin: A Comparison of Vinblastine, Vincristine, and Vinorelbine. *Biochemistry* **1996**, *35* (21), 6806–6814. https://doi.org/10.1021/bi953037i.

(10) Safa, A. R.; Hamel, E.; Felsted, R. L. Photoaffinity Labeling of Tubulin Subunits with a Photoactive Analog of Vinblastine. *Biochemistry* **1987**, *26* (1), 97–102. https://doi.org/10.1021/bi00375a014.

(11) Prakash, V.; Timasheff, S. N. Mechanism of Interaction of Vinca Alkaloids with Tubulin: Catharanthine and Vindoline. *Biochemistry* **1991**, *30* (3), 873–880. https://doi.org/10.1021/bi00217a042.

(12) Hart, M. J.; Glicksman, M.; Liu, M.; Sharma, M. K.; Cuny, G.; Galvan, V. Development of a High-Throughput Screen Targeting Caspase-8-Mediated Cleavage of the Amyloid Precursor Protein. *Anal. Biochem.* **2012**, *421* (2), 467–476. https://doi.org/10.1016/j.ab.2011.11.020.

(13) Dias, D. A.; Urban, S.; Roessner, U. A Historical Overview of Natural Products in Drug Discovery. *Metabolites* **2012**, *2* (2), 303–336. https://doi.org/10.3390/metabo2020303.

(14) Burnell, R. H.; Medina, J. D.; Ayer, W. A. Alkaloids of the Seeds of Aspidosperma Fendleri Woodson. *Can. J. Chem.* **1966**, *44* (1), 28–31. https://doi.org/10.1139/v66-005.

(15) Mitaine, A.-C.; Mesbah, K.; Richard, B.; Petermann, C.; Arrazola, S.; Moretti, C.; Zèches-Hanrot, M.; Men-Olivier, L. L. Alkaloids from Aspidosperma Species from Bolivia. *Planta Med.* **1996**, *62* (5), 458–461. https://doi.org/10.1055/s-2006-957939.

(16) Estrada, O.; González-Guzmán, J. M.; Salazar-Bookman, M. M.; Cardozo, A.; Lucena, E.; Alvarado-Castillo, C. P. Hypotensive and Bradycardic Effects of Quinovic Acid Glycosides from Aspidosperma Fendleri in Spontaneously Hypertensive Rats. *Nat. Prod. Commun.* **2015**, *10* (2), 281–284.

(17) Ceravolo, I. P.; Zani, C. L.; Figueiredo, F. J. B.; Kohlhoff, M.; Santana, A. E. G.; Krettli, A. U. Aspidosperma Pyrifolium, a Medicinal Plant from the Brazilian Caatinga, Displays a High Antiplasmodial Activity and Low Cytotoxicity. *Malar. J.* **2018**, *17* (1), 436. https://doi.org/10.1186/s12936-018-2568-y.

(18) Atta-ur-Rahman. *Bioactive Natural Products (Part B)*; Elsevier, 2000.

(19) Sears, J. E.; Boger, D. L. Tandem Intramolecular Diels–Alder/1,3-Dipolar Cycloaddition Cascade of 1,3,4-Oxadiazoles: Initial Scope and Applications. *Acc. Chem. Res.* **2016**, *49* (2), 241–251. https://doi.org/10.1021/acs.accounts.5b00510.

(20) Liu, Y.; Luo, S.; Fu, X.; Fang; Zhuang, Z.; Xiong, W.; Jia, X.; Zhai, H. Facile Construction of the Pentacyclic Framework of Subincanadine B. Synthesis of 20-Deethylenylated Subincanadine B and 19,20-Dihydrosubincanadine B. *Org. Lett.* **2006**, *8* (1), 115–118. https://doi.org/10.1021/ol0526367.

(21) Ende, A. E. van der; Kravitz, E. J.; Harth, E. Approach to Formation of Multifunctional Polyester Particles in Controlled Nanoscopic Dimensions. *J. Am. Chem. Soc.* **2008**, *130* (27), 8706–8713. https://doi.org/10.1021/ja711417h.

(22) Christl, M.; Lanzendörfer, U.; Grötsch, M. M.; Ditterich, E.; Hegmann, J. Cycloadditionen von 1,3,4-Oxadiazin-6-Onen (4,5-Diaza-α-Pyronen), 9. 6-Oxo-5-Phenyl-1,3,4-Oxadiazin-2-Carbonsäure-Methylester — Synthese Und Reaktionen Mit Norbornen, Norbornadien, Cyclopropenen, Cyclobuten Und Benzvalen. *Chem. Ber.* **1990**, *123* (10), 2031–2037. https://doi.org/10.1002/cber.19901231014.

(23) Mewald, M.; Medley, J. W.; Movassaghi, M. Concise and Enantioselective Total Synthesis of (−)-Mehranine, (−)-Methylenebismehranine, and Related Aspidosperma Alkaloids. *Angew. Chem. Int. Ed.* **2014**, *53* (43), 11634–11639. https://doi.org/10.1002/anie.201405609.

(24) Schultz, A. G.; Dittami, J. P.; Myong, S. O.; Sha, C. K. A New 2-Azatricyclo[4.4.0.02,8]Decenone Synthesis and Ketene Formation by Retro-Diels-Alder Reaction. *J. Am. Chem. Soc.* **1983**, *105* (10), 3273–3279. https://doi.org/10.1021/ja00348a051.

(25) Behenna, D. C.; Stoltz, B. M. The Enantioselective Tsuji Allylation. *J. Am. Chem. Soc.* **2004**, *126* (46), 15044–15045. https://doi.org/10.1021/ja044812x.

(26) Tsuji, J.; Takahashi, H.; Morikawa, M. Organic Syntheses by Means of Noble Metal Compounds XVII. Reaction of π-Allylpalladium Chloride with Nucleophiles. *Tetrahedron Lett.* **1965**, *6* (49), 4387–4388. https://doi.org/10.1016/S0040-4039(00)71674-1.

(27) Trost, B. M.; Fullerton, T. J. New Synthetic Reactions. Allylic Alkylation. *J. Am. Chem. Soc.* **1973**, *95* (1), 292–294. https://doi.org/10.1021/ja00782a080.

(28) Keith, J. A.; Behenna, D. C.; Sherden, N.; Mohr, J. T.; Ma, S.; Marinescu, S. C.; Nielsen, R. J.; Oxgaard, J.; Stoltz, B. M.; Goddard, W. A. The Reaction Mechanism of the Enantioselective Tsuji Allylation: Inner-Sphere and Outer-Sphere Pathways, Internal Rearrangements, and Asymmetric C–C Bond Formation. *J. Am. Chem. Soc.* **2012**, *134* (46), 19050–19060. https://doi.org/10.1021/ja306860n.

(29) Weaver, J. D.; Recio, A.; Grenning, A. J.; Tunge, J. A. Transition Metal-Catalyzed Decarboxylative Allylation and Benzylation Reactions. *Chem. Rev.* **2011**, *111* (3), 1846–1913. https://doi.org/10.1021/cr1002744.

(30) Bennett, N. B.; Duquette, D. C.; Kim, J.; Liu, W.-B.; Marziale, A. N.; Behenna, D. C.; Virgil, S. C.; Stoltz, B. M. Expanding Insight into Asymmetric Palladium-Catalyzed Allylic Alkylation of N-Heterocyclic Molecules and Cyclic Ketones. *Chem. – Eur. J.* **2013**, *19* (14), 4414–4418. https://doi.org/10.1002/chem.201300030.

(31) Gramain, J.-C.; Troin, Y.; Husson, H.-P. A Short and Efficient Synthesis of 4a-Substituted Cis-Hexahydro-1,2,3,4,4a,9a-Carbazol-4-Ones. *J. Heterocycl. Chem.* **1988**, *25* (1), 201–203. https://doi.org/10.1002/jhet.5570250130.

(32) Dugat, D.; Gramain, J.-C. Structure, Stereochemistry, and Conformation of Diastereoisomericcis- and Trans-3-Ethyl-l,2,3,4,4a,9a-Hexahydrocarbazol-4-Ones by Means of 13Cand Two- Dimensional H Nuclear Magnetic Resonance Spectroscopy. An Example of Diastereoselection in a Photocyclisation Reaction l. *J CHEM SOC PERKIN TRANS* **1990**, 7.

(33) Gramain, J.-C.; Husson, H. P.; Troin, Y. A Novel and Efficient Synthesis of the Aspidosperma Alkaloid Ring System: N(a)-Benzyldeethylaspidospermidine. *J. Org. Chem.* **1985**, *50* (26), 5517–5520. https://doi.org/10.1021/jo00350a016.

(34) Hoffmann, R.; Woodward, R. B. Conservation of Orbital Symmetry. *Acc. Chem. Res.* **1968**, *1* (1), 17–22. https://doi.org/10.1021/ar50001a003.

(35) Modha, S. G.; Pöthig, A.; Dreuw, A.; Bach, T. [6π] Photocyclization to Cis-Hexahydrocarbazol-4-Ones: Substrate Modification, Mechanism, and Scope. *J. Org. Chem.* **2019**, *84* (3), 1139–1153. https://doi.org/10.1021/acs.joc.8b03144.

(36) Ikawa, T.; Hattori, K.; Sajiki, H.; Hirota, K. Solvent-Modulated Pd/C-Catalyzed Deprotection of Silyl Ethers and Chemoselective Hydrogenation. *Tetrahedron* **2004**, *60* (32), 6901–6911. https://doi.org/10.1016/j.tet.2004.05.098.

(37) Kim, S.; Marie Jacobo, S.; Chang, C.-T.; Bellone, S.; Powell, W. S.; Rokach, J. Silyl Group Deprotection by Pd/C/H2. A Facile and Selective Method. *Tetrahedron Lett.* **2004**, *45* (9), 1973–1976. https://doi.org/10.1016/j.tetlet.2003.12.145.

(38) Walser, A.; Djerassi, C. Alkaloid-Studien LII. Die Alkaloide aus Vallesia dichotoma RUIZet PAV. *Helv. Chim. Acta* **1965**, *48* (2), 391–404. https://doi.org/10.1002/hlca.19650480220.

(39) Azarian, D.; Dua, S. S.; Eaborn, C.; Walton, D. R. M. Reactions of Organic Halides with R3 MMR3 Compounds (M = Si, Ge, Sn) in the Presence of Tetrakis(Triarylphosphine)Palladium. *J. Organomet. Chem.* **1976**, *117* (3), C55–C57. https://doi.org/10.1016/S0022-328X(00)91902-8.

(40) Kosugi, M.; Sasazawa, K.; Shimizu, Y.; Migita, T. Reactions of Allyltin Compounds Iii. Allylation of Aromatic Halides with Allyltributyltin in the Presence of Tetrakis(Triphenylphosphine)Palladium(o). *Chem. Lett.* **1977**, *6* (3), 301–302. https://doi.org/10.1246/cl.1977.301.

(41) Kosugi, M.; Shimizu, Y.; Migita, T. Alkylation, Arylation, and Vinylation of Acyl Chlorides by Means of Organotin Compounds in the Presence of Catalytic Amounts of Tetrakis(Triphenylphosphine)Palladium(o). *Chem. Lett.* **1977**, *6* (12), 1423–1424. https://doi.org/10.1246/cl.1977.1423.

(42) Milstein, D.; Stille, J. K. A General, Selective, and Facile Method for Ketone Synthesis from Acid Chlorides and Organotin Compounds Catalyzed by Palladium. *J. Am. Chem. Soc.* **1978**, *100* (11), 3636–3638. https://doi.org/10.1021/ja00479a077.

(43) Stille, J. K. John K. Stille. Biographical Sketch. *Organometallics* **1990**, *9* (12), 3007–3008. https://doi.org/10.1021/om00162a001.

(44) Lenz, R. W. In Memory of John Kenneth Stille. *Macromolecules* **1990**, *23* (9), 2417–2418. https://doi.org/10.1021/ma00211a001.

(45) Cordovilla, C.; Bartolomé, C.; Martínez-Ilarduya, J. M.; Espinet, P. The Stille Reaction, 38 Years Later. *ACS Catal.* **2015**, *5* (5), 3040–3053. https://doi.org/10.1021/acscatal.5b00448.

(46) Farina, V.; Kapadia, S.; Krishnan, B.; Wang, C.; Liebeskind, L. S. On the Nature of the "Copper Effect" in the Stille Cross-Coupling. *J. Org. Chem.* **1994**, *59* (20), 5905–5911. https://doi.org/10.1021/jo00099a018.

(47) Mee, S. P. H.; Lee, V.; Baldwin, J. E. Stille Coupling Made Easier—The Synergic Effect of Copper(I) Salts and the Fluoride Ion. *Angew. Chem. Int. Ed.* **2004**, *43* (9), 1132–1136. https://doi.org/10.1002/anie.200352979.

(48) Piers, E.; Wong, T. Copper(I) Chloride-Mediated Intramolecular Coupling of Vinyltrimethylstannane and Vinyl Halide Functions. *J. Org. Chem.* **1993**, *58* (14), 3609–3610. https://doi.org/10.1021/jo00066a006.

(49) Falck, J. R.; Bhatt, R. K.; Ye, J. Tin-Copper Transmetalation: Cross-Coupling of .Alpha.-Heteroatom-Substituted Alkyltributylstannanes with Organohalides. *J. Am. Chem. Soc.* **1995**, *117* (22), 5973–5982. https://doi.org/10.1021/ja00127a010.

(50) The Copper(I) Iodide-promoted Allylation of Vinylstannanes with Allylic Halides | Chemistry Letters https://www.journal.csj.jp/doi/abs/10.1246/cl.1995.771 (accessed Nov 8, 2019).

(51) Allred, G. D.; Liebeskind, L. S. Copper-Mediated Cross-Coupling of Organostannanes with Organic Iodides at or below Room Temperature. *J. Am. Chem. Soc.* **1996**, *118* (11), 2748–2749. https://doi.org/10.1021/ja9541239.

(52) Kang, S.-K.; Kim, J.-S.; Choi, S.-C. Copper- and Manganese-Catalyzed Cross-Coupling of Organostannanes with Organic Iodides in the Presence of Sodium Chloride. *J. Org. Chem.* **1997**, *62* (13), 4208–4209. https://doi.org/10.1021/jo970656j.

(53) Nudelman, N. S.; Carro, C. Cu(I)-Catalyzed Regioselective Synthesis of Substituted Allyl Furans and Thiophenes Using Organostannanes. *Synlett* **1999**, *1999* (12), 1942–1944. https://doi.org/10.1055/s-1999-2984.

(54) Wang, Y.; Burton, D. J. Copper(I)-Only Catalyzed Reactions of (E)-2,3-Difluoro-3-Stannylacrylic Ester with Acid Chlorides and Mechanistic Studies of the "Copper Effect" in Stille Coupling Reactions. *Org. Lett.* **2006**, *8* (6), 1109–1111. https://doi.org/10.1021/ol053023x.

(55) Casado, A. L.; Espinet, P. Quantitative Evaluation of the Factors Contributing to the "Copper Effect" in the Stille Reaction. *Organometallics* **2003**, *22* (6), 1305–1309. https://doi.org/10.1021/om020896b.

(56) Wang, M.; Lin, Z. Stille Cross-Coupling Reactions of Alkenylstannanes with Alkenyl Iodides Mediated by Copper(I) Thiophene-2-Carboxylate: A Density Functional Study. *Organometallics* **2010**, *29* (14), 3077–3084. https://doi.org/10.1021/om100304t.

(57) Braga, A. A. C.; Ujaque, G.; Maseras, F. A DFT Study of the Full Catalytic Cycle of the Suzuki−Miyaura Cross-Coupling on a Model System. *Organometallics* **2006**, *25* (15), 3647–3658. https://doi.org/10.1021/om060380i.

(58) Yamanaka, M.; Kato, S.; Nakamura, E. Mechanism and Regioselectivity of Reductive Elimination of π-Allylcopper (III) Intermediates. *J. Am. Chem. Soc.* **2004**, *126* (20), 6287–6293. https://doi.org/10.1021/ja049211k.

(59) Preparation of σ- and π-Allylcopper(III) Intermediates in SN2 and SN2′ Reactions of Organocuprate(I) Reagents with Allylic Substrates | Journal of the American Chemical Society https://pubs.acs.org/doi/full/10.1021/ja801186c (accessed Feb 4, 2020).

(60) Lee, V. Application of Copper(I) Salt and Fluoride Promoted Stille Coupling Reactions in the Synthesis of Bioactive Molecules. *Org. Biomol. Chem.* **2019**, *17* (41), 9095–9123. https://doi.org/10.1039/C9OB01602C.

(61) Gilman, H.; Jones, R. G.; Woods, L. A. The Preparation of Methylcopper and Some Observations on the Decomposition of Organocopper Compounds. *J. Org. Chem.* **1952**, *17* (12), 1630–1634. https://doi.org/10.1021/jo50012a009.

(62) Experimental Evidence Supporting a CuIII Intermediate in Cross-Coupling Reactions of Allylic Esters with Diallylcuprate Species - Karlström - 2001 - Chemistry – A European Journal - Wiley Online Library https://onlinelibrary.wiley.com/doi/10.1002/1521-3765%2820010504%297%3A9%3C1981%3A%3AAID-CHEM1981%3E3.0.CO%3B2-C (accessed Feb 4, 2020).

(63) Wang, Y.; Ho, C.-T. Formation of 2,5-Dimethyl-4-Hydroxy-3(2H)-Furanone through Methylglyoxal: A Maillard Reaction Intermediate. *J. Agric. Food Chem.* **2008**, *56* (16), 7405–7409. https://doi.org/10.1021/jf8012025.

(64) Soliman, M. A.; El-Sawy, A. A.; Fadel, H. M.; Osman, F. Effect of Antioxidants on the Volatiles of Roasted Sesame Seeds. *J. Agric. Food Chem.* **1985**, *33* (3), 523–528. https://doi.org/10.1021/jf00063a046.

(65) Watanabe, K.; Sato, Y. Shallow-Fried Beef. Additional Flavor Components. *J. Agric. Food Chem.* **1972**, *20* (2), 174–176. https://doi.org/10.1021/jf60180a001.

(66) Buttery, R. G.; Stern, D. J.; Ling, L. C. Studies on Flavor Volatiles of Some Sweet Corn Products. *J. Agric. Food Chem.* **1994**, *42* (3), 791–795. https://doi.org/10.1021/jf00039a038.

(67) Harrowven, D. C.; Curran, D. P.; Kostiuk, S. L.; Wallis-Guy, I. L.; Whiting, S.; Stenning, K. J.; Tang, B.; Packard, E.; Nanson, L. Potassium Carbonate–Silica: A Highly Effective Stationary Phase for the Chromatographic Removal of Organotin Impurities. *Chem. Commun.* **2010**, *46* (34), 6335–6337. https://doi.org/10.1039/C0CC01328E.

(68) Spliceosome Structure and Function https://cshperspectives.cshlp.org/content/3/7/a003707 (accessed Nov 8, 2019).

(69) Targeting the spliceosome | Nature Chemical Biology https://www.nature.com/articles/nchembio0907-533 (accessed Nov 8, 2019).

(70) The Spliceosome: Design Principles of a Dynamic RNP Machine - ScienceDirect https://www.sciencedirect.com/science/article/pii/S0092867409001469?via%3Dihub (accessed Nov 8, 2019).

(71) Spliceostatin A inhibits spliceosome assembly subsequent to prespliceosome formation | Nucleic Acids Research | Oxford Academic https://academic.oup.com/nar/article/38/19/6664/2409469 (accessed Nov 8, 2019).

(72) Lee, S. C.-W.; Abdel-Wahab, O. Therapeutic Targeting of Splicing in Cancer. *Nat. Med.* **2016**, *22* (9), 976–986. https://doi.org/10.1038/nm.4165.

(73) Singh, R. K.; Cooper, T. A. Pre-MRNA Splicing in Disease and Therapeutics. *Trends Mol. Med.* **2012**, *18* (8), 472–482. https://doi.org/10.1016/j.molmed.2012.06.006.

(74) van Alphen, R. J.; Wiemer, E. a. C.; Burger, H.; Eskens, F. a. L. M. The Spliceosome as Target for Anticancer Treatment. *Br. J. Cancer* **2009**, *100* (2), 228–232. https://doi.org/10.1038/sj.bjc.6604801.

(75) Karp's Cell and Molecular Biology: Concepts and Experiments, 8th Edition | Wiley https://www.wiley.com/en-us/Karp%27s+Cell+and+Molecular+Biology%3A+Concepts+and+Experiments%2C+8th+Edition-p-ES81118883846 (accessed Mar 2, 2020).

(76) Effenberger, K. A.; Urabe, V. K.; Jurica, M. S. Modulating Splicing with Small Molecular Inhibitors of the Spliceosome. *Wiley Interdiscip. Rev. RNA* **2017**, *8* (2). https://doi.org/10.1002/wrna.1381.

(77) Effenberger, K. A.; Urabe, V. K.; Prichard, B. E.; Ghosh, A. K.; Jurica, M. S. Interchangeable SF3B1 Inhibitors Interfere with Pre-MRNA Splicing at Multiple Stages. *RNA* **2016**, *22* (3), 350–359. https://doi.org/10.1261/rna.053108.115.

(78) Kahlscheuer, M. L.; Widom, J.; Walter, N. G. Chapter Eighteen - Single-Molecule Pull-Down FRET to Dissect the Mechanisms of Biomolecular Machines. In *Methods in Enzymology*; Woodson, S. A., Allain, F. H. T., Eds.; Structures of Large RNA Molecules and Their Complexes; Academic Press, 2015; Vol. 558, pp 539–570. https://doi.org/10.1016/bs.mie.2015.01.009.

(79) Nakajima, H.; Sato, B.; Fujita, T.; Takase, S.; Terano, H.; Okuhara, M. New Antitumor Substances, FR901463, FR901464 and FR901465. *J. Antibiot. (Tokyo)* **1996**, *49* (12), 1196–1203. https://doi.org/10.7164/antibiotics.49.1196.

(80) Nakajima, H.; Hori, Y.; Terano, H.; Okuhara, M.; Manda, T.; Matsumoto, S.; Shimomura, K. New Antitumor Substances, FR901463, FR901464 and FR901465. *J. Antibiot. (Tokyo)* **1996**, *49* (12), 1204–1211. https://doi.org/10.7164/antibiotics.49.1204.

(81) Nakajima, H.; Takase, S.; Terano, H.; Tanaka, H. New Antitumor Substances, FR901463, FR901464 and FR901465. *J. Antibiot. (Tokyo)* **1997**, *50* (1), 96–99. https://doi.org/10.7164/antibiotics.50.96.

(82) Thompson, C. F.; Jamison, T. F.; Jacobsen, E. N. FR901464: Total Synthesis, Proof of Structure, and Evaluation of Synthetic Analogues. *J. Am. Chem. Soc.* **2001**, *123* (41), 9974–9983. https://doi.org/10.1021/ja016615t.

(83) Ghosh, A. K.; Veitschegger, A. M.; Nie, S.; Relitti, N.; MacRae, A. J.; Jurica, M. S. Enantioselective Synthesis of Thailanstatin A Methyl Ester and Evaluation of in Vitro Splicing Inhibition. *J. Org. Chem.* **2018**, *83* (9), 5187–5198. https://doi.org/10.1021/acs.joc.8b00593.

(84) Ghosh, A. K.; Veitschegger, A. M.; Sheri, V. R.; Effenberger, K. A.; Prichard, B. E.; Jurica, M. S. Enantioselective Synthesis of Spliceostatin E and Evaluation of Biological Activity. *Org. Lett.* **2014**, *16* (23), 6200–6203. https://doi.org/10.1021/ol503127r.

(85) Ghosh, A. K.; Reddy, G. C.; MacRae, A. J.; Jurica, M. S. Enantioselective Synthesis of Spliceostatin G and Evaluation of Bioactivity of Spliceostatin G and Its Methyl Ester. *Org. Lett.* **2018**, *20* (1), 96–99. https://doi.org/10.1021/acs.orglett.7b03456.

(86) Ghosh, A. K.; Reddy, G. C.; Kovela, S.; Relitti, N.; Urabe, V. K.; Prichard, B. E.; Jurica, M. S. Enantioselective Synthesis of a Cyclopropane Derivative of Spliceostatin A and Evaluation of Bioactivity. *Org. Lett.* **2018**, *20* (22), 7293–7297. https://doi.org/10.1021/acs.orglett.8b03228.

(87) Ghosh, A. K.; Chen, Z.-H. Enantioselective Syntheses of FR901464 and Spliceostatin A: Potent Inhibitors of Spliceosome. *Org. Lett.* **2013**, *15* (19), 5088–5091. https://doi.org/10.1021/ol4024634.

(88) Ghosh, A. K.; Chen, Z.-H.; Effenberger, K. A.; Jurica, M. S. Enantioselective Total Syntheses of FR901464 and Spliceostatin A and Evaluation of Splicing Activity of Key Derivatives. *J. Org. Chem.* **2014**, *79* (12), 5697–5709. https://doi.org/10.1021/jo500800k.

(89) Nicolaou, K. C.; Rhoades, D.; Kumar, S. M. Total Syntheses of Thailanstatins A–C, Spliceostatin D, and Analogues Thereof. Stereodivergent Synthesis of Tetrasubstituted Dihydro- and Tetrahydropyrans and Design, Synthesis, Biological Evaluation, and Discovery of Potent Antitumor Agents. *J. Am. Chem. Soc.* **2018**, *140* (26), 8303–8320. https://doi.org/10.1021/jacs.8b04634.

(90) US20190084996 Thailanstatin analogs https://patentscope.wipo.int/search/en/detail.jsf?docId=US239436404&recNum=118&docAn=16135287&queryString=FP:(%22Antibody%20drug%20conjugate%22)&maxRec=2831 (accessed Feb 3, 2020).

(91) Synthesis of a C4-epi-C1−C6 Fragment of FR901464 Using a Novel Bromolactolization | Organic Letters https://pubs.acs.org/doi/10.1021/ol049160w (accessed Feb 17, 2020).

(92) Total Synthesis of Thailanstatin A | Journal of the American Chemical Society https://pubs.acs.org/doi/abs/10.1021/jacs.6b04781 (accessed Feb 17, 2020).

(93) Motoyoshi, H.; Horigome, M.; Watanabe, H.; Kitahara, T. Total Synthesis of FR901464: Second Generation. *Tetrahedron* **2006**, *62* (7), 1378–1389. https://doi.org/10.1016/j.tet.2005.11.031.

(94) Horigome, M.; Motoyoshi, H.; Watanabe, H.; Kitahara, T. A Synthesis of FR901464. *Tetrahedron Lett.* **2001**, *42* (46), 8207–8210. https://doi.org/10.1016/S0040-4039(01)01763-4.

(95) Albert, B. J.; Sivaramakrishnan, A.; Naka, T.; Czaicki, N. L.; Koide, K. Total Syntheses, Fragmentation Studies, and Antitumor/Antiproliferative Activities of FR901464 and Its Low Picomolar Analogue. *J. Am. Chem. Soc.* **2007**, *129* (9), 2648–2659. https://doi.org/10.1021/ja067870m.

(96) Total Synthesis of FR901464, an Antitumor Agent that Regulates the Transcription of Oncogenes and Tumor Suppressor Genes | Journal of the American Chemical Society https://pubs.acs.org/doi/10.1021/ja058216u (accessed Feb 17, 2020).

(97) Li, Z.; Tong, R. Catalytic Environmentally Friendly Protocol for Achmatowicz Rearrangement. *J. Org. Chem.* **2016**, *81* (11), 4847–4855. https://doi.org/10.1021/acs.joc.6b00469.

(98) Hoberg, J. O. Synthesis and Chemistry of 4,6-O-Di-(Tert-Butyl)Silanediyl-d-Glucal. *Carbohydr. Res.* **1997**, *300* (4), 365–367. https://doi.org/10.1016/S0008-6215(97)00068-2.

(99) Pazos, G.; Pérez, M.; Gándara, Z.; Gómez, G.; Fall, Y. A New, Enantioselective Synthesis of (+)-Isolaurepan. *Tetrahedron Lett.* **2009**, *50* (37), 5285–5287. https://doi.org/10.1016/j.tetlet.2009.07.041.

(100) Abdel-Magid, A. F.; Carson, K. G.; Harris, B. D.; Maryanoff, C. A.; Shah, R. D. Reductive Amination of Aldehydes and Ketones with Sodium Triacetoxyborohydride. Studies on Direct and Indirect Reductive Amination Procedures1. *J. Org. Chem.* **1996**, *61* (11), 3849–3862. https://doi.org/10.1021/jo960057x.

(101) Marchand, A. P.; Lehr, R. E. *Pericyclic Reactions: Organic Chemistry: A Series of Monographs, Vol. 35.2*; Academic Press, 2013.

(102) Dang, H. T.; Nguyen, V. T.; Nguyen, V. D.; Arman, H. D.; Larionov, O. V. Efficient Synthesis of 3-Sulfolenes from Allylic Alcohols and 1,3-Dienes Enabled by Sodium Metabisulfite as a Sulfur Dioxide Equivalent. *Org. Biomol. Chem.* **2018**, *16* (19), 3605–3609. https://doi.org/10.1039/C8OB00745D.

(103) Fujii, A.; Hashiguchi, S.; Uematsu, N.; Ikariya, T.; Noyori, R. Ruthenium(II)-Catalyzed Asymmetric Transfer Hydrogenation of Ketones Using a Formic Acid−Triethylamine Mixture. *J. Am. Chem. Soc.* **1996**, *118* (10), 2521–2522. https://doi.org/10.1021/ja954126l.

(104) Takeshi Ohkuma, ‡; Noriyuki Utsumi, §; Kunihiko Tsutsumi, §; Kunihiko Murata, §; Christian Sandoval, † and; Ryoji Noyori*, †. The Hydrogenation/Transfer Hydrogenation Network: Asymmetric Hydrogenation of Ketones with Chiral η6-Arene/N-Tosylethylenediamine−Ruthenium(II) Catalysts https://pubs.acs.org/doi/full/10.1021/ja0620989 (accessed Apr 10, 2020). https://doi.org/10.1021/ja0620989.

(105) Dub, P. A.; Gordon, J. C. The Mechanism of Enantioselective Ketone Reduction with Noyori and Noyori–Ikariya Bifunctional Catalysts. *Dalton Trans.* **2016**, *45* (16), 6756–6781. https://doi.org/10.1039/C6DT00476H.

(106) Woodward, S. Decoding the ‘Black Box’ Reactivity That Is Organocuprate Conjugate Addition Chemistry. *Chem. Soc. Rev.* **2000**, *29* (6), 393–401. https://doi.org/10.1039/B002690P.

(107) Human Metabolome Database: Showing metabocard for 2-Acetylfuran (HMDB0033127) http://www.hmdb.ca/metabolites/HMDB0033127 (accessed Feb 19, 2020).

(108) Dang, Q.; Kasibhatla, S. R.; Reddy, K. R.; Jiang, T.; Reddy, M. R.; Potter, S. C.; Fujitaki, J. M.; van Poelje, P. D.; Huang, J.; Lipscomb, W. N.; Erion, M. D. Discovery of Potent and Specific Fructose-1,6-Bisphosphatase Inhibitors and a Series of Orally-Bioavailable Phosphoramidase-Sensitive Prodrugs for the Treatment of Type 2 Diabetes. *J. Am. Chem. Soc.* **2007**, *129* (50), 15491–15502. https://doi.org/10.1021/ja074871l.

(109) Yildizhan, S.; Schulz, S. Easy Access to (E)-β-Ocimene. *Synlett* **2011**, *2011* (19), 2831–2833. https://doi.org/10.1055/s-0031-1289869.

VITA

Joshua Ryan Born was born in Evansville, Indiana on September 30, 1993 to Tim and Brenda Born. After growing up and graduating from Evansville Mater Dei Catholic High School in May 2012, he continued his pursuit of higher education at Purdue University in West Lafayette, Indiana and graduated with an ACS accredited Bachelor of Science in Chemistry in May 2016. While there he studied under the direction of Prof. Mark Lipton working on solid-phase peptide synthesis and methodology. It was during this time that he accumulated his passion for organic synthesis. In August 2016 he joined Professor Arun Ghosh's laboratory where he started his seminal total synthesis work. His PhD work spans the fields of total synthesis, methodology, and medicinal chemistry.

Upon completion of his studies, Josh will be continuing his work as a post-doctoral researcher in Prof. Ghosh's lab, pursuing industrial positions in the pharmaceutical, agricultural, or food science fields.

JOC The Journal of Organic Chemistry Article
Cite This: J. Org. Chem. 2019, 84, 5167−5175 pubs.acs.org/joc

Enantioselective Total Syntheses of (+)-Fendleridine and (+)-Acetylaspidoalbidine

Arun K. Ghosh,* Joshua R. Born, and Luke A. Kassekert

Department of Chemistry and Department of Medicinal Chemistry, Purdue University, 560 Oval Drive, West Lafayette, Indiana 47907, United States

Supporting Information

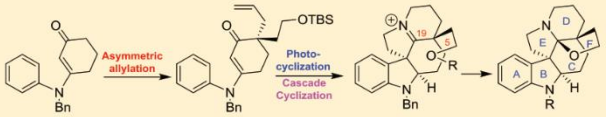

ABSTRACT: Enantioselective syntheses of hexacyclic aspidoalbidine alkaloids (+)-fendleridine (**2**) and (+)-acetylaspidoalbidine (**3**) are described. These syntheses feature an asymmetric decarboxylative allylation and photocyclization of a highly substituted enaminone. Also, the synthesis highlights the formation of a C19-hemiaminal ether via a reduction/condensation/intramolecular cyclization cascade with the C21-alcohol. The present synthesis provides convenient access to the aspidoalbidine hexacyclic alkaloid family in an efficient manner.

INTRODUCTION

The indoline alkaloids constitute a large family of monoterpene natural products that display immense structural diversity.[1,2] The structural core of these natural products is composed of polycyclic fused ring systems with contiguous chiral centers as represented in aspidospermidine (**1**, Figure 1), one of the parent members.[3,4] Several *Aspidosperma* alkaloids exhibit a broad range of intriguing pharmacological activity, including anticancer and antibacterial among many others.[5−7] Over the years, many strategies have been developed for their syntheses in both racemic and enantioselective manner.[1,2,8−10] However, general strategies for the synthesis of the subset aspidoalbidine family of alkaloids received relatively less attention because of further structural complexity. As shown, (+)-fendleridine (**2**), also known as aspidoalbidine, and (+)-1-acetylaspidoalbidine (**3**) contain a unique C19-hemiaminal ether functionality in place of the C19 C−N linkage typical of *aspidosperma* alkaloids.[11,12] Other representative oxidized forms of these natural products include (+)-haplocine (**4**), (+)-haplocidine (**5**), (+)-cimicine (**6**), and (−)-aspidophytine (**7**).[13,14]

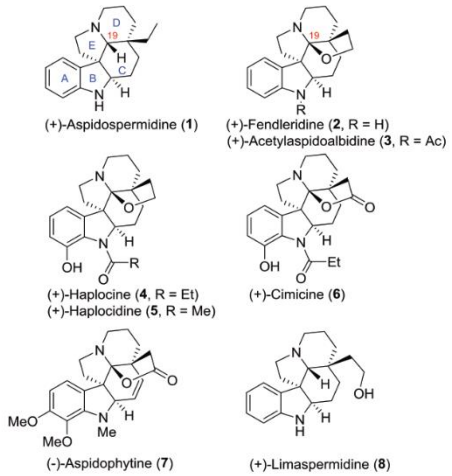

Figure 1. Structures of selected aspidosperma alkaloids.

Fendleridine (**2**) was isolated from the Venezuelan tree *Aspidosperma fendleri* Woodson in 1964.[15] Later, it was also isolated from the Venezuelan tree species *Aspidosperma rhombeosignatum* Markgraph in 1979.[16] The corresponding 1-acetyl derivative, 1-acetylaspidoalbidine, was first isolated from the Peruvian plant *Vallesia dichotoma* Ruiz et Pav in 1963.[17] Fendleridine can be viewed as a biosynthetic product of the cyclization of N-protected derivative of (+)-limaspermidine (**8**). A few syntheses of 1-acetylaspidoalbidine were carried out by the oxidation and cyclization of **8**.[18−20] The first total synthesis of fendleridine (**2**) and 1-acetylaspidoalbidine (**3**) was reported by Ban and co-workers in 1975 and 1976.[19,21] Overman and co-workers in 1991 also reported a formal synthesis of 1-acetylaspidoalbidine (**3**) in racemic form, using the aza-Cope−Mannich reaction as the key transformation.[22]

Received: January 15, 2019
Published: April 2, 2019

DOI: 10.1021/acs.joc.9b00145
J. Org. Chem. 2019, 84, 5167−5175

Subsequently, syntheses of (−)-aspidophytine (**7**) and haplophytine, related members of the aspidoalbine family, were reported.[23,24] Boger and co-workers first reported a total synthesis of (+)-fendleridine (**2**) and (+)-1-acetylaspidoalbidine (**3**) and unambiguously established an absolute configuration of these parent members.[25] They utilized a (4 + 2)/(3 + 2) cycloaddition cascade reaction that constructed the pentacyclic framework.[26] Movassaghi and co-workers recently reported the syntheses of these alkaloids via oxidation of the C19-iminium ion to install the C19-hemiaminal functionality.[27] These two syntheses employed the use of chiral high-performance liquid chromatography (HPLC) and enzymatic resolution, respectively, to separate out the sought after intermediates. In this paper, we report an enantioselective synthesis of (+)-fendleridine (**2**) and (+)-acetylaspidoalbidine (**3**) in 10 and 11 steps, respectively, starting from readily accessible starting materials.

RESULTS AND DISCUSSION

Our retrosynthetic analysis of (+)-fendleridine and (+)-1-acetylaspidoalbidine is shown in Scheme 1. As depicted, an N-

Scheme 1. Retrosynthesis of (+)-fendleridine and (+)-acetylaspidoalbidine

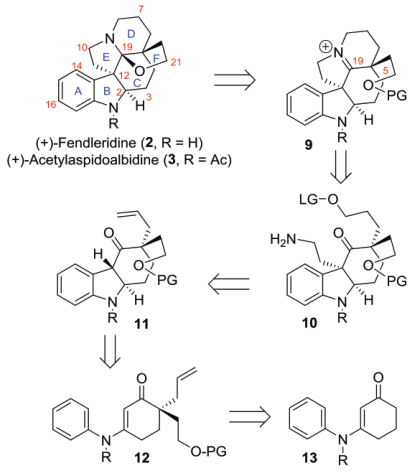

protected fendleridine would be obtained from the iminium ion **9**. We planned to construct the C19-hemiaminal ether functionality with a defined stereochemistry through the formation of a C19 imine from the C19 ketone and a C10 amine followed by intramolecular alkylation at C8 forming the iminium ion structure **9**. Removal of the protecting group on the C21 alcohol would construct the C19-hemiaminal ether functionality. The stereochemistry of the C19 stereocenter will be defined based on the stereochemistry of the C12-ethylamine and the C5 alkoxyethyl group on structure **10**. The elaboration of the C12 aminoethyl functionality can be achieved by alkylation of the hexahydrocarbazol-4-one **11**. The alkylation reaction with an appropriate electrophile will presumably ensure the desired cis-stereochemistry depicted on the substituted cyclohexanone derivative **10**. We plan to construct the hexahydrocarbozolone **11** by a photocyclization of an optically active enaminone **12** (R = Bn). Such photocyclization would provide a mixture of diastereomers at the C2 and C12 carbons. Our plan for photocyclization is motivated by previous work by Gramain and co-workers who have demonstrated photocyclization of related aryl enaminones to form hexahydrocarbazolones with trans-ring junction stereochemistry.[28] The synthesis of enaminone **12** in an optically active form can be achieved conveniently by using an enantioselective Stoltz decarboxylative allylation reaction.[29] Enaminone **13** (R = Bn) can be prepared on a multigram scale from readily available starting materials, *N*-benzylaniline and 1,3-cyclohexanedione.

As shown in Scheme 2, our synthesis commenced with the formation of a multigram quantity of enaminone **13** by

Scheme 2. Enantioselective Synthesis of Enaminone 17

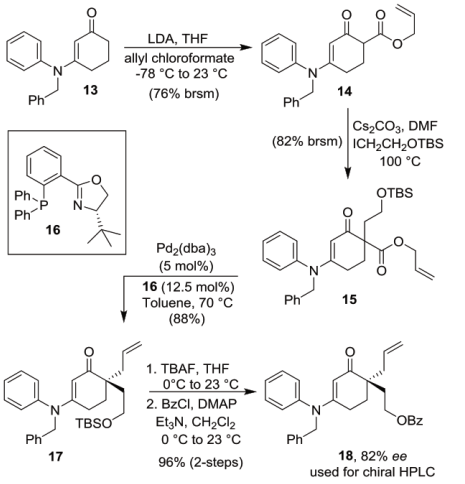

condensation of *N*-benzylaniline and 1,3-cyclohexanedione in toluene in the presence of *p*-TSA·H_2O at reflux for 40 h. Subsequently, enaminone **13** was alkylated with LDA and allylchloroformate at −78 to 23 °C for 18 h to afford *β*-keto ester **14** in 62% yield. Alkylation of the *β*-keto ester **14** with *tert*-butyl(2-iodoethoxy)dimethylsilane was carried out in dimethylformamide (DMF) in the presence of Cs_2CO_3 at 100 °C for 32 h to furnish a racemic keto ester **15** in 70% yield.[30] For catalytic asymmetric allylation, we planned to utilize $Pd_2(dba)_3$ in combination with (*S*)-*t*-Bu-Phox ligand as the prior work by Stoltz and co-workers already established that (*S*)-*t*-Bu-Phox provides the best enantioselectivity for allylation of enaminones.[31] Therefore, we investigated enantioselective allylation in a number of solvents by exposure of enaminone **15** to $Pd_2(dba)_3$ (5 mol %) and (*S*)-*t*-Bu-Phox ligand (12.5 mol %) at 23 °C followed by heating the reaction mixture to a specified temperature. As shown in Table 1, the initial attempts to use toluene without deoxygenation resulted in only a trace amount of the desired allylated product, with a largely recovered starting material and a dealkylated by-product.[32] Subsequently, we deoxygenated all solvents by bubbling with argon for at least an hour prior to use. The reaction in methyl *tert*-butyl ether was carried out at lower

DOI: 10.1021/acs.joc.9b00145
J. Org. Chem. 2019, 84, 5167−5175

Table 1. Asymmetric Allylation of Enaminone 15

solvent	temperature (°C)	duration	percent yield of **17**	% ee of **18**
toluene[a]	70	12 h	trace	N/A
MTBE	40	12 h	trace	N/A
THF	70	30 min	97%	77%
benzene	70	30 min	98%	81%
toluene[b]	70	30 min	88%	82%

[a]Solvent not degassed. [b]Reaction carried out on a multigram scale.

temperature because of the volatility of the solvent. This condition resulted in a trace amount of allylated product **17**. The reactions in tetrahydrofuran (THF) and benzene at 70 °C however resulted in excellent yields of the allylated product **17**. To determine enantiomeric purity, compound **17** was converted to the benzoate derivative **18**. The HPLC analysis of **18** using a CHIRALCEL OD-H column showed that enantioselectivity of **17** was 77 and 81% ee, respectively (see the Supporting Information for further details). Freshly deoxygenated toluene was tested last and found to furnish the optically active enaminone **17** in 88% yield and 82% ee. We utilized this condition to prepare optically active enaminone **17** on a multigram scale.

The synthesis of the hexahydrocarbazolone ring system is shown in Scheme 3. Our initial attempt to photocyclize **17** in

Scheme 3. Synthesis of Diastereomeric Alcohols 24 and 25

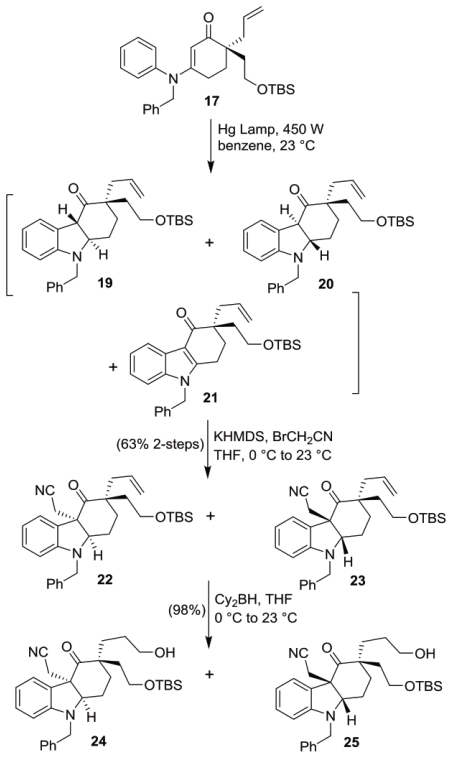

benzene with a mercury lamp (450 W) provided an inseparable mixture (1:1) of *trans*-diastereomic indoline derivatives **19** and **20** along with the corresponding oxidized indole byproduct **21**. Gramain and co-workers reported such a photocyclization on an unsubstituted enaminone to provide a hexahydrocarbazolone and the corresponding oxidized indole product.[28] We attempted optimization of the photocyclization to inhibit the formation of indole byproduct **21**. It turns out that careful degassing of the apparatus with benzene as the solvent and shorter reaction times afforded indolines **19** and **20** as the major products and only a trace amount of indole byproduct **21**. It is important to note that the photochemical *trans*-indoline products are quite prone to oxidation to the indole byproduct **21**. Mechanistic insights into this photocyclization reaction were recently reported by Bach and co-workers.[33] For our synthesis, we utilized the crude mixture of diastereomers for the next alkylation reaction immediately. The crude photocyclization product mixture was treated with KHMDS in THF at 23 °C, cooled to 0 °C, and then stirred under the same temperature for 10 min. Bromoacetonitrile was added and the reaction was stirred for 40 min at 0 °C. This provided inseparable *cis*-diastereomeric products **22** and **23** in 63% yield in two steps.[28b]

Hydroboration of the mixture of nitrile derivatives with in situ formed Cy_2BH in freshly distilled THF at 0−23 °C for 2.5 h followed by oxidation with $NaBO_3{\cdot}4H_2O$ afforded a 1:1 mixture of alcohols in 98% combined yield.[34] The mixture was separated by silica gel chromatography to provide alcohols **24** and **25** as pure separable compounds. The stereochemical identity of **24** and **25** was primarily determined using extensive ^{1}H NMR NOESY experiments (see the Supporting Information for details).

To further ascertain the stereochemical identity of alcohols **24** and **25**, our plan was to convert them to the respective spiroketal derivative, thus creating a more rigid conformation for two-dimensional (2D) nuclear magnetic resonance (NMR) analysis. As shown in Scheme 4, alcohols **24** and **25** were converted to the corresponding tosylate derivatives **26** and **27** in 79 and 85% yields, respectively. The TBS group of tosylate **26** was then removed by exposure to TBAF in THF at 23 °C for 7.5 h. This resulted in the formation of a spiroketal derivative **28** in the near-quantitative yield. Similarly, we have converted **27** to a spiroketal derivative **29** in excellent yields. The stereochemical assignment of the diastereomeric spiroketals **28** and **29** was carried out by extensive 2D NMR studies. The results are summarized in Figure 2. The observed specific NOESY interactions between H_a−H_b and H_a−H_c for spiroketal **28** are consistent with the depicted chemistry. Similarly, the observed NOESY interactions between H_a−H_d and H_a−H_e support the assigned stereochemistry of spiroketal **29** (see the Supporting Information for more details). On the basis of these stereochemical assignments of spiroketal structures **28** and **29**, we then speculated that if the assigned stereochemistry of tosylate **27** is correct, our planned formation of iminium ion **9** (R = Bn, PG = TBS) may not be feasible upon reduction of nitrile to amine from **27**. Reduction of nitrile **27** was carried out by exposure to Ra−Ni 2800 in methanol under 60 psi hydrogen in a parr apparatus at 23 °C for 21 h. These conditions resulted in the formation of the corresponding ethyl amine, which concomitantly cyclized to imine **30**. This further corroborated our assignment of stereochemical identity.

DOI: 10.1021/acs.joc.9b00145
J. Org. Chem. 2019, 84, 5167−5175

Scheme 4. Stereochemical Studies of Ketal Products 28 and 29

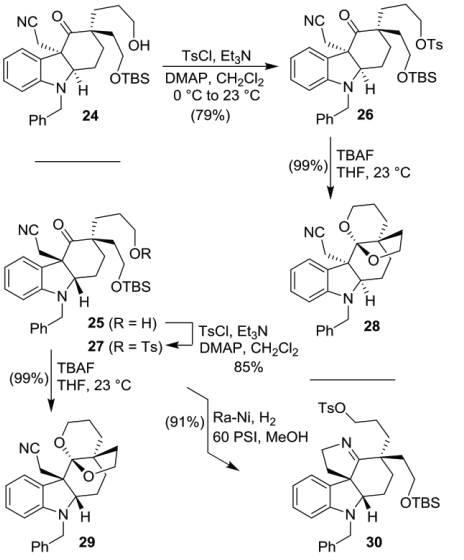

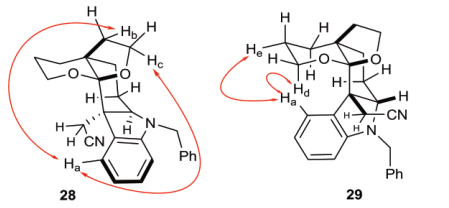

Figure 2. Representative NOESY correlation of compounds **28** and **29**.

Scheme 5. Synthesis of (+)-Fendleridine and (+)-1-Acetylaspidoalbidine

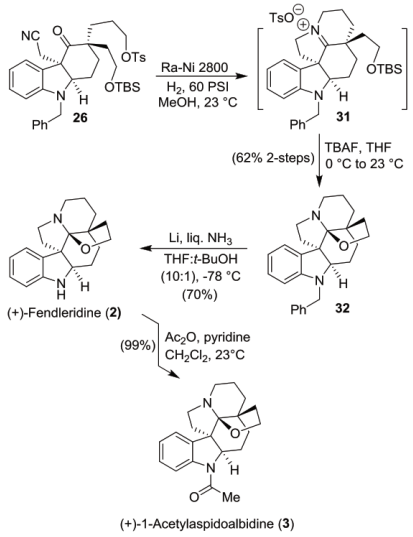

Tosyl derivative **26** was readily converted to (+)-fendleridine **2** as shown in Scheme 5. Tosylate **26** was subjected to Ra−Ni 2800 under hydrogen at 60 psi to afford a highly polar iminium salt **31**. Treatment of the crude salt **31** with TBAF at 0−23 °C for 13.5 h removed the silyl group and concomitantly formed the C19-hemiaminal ether. Purification over basic alumina provided benzyl derivative **32** in 62% yield over two steps. The *N*-benzyl group was successfully deprotected using lithium in liquid NH_3 at −78 °C for 1.5 h to furnish synthetic (+)-fendleridine **2** in 70% yield after purification by alumina using 5% ethyl acetate in hexanes as the eluent. The ^{1}H NMR and ^{13}C NMR spectra of synthetic (+)-fendleridine **2** {$[\alpha]_D^{20}$ +53.7 (*c* 0.2, $CHCl_3$)} are in complete agreement with the reported[25,27] spectra for synthetic and natural (+)-fendleridine. We have also converted (+)-fendleridine **2** to its acetyl derivative by acetylation with acetic anhydride and pyridine in CH_2Cl_2 at 23 °C for 1 h to provide synthetic (+)-1-acetyl-aspidoalbidine **3** {$[\alpha]_D^{20}$ +30.2 (*c* 0.15, $CHCl_3$)} in quantitative yield after purification over alumina column. The ^{1}H NMR and ^{13}C NMR spectra of synthetic (+)-1-acetyl-aspidoalbidine **3** are in complete agreement with the reported[25,27] spectra with rotational isomers.

■ CONCLUSIONS

In summary, we have developed a short and enantioselective total syntheses of (+)-fendleridine and (+)-1-acetylaspidoalbidine. The syntheses of (+)-fendleridine and (+)-1-acetylaspidoalbidine were achieved in 10 and 11 steps, respectively, from readily available starting materials. The synthesis highlights the construction of the highly substituted hexahydrocarbazolone ring system by a photochemical reaction. The synthesis also utilizes the enantioselective formation of an enaminone containing a quaternary carbon center by Stoltz decarboxylative allylation processes. The chirality on the enaminone ensures the formation of the unique C19-hemiaminal ether functionality inherent to the aspidoalbine family of alkaloids. The Ra−Ni-catalyzed reduction of nitrile and subsequent cascade cyclization to iminium salt lead to the formation of C19-hemiaminal ether very efficiently. Further application of photocyclization and synthesis of pharmacologically important indoline alkaloids are underway.

■ EXPERIMENTAL SECTION

General Procedural/Analytical Methods. All reactions were performed in oven-dried round-bottom flasks followed by flame-drying in the case of moisture-sensitive reactions. The flasks were fitted with rubber septa and kept under a positive pressure of argon. Cannula were used in the transfer of moisture-sensitive liquids. Heated reactions were allowed to run using an oil bath on a hot plate equipped with a temperature probe. Hydrogenations were carried out using a Parr shaking apparatus inside a thick-walled nonreactant borosilicate glass vessel. Photochemical transformations were done using a Hanovia 450 W Hg lamp. TLC analysis was conducted using glass-backed thin-layer silica gel chromatography plates (60 Å, 250 μm thickness, F-254 indicator) or with glass-backed thin-layer alumina N chromatography plates (250 μm thickness, UV 254).

DOI: 10.1021/acs.joc.9b00145
J. Org. Chem. 2019, 84, 5167−5175

Flash chromatography was done using a 230−400 mesh, a 60 Å pore diameter silica gel, or a with 80−200 mesh alumina. Organic solutions were concentrated at 30−35 °C on rotary evaporators capable of achieving a minimum pressure of ∼30 Torr and further concentrated on a Hi-vacuum pump capable of achieving a minimum pressure of ∼4 Torr. ^{1}H NMR spectra were recorded on 400, 500, and 800 MHz spectrometers. ^{13}C NMR spectra were recorded at 100, 125, and 200 MHz on the respective NMRs. Chemical shifts are reported in parts per million and referenced to the deuterated residual solvent peak ($CDCl_3$, 7.26 ppm for ^{1}H and 77.16 ppm for ^{13}C). NMR data are reported as δ value (chemical shift), J-value (Hz), and integration, where s = singlet, bs = broad singlet, d = doublet, t = triplet, q = quartet, p = quintet, m = multiplet, dd = doublet doublets, and so on. Optical rotations were recorded on a digital polarimeter. Low-resolution mass spectra (LRMS) spectra were recorded using a quadrupole LCMS under positive electrospray ionization (ESI+). High-resolution mass spectrometry (HRMS) spectra were recorded at the Purdue University Department of Chemistry Mass Spectrometry Center. These experiments were performed under ESI+ and positive atmospheric pressure chemical ionization (APCI+) conditions using an Orbitrap XL Instrument.

*3-(Benzyl(phenyl)amino)cyclohex-2-en-1-one (**13**).*[28c,35] To a 500 mL one-neck round-bottom flask equipped with a stir bar, 1,3-dicyclohexadiene (15 g, 133.8 mmol, 1.0 equiv), *N*-benzylaniline (26.97 g, 147.2 mmol, 1.1 equiv), and *p*-toluenesulfonic acid monohydrate (4.07 g, 21.4 mmol, 0.16 equiv) were added sequentially. A Dean−Stark apparatus with a reflux condenser was then attached and the entire vessel was evacuated and flushed with argon several times. Toluene (267 mL) was added, and the reaction was heated at 160 °C for 40 h. After this period, the reaction was cooled, diluted with EtOAc, washed with 1 M NaOH, brine, dried over Na_2SO_4, and concentrated. The crude mixture was purified via column chromatography over silica gel using 100% EtOAc as the eluent. Enaminone **13** was obtained as brown oil (34.57 g, 93%) TLC: silica gel (100% EtOAc), R_f = 0.31. ^{1}H NMR (400 MHz, $CDCl_3$): δ 7.36−7.15 (m, 8H), 7.11 (d, J = 7.1 Hz, 2H), 5.36 (s, 1H), 4.80 (s, 2H), 2.28 (dd, J = 14.2, 6.4 Hz, 4H), 1.88 (p, J = 6.4 Hz, 2H); ^{13}C{^{1}H} NMR (101 MHz, $CDCl_3$): δ 197.6, 164.9, 144.4, 136.3, 129.6, 128.6, 127.7, 127.5, 127.4, 126.8, 101.6, 56.6, 36.1, 28.6, 22.5; LRMS-ESI (+) m/z: 278.1 $[M + H]^+$.

*Allyl 4-(Benzyl(phenyl)amino)-2-oxocyclohex-3-ene-1-carboxylate ((±)-**14**).* To a flame-dried 1 L round-bottom flask under argon, diisopropylamine (34.1 mL, 243 mmol, 2.5 equiv) in freshly distilled THF (144 mL) was added. To this solution at 0 °C, *n*-BuLi (1.6 M in hexanes, 152 mL, 243 mmol, 2.5 equiv) was added and the reaction was stirred for 50 min. In a separate flame-dried 1 L flask, enaminone **13** (27 g, 97.2 mmol, 1 equiv) was dissolved in THF (125 mL) and the solution was cannulated to the yellow solution with the above LDA at −78 °C. The resulting mixture was stirred at −78 °C for 1 h and then allyl chloroformate (13.4 mL, 126.4 mmol, 1.3 equiv) was added dropwise. The resulting reaction was allowed to warm slowly to 23 °C for 12 h. The reaction was quenched with saturated NH_4Cl (250 mL), extracted with EtOAc (3×), washed with brine, dried over Na_2SO_4, and concentrated. The crude mixture was purified via column chromatography over silica gel to provide the product as a viscous dark red oil (21.8 g, 62% yield) and an unreacted starting material (4.9 g) was recovered (76% yield, brsm). TLC: silica gel (50% EtOAc/hexanes), R_f = 0.34. ^{1}H NMR (400 MHz, $CDCl_3$): δ 7.37−7.20 (m, 6H), 7.17 (d, J = 7.0 Hz, 2H), 7.11 (d, J = 7.0 Hz, 2H), 5.90 (ddt, J = 17.2, 10.5, 5.6 Hz, 1H), 5.39 (s, 1H), 5.31 (dq, J = 17.2, 1.5 Hz, 1H), 5.19 (dq, J = 10.4, 1.2 Hz, 1H), 4.82 (s, 2H), 4.69−4.58 (m, 2H), 3.32 (dd, J = 8.7, 5.0 Hz, 1H), 2.57−2.46 (m, 1H), 2.36−2.23 (m, 2H), 2.17−2.06 (m, 1H); ^{13}C{^{1}H} NMR (101 MHz, $CDCl_3$): δ 191.0, 170.7, 164.6, 144.0, 136.0, 132.0, 129.7, 128.7, 127.8, 127.7, 127.5, 126.9, 118.1, 100.5, 65.5, 56.7, 51.5, 26.6, 25.2; HRMS-ESI (+) m/z: calcd for $C_{23}H_{23}NO_3$ $[M + H]^+$, 362.1751; found, 362.1755.

*Allyl 4-(Benzyl(phenyl)amino)-1-(2-((tert-butyldimethylsilyl)oxy)-ethyl)-2-oxocyclohex-3-ene-1-carboxylate ((±)-**15**).* To a flame-dried 1 L round-bottom flask under argon equipped with a stir bar and a reflux condenser, racemic **14** (21.8 g, 60.2 mmol, 1 equiv) in DMF (500 mL) was added. To this solution, *tert*-butyl(2-iodoethoxy)dimethylsilane (33.4 mL, 150.4 mmol, 2.5 equiv) followed by Cs_2CO_3 (39.2 g, 120.4 mmol, 2.0 equiv) was added. The resulting reaction was heated in an oil bath to 100 °C for 32 h. After this period, the reaction was quenched with H_2O and brine (100 mL each). The resulting mixture was extracted with CH_2Cl_2 and washed with 5% aqueous LiCl solution. The crude mixture was concentrated and purified via column chromatography over silica gel using 25−55% EtOAc/hexanes as the eluent to yield allyl carbonate **15** (21.9 g, 70.1% yield) as an orange amorphous solid. An unreacted starting material was recovered (3.2 g, 82% yield, brsm). TLC: silica gel (25% EtOAc/hexanes), R_f = 0.2. ^{1}H NMR (400 MHz, $CDCl_3$): δ 7.38−7.27 (m, 5H), 7.25 (d, J = 7.0 Hz, 1H), 7.18 (d, J = 6.7 Hz, 2H), 7.10 (d, J = 6.8 Hz, 2H), 5.89 (ddt, J = 17.2, 10.7, 5.5 Hz, 1H), 5.36 (s, 1H), 5.29 (dq, J = 16.8, 1.4 Hz, 1H), 5.19 (dq, J = 10.5, 1.4 Hz, 1H), 4.81 (s, 2H), 4.61 (dtdd, J = 14.9, 13.4, 5.0, 1.5 Hz, 2H), 3.72 (t, J = 6.6 Hz, 2H), 2.60−2.26 (m, 4H), 1.98 (dq, J = 14.0, 7.4, 6.6 Hz, 2H), 0.85 (s, 9H), 0.02 (d, J = 2.7 Hz, 6H); ^{13}C{^{1}H} NMR (101 MHz, $CDCl_3$): δ 193.5, 172.2, 163.9, 144.2, 136.3, 132.2, 129.8, 128.8, 127.9, 127.8, 127.6, 127.0, 118.0, 100.3, 65.5, 60.2, 56.7, 54.4, 36.5, 29.6, 26.0, 25.9, 18.3, −5.3; HRMS-ESI (+) m/z: calcd for $C_{31}H_{42}NO_4Si$ $[M + H]^+$, 520.2878; found, 520.2874.

*(S)-6-Allyl-3-(benzyl(phenyl)amino)-6-(2-((tert-butyldimethylsilyl)oxy)ethyl)cyclohex-2-en-1-one (**17**).* To a flame-dried round-bottom flask under argon equipped with a stir bar and a reflux condenser, (*S*)-*t*Bu-Phox (429.6 mg, 1.11 mmol, 12.5 mol %) and $Pd_2(dba)_3$ (406 mg, 0.44 mmol, 5 mol %) were added. Deoxygenated toluene (61 mL) was added and the resulting mixture was stirred at 23 °C for 30 min. A solution of allyl carbonate **15** (4.61 g, 8.87 mmol, 1 equiv) in toluene (61 mL) was then slowly cannulated to the orange solution containing the catalyst at 23 °C. The resulting reaction mixture was heated to 70 °C for 35 min. After this period, the orange reaction mixture was cooled and then filtered over Celite. The filter cake was washed with CH_2Cl_2. The solvent was concentrated, and the residue was purified via column chromatography over silica gel using 15−20% EtOAc/hexanes as the eluent to provide the allylated product **17** (3.69 g, 88% yield) as viscous brown oil. TLC: silica gel (15% EtOAc/hexanes), R_f = 0.16. $[\alpha]_D^{20}$ −2.9 (*c* 0.068, $CHCl_3$); ^{1}H NMR (500 MHz, $CDCl_3$): δ 7.37−7.27 (m, 5H), 7.24 (m, 1H), 7.19 (d, J = 7.2 Hz, 2H), 7.12 (d, J = 7.1 Hz, 2H), 5.82−5.70 (m, 1H), 5.29 (s, 1H), 5.04 (s, 1H), 5.02 (d, J = 4.3 Hz, 1H), 4.82 (s, 2H), 3.72 (ddd, J = 10.1, 8.5, 6.2 Hz, 1H), 3.63 (ddd, J = 10.3, 8.7, 5.7 Hz, 1H), 2.42 (m, 2H), 2.30 (dt, J = 17.5, 5.7 Hz, 1H), 2.21 (dd, J = 13.9, 8.0 Hz, 1H), 1.87−1.78 (m, 3H), 1.75−1.69 (m, 1H), 0.87 (s, 9H), 0.03 (s, 6H); ^{13}C{^{1}H} NMR (126 MHz, $CDCl_3$): δ 200.5, 163.2, 144.5, 136.7, 135.2, 129.8, 128.8, 128.0, 127.59, 127.55, 127.1, 117.6, 100.9, 59.9, 56.7, 44.5, 40.3, 37.9, 31.0, 26.1, 25.5, 18.4, −5.1, −5.2; HRMS-ESI (+) m/z: calcd for $C_{30}H_{42}NO_2Si$ $[M + H]^+$, 476.2979; found, 476.2969.

*(S)-2-(1-Allyl-4-(benzyl(phenyl)amino)-2-oxocyclohex-3-en-1-yl)-ethyl Benzoate (**18**).* To a flame-dried round-bottom flask under argon equipped with a stir bar, allyl derivative **17** (21 mg, 0.04 mmol, 1.0 equiv) was added in freshly distilled THF (0.5 mL, 0.1 M). To this solution, TBAF (1.0 M in THF, 46 μL, 0.05 mmol, 1.05 equiv) was added dropwise at 0 °C and the resulting mixture was stirred at 0−23 °C for 12 h. The reaction was then quenched with H_2O and brine (∼0.5 mL each), extracted with EtOAc (3×), washed with brine, dried over Na_2SO_4, and concentrated. The crude mixture was purified via silica gel column chromatography, using 65% EtOAc/hexanes as the eluent to provide the corresponding alcohol as an amorphous solid (16 mg, 100% yield). TLC: silica (65% EtOAc/hexanes), R_f = 0.50 (UV and PMA). ^{1}H NMR (400 MHz, $CDCl_3$): δ 7.40−7.19 (m, 6H), 7.19 (m, 2H), 7.13 (m, 2H), 5.72 (m, 1H), 5.34 (s, 1H), 5.09 (m, 1H), 5.06 (m, 1H), 4.84 (s, 2H), 3.86 (br s, 1H), 3.81 (ddd, J = 12.1, 8.2, 4.4 Hz, 1H), 3.64 (dt, J = 10.7, 4.9 Hz, 1H), 2.46−2.29 (m, 4H), 1.84−1.67 (m, 4H). ^{13}C{^{1}H} NMR (101 MHz, $CDCl_3$): δ 202.6, 164.4, 144.2, 136.3, 134.2, 129.9, 128.9, 127.9 (2C), 127.7, 127.1, 118.4, 100.5, 58.9, 56.9, 45.0, 38.9, 37.9, 32.0, 25.4. LRMS-ESI (+) m/z: 362.1$[M + H]^+$.

DOI: 10.1021/acs.joc.9b00145
J. Org. Chem. 2019, 84, 5167−5175

To a flame-dried round-bottom flask under argon, equipped with a stir bar, the above alcohol (15 mg, 41 μmol, 1.0 equiv) was added in CH_2Cl_2 (0.5 mL). To this solution at 0 °C, DMAP (1.0 mg, 8 μmol, 0.2 equiv), triethylamine (8.4 mg, 12 μL, 0.08 mmol, 2.0 equiv), and benzoyl chloride (7 mg, 6 μL, 0.05 mmol, 1.2 equiv) were added. The resulting reaction mixture was stirred at 0−23 °C for 2.5 h. The reaction was then quenched with H_2O and brine (~0.5 mL each), extracted with CH_2Cl_2 (3×), washed with brine, dried over Na_2SO_4, and concentrated. The crude mixture was purified via column chromatography over silica gel to provide benzoate **18** (18.5 mg, 96% yield) as an oil. TLC: silica (30% EtOAc/hexanes), R_f = 0.32 (UV and PMA); ^{1}H NMR (400 MHz, $CDCl_3$): δ 8.01 (d, *J* = 7.1 Hz, 2H), 7.54 (t, *J* = 7.4 Hz, 1H), 7.41 (t, *J* = 7.7 Hz, 2H), 7.35 (t, *J* = 7.5 Hz, 2H), 7.31−7.22 (m, 4H), 7.18 (d, *J* = 6.8 Hz, 2H), 7.12 (d, *J* = 7.6 Hz, 2H), 5.85−5.75 (m, 1H), 5.34 (s, 1H), 5.09 (s, 1H), 5.06 (d, *J* = 4.4 Hz, 1H), 4.81 (s, 2H), 4.44−4.34 (m, 2H), 2.48−2.28 (m, 4H), 2.23−2.16 (m, 1H), 1.93−1.85 (m, 3H). $^{13}C\{^1H\}$ NMR (101 MHz, $CDCl_3$): δ 199.78, 166.71, 163.20, 144.34, 136.49, 134.45, 132.92, 130.51, 129.82, 129.69, 128.86, 128.44, 127.97, 127.70, 127.60, 127.02, 118.25, 100.73, 62.13, 56.71, 44.42, 40.41, 33.79, 30.44, 25.32. LRMS-ESI (+) *m*/*z*: 466.2 $[M + H]^+$.

*2-((3S)-3-Allyl-9-benzyl-3-(2-((tert-butyldimethylsilyl)oxy)ethyl)-4-oxo-1,2,3,4,9,9a-hexahydro-4aH-carbazol-4a-yl)acetonitrile (**22** and **23**).* To a flame-dried round-bottom flask under argon fitted with a reflux condenser and a stir bar, allylated **17** (1.55 g, 3.26 mmol, 1.0 equiv) was added. Deoxygenated benzene (163 mL) was added and the resulting mixture was flushed under argon multiple times. Photocyclization reaction then was carried out with a 450 W Hg lamp for 1.5 h. After this period, the reaction was concentrated under reduced pressure in the dark. The resulting crude product was immediately subjected to the next step.

To the above mixture, freshly distilled THF (21.7 mL) and KHMDS (0.7 M in toluene, 5.12 mL, 3.58 mmol, 1.1 equiv) were added sequentially at 23 °C (the solution went from orange gold to dark brown). The reaction was cooled to 0 °C, and after 10 min, $BrCH_2CN$ (238 μL, 3.42 mmol, 1.05 equiv) was added dropwise. The resulting mixture was stirred for 40 min at 0 °C. After this period, the reaction was quenched with saturated NH_4Cl (15 mL). The reaction was extracted with EtOAc (3×), and the combined extracts were washed with brine, dried with Na_2SO_4, and concentrated. The crude mixture was purified via column chromatography over silica gel using 5% EtOAc/hexanes as the eluent to provide **22** and **23** as an inseparable mixture as an oil (1.05 g, 63% over two steps). TLC: silica gel (15% EtOAc/hexanes), R_f = 0.44. ^{1}H NMR (500 MHz, $CDCl_3$): δ 7.40−7.28 (m, 5H), 7.13 (t, *J* = 7.0 Hz, 1H), 6.93 (d, *J* = 7.6 Hz, 1H), 6.66 (t, *J* = 8.7 Hz, 1H), 6.49 (d, *J* = 7.9 Hz, 1H), 5.76 (m, 0.5H), 5.54 (m, 0.5H), 5.08 (m, 1H), 5.00 (d, *J* = 10.1 Hz, 0.5H), 4.87 (d, *J* = 17.0 Hz, 0.5H), 4.53 (d, *J* = 12.4 Hz, 1H), 4.32 (d, *J* = 12.4 Hz, 1H), 3.95 (m, 1H), 3.68 (t, *J* = 7.1 Hz, 1H), 3.50−3.45 (m, 0.5H), 3.42−3.38 (m, 0.5H) 3.07 (d, *J* = 10.4 Hz, 1H), 2.59−2.52 (m, 1.5H), 2.28 (dd, *J* = 11.1, 6.38, Hz, 0.5H), 2.09−2.05 (m, 0.5H), 2.02−1.96 (m, 1H), 1.91−1.45 (m, 5.5H), 0.89 (s, 5H), 0.83 (s, 4H), 0.06 (d, *J* = 4.1 Hz, 3H), −0.04 (d, *J* = 9.4 Hz, 3H). $^{13}C\{^1H\}$ NMR (126 MHz, $CDCl_3$): δ 210.9, 210.5, 150.1, 149.9, 137.7, 137.7, 133.9, 132.6, 130.5, 130.4, 128.9, 127.7, 127.5, 127.03, 126.97, 124.0, 123.8, 118.9, 118.8, 118.5, 118.3, 117.69, 117.67, 107.7, 68.99, 68.97, 59.6, 59.0, 58.2, 57.9, 49.7, 49.6, 49.5, 43.2, 41.0, 40.3, 39.3, 31.7, 27.2, 26.7, 26.6, 26.1, 26.0, 25.4, 22.8, 22.3, 22.2, 18.4, 18.3, 14.2, −5.2, −5.3; HRMS-ESI (+) *m*/*z*: calcd for $C_{32}H_{43}N_2O_2Si$ $[M + H]^+$, 515.3088; found, 515.3095.

*2-((3S)-9-Benzyl-3-(2-((tert-butyldimethylsilyl)oxy)ethyl)-3-(3-hydroxypropyl)-4-oxo-1,2,3,4,9,9a-hexahydro-4aH-carbazol-4a-yl)-acetonitrile (**24** and **25**).* To a flame-dried round-bottom flask under argon equipped with a stir bar, cyclohexene (1.4 mL, 13.9 mmol, 6.5 equiv) was added to freshly distilled THF (6 mL) at 0 °C. To this solution at 0 °C, a borane dimethyl sulfide complex (neat, 607 μL, 6.4 mmol, 3.0 equiv) was added dropwise. A thick white slurry started to form after 1 min. Additional amounts of THF (1 mL) was added and the reaction was continuously stirred at 0 °C for 1 h. After this period, a solution of **22** and **23** (1.10 g, 2.1 mmol, 1.0 equiv) was cannulated in THF (5 mL) at 0 °C and the resulting reaction was warmed slowly to 23 °C for 2.5 h. The reaction was quenched with slow addition of $NaBO_3{\cdot}4H_2O$ (3.3 g, 21.3 mmol, 10 equiv) and H_2O (7 mL, 0.3 M), and the resulting reaction mixture was continuously stirred for 12 h. The reaction was diluted in brine, extracted with EtOAc (3×), dried with Na_2SO_4, and concentrated. The crude mixture was purified via column chromatography over silica gel using 40% EtOAc/hexanes as the eluent to provide alcohol diastereomers **24** and **25** (1.12 g, 98% combined yield), which were separated. TLC: silica gel (40% EtOAc/hexanes), R_f = 0.52 and 0.38 (lower spot desired diastereomer).

*2-((3S,4aS,9aS)-9-Benzyl-3-(2-((tert-butyldimethylsilyl)oxy)-ethyl)-3-(3-hydroxypropyl)-4-oxo-1,2,3,4,9,9a-hexahydro-4aH-carbazol-4a-yl)acetonitrile (**25**).* ^{1}H NMR (500 MHz, $CDCl_3$): δ 7.39−7.28 (m, 5H), 7.12 (td, *J* = 7.7, 1.3 Hz, 1H), 6.90 (dd, *J* = 7.5, 1.2 Hz, 1H), 6.64 (td, *J* = 7.5, 1.0 Hz, 1H), 6.49 (d, *J* = 7.8 Hz, 1H), 4.53 (d, *J* = 15.5 Hz, 1H), 4.31 (d, *J* = 15.5 Hz, 1H), 3.95 (dd, *J* = 7.1, 4.3 Hz, 1H), 3.65 (m, 2H), 3.35 (m, 2H), 3.04 (d, *J* = 16.4 Hz, 1H), 2.56 (d, *J* = 16.4 Hz, 1H), 2.04 (m, 1H), 1.88−1.65 (m, 5H), 1.44−1.35 (m, 1H), 1.34−1.29 (m, 2H), 1.25 (m, 1H), 0.88 (s, 9H), 0.05 (d, *J* = 3.9 Hz, 6H); $^{13}C\{^1H\}$ NMR (126 MHz, $CDCl_3$): δ 210.6, 150.0, 137.6, 130.6, 129.0, 127.8, 127.6, 127.1, 123.6, 118.1, 117.8, 107.9, 69.1, 62.9, 59.6, 58.0, 49.6, 49.4, 38.7, 35.0, 28.4, 26.9, 26.7, 26.1, 22.5, 18.4, −5.2; LRMS-ESI (+) *m*/*z*: 533.3 $[M + H]^+$.

*2-((3S,4aR,9aR)-9-Benzyl-3-(2-((tert-butyldimethylsilyl)oxy)-ethyl)-3-(3-hydroxypropyl)-4-oxo-1,2,3,4,9,9a-hexahydro-4aH-carbazol-4a-yl)acetonitrile (**24**).* $[\alpha]_D^{20}$ −144 (*c* 0.08, $CHCl_3$); ^{1}H NMR (500 MHz, $CDCl_3$): δ 7.39−7.28 (m, 5H), 7.12 (td, *J* = 7.7, 1.3 Hz, 1H), 6.91 (dd, *J* = 7.5, 1.2 Hz, 1H), 6.66 (td, *J* = 7.5, 0.9 Hz, 1H), 6.48 (d, *J* = 7.9 Hz, 1H), 4.52 (d, *J* = 15.4 Hz, 1H), 4.30 (d, *J* = 15.4 Hz, 1H), 3.93 (m, 1H), 3.62 (m, 2H), 3.47 (m, 1H), 3.39 (m, 1H), 3.08 (d, *J* = 16.3 Hz, 1H), 2.52 (d, *J* = 16.3 Hz, 1H), 1.87−1.76 (m, 4H), 1.69−1.59 (m, 3H), 1.55 (m, 1H), 1.51−1.40 (m, 2H), 0.81 (s, 9H), −0.06 (d, *J* = 9.4 Hz, 6H); $^{13}C\{^1H\}$ NMR (126 MHz, $CDCl_3$): δ 211.4, 149.8, 137.7, 130.4, 129.0, 127.8, 127.5, 127.3, 123.8, 118.6, 117.9, 107.9, 69.0, 63.3, 59.0, 58.1, 49.6, 49.4, 40.3, 32.5, 27.6, 27.3, 26.6, 26.0, 22.1, 18.3, −5.3; HRMS-ESI (+) *m*/*z*: calcd for $C_{32}H_{44}N_2O_3SiNa$ $[M + Na]^+$, 555.3013; found, 555.3009.

*3-((3S,4aR,9aR)-9-Benzyl-3-(2-((tert-butyldimethylsilyl)oxy)-ethyl)-4a-(cyanomethyl)-4-oxo-2,3,4,4a,9,9a-hexahydro-1H-carbazol-3-yl)propyl 4-Methylbenzenesulfonate (**26**).* To a flame-dried round-bottom argon flask equipped with a stir bar, TsCl (50.1 mg, 0.26 mmol, 2.0 equiv) and DMAP (1.6 mg, 0.01 mmol, 10 mol %) in 0.3 mL of CH_2Cl_2were added at 0 °C. To this solution, alcohol **24** (70 mg, 0.13 mmol, 1.0 equiv) in CH_2Cl_2 (0.3 mL) followed by triethylamine addition (20.1 μL, 0.14 mmol, 1.1 equiv) was added. Additional amounts of TsCl and trimethylamine (0.5 and 0.4 equiv, respectively) were further added. The resulting reaction was warmed to 23 °C, quenched with saturated $NaHCO_3$ (5 mL), extracted with CH_2Cl_2 (3×), washed with brine, dried with Na_2SO_4, and concentrated. The crude mixture was purified via column chromatography over silica gel using 10−15% EtOAc/hexanes as the eluent to provide tosylate **26** as an oil (71.4 mg, 79% yield). TLC: silica gel (20% EtOAc/hexanes), R_f = 0.31. $[\alpha]_D^{20}$ −101.20 (*c* 0.171, $CHCl_3$); ^{1}H NMR (500 MHz, $CDCl_3$): δ 7.78 (d, *J* = 8.3 Hz, 2H), 7.39−7.28 (m, 7H), 7.12 (td, *J* = 7.7, 1.3 Hz, 1H), 6.87 (dd, *J* = 7.5, 1.2 Hz, 1H), 6.65 (td, *J* = 7.5, 1.0 Hz, 1H), 6.47 (d, *J* = 7.9 Hz, 1H), 4.51 (d, *J* = 15.4 Hz, 1H), 4.28 (d, *J* = 15.4 Hz, 1H), 4.00 (m, 2H), 3.89 (dd, *J* = 7.4, 4.5 Hz, 1H), 3.46−3.40 (m, 1H), 3.38−3.31 (m, 2H), 3.03 (d, *J* = 16.3 Hz, 1H), 2.48 (d, *J* = 16.3 Hz, 1H), 2.44 (s, 3H), 1.84−1.77 (m, 2H), 1.77−1.65 (m, 3H), 1.58−1.47 (m, 4H), 1.40 (ddd, *J* = 14.0, 8.3, 5.7 Hz, 1H), 0.80 (s, 9H), −0.07 (d, *J* = 9.0 Hz, 6H); $^{13}C\{^1H\}$ NMR (126 MHz, $CDCl_3$): δ 210.9, 149.6, 144.9, 137.6, 133.1, 130.5, 130.0, 129.0, 128.1, 127.8, 127.5, 127.2, 123.7, 118.6, 117.8, 107.9, 71.0, 68.9, 58.8, 58.1, 49.5, 49.3, 40.0, 32.3, 27.3, 26.4, 26.0, 24.0, 22.0, 21.8, 18.3, −5.3; HRMS-ESI (+) *m*/*z*: calcd for $C_{39}H_{51}N_2O_5SSi$ $[M + H]^+$, 687.3283; found, 687.3276.

*3-((3S,4aS,9aS)-9-Benzyl-3-(2-((tert-butyldimethylsilyl)oxy)-ethyl)-4a-(cyanomethyl)-4-oxo-2,3,4,4a,9,9a-hexahydro-1H-carbazol-3-yl)propyl 4-Methylbenzenesulfonate (**27**).* The experimental is same as in the transformation of **24** to **26**. The crude mixture was isolated via column chromatography over silica gel using 15−20%

DOI: 10.1021/acs.joc.9b00145
J. Org. Chem. 2019, 84, 5167−5175

EtOAc/hexanes as the eluent to provide tosylate **27** as yellow oil (463.2 mg, 85% yield). TLC: silica (20% EtOAc/hexanes), R_f = 0.29. ^{1}H NMR (400 MHz, $CDCl_3$): δ 7.68 (d, J = 8.3 Hz, 2H), 7.40−7.28 (m, 7H), 7.11 (td, J = 7.7, 1.3 Hz, 1H), 6.80 (dd, J = 7.6, 1.3 Hz, 1H), 6.58 (td, J = 7.4, 0.9 Hz, 1H), 6.49 (d, J = 7.9 Hz, 1H), 4.52 (d, J = 15.5 Hz, 1H), 4.30 (d, J = 15.5 Hz, 1H), 3.97−3.87 (m, 1H), 3.76 (m, 1H), 3.67 (m, 1H), 3.59 (td, J = 6.8, 1.5 Hz, 2H), 3.00 (d, J = 16.3 Hz, 1H), 2.53 (d, J = 16.4 Hz, 1H), 2.45 (s, 3H), 1.95 (m, 1H), 1.84−1.65 (m, 4H), 1.61 (m, 1H), 1.54−1.44 (m, 1H), 1.44−1.32 (m, 1H), 1.27 (td, J = 12.7, 4.5 Hz, 2H), 1.09 (td, J = 13.1, 3.4 Hz, 1H), 0.86 (s, 9H), 0.02 (d, J = 2.6 Hz, 6H); ^{13}C{^{1}H} NMR (101 MHz, $CDCl_3$): δ 210.4, 150.1, 144.8, 137.6, 133.1, 130.7, 129.9, 129.0, 128.0, 127.8, 127.6, 126.8, 123.4, 118.3, 117.7, 107.9, 70.4, 69.0, 59.5, 58.0, 49.7, 49.1, 38.4, 34.7, 28.3, 26.7, 26.1, 23.4, 22.5, 21.8, 18.4, −5.2; LRMS-ESI (+) m/z: 687.3 $[M + H]^+$.

*2-((4aS,6aR,11bR,11cS)-7-Benzyl-3,4,5,6,6a,7-hexahydro-2H,11bH-11c,4a-(epoxyethano)pyrano[3,2-c]carbazol-11b-yl)-acetonitrile (**28**).* To a flame-dried round-bottom flask under argon equipped with a stir bar, tosylate **26** (27 mg, 39 μmol, 1.0 equiv) was dissolved in freshly distilled THF (0.4 mL, 0.1 M). To this solution at 23 °C, TBAF (1.0 M in THF, 47 μL, 47 μmol, 1.2 equiv) was added dropwise and the reaction mixture was stirred for 12 h. Reaction was then quenched with H_2O and brine (∼0.5 mL each), extracted with EtOAc (3×), washed with brine, dried with Na_2SO_4, and concentrated. The crude mixture was purified via column chromatography over silica gel using 15% EtOAc/hexanes as the eluent to provide tosylate **28** (15.7 mg, 99% yield) as a white amorphous solid. TLC: silica (20% EtOAc/hexanes), R_f = 0.34. $[\alpha]_D^{20}$ +45.13 (c 0.203, $CHCl_3$); ^{1}H NMR (400 MHz, chloroform-d): δ 7.34−7.24 (m, 6H), 7.07 (td, J = 7.7, 1.3 Hz, 1H), 6.62 (td, J = 7.4, 1.0 Hz, 1H), 6.34 (d, J = 8.3 Hz, 1H), 4.45 (d, J = 16.0 Hz, 1H), 4.35 (d, J = 16.0 Hz, 1H), 4.09 (ddd, J = 10.8, 8.4, 6.2 Hz, 1H), 3.91 (td, J = 8.6, 1.1 Hz, 1H), 3.77 (m, 2H), 3.68 (m, 1H), 2.95 (d, J = 16.6 Hz, 1H), 2.80 (d, J = 16.6 Hz, 1H), 2.02 (tt, J = 13.6, 3.5 Hz, 1H), 1.81−1.58 (m, 6H), 1.54−1.36 (m, 3H); ^{13}C{^{1}H} NMR (101 MHz, chloroform-d): δ 152.1, 138.9, 129.9, 129.5, 128.7, 127.4, 127.2, 125.9, 119.3, 117.2, 108.8, 105.9, 68.3, 67.3, 61.3, 54.9, 50.9, 41.4, 38.6, 36.5, 31.3, 28.0, 24.9, 21.3; HRMS-APCI (+) m/z: calcd for $C_{26}H_{29}N_2O_2$ $[M + H]^+$, 401.2223; found, 401.2220.

*2-((4aS,6aS,11bS,11cS)-7-Benzyl-3,4,5,6,6a,7-hexahydro-2H,11bH-11c,4a-(epoxyethano)pyrano[3,2-c]carbazol-11b-yl)-acetonitrile (**29**).* To a flame-dried round-bottom flask under argon equipped with a stir bar, compound **27** (30 mg, 44 μmol, 1.0 equiv) was added in freshly distilled THF (0.44 mL, 0.1 M). To this solution at 23 °C, TBAF (1.0 M in THF, 52 μL, 52 μmol, 1.2 equiv) was added and the resulting reaction was stirred for 12 h. The reaction was then quenched with H_2O (0.5 mL), extracted with EtOAc (3×), washed with brine, dried with Na_2SO_4, and concentrated. The crude mixture was purified via column chromatography over silica gel using 20% EtOAc/hexanes as the eluent to provide product **29** (17.5 mg, quantitative yield) as an amorphous white solid. TLC: silica (20% EtOAc/hexanes), R_f = 0.30. $[\alpha]_D^{20}$ −68.82 (c 0.364, $CHCl_3$); ^{1}H NMR (500 MHz, $CDCl_3$): δ 7.53 (dd, J = 7.5, 1.3 Hz, 1H), 7.37−7.30 (m, 4H), 7.26 (m, 1H), 7.05 (td, J = 7.7, 1.4 Hz, 1H), 6.58 (td, J = 7.5, 1.0 Hz, 1H), 6.30 (dd, J = 7.9, 0.9 Hz, 1H), 4.47 (d, J = 15.9 Hz, 1H), 4.39 (d, J = 15.9 Hz, 1H), 4.17 (ddd, J = 10.6, 8.7, 4.9 Hz, 1H), 3.98 (ddd, J = 12.0, 9.8, 1.9 Hz, 1H), 3.93 (ddd, J = 9.6, 8.6, 7.5 Hz, 1H), 3.75 (ddd, J = 12.3, 10.4, 6.9 Hz, 1H), 3.66 (d, J = 3.7 Hz, 1H), 2.98 (d, J = 16.6 Hz, 1H), 2.93 (d, J = 16.5 Hz, 1H), 2.51 (ddd, J = 13.5, 10.6, 7.5 Hz, 1H), 1.99−1.89 (m, 1H), 1.83 (ddd, J = 14.0, 9.6, 4.9 Hz, 1H), 1.73−1.63 (m, 2H), 1.58−1.45 (m, 3H), 1.38−1.34 (m, 1H), 1.23−1.15 (m, 1H); ^{13}C{^{1}H} NMR (126 MHz, $CDCl_3$): δ 152.4, 138.9, 129.4, 128.7, 128.4, 127.5, 127.2, 126.5, 119.2, 116.7, 109.4, 105.2, 67.8, 67.0, 58.6, 53.1, 50.4, 43.3, 38.2, 35.1, 28.4, 27.8, 23.8, 19.0; HRMS-APCI (+) m/z: calcd for $C_{26}H_{29}N_2O_2$ $[M + H]^+$, 401.2223; found, 401.2219.

*3-((4S,6aS,11bS)-7-Benzyl-4-(2-((tert-butyldimethylsilyl)oxy)-ethyl)-2,4,5,6,6a,7-hexahydro-1H-pyrrolo[2,3-d]carbazol-4-yl)-propyl 4-Methylbenzenesulfonate (**30**).* To a Parr reactor vessel under argon, 2800 Ra−Ni (1.21 g, 300 wt %) was added. A solution of tosylate **27** (403 mg, 0.59 mmol, 1.0 equiv) in MeOH (22 mL, 27 mM) was then cannulated in the flask. The mixture was shaken in a Parr apparatus under hydrogen at 60 psi pressure for 46 h. After this period, the resulting white solution mixture was filtered through Celite and the filter cake was washed with MeOH and CH_2Cl_2 (15 mL each). Solvents were evaporated to yield imine **30** (359.5 mg, 90.8% yield). TLC: silica (30% EtOAc/hexanes), R_f = 0.46. ^{1}H NMR (500 MHz, $CDCl_3$): δ 7.68 (d, J = 8.3 Hz, 2H), 7.36−7.27 (m, 7H), 7.03 (td, J = 7.7, 1.3 Hz, 1H), 6.63 (dd, J = 7.3, 1.2 Hz, 1H), 6.48 (t, J = 5.9 Hz, 1H), 6.40 (d, J = 7.9 Hz, 1H), 4.48 (d, J = 15.5 Hz, 1H), 4.24 (d, J = 15.5 Hz, 1H), 3.91 (dd, J = 15.4, 8.5 Hz, 1H), 3.80 (m, 1H), 3.74 (m, 1H), 3.68 (m, 1H), 3.62 (td, J = 7.2, 3.0 Hz, 2H), 3.47 (t, J = 5.7 Hz, 1H), 2.45 (s, 3H), 2.19 (dt, J = 12.2, 6.6 Hz, 1H), 1.91 (m, 1H), 1.80 (dt, J = 13.9, 6.7 Hz, 1H), 1.69 (m, 2H), 1.57 (m, 2H), 1.46 (m, 2H), 1.16 (td, J = 13.0, 5.3 Hz, 1H), 1.04 (td, J = 13.1, 3.2 Hz, 1H), 0.85 (s, 9H), 0.01 (d, J = 1.9 Hz, 7H); ^{13}C{^{1}H} NMR (126 MHz, $CDCl_3$): δ 180.8, 149.2, 144.5, 138.4, 133.2, 132.4, 129.8, 128.7, 128.7, 127.9, 127.4, 127.3, 122.0, 117.4, 107.2, 71.6, 71.0, 61.0, 59.4, 56.9, 49.2, 43.5, 41.8, 38.6, 32.6, 31.4, 26.0, 23.7, 22.5, 21.7, 18.3, −5.3; LRMS-ESI (+) m/z: 673.3 $[M + H]^+$.

*1-Benzyl Fendleridine (**32**).*[25] To a Parr reactor vessel under argon, 2800 Ra−Ni (51 mg, 300 wt %) was added. A solution of tosylate **26** (17 mg, 25 μmol, 1.0 equiv) in MeOH (1 mL, 27 mM) was then cannulated in the flask. The mixture was shaken in a Parr apparatus under hydrogen at 60 psi pressure for 21 h. After this period, the resulting white solution mixture was filtered through Celite and the filter cake was washed with MeOH and CH_2Cl_2 (10 mL each). Solvents were evaporated and the crude material (**31**) was used directly for the next reaction. LRMS-ESI (+) m/z: 501.3 $[M]^+$.

To a flame-dried flask under argon equipped with a stir bar, the above crude product (**31**) was dissolved in freshly distilled THF (0.3 mL, 0.1 M), TBAF (1 M in THF, 30 μL, 0.03 mmol, 1.2 equiv) was added, and the resulting reaction mixture was stirred for 12 h. The reaction was then quenched with H_2O (∼0.5 mL), extracted with EtOAc (3×), washed with brine, dried with Na_2SO_4, and concentrated. The crude mixture was purified via column chromatography over silica gel using 70−80% EtOAc/hexanes as the eluent to provide benzyl derivative **32** (5.9 mg, 62% yield over 2 steps) as an off-white amorphous solid. TLC: alumina (5% EtOAc/hexanes), R_f = 0.50. $[\alpha]_D^{20}$ +3.0 (c 0.155, $CHCl_3$); ^{1}H NMR (400 MHz, $CDCl_3$): δ 7.36 (dd, J = 7.4, 1.3 Hz, 1H), 7.29−7.15 (m, 5H), 6.94 (td, J = 7.6, 1.3 Hz, 1H), 6.59 (td, J = 7.4, 1.1 Hz, 1H), 6.27 (dd, J = 7.8, 1.0 Hz, 1H), 4.34 (d, J = 15.4 Hz, 1H), 4.06 (d, J = 15.4 Hz, 1H), 3.89−3.75 (m, 2H), 3.22 (dd, J = 7.6, 4.1 Hz, 1H), 2.91−2.82 (m, 2H), 2.74−2.64 (m, 1H), 2.59−2.51 (m, 1H), 2.14 (ddd, J = 13.2, 8.9, 6.6 Hz, 1H), 1.98−1.84 (m, 2H), 1.77 (dd, J = 21.1, 10.6 Hz, 1H), 1.64−1.50 (m, 3H), 1.50−1.38 (m, 3H), 1.29−1.19 (m, 2H); ^{13}C{^{1}H} NMR (101 MHz, $CDCl_3$): δ 151.2, 139.0, 135.0, 128.6, 127.7, 127.5, 127.1, 125.9, 117.9, 106.5, 101.9, 71.5, 64.9, 57.9, 49.6, 49.2, 44.1, 38.6, 38.3, 36.9, 34.7, 27.4, 21.64, 21.56; HRMS-ESI (+) m/z: calcd for $C_{26}H_{31}N_2O$ $[M + H]^+$, 387.2431; found, 387.2429.

*(+)-Fendleridine (**2**).*[25,27a] A flame-dried round-bottom flask under argon was equipped with a stir bar and a cold-finger condenser with dry ice and acetone. NH_3 was allowed to condense into the flask (1 mL), the cold finger condenser was removed, and a septum with an argon balloon quickly replaced it. To this, small chunks of freshly cut Li (30 mg, 167 equiv) washed with hexanes were added. The solution turned dark blue. The benzyl derivative **32** (10 mg, 0.03 mmol, 1 equiv) in a mixture (10:1) of THF and t-BuOH (0.5 mL) was added and the reaction was stirred for 2 h. Reaction was quenched with solid NH_4Cl (∼100 mg, 72.3 equiv), the cooling bath was removed, and the reaction was warmed to 23 °C. The reaction was diluted with EtOAc (1 mL), filtered through cotton plug with CH_2Cl_2 and EtOAc (5 mL each), and concentrated. The crude mixture was purified via column chromatography over alumina using 5% EtOAc/hexanes as the eluent to provide synthetic (+)fendleridine, (+)-**2** as off-white amorphous solid (5.3 mg, 70%). TLC: alumina (5% EtOAc/hexanes), R_f = 0.13. $[\alpha]_D^{20}$ +53.7 (c 0.177, $CHCl_3$); ^{1}H NMR (800 MHz, $CDCl_3$): δ 7.45 (d, J = 7.5 Hz, 1H), 7.01 (t, J = 7.6 Hz, 1H), 6.73 (t, J = 7.5 Hz, 1H), 6.60 (d, J = 7.7 Hz, 1H), 4.03−3.95 (m, 2H), 3.52 (br

DOI: 10.1021/acs.joc.9b00145
J. Org. Chem. 2019, 84, 5167−5175

s, 1H), 3.40 (dd, J = 9.5, 4.8 Hz, 1H), 3.00 (td, J = 8.7, 4.1 Hz, 1H), 2.92 (dt, J = 15.6, Hz, 1H), 2.79 (t, J = 11.4 Hz, 1H), 2.65 (d, J = 11.1 Hz, 1H), 2.24 (ddd, J = 13.4, 8.7, 5.9 Hz, 1H), 1.92−1.83 (m, 2H), 1.81 (td, J = 12.9, 4.0 Hz, 1H), 1.78−1.71 (m, 2H), 1.71−1.59 (m, 2H), 1.51 (dt, J = 12.1, 3.2 Hz, 1H), 1.45 (dt, J = 13.8, 4.8 Hz, 1H), 1.35 (d, J = 13.0 Hz, 1H), 1.24 (dd, J = 11.9, 5.5 Hz, 1H); $^{13}C\{^1H\}$ NMR (201 MHz, $CDCl_3$): δ 150.3, 134.4, 127.3, 126.1, 119.4, 110.0, 102.1, 66.6, 64.9, 58.9, 49.3, 44.1, 39.2, 37.0, 35.8, 34.1, 27.3, 27.0, 21.5; HRMS-ESI (+) m/z: calcd for $C_{19}H_{25}N_2O$ $[M + H]^+$, 297.1961; found, 297.1964.

(+)-Acetylaspidoalbidine (3).[25,27a] To a flame-dried round-bottom flask under argon equipped with a stir bar, synthetic fendleridine (7.9 mg, 0.027 mmol, 1.0 equiv) was dissolved in CH_2Cl_2 (1 mL). Pyridine (11 μL, 0.13 mmol, 5.0 equiv) and acetic anhydride (7.5 μL, 0.08 mmol, 3.0 equiv) were added sequentially. The reaction was quenched with saturated $NaHCO_3$ (∼0.1 mL), extracted 3× with CH_2Cl_2, dried with Na_2SO_4, and concentrated. The crude mixture was purified via column chromatography using 15−20% EtOAc/hexanes as the eluent to provide products (+)-**3** (rotamers) as white amorphous solid (9 mg, quantitative yield). TLC: alumina (5% EtOAc/hexanes), R_f = 0.08. $[\alpha]_D^{20}$ +30.2 (c 0.145, $CHCl_3$); ^1H NMR (800 MHz, $CDCl_3$): δ 8.14 (d, J = 8.0 Hz, 1H), 7.67 (d, J = 3.5 Hz, 0.3H) 7.60 (d, J = 7.7 Hz, 1H, minor rotamer), 7.19 (t, J = 7.7 Hz, 1H), 7.05 (t, J = 7.5 Hz, 1H), 4.42 (dd, J = 9.12, 4.16 Hz, minor rotamer), 4.16 (t, J = 8.6 Hz, 1H), 4.09 (dt, J = 10.5, 7.5 Hz, 1H), 3.86 (dd, J = 11.0, 5.2 Hz, 1H), 3.02 (td, J = 8.8, 4.1 Hz, 1H), 2.93 (dd, J = 15.7, 9.0 Hz, 1H), 2.80 (td, J = 11.5, 2.8 Hz, 1H), 2.65 (d, J = 10.7 Hz, 1H), 2.39 (s, 0.6H, minor rotamer), 2.26 (s, 2.1H), 2.10 (ddd, J = 14.6, 9.1, 6.1 Hz, 1H), 2.07−2.00 (m, 1H), 1.93 (m, 1H), 1.86 (m, 1H), 1.83−1.66 (m, 4H), 1.55 (dt, J = 12.7, 3.6 Hz, 0.8H), 1.50 (t, J = 13.9 Hz, 0.2H, minor rotamer), 1.43 (dt, J = 14.0, 3.9 Hz, 1H), 1.38 (d, J = 12.9 Hz, 1H), 1.27 (m, 1H); $^{13}C\{^1H\}$ NMR (201 MHz, $CDCl_3$, major rotamer): δ 168.2, 141.2, 137.9, 127.5, 124.9, 124.8, 117.9, 102.2, 69.0, 65.1, 58.4, 49.1, 44.1, 39.8, 37.3, 34.9, 33.2, 26.6, 25.5, 23.5, 21.2; $^{13}C\{^1H\}$ NMR (201 MHz, $CDCl_3$, minor rotamer): δ 168.0, 140.6, 140.1, 127.1, 126.1, 124.3, 115.1, 102.5, 67.1, 65.0, 57.2, 48.9, 43.9, 39.6, 37.0, 35.2, 33.5, 26.8, 24.4, 23.8, 21.2; HRMS-ESI (+) m/z: calcd for $C_{21}H_{27}N_2O_2$ $[M + H]^+$, 339.2067; found, 339.2064.

■ ASSOCIATED CONTENT

Supporting Information

The Supporting Information is available free of charge on the ACS Publications website at DOI: 10.1021/acs.joc.9b00145.

^1H and ^{13}C NMR spectra for all new compounds and HPLC data for asymmetric allylation reaction (PDF)

■ AUTHOR INFORMATION

Corresponding Author

*E-mail: akghosh@purdue.edu.

ORCID

Arun K. Ghosh: 0000-0003-2472-1841

Notes

The authors declare no competing financial interest.

■ ACKNOWLEDGMENTS

Financial support of this work was provided by the National Institutes of Health (GM122279) and Purdue University.

■ REFERENCES

(1) (a) Lopchuk, J. M. In *Progress in Heterocyclic Chemistry*; Gribble, G. W., Joule, J. A., Eds.; Elsevier, 2011; Vol. *23*, pp 1−25. (b) O'Connor, S. E. 1.25—Alkaloids. In *Comprehensive Natural Products II*; Liu, H.-W., Mander, L., Eds.; Elsevier: Oxford, 2010; pp 977−1007.

(2) (a) Saxton, J. E. In *The Alkaloids: Chemistry and Biology*; Cordell, G. A., Ed.; Academic Press, 1998; Vol. *50*, pp 343−376. (b) Saxton, J. E. In *The Alkaloids: Chemistry and Biology*; Cordell, G. A., Ed.; Academic Press, 1998; Vol. *51*, pp 1−197.

(3) Blair, L. M.; Calvert, M. B.; Gaich, T.; Lindel, T.; Phaffenbach, M.; Sperry, J. In *The Alkaloids: Chemistry and Biology*; Knölker, H.-J., Ed.; Academic Press: New York, 2017; Vol. *77*, pp 1−84.

(4) O'Connor, S. E.; Maresh, J. Chemistry and biology of monoterpene indole alkaloid biosynthesis. *Nat. Prod. Rep.* **2006**, *23*, 532−547.

(5) (a) Lobert, S.; Vulevic, B.; Correia, J. J. Interaction of Vinca Alkaloids with Tubulin: A Comparison of Vinblastine, Vincristine, and Vinorelbine. *Biochemistry* **1996**, *35*, 6806−6814. (b) Prakash, V.; Timasheff, S. N. Mechanism of interaction of vinca alkaloids with tubulin: catharanthine and vindoline. *Biochemistry* **1991**, *30*, 873−880. (c) Safa, A. R.; Hamel, E.; Felsted, R. L. Photoaffinity labeling of tubulin subunits with a photoactive analog of vinblastine. *Biochemistry* **1987**, *26*, 97−102.

(6) Tanaka, J. C. A.; Silva, C. C. d.; Oliveira, A. J. B. d.; Nakamura, C. V.; Dias Filho, B. P. Antibacterial activity of indole alkaloids from Aspidosperma ramiflorum. *Braz. J. Med. Biol. Res.* **2006**, *39*, 387−391.

(7) Aquino, P. G. V.; de Aquino, T. M.; Alexandre-Moreira, M. S.; Santos, B. V. d. O.; Santana, A. E. G.; de Araujo, J. X. Aspidosperma Terpenoid Alkaloids—Biosynthetic Origin, Chemical Synthesis and Importance. *Phytochemicals—Isolation, Characterisation and Role in Human Health*; IntechOpen, 2015.

(8) For pioneering earlier studies, see the following references (a) Stork, G.; Dolfini, J. E. The Total Synthesis of dl-Aspidospermine and of dl-Quebrachamine. *J. Am. Chem. Soc.* **1963**, *85*, 2872−2873. (b) Harley-Mason, J.; Kaplan, M. A simple total synthesis of (±)-aspidospermidine. *Chem. Commun.* **1967**, 915−916. (c) Buechi, G.; Matsumoto, K. E.; Nishimura, H. Total synthesis of (+-)-vindorosine. *J. Am. Chem. Soc.* **1971**, *93*, 3299−3301. (d) Kuehne, M. E.; Roland, D. M.; Hafter, R. Studies in biomimetic alkaloid syntheses. 2. Synthesis of vincadifformine from tetrahydro-.beta.-carboline through a secodine intermediate. *J. Org. Chem.* **1978**, *43*, 3705−3710. (e) Andriamialisoa, R. Z.; Langlois, N.; Langlois, Y. A new efficient total synthesis of vindorosine and vindoline. *J. Org. Chem.* **1985**, *50*, 961−967. (f) Cardwell, K.; Hewitt, B.; Ladlow, M.; Magnus, P. Methods for indole alkaloid synthesis. A study of the compatibility of the indole-2,3-quinodimethane strategy for the synthesis of 16-methoxy-substituted aspidosperma-type alkaloids. Synthesis of (+)- and (-)-16-methoxytabersonine. *J. Am. Chem. Soc.* **1988**, *110*, 2242−2248. (g) Kozmin, S. A.; Iwama, T.; Huang, Y.; Rawal, V. H. An Efficient Approach to Aspidosperma Alkaloids via [4+2] Cycloadditions of Aminosiloxydienes: Stereocontrolled Total Synthesis of (±)-Tabersonine. Gram-Scale Catalytic Asymmetric Syntheses of (+)-Tabersonine and (+)-16-Methoxytabersonine. Asymmetric Syntheses of (+)-Aspidospermidine and (-)-Quebrachamine. *J. Am. Chem. Soc.* **2002**, *124*, 4628−4641.

(9) (a) Zhao, S.; Andrade, R. B. Domino Michael/Mannich/N-Alkylation Route to the Tetrahydrocarbazole Framework of Aspidosperma Alkaloids: Concise Total Syntheses of (−)-Aspidospermidine, (−)-Tabersonine, and (−)-Vincadifformine. *J. Am. Chem. Soc.* **2013**, *135*, 13334−13337. (b) Liu, Y.; Liniger, M.; McFadden, R. M.; Roizen, J. L.; Malette, J.; Reeves, C. M.; Behenna, D. C.; Seto, M.; Kim, J.; Mohr, J. T.; Virgil, S. C.; Stoltz, B. M. Formal total syntheses of classic natural product target molecules via palladium-catalyzed enantioselective alkylation. *Beilstein J. Org. Chem.* **2014**, *10*, 2501−2512.

(10) (a) Horinouchi, R.; Kamei, K.; Watanabe, R.; Hieda, N.; Tatsumi, N.; Nakano, K.; Ichikawa, Y.; Kotsuki, H. Enantioselective Synthesis of Quaternary Carbon Stereogenic Centers through the Primary Amine-Catalyzed Michael Addition Reaction of α-Substituted Cyclic Ketones at High Pressure. *Eur. J. Org. Chem.* **2015**, 4457−4463. (b) Mori, M.; Nakanishi, M.; Kajishima, D.; Sato, Y. A Novel and General Synthetic Pathway to Strychnos Indole Alkaloids: Total Syntheses of (−)-Tubifoline, (−)-Dehydrotubifoline, and

(−)-Strychnine Using Palladium-Catalyzed Asymmetric Allylic Substitution. *J. Am. Chem. Soc.* **2003**, *125*, 9801−9807.
(11) (a) Cava, M. P.; Talapatra, S. K.; Nomura, K.; Weisbach, J. A.; Douglas, B.; Shoop, E. C. Haplocine and Haplocidine: Aspidospermine-Type Alkaloids from Haplophyton cimicidum. *Chem. Ind.* **1963**, 1242−1243. (b) Cava, M. P.; Nomura, K.; Talapatra, S. K. The stereochemistry of limaspermine, haplocine and haplocidine. *Tetrahedron* **1964**, *20*, 581−583.
(12) Hart, M. J.; Glicksman, M.; Liu, M.; Sharma, M. K.; Cuny, G.; Galvan, V. Development of a high-throughput screen targeting caspase-8-mediated cleavage of the amyloid precursor protein. *Anal. Biochem.* **2012**, *421*, 467−476.
(13) (a) Cava, M. P.; Talapatra, S. K.; Yates, P.; Rosenberger, M.; Szano, A. G.; Douglas, B.; Raffauf, R. F.; Shoop, E. C.; Weisbach, J. A. Cimicine and Cimicidine: Lactonic Alkaloids of the Aspidospermine Skeletal Type. *Chem. Ind.* **1963**, 1875−1876. (b) Cava, M. P.; Lakshmikantham, M. V.; Talapatra, S. K.; Yates, P.; Rae, I. D.; Rosenberger, M.; Szabo, A. G.; Douglas, B.; Weisbach, J. A. Cimicine and Cimicidine, Lactonic Alkaloids from Haplophyton cimicidum. *Can. J. Chem.* **1973**, *51*, 3102−3109.
(14) Satoh, H.; Ueda, H.; Tokuyama, H. Divergent total synthesis of (−)-aspidophytine and its congeners via Fischer indole synthesis. *Tetrahedron* **2013**, *69*, 89−95.
(15) Burnell, R. H.; Medina, J. D.; Ayer, W. A. Alkaloids of the Seeds of Aspidosperma Fendleri WOODSON. *Can. J. Chem.* **1966**, *44*, 28−31.
(16) Medina, J.; Genova, L. Alkaloids of the Bark of Aspidosperma rhombeosignatum. *Planta Med.* **1979**, *37*, 165−167.
(17) (a) Brown, K. S.; Budzikiewicz, H.; Djerassi, C. Alkaloid studies XLII. The structures of dichotamine, 1-acetyl-aspidoalbidine and 1-acetyl-17-hydroxyaspidoalbidine: three new alkaloids from vallesia-dichotoma ruiz et pav. *Tetrahedron Lett.* **1963**, *4*, 1731−1736. (b) Walser, A.; Djerassi, C. Alkaloid-Studien LII. Die Alkaloide aus Vallesia dichotoma RUIZet PAV. *Helv. Chim. Acta* **1965**, *48*, 391−404.
(18) Tan, S. H.; Banwell, M. G.; Willis, A. C.; Reekie, T. A. Application of a Raney-Cobalt-Mediated Tandem Reductive Cyclization Protocol to Total Syntheses of the Aspidosperma Alkaloids (±)-Limaspermidine and (±)-1-Acetylaspidoalbidine. *Org. Lett.* **2012**, *14*, 5621−5623.
(19) Ban, Y.; Ohnuma, T.; Seki, K.; Oishi, T. The total synthesis of the alkaloid (±)-1-acetylaspidoalbidine. *Tetrahedron Lett.* **1975**, *16*, 727−730.
(20) Jin, J.; Qiu, F. G. Total Synthesis of (±)-1-Acetylaspidoalbidine and (±)-1-Methylaspidospermidine. *Adv. Synth. Catal.* **2014**, *356*, 340−346.
(21) (a) Ban, Y.; Honma, Y.; Ohnuma, T. A Total Synthesis of (±)-Fendleridine. *Heterocycles* **1976**, *5*, 47−51. (b) Yoshida, K.; Sakuma, Y.; Ban, Y. Synthetic Studies on Oxygenated Aspidoserma Alkaloids: Facile Syntheses of 1-Acetylaspidoalbidine and Deoxyaspidodispermine. *Heterocycles* **1987**, *25*, 47−50.
(22) Overman, L. E.; Sworin, M.; Burk, R. M. Synthesis applications of aza-Cope rearrangements. Part 10. A new approach for the total synthesis of pentacyclic Aspidosperma alkaloids. Total synthesis of dl-16-methoxytabersonine. *J. Org. Chem.* **1983**, *48*, 2685−2690.
(23) For the total synthesis of the related alkaloid aspidophytine, see: (a) He, F.; Bo, Y.; Altom, J. D.; Corey, E. J. Enantioselective Total Synthesis of Aspidophytine. *J. Am. Chem. Soc.* **1999**, *121*, 6771−6772. (b) Sumi, S.; Matsumoto, K.; Tokuyama, H.; Fukuyama, T. Stereocontrolled total synthesis of (−)-aspidophytine. *Tetrahedron* **2003**, *59*, 8571−8587. (c) Mejía-Oneto, J. M.; Padwa, A. Application of the Rh(II) Cyclization/Cycloaddition Cascade for the Total Synthesis of (±)-Aspidophytine. *Org. Lett.* **2006**, *8*, 3275−3278. (d) Marino, J. P.; Cao, G. Total synthesis of aspidophytine. *Tetrahedron Lett.* **2006**, *47*, 7711−7713. (e) Nicolaou, K. C.; Dalby, S. M.; Majumder, U. A Concise Asymmetric Total Synthesis of Aspidophytine. *J. Am. Chem. Soc.* **2008**, *130*, 14942−14943.
(24) Doris, E. Total syntheses of (+)-haplophytine. *Angew. Chem., Int. Ed.* **2009**, *48*, 7480−7483.
(25) Campbell, E. L.; Zuhl, A. M.; Liu, C. M.; Boger, D. L. Total Synthesis of (+)-Fendleridine (Aspidoalbidine) and (+)-1-Acetylaspidoalbidine. *J. Am. Chem. Soc.* **2010**, *132*, 3009−3012.
(26) Wilkie, G. D.; Elliott, G. I.; Blagg, B. S. J.; Wolkenberg, S. E.; Soenen, D. R.; Miller, M. M.; Pollack, S.; Boger, D. L. Intramolecular Diels−Alder and Tandem Intramolecular Diels−Alder/1,3-Dipolar Cycloaddition Reactions of 1,3,4-Oxadiazoles. *J. Am. Chem. Soc.* **2002**, *124*, 11292−11294.
(27) (a) White, K. L.; Movassaghi, M. Concise Total Syntheses of (+)-Haplocidine and (+)-Haplocine via Late-Stage Oxidation of (+)-Fendleridine Derivatives. *J. Am. Chem. Soc.* **2016**, *138*, 11383−11389. (b) Mewald, M.; Medley, J. W.; Movassaghi, M. Concise and enantioselective total synthesis of (-)-mehranine, (-)-methylenebismehranine, and related Aspidosperma alkaloids. *Angew. Chem., Int. Ed.* **2014**, *53*, 11634−11639.
(28) (a) Dugat, D.; Gramain, J.-C.; Dauphin, G. r. Structure, stereochemistry, and conformation of diastereoisomeric cis- and trans-3-ethyl-1,2,3,4,4a,9a-hexahydrocarbazol-4-ones by means of ^{13}C and two-dimensional ^{1}H nuclear magnetic resonance spectroscopy. An example of diastereoselection in a photocyclisation reaction. *J. Chem. Soc., Perkin Trans. 2* **1990**, 605−611. (b) Gramain, J.-C.; Troin, Y.; Husson, H.-P. A short and efficient synthesis of 4a-substituted cis-hexahydro-1,2,3,4,4a,9a-carbazol-4-ones. *J. Heterocycl. Chem.* **1988**, *25*, 201−203. (c) Gramain, J.-C.; Husson, H. P.; Troin, Y. A novel and efficient synthesis of the aspidosperma alkaloid ring system: N(a)-benzyldeethylaspidospermidine. *J. Org. Chem.* **1985**, *50*, 5517−5520.
(29) (a) McFadden, R. M.; Stoltz, B. M. The Catalytic Enantioselective, Protecting Group-Free Total Synthesis of (+)-Dichroanone. *J. Am. Chem. Soc.* **2006**, *128*, 7738−7739. (b) Behenna, D. C.; Mohr, J. T.; Sherden, N. H.; Marinescu, S. C.; Harned, A. M.; Tani, K.; Seto, M.; Ma, S.; Novák, Z.; Krout, M. R.; McFadden, R. M.; Roisen, J. L.; Enquist, J. A., Jr.; White, D. E.; Leine, S. R.; Petrova, K. V.; Iwashita, A.; Virgil, S. C.; Stoltz, B. M. Enantioselective Decarboxylative Alkylation Reactions: Catalyst Development, Substrate Scope, and Mechanistic Studies. *Chem.—Eur. J.* **2011**, *17*, 14199−14223. (c) Mohr, J. T.; Stoltz, B. M. Enantioselective Tsuji Allylations. *Chem.—Asian J.* **2007**, *2*, 1476−1491. (d) Bennett, N. B.; Duquette, D. C.; Kim, J.; Liu, W.; Marziale, A. N.; Behenne, D. C.; Virgil, S. C.; Stoltz, B. M. Expanding Insight into Asymmetric Palladium-Catalyzed Allylic Alkylation of N-Heterocyclic Molecules and Cyclic Ketones. *Chem.—Eur. J.* **2013**, *19*, 4414−4418.
(30) Zhao, X.; Li, W.; Wang, J.; Ma, D. Convergent Route to ent-Kaurane Diterpenoids: Total Synthesis of Lungshengenin D and 1α,6α-Diacetoxy-ent-kaura-9(11),16-dien-12,15-dione. *J. Am. Chem. Soc.* **2017**, *139*, 2932−2935.
(31) Bennett, N. B.; Duquette, D. C.; Kim, J.; Liu, W.-B.; Marziale, A. N.; Behenna, D. C.; Virgil, S. C.; Stoltz, B. M. Expanding Insight into Asymmetric Palladium-Catalyzed Allylic Alkylation of N-Heterocyclic Molecules and Cyclic Ketones. *Chem.—Eur. J.* **2013**, *19*, 4414−4418.
(32) Weaver, J. D.; Recio, A.; Grenning, A. J.; Tunge, J. A. Transition Metal-Catalyzed Decarboxylative Allylation and Benzylation Reactions. *Chem. Rev.* **2011**, *111*, 1846−1913.
(33) Modha, S. G.; Pöthig, A.; Dreuw, A.; Bach, T. [6π] Photocyclization to cis Hexahydrocarbazol-4-ones: Substrate Modification, Mechanism, and Scope. *J. Org. Chem.* **2019**, *84*, 1139−1153.
(34) (a) Brown, H. C.; Prasad, J. V. N. V.; Zee, S. H. Hydroboration. 71. Hydroboration of representative heterocyclic olefins with borane-methyl sulfide, 9-borabicyclo[3.3.1]nonane, dicyclohexylborane, and disiamylborane. Synthesis of heterocyclic alcohols. *J. Org. Chem.* **1985**, *50*, 1582−1589. (b) Brown, H. C.; Prasad, J. V. N. V.; Zee, S. H. Hydroboration. 75. Directive effects in the hydroboration of vinyl and propenyl heterocycles with representative hydroborating agents. *J. Org. Chem.* **1986**, *51*, 439−445.
(35) Schultz, A. G.; Dittami, J. P.; Myong, S. O.; Sha, C. K. A New 2-Azatricyclo[4.4.0.$0^{2,8}$]decenone Synthesis and Ketene Formation by Retro-Diels-Alder Reaction. *J. Am. Chem. Soc.* **1983**, *105*, 3273−3279.

DOI: 10.1021/acs.joc.9b00145
J. Org. Chem. 2019, 84, 5167−5175